

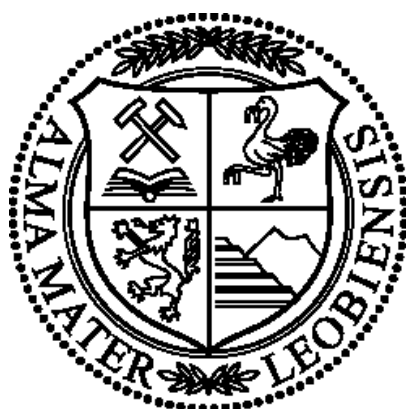
# **Thiol-yne Derived Resins for 3D Printing of Biocompatible Structures**

**Doctoral Thesis**

Dissertation

by

**Andreas Oesterreicher**



Montanuniversität Leoben

Institute of Chemistry of Polymeric Materials

Leoben, November 2016

Supervisor:

Assoc. Prof. Dipl.-Ing. Dr. Thomas Griesser

# ABSTRACT

The present thesis deals with the synthesis and investigation of new, low-cytotoxic alkyne and thiol monomers and their thiol-yne derived photopolymers. Furthermore, polymerizable photoinitiators featuring low migration in thiol-based resins have been studied. This research is driven by the vision to produce custom-made, biomedical devices by lithography-based additive manufacturing technologies.

In the first part of this work alkyne ethers and alkyne carbonates have been explored as low cytotoxic alternatives to the commonly used (meth)acrylates. The work describes the synthesis, the cytotoxic behavior and the characterization of the photoreactivity of alkynes in combination with different thiol monomers. While featuring high reaction rates and also high monomer conversions, investigations on the network properties of cured thiol-yne resins by dynamic thermo-mechanical analysis (DMA), double quantum (DQ) solid state NMR spectroscopy and photorheology have revealed that these monomers show the potential to realize photopolymers with very homogenous network structures, leading to excellent mechanical properties in terms of modulus and polymer toughness. Different stabilizers have been evaluated in the resin that significantly improved the storage stability. It is also shown how the degradation behavior of cured photopolymers can be tuned from hydrolytic susceptibility to hydrolytic stability, dependent on the applied thiol or alkyne monomer. In this context, a new silicone-based thiol has been introduced as non-degradable monomer, which also leads to polymers with reduced water absorption and improved mechanical properties. Printing experiments revealed, that the presented alkyne resins have shown excellent 3D printing behavior with high accuracy as it has been demonstrated on a digital light processing (DLP) based 3D printer.

The second part of this work describes the synthesis and characterization of new type I alkyne-functionalized photoinitiators for thiol-ene and thiol-yne resins. It is the aim to realize low photoinitiator migration in biocompatible photopolymers, while still maintaining high initiation performance. Therefore, two different types of photoinitiators have been studied and their overall performances in a biocompatible thiol-ene and thiol-yne resins are discussed intensively.

Due to the versatile properties of the presented thiol-yne photopolymers, including low monomer cytotoxicity, high photoreactivity and high monomer conversion together with excellent thermo-mechanical and impact properties, these material shows very high potential for the 3D printing of medical devices.

# KURZFASSUNG

Die vorliegende Doktorarbeit beschäftigt sich mit der Synthese und Untersuchung von neuen Alkin- und Thiolmonomeren niedriger Zytotoxizität, sowie mit der Untersuchung der darauf basierenden Thiol-in Photopolymere. Zudem umfasst diese Arbeit die Synthese polymerisierbarer Photoinitiatoren, welche ein geringes Migrationsverhalten in thiol-basierenden Harzen aufweisen. Motivation dieser Forschung ist die Herstellung patientenspezifischer, biomedizinischer Produkte mittels lithographischer 3D-Drucktechnologien.

Im ersten Teil werden Alkinether und Alkincarbonate als niedrig-zytotoxische Alternativen zu kommerziellen (Meth)acrylaten vorgestellt. Es wird sowohl deren Synthese, deren Zytotoxizität als auch deren Photoreaktivität in Harzformulierungen in Kombination mit verschiedenen Thiolmonomeren beschrieben. Während sich die untersuchten Harze durch hohe Photoreaktivitäten und hohe Monomerumsätze auszeichnen, konnten Untersuchungen der Netzwerkeigenschaften mittels Dynamisch Mechanischer Analyse (DMA), Doppelquantum (DQ) Festkörper NMR Spektroskopie und Photorheologie zeigen, dass diese Photopolymere sehr homogene Netzwerkstrukturen aufweisen, die zu hervorragenden mechanischen Eigenschaften hinsichtlich Modul und Polymerzähigkeit führen. Es wurden außerdem verschiedenen Stabilisatoren untersucht, welche in der Lage sind die Lagerstabilität von Thiol-in Harzen deutlich zu steigern. Außerdem wird gezeigt, dass sich die Degradierbarkeit dieser Polymere durch den Einsatz unterschiedlicher Alkine und Thiole gezielt steuern lässt. In diesem Zusammenhang wird ein silizium-basierendes Thiol als nichtabbaubares Monomer vorgestellt. Neben geringeren Wasseraufnahmen führt dieses zusätzlich zu verbesserten mechanischen Eigenschaften der hergestellten Photopolymere. Durchgeführte 3D Druckexperimente zeigten, dass sich diese Alkinharze in einem DLP Prozess mit sehr hoher Genauigkeit drucken lassen.

Im zweiten Teil dieser Doktorarbeit wird die Synthese und Charakterisierung neuer, alkin-funktionalisierter Typ-I Photoinitiatoren für den Einsatz in Thiol-en und Thiol-in Harzen beschrieben. Ziel war es, die Migration von Photoinitiatoren in biokompatiblen Photopolymeren deutlich zu reduzieren. Hierfür wurden zwei Photoinitiatoren hergestellt und deren Einfluss in den Harzen untersucht und diskutiert. Aufgrund der vielfältigen Eigenschaften der präsentierten Thiol-in Photopolymere (niedrige Zytotoxizität, hohe Photoreaktivität und Monomerumsätze, gute thermomechanische Eigenschaften und Schlagzähigkeiten, gute Druckeigenschaften), zeigen diese ein hohes Potential für den 3D Druck medizinischer Produkte.

# ACKNOWLEDGEMENT

Many people supported me along the way and directly or indirectly contributed to this thesis. First of all, I want to express my gratitude to my parents Elfriede and Wolf-Dieter who have always supported me in every sense for my whole life. Special thanks go to my brother Roland for being there as a friend and for inspiring me in life. I hope there are lots of surfing, skiing and climbing trips ahead of us!

With no doubt, this work would not have been possible without my supervisor, Prof. Thomas Griesser who offered me the opportunity to perform this work at the Christian Doppler Laboratory (CDL) for Functional and Polymer Based Inkjet Inks at the Institute of Chemistry of Polymeric Materials. His motivation, enthusiasm and optimism were inspiring. I want to thank him for his kind support and friendship that has built up over the last years. Additionally, I want to thank the head of the Institute of Chemistry of Polymeric Materials, Prof. Wolfgang Kern.

Next, I want to thank my colleagues from the institute including our secretary Claudia Wieser and Heike Noll for their kind support. Special thanks go to my close colleagues from the CDL and our student assistants, Stefan, Hojabr, Paul and Hannes for their great scientific support, but also for being a great team. It was a lot of fun to work with you guys!

Additional thanks go to Andreas Moser and his supervisor Prof. Gerald Pinter from the Institute of Material Science and Testing of Polymers of the Montanuniversität Leoben, Dr. Santhosh Ayalur-Karunakaran and Dr. Sandra Schlögl from the Polymer Competence Center Leoben GmbH, Dr. Christoph Walkner from the Institute of General and Analytical Chemistry of the Montanuniversität Leoben, Dr. Christian Gorsche and his supervisor Prof. Robert Liska from the Institute of Applied Synthetic Chemistry of the TU Vienna, Robert Gmeiner from Cubicure GmbH, Dr. Dietmar Scheddin from CYTOX biologische Sicherheitsprüfungen, Dr. Josef Spreitz from Aglycon Dr. Spreitz KG, Dr. Petra Kaschnitz and Prof. Gregor Trimmel from the Institute of Chemistry and Technology of Materials of the TU Graz.

Furthermore, I want to thank all my friends from Leoben, Graz, Bludenz, and Vienna, as well as outside of Austria (Sweden, Switzerland, Germany, France and Sierra Leone) for the great times we have had in the last few years.

Financial support by Durst Phototechnik AG, the Christian Doppler Research Association and the Austrian Federal Ministry of Science, Research and Economy (BMWFW) is gratefully acknowledged.

# AFFIDAVIT

I declare in lieu of oath, that I wrote this thesis and performed the associated research myself, using only literature cited in this volume.

Leoben, November 2016

Dipl.-Ing. Andreas Oesterreicher

# INDEX

1	Motivation and outline.....	1
2	Exploring alkyne ethers, alkyne carbonates and new ester-free thiols in thiol-yne derived photopolymers for 3D printing .....	2
2.1	State of the art .....	2
2.2	Results and discussion .....	6
2.2.1	Reactivity of monomer model compounds under physiological conditions .....	6
2.2.2	Synthesis of alkyne monomers.....	7
2.2.3	In-vitro cytotoxicity .....	9
2.2.4	Investigated thiol monomers.....	10
2.2.5	Photoreactivity and Conversion.....	11
2.2.6	Storage Stability .....	15
2.2.6.1	Stability of alkyne ether formulations.....	15
2.2.6.2	Investigation of different stabilizers in alkyne carbonate formulations .....	15
2.2.7	Network structure and thermo-mechanical properties .....	17
2.2.7.1	Alkyne ethers networks .....	17
2.2.7.2	Alkyne carbonates networks.....	19
2.2.7.3	Impact properties of thiol-yne photopolymers .....	22
2.2.7.4	In-depth investigations on the network formation.....	23
2.2.8	Degradation of alkyne carbonates derived photopolymers.....	26
2.2.9	3D printing of tough thiol-yne derived photopolymers .....	27
3	Low Migration Type I Photoinitiators for Thiol-based Resins .....	28
3.1	State of the art .....	28
3.2	Results and Discussion .....	29
3.2.1	Synthesis .....	29
3.2.2	Absorption by UV-vis Spectroscopy .....	30
3.2.3	Photoreactivity .....	31
3.2.4	Migration Studies .....	33

4	Summary .....	35
5	List of Enclosed Publications .....	37
6	Co-Authorship Publications, Patents and Conference Contributions .....	128
6.1	Patents .....	129
6.2	Conference Contributions .....	129
7	APPENDIX .....	131
7.1	List of Abbreviations and Acronyms .....	131
7.2	List of Figures .....	134
7.3	List of Tables .....	136
7.4	List of Schemes .....	136
8	References .....	137
9	Curriculum Vitae .....	142

# 1 Motivation and outline

Photopolymers have evolved into a rapidly progressing research field in the last years, mainly driven by the demand of high-performance materials for UV-based additive manufacturing technology (AMT) processes.<sup>1,2</sup> Advances are being expected especially in the healthcare industry as the production of biomedical devices by means of AMTs offers the possibility of patient-specific customization of individually shaped parts, reaching from surgical or dental implants to prosthetics. 3D images can be directly obtained from CT, X-ray or MRI scans which significantly reduces costs, production time and inventory.<sup>3,4,5,6</sup> The pallet of 3D printable biomaterials includes metals,<sup>7,8</sup> ceramics<sup>8,9,10</sup> and polymers,<sup>11,12,2</sup> however, each type of material has its limitations in terms of its specific material and mechanical properties, processing methods, chemical properties, cell-material interactions and biocompatibility.<sup>13</sup> From the UV-based 3D printing technologies, especially stereolithography (SLA) and digital light processing (DLP) are promising technologies for the processing of biomaterials as they offer several advantages, such as fast and precise fabrication with very high feature resolutions up to 10  $\mu\text{m}$ , enabling the production of medical parts with complex geometries, smooth surface finish and variable mechanical properties.<sup>14,15,16,17</sup> However, one major disadvantage of these technologies is the limited availability of biocompatible, photocurable resins.<sup>13</sup> Furthermore the mechanical properties of common photopolymers are subject to improvement for many end-use applications.<sup>18</sup>

In this contrast, the present thesis focuses on the development of new biocompatible, photoreactive resin systems based on the radical mediated reaction of alkyne and thiol monomers (thiol-yne reaction). In the first part, two classes of photopolymers, alkyne ethers and alkyne carbonates are presented which show low cytotoxicity, as well as high photoreactivities and conversions in combination with different commercially available, but also a newly synthesized thiol under UV curing conditions. Specific focus was set on the network structure and the mechanical properties of derived photopolymers and their degradation behavior in acidic or alkaline medium. In the second part new alkyne-functionalized photoinitiators were synthesized and their performance in thiol-based resins was investigated. Particular focus was set on their photoreactivity in a biocompatible thiol-ene resin and their migration behavior.

Covering these aspects this thesis gives insights into the challenges of the development of biocompatible, photocurable materials and paves the way towards the 3D printing of medical devices.



## 2 Exploring alkyne ethers, alkyne carbonates and ester-free thiols in thiol-yne derived photopolymers for 3D printing

*The following results have been published in peer-reviewed journals or have been submitted to journals which are listed in chapter 5 of this thesis.*<sup>19,20,21,22,23</sup>

### 2.1 State of the art

The concept of photopolymerization which describes structural changes of monomers, oligomers or polymers upon light exposure, is hardly new. Thus, photosensitive materials that harden by sunlight-induced crosslinking have already been used in ancient times for mummification or for caulking of wooden ships, known under Judean asphalt or Syrian bitumen.<sup>24</sup> Nowadays, a multitude of photopolymers can be found in industrial products like coatings, adhesives, paints, ink-jet inks, photoresists, or optical materials.<sup>25,26,27</sup> Especially in the last years, photopolymers gained increasing importance for UV-based AMT processes, such as lithography based 3D printing or 3D ink-jet printing.<sup>11</sup>

It was already in the early 1980s when Chuck Hull invented the first rapid prototyping method, known as stereolithography (SLA).<sup>4,28</sup> This layer-by-layer based AMT underlies the principle of photopolymerization, as a liquid, photoreactive resin solidifies upon irradiation with UV light by a computer-controlled laser beam (direct laser writing) or a digital light projector (DLP) creating a pattern on the surface of a resin. The solidified layer is moved on the building platform in order to recoat a fresh layer of resin which solidifies by a subsequent light-induced patterning step. Repeating these steps allows the construction of a three-dimensional object.<sup>29</sup> The object is washed after the completed structuring process to remove excess resin and it is post-cured afterward by UV light to increase the rather low monomer conversion during the patterning process and therefore, improve the mechanical properties of the built device.

The device geometry and shape are defined by a CAD file which can be directly conducted from 3D imaging data as tomographic or magnet resonance scans, making rapid prototyping also interesting for the individualized fabrication of medical devices.<sup>5,30</sup> The design is usually transferred into an STL file which is virtually sliced into layers of the thickness of the layer-by-layer fabrication process, therefore allowing easy data processing.<sup>29</sup>

3D printing technologies as SLA and DLP represent a huge potential for the health care industry. While ear-shaped hearing aids or dental implantation drilling guides printed by lithographic processes are already well-established processes,<sup>31,3</sup> the fabrication of patient-specific implants or prosthetics by UV-based AMTs are future challenges to overcome.<sup>29</sup> Especially due to its high printing resolution, bone replacement materials (tissue engineering scaffolds), where porous implants with pore sizes between 50 – 1000  $\mu\text{m}$  are known for optimal bone ingrowth,<sup>32,33,34</sup> are challenging applications for lithographic 3D printing processes.<sup>29,35,36</sup>

Many of the nowadays used photocurable resins for SLA and DLP are based on commercial, multifunctional acrylate or methacrylate monomers.<sup>18</sup> Especially methacrylates are being favored for lithographic 3D printing processes due to their lower cytotoxicity and higher heat resistance compared to acrylates.<sup>37</sup> However, the requirements on the material properties of AMT processed polymers differ from conventional photopolymers. Especially the mechanical performance, particularly the material toughness at sufficiently high heat deflection temperatures become essential key parameters for the production of 3D processed high-performance materials.<sup>18,38</sup> Although common resins based on (meth)acrylates show fast curing rates and excellent storage behavior, they are associated with brittleness of the manufactured parts which is a result of an inhomogeneous network formation during the radical mediated chain-growth mechanism and due to its low monomer conversion at the gel point, leading to internal shrinkage stress.<sup>37,18,39</sup>

Another drawback of (meth)acrylates, especially for the production of medical devices is their rather high irritancy or even monomer cytotoxicity as they can serve as Michael acceptors for thiols and amines and therefore can interact with human proteins or DNA.<sup>40,41</sup> In connection with rather low double bond conversions of reportedly 60 - 90%, cytotoxic residual monomers that remain in the cured polymer matrix state a health risk. Furthermore, methacrylates are known to form of high molecular weight (meth)acrylic acid upon hydrolytic degradation which limits their applicability for the production of implants or scaffolds.<sup>42</sup> Elevated concentrations of acidic moieties can lead to a local decrease in the pH in the human body, which can cause inflammatory reactions or tissue necrosis in the worst case.<sup>43,44</sup>

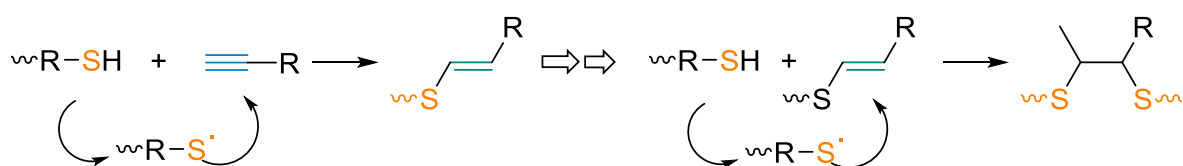
To overcome those challenges, different approaches can be found in the literature that focus on alternative photocurable systems to (meth)acrylates. Already in 2002, Matsuda et al. reported about biodegradable and biocompatible needles produced of poly( $\epsilon$ -caprolactone-co-trimethylene carbonate) resins by traditional stereolithography.<sup>45</sup> Further very recent studies have investigated vinyl carbonate, -carbamates and -esters demonstrating their high biocompatibility under in-vitro and in-vivo tests.<sup>46,47,48</sup> Their mechanical properties,

mentionable their impact properties can be significantly improved by modified backbone structures.<sup>49</sup> As one major disadvantage they show rather low reactivity which, however, can be enhanced by the addition of multifunctional thiols.<sup>33</sup> Thereby, higher monomer conversion can be reached, which is, however, at the expense of their mechanical performance. Such thiol-ene systems feature high monomer conversions at the gel point due to their step-growth mechanism which leads to homogeneously crosslinked networks with low shrinkage stress compared to conventional (meth)acrylates.<sup>50,51,52</sup> Thiol-ene photopolymerization is not inhibited by oxygen<sup>53,54</sup> and due to the low cytotoxicity of conventional thiols, several concepts for the development of medical materials are based on thiol chemistry.<sup>55,56,57,58,59</sup>

Major drawbacks of thiol chemistry are the distinct odor of many of the commercially available thiols and the rather low resin stability.<sup>51</sup> Moreover, thiol-ene derived polymers are rather soft as their glass transition temperatures are often not higher than room temperature, with only a few exceptions reported very recently.<sup>57,60</sup> This fact can be attributed to the rather flexible thioether linkages, but also to their rather low crosslink density.<sup>56,42,61</sup> Also the presence of the ester groups originating from the commonly used low-odor, multifunctional thiols, the mercapto propionic acid or mercapto acetic acid derivatives, reduces the modulus and also leads to hydrolytic degradation of derived photopolymers under acidic or alkaline conditions.<sup>56,42,61</sup> Additionally, water absorption is favored due to the polarity of the ester group, significantly reducing the mechanical performance of thiol-ene photopolymers upon water storage.<sup>56,62</sup> As the formed thioether bond in thiol-derived photopolymers is rather stable, the hydrolytic stability of derived photopolymers is expected to significantly increase when thiols without hydrolytic sensitive groups (e.g. ester groups) are used. Nevertheless, only a few reports are available that deal with new ester-free thiols and their impact on the polymeric properties of thiol-ene photopolymers.<sup>63,57,62</sup>

To improve the thermo-mechanical properties of thiol-ene photopolymers one strategy is the use of rigid ene structures as for example triallyl-1,3,5-triazine,2,4,6(1H,3H,5H)trione (TATT), norbornene derivatives or maleimides.<sup>57,62,60,64</sup> Another strategy is to improve the overall crosslink density of photopolymers. This can be achieved by thiol-yne chemistry which describes the radical reaction of an alkyne with two thiol functional groups.<sup>65</sup> Herein, each yne moiety reacts with a thiyl radical in a first step under formation of a vinyl sulfide intermediate which subsequently undergoes a reaction with a second thiyl moiety to form a 1,2-disubstituted adduct as depicted in Scheme 1.<sup>66</sup> The reaction of the thiyl radicals with the vinyl sulfide intermediate proceeds ~3 times faster than with the alkyne moiety in the first step.<sup>65</sup> Using multifunctional alkynes and thiols, highly crosslinked polymers can be obtained that profit from the beneficial features of thiol click chemistry. Thus, it is mostly unaffected by

oxygen and humidity and proceeds at high reaction rates to high conversions, while forming highly homogeneous networks.<sup>67,68,59</sup> Thiol-yne derived photopolymers offer an about six times higher crosslink density than their analogous thiol-ene species, which significantly increases their glass transitions temperatures far above room temperature.<sup>65</sup> Investigation on the relative reactivity of alkyne monomers revealed that terminal alkynes show the highest reactivity towards thiols, followed by propargyl esters and propargyl ethers and internal alkynes while cyclooctyne, methyl propargylamine and ethyl propiolate did show this typical bireactive character.<sup>69</sup>



Scheme 1: Radical mediated thiol-yne reaction.

Generally, internal alkynes have shown low cytotoxicity in previous studies and seem to be promising candidates for the fabrication of medical materials.<sup>70</sup> Thiol-yne resins showed good printability with high accuracy under direct laser writing techniques and also offer the possibility of surface post-modifications, which is another advantage for medical devices.<sup>71,72</sup>

Inspired by the well-described concept of thiol-yne photopolymerization, we have therefore investigated alkyne carbonates and alkyne ethers as potential candidates for the UV-based AMT fabrication of medical devices. Also, a new ester-free thiol is presented in combination with these alkynes. This thesis describes our findings that have also been published in peer-reviewed journals.<sup>20,19,21,22</sup>

## 2.2 Results and discussion

### 2.2.1 Reactivity of monomer model compounds under physiological conditions

In an initial study, the reactivity of (meth)acrylate and alkyne model compounds under simulated physiological conditions were investigated. (Meth)acrylates are known to interact with human DNA via Michael addition reactions with thiols and amino groups.<sup>41</sup> Especially the electron density of the Michael acceptors determines the reactivity towards its donor.<sup>73,74</sup> The lower electron density of acrylates compared to methacrylates, therefore, explains their generally higher reactivity, hence higher cytotoxicity. While reportedly, terminal alkynes without electron drawing neighboring groups are known to be mostly inert to Michael reactions, even under basic conditions,<sup>75</sup> we investigated the reactivity of water-soluble model compounds (Figure 1, left) in buffered D<sub>2</sub>O at 37 °C by <sup>1</sup>H-NMR. It was observed that especially 2-hydroxyethyl acrylate (HEA), but also 2-hydroxyethyl methacrylate (HEMA) reacted very fast with the thiol compound, 2-(2-methoxyethoxy)ethanethiol (MTE), forming the expected Michael adduct (Figure 1, right) The reaction with ethanolamine hydrochloride (ETAHC) could only be observed for HEA in the given time frame. Most importantly, no reaction occurred for 3-butyne-1-ol (BuOH) with any of the two Michael donors, underlining previously observed results in the literature and expecting a lower cytotoxicity for this type of monomers.<sup>75</sup>

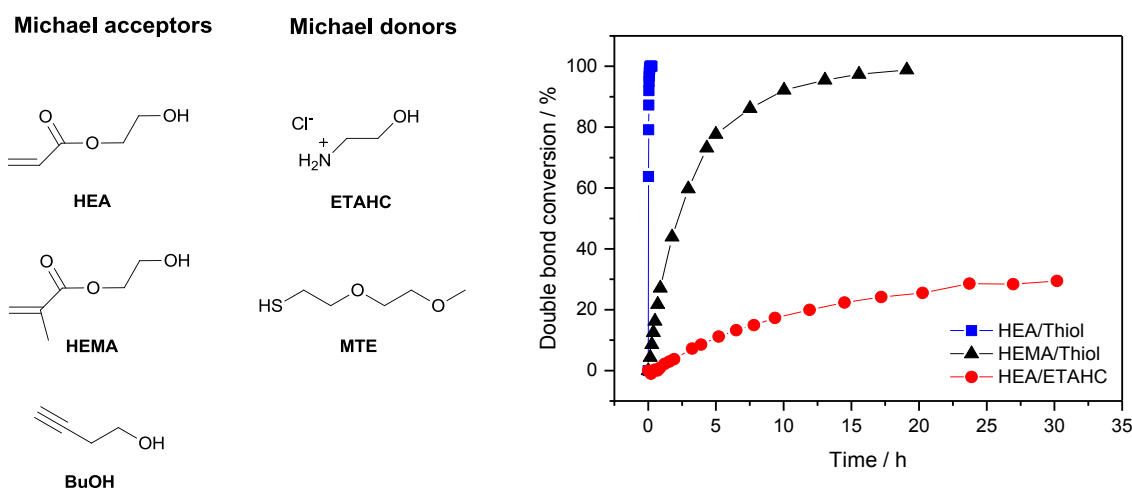
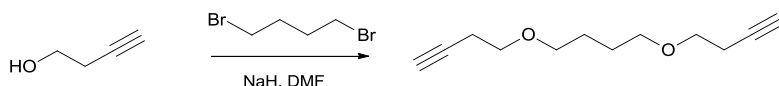


Figure 1: Left: Water-soluble model compounds [HEA = 2-hydroxyethyl acrylate, HEMA = 2-hydroxymethyl acrylate, BuOH = 3-butyne-1-ol, ETAHC = ethanolamine hydrochloride, MTE = 2-(2-methoxyethoxy)ethanethiol]. Right: Double bond conversion of HEA/MTE (squares), HEMA/MTE (triangle) and HEA/ETAHC (circles) under simulated physiological conditions.

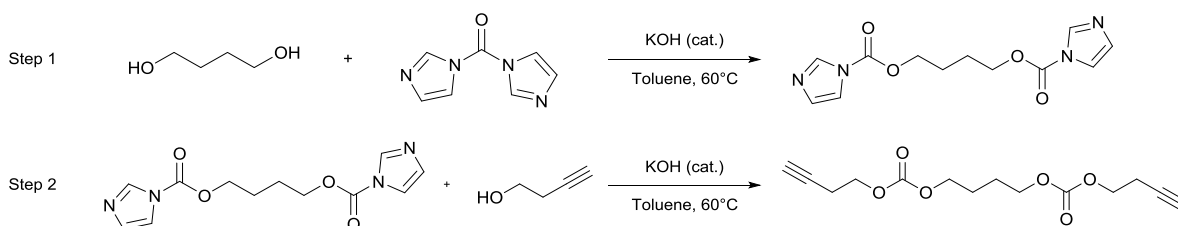
## 2.2.2 Synthesis of alkyne monomers

Two different types of monomers have been synthesized in straightforward procedures. Firstly, the synthesis of alkyne ethers was carried out via the well-described Williamson ether synthesis.<sup>76</sup> Hereby, propargyl ether derivatives were obtained by reacting sodium hydride with the corresponding hydroxyl functionalized backbone structure to its sodium alkoxylate which was further converted with propargyl bromide to the desired propargyl ether derivatives in good yields.<sup>19</sup> This reaction analogy failed for the synthesis of but-1-yn-4-yl ethers as an isomerization of the alkyne group from the terminal alkyne to its corresponding 2-yne occurred. Therefore, 1-but-yn-3-ol was converted with sodium hydride to its alkoxylate and further reacted with the 1,4-dibromobutane to the desired product as described in the literature (see Scheme 2) in moderate yields.<sup>77</sup>



Scheme 2: Synthesis of but-1-yn-4-yl ethers.

Alkyne carbonates were synthesized in a KOH-catalyzed two-step reaction of alcohols with 1,1'-carbonyldiimidazole (CDI) in good to very high yields as depicted in Scheme 3.<sup>20,78</sup> Di(but-1-yn-4-yl)carbonate (DBC), which was obtained in a single-step reaction of CDI using an excess of BuOH even showed quantitative conversion.

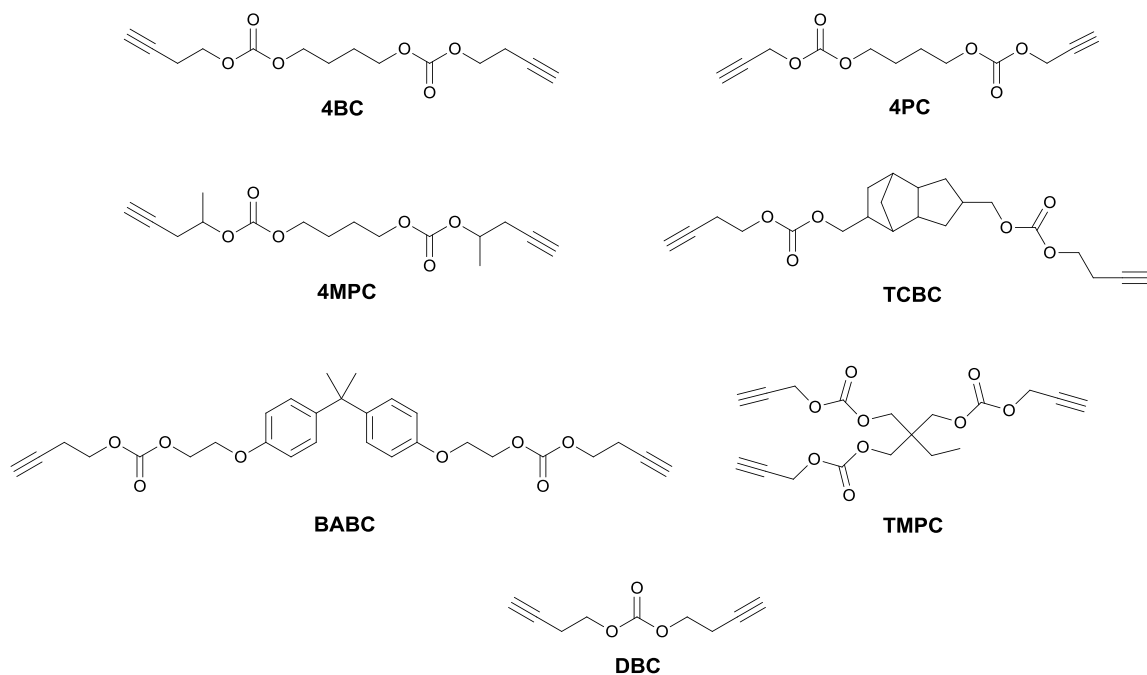


Scheme 3: Synthesis of alkyne carbonates.

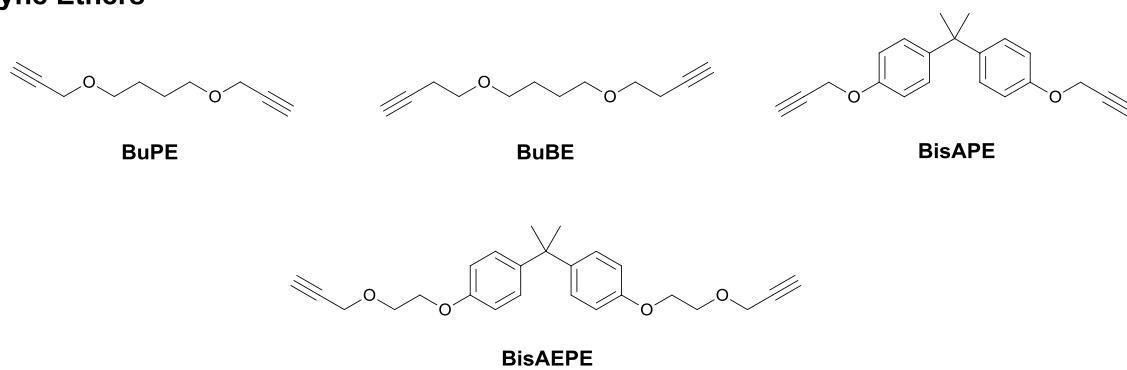
In general, all alkyne ethers and carbonates were synthesized from commercially available hydroxyl functionalized backbones with exception of BisAEPE and BABC. Here the backbone molecule, 2,2-bis[4-(2-hydroxy)ethoxyphenyl]propane was obtained by the reaction of bisphenol A with ethylene carbonate as described in the literature.<sup>57</sup> This backbone was then converted to BisAEPE via the described Williamson ether synthesis or to

BABC according to Scheme 3. The synthesized alkyne ethers and carbonates are listed in Scheme 4. The  $^1\text{H}$ - and  $^{13}\text{C}$ -NMR spectra of all compounds were in good agreement with the proposed structures.

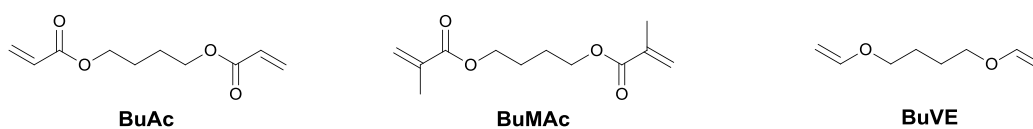
### Alkyne Carbonates



### Alkyne Ethers



### References



Scheme 4: Structures of the investigated alkyne monomers including reference substances.

### 2.2.3 In-vitro cytotoxicity

Not only the unsaturated polymerizable moiety and its reactivity towards thio- and aza-Michael donors is responsible for the cytotoxicity of photoactive monomers, but also the spacer group of these building blocks influences their cytotoxicity. As UV curable resins contain certain amounts of leachable residual monomers, the evaluation of monomer cytotoxicity is very important for the fabrication of biomedical applications. Due to the fact that thiols have shown low cytotoxicity as Mautner et al. reported in the literature,<sup>49</sup> the focus of the cytotoxicity test was set on alkyne monomers.

For that reason the cytotoxic potential of the synthesized alkyne ether and carbonate monomers with aliphatic C4 spacers and DBC, as well as tricyclo[5.2.1.0<sup>2,6</sup>]decane-4,8-dimethanol dibut-3-yn-1-yl carbonate (TCBC), which was used in 3D printing experiments (vide infra) was determined by in-vitro tests using L929 mouse fibroblast cells (due to ISO 10993-5:2009) and compared to the cytotoxicity of 1,4-butanediol diacrylate (BuAc) and 1,4-butanediol dimethacrylate (BuMAc) serving as reference compounds. The cells were incubated in a defined media with increasing concentrations of each monomer in DMSO, respectively, for 48 h at 37 °C. After an alkaline lysis step the cell protein concentration was determined via the Bradford method. The extrapolated concentration of which the half of the cells remained alive compared to the negative control (the cell culture medium) was assessed as the cell viability (EC50). The EC50 values of several investigated alkynes are listed in Table 1.

Table 1: EC50 values obtained from cytotoxicity tests.

Monomer	Alkyne ethers		Alkyne carbonates					References	
	BuPE	BuBE	4MPC	4PC	4BC	TCBC	DBC	BuAc	BuMAc
EC50 / mM	3	2	10.0	0.55	2.0	2.4	1.6	< 0.16	< 0.16

Apparently, cells show much higher tolerance of the investigated alkynes, compared to the reference substances BuAc and BuMAc, which is reflected by at least the factor of three and much higher EC50 values. As an example, the detailed test results of BuAc and BuBE depicted in Figure 2 visualize the difference of their cytotoxic behavior. Here, the direct dependency of the cell protein concentration and the applied test concentration are shown. While the medium served as negative control, triton x100 was used as the cytotoxic positive control. Compared to BuBE, BuAc appears to be highly cytotoxicity even at the lowest tested



concentration of 0.16 mM. The obtained results reveal the superiority of alkyne ethers and carbonates in terms of monomer cytotoxicity compared to (meth)acrylates.

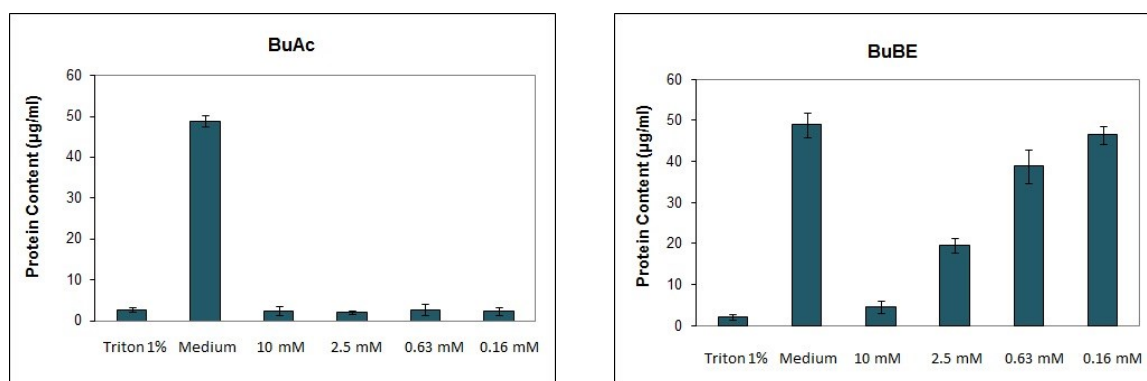
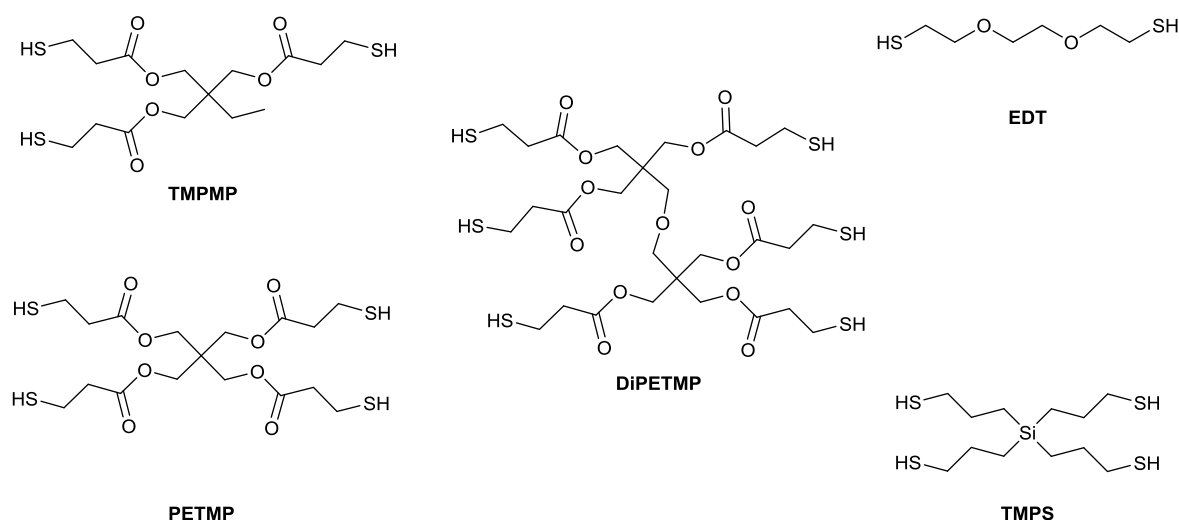


Figure 2: Test results of in-vitro cytotoxicity tests.

## 2.2.4 Investigated thiol monomers

Thiol-yne resins were formulated using the commercially available 3-mercaptopropionic acid derivatives, trimethylolpropanetris(3-mercaptopropionat) (TMPMP), pentaerythritoltetra(3-mercaptopropionat) (PETMP) and dipentaerythritolhexa(3-mercaptopropionate) (DiPETMP). Additionally, the commercially available 2,2'-(ethylenedioxy)diethanethiol (EDT) was used. Furthermore, silanetetrayltetrakis(propane-1-thiol) (TMPS) was synthesized via the radically induced thiol-ene reaction of the alkene precursor, tetraallyl silane with thioacetic acid. The intermediate thioester generated by this reaction was hydrolyzed under alkaline conditions to yield the corresponding thiol TMPS. The investigated thiols are depicted in Scheme 5.



Scheme 5: Chemical structures of investigated thiols.

The characterization of the physiochemical properties of the newly synthesized thiol TMPS revealed a slightly lower density and surface tension, but a much lower viscosity compared to PETMP as shown in Table 2. This makes this thiol an interesting candidate for the 3D printing industry but also for the coating industry.

Table 2: Density ( $\rho$ ), surface tension ( $\sigma$ ) and viscosity ( $\eta$ ) of TMPS and PETMP.

Thiol Monomer	$\rho / \text{g} \cdot \text{cm}^{-3}$	$\sigma / \text{mN} \cdot \text{m}^{-1}$	$\eta (25^\circ\text{C}) / \text{mPa} \cdot \text{s}$
TMPS	1.10	43.9	49.7
PETMP	1.28	47.9	450.8

### 2.2.5 Photoreactivity and Conversion

For the development of biomedical materials two parameters, the curing rate and the conversion of UV curable monomers are important as they determine the 3D printing speed and the amount of leachable monomers in the built medical device. Photo Differential Scanning Calorimetry (photo-DSC) is a unique method that gives access to kinetic parameters of the photoactive resins. The hereby evaluated reaction time  $t_{\text{max}}$ , which is the time to reach the maximum of polymerization enthalpy, in combination with the peak shape reveals information about the overall photoreactivity.

Figure 3 (left) displays the photo-DSC plots of the investigated thiol-yne formulations of alkyne carbonates bearing the same C4 spacer and the reference substances BuAc and BuMAc. It is shown that the thiol-yne resins offer photoreactivities that are comparable to the corresponding acrylate while only moderate curing performance were observed for the reference methacrylate BuMAc. The  $t_{\text{max}}$  values of investigated alkyne ethers and carbonates are summarized in Table 3. Comparison of the propargyl ether (4PE) with its analogous but-1-yn-4-yl ether (4BE) reveals a significant difference in the curing performance which can be attributed to the additional  $\text{CH}_2$  group, reducing the inductive effect of the neighboring ether group on the terminal alkyne. Therefore, the overall photoreaction for 4BE is accelerated which is indicated by its low  $t_{\text{max}}$  value that is comparable to the reference acrylate. The same retardation effect can be seen in Figure 3 (left) for alkyne carbonates by comparing the propargyl derivative 4PC with the but-1-yn-4-yl derivative 4BC, thus making but-1-yn-4-yl derivative interesting candidates for fast curing 3D printing resins comparable to acrylates.

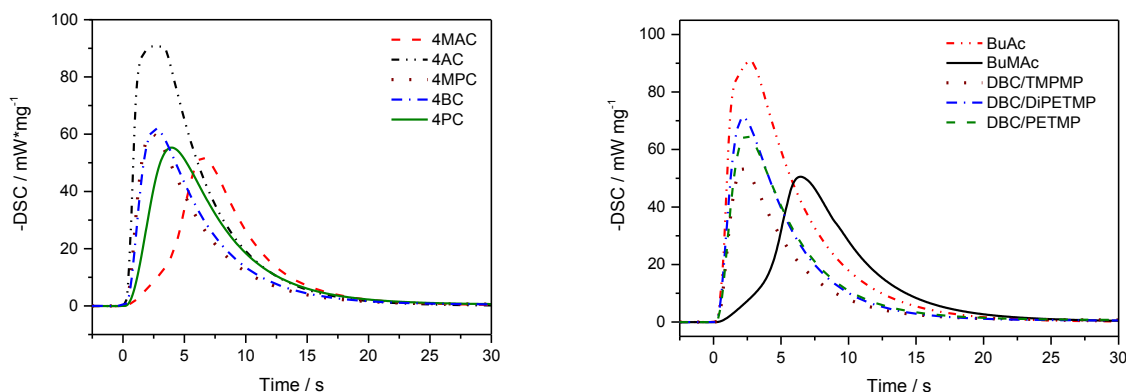


Figure 3: Photo-DSC plots of investigated monomers. Left: 4PC (solid), 4BC (chain dotted), 4MPC (dotted), BuAc (chain double dotted) and BuMAc (dashed). Right: BuAc (chain double dotted), BuMAc (solid), DBC/TMPMP (dotted), DBC/DiPETMP (chain dotted), DBC/PETMP (dashed). Light starts at 0 s.

Figure 3 (right) shows the plots of DBC in combination with different thiols and the references. As it is shown, the curing speed  $t_{\max}$  is mostly independent on the applied thiol. In general, the photoreactivity of monomers with higher molecular weight decreases as it is shown in Table 3. This can be attributed to their higher monomer viscosity, reducing the monomer mobility during the photoreaction which also leads to lower monomer conversions (vide infra).

Table 3: Summary of photo-DSC ( $t_{\max}$ ) and RT-FT-IR measurements (conversion) of alkyne monomers in combination with thiols, including reference samples (BuAc and BuMAc).

	Monomer	$t_{\max}$ / s	Conversion / %
Alkyne Ethers	BuPE	5.2 <sup>a</sup>	94 <sup>a</sup>
	BuBE	2.3 <sup>a</sup>	99 <sup>a</sup>
	BisAEPE	6.2 <sup>a</sup>	65 <sup>b</sup> (98) <sup>b,c</sup>
	BisAPE	8.1 <sup>a</sup>	62 <sup>b</sup> (92) <sup>b,c</sup>
Ref.	BuMAc	6.7	74
	BuAc	1.8	79
Alkyne Carbonates	4PC	3.8 <sup>d</sup>	98 <sup>a</sup>
	4BC	2.8 <sup>d</sup>	98 <sup>a</sup>
	4MPC	2.5 <sup>d</sup>	96 <sup>a</sup>
	TCBC	2.6 <sup>d</sup>	94 <sup>a</sup>
	TMPC	3.7 <sup>d</sup>	91 <sup>a</sup>
	BABC	3.5 <sup>d</sup>	84 <sup>a</sup>

<sup>a</sup> Corresponds to a formulation with a stoichiometric amount of TMPMP

<sup>b</sup> Corresponds to a formulation with a stoichiometric amount of TMPS

<sup>c</sup> Measured after post-curing at 100 °C

<sup>d</sup> Corresponds to a formulation with a stoichiometric amount of PETMP

The findings of the photo-DSC measurements of the alkyne ethers was confirmed by real-time Fourier Transformed Infrared Spectroscopy (FT-IR) measurements which were used to observe the conversion of the alkyne triple bonds, the double bonds of the reference meth(acrylates) and the thiol groups during illumination. As shown in Figure 4 (right), BuBE/TMPMP outperforms BuPE/TMPMP in terms of photoreactivity, also leading to higher overall conversions. Mentionable the conversion of the thiol group happens simultaneously with the consumption of the alkyne bond, revealing the absence of any side reactions. Thus, the conversion after 2 min of illumination is almost quantitative for BuBE as shown in Table 3, while BuPE reaches a high conversion of 94%. In contrast, the references show only a conversion of 79% for the acrylate, BuAc and only 75% for the methacrylate, BuMAc, revealing the superiority of alkyne ether monomers in terms of monomer conversion.

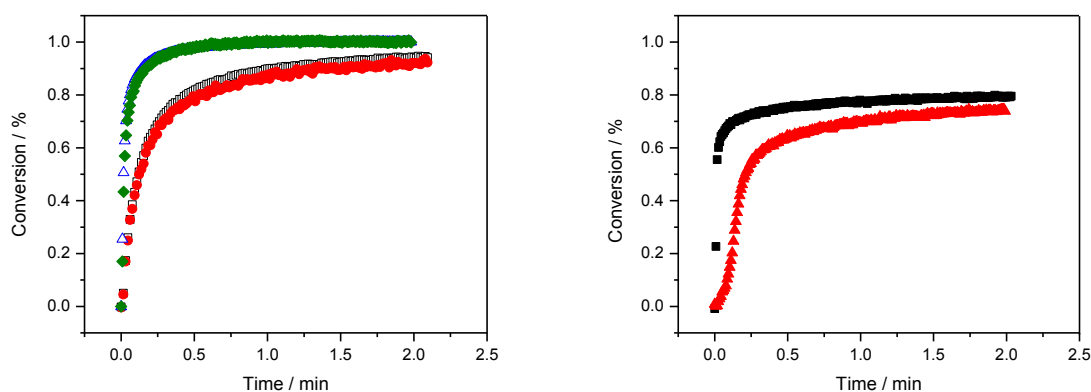


Figure 4: Real-time FT-IR measurements: Conversion of alkyne and thiol moieties. Left: BuBE (open triangle) / TMPMP (diamond), BuPE (open square) / TMPMP (circle). Right: Conversion of (meth)acrylates. Right: BuAc (square) and BuMAc (triangle).

Similar high conversion rates were observed for alkyne carbonates, which also show much higher conversions compared to the reference acrylate and methacrylate as it is shown in Figure 5 and Table 3. As already mentioned, generally lower conversions were observed for the alkyne monomers of higher molecular weight (TMPC, TCBC, BABC, BisAEPE or BisAPE). This fact is explained by their higher monomer viscosity reducing the overall monomer mobility during the curing process (e.g.: BuPE = 4.7 mPa\*s v.s. BisAEPE = 949 mPa\*s; 4PE = 44 mPa\*s v.s. TCBE = 2330 mPa\*s).

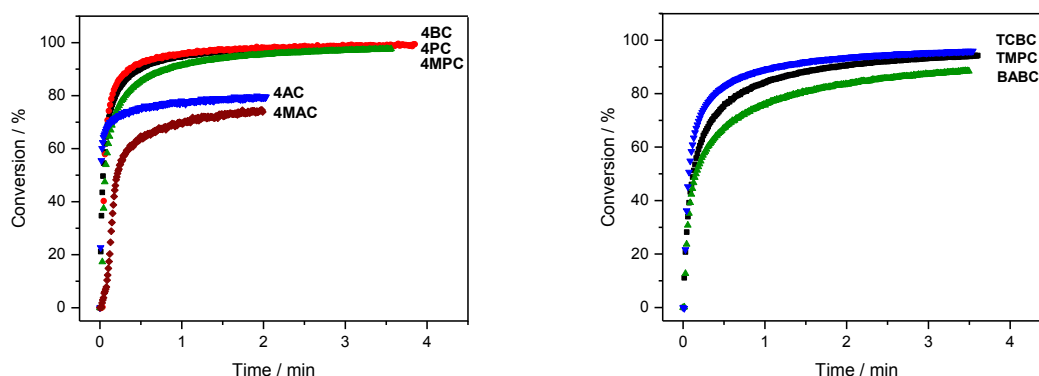


Figure 5: Triple bond (alkyne carbonates) and double bond ((meth)acrylates) conversion versus illumination time.

Nevertheless, it was demonstrated that it is possible to increase the overall monomer conversion of thiol-yne networks by post-illumination in combination with heating the sample above its  $T_g$  as it is demonstrated for formulations containing bisphenol A derivatives (see Figure 6). Hereby it was possible to improve the monomer conversion from 62% to 92% for BisAPE and 65% to 95% for BisAEPE while significantly reducing the amount of leachable monomers. For these tests, the thiol TMPS was used instead of TMPMP and PETMP in order to improve the network properties as this type of ester-free thiol is known to provide hydrolytically stable networks with good mechanical properties, even after water storage (vide infra).<sup>62,22</sup>

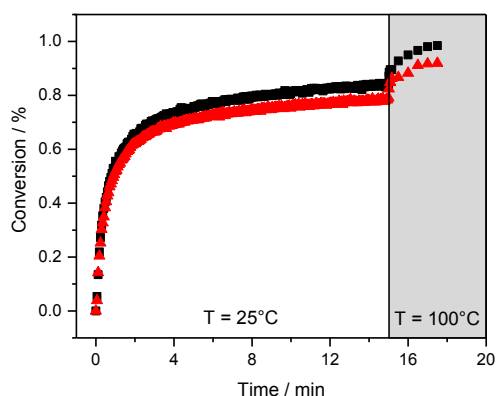


Figure 6: Conversion of the alkyne monomers BisAEPE (square) and BisAPE (triangle) in alkyne/TMPS formulations versus illumination time including thermal post-curing.

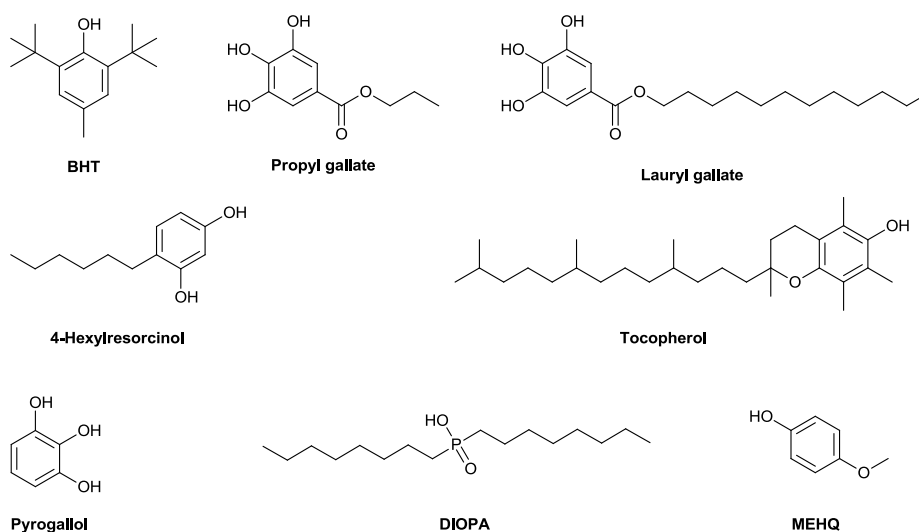
## 2.2.6 Storage Stability

### 2.2.6.1 Stability of alkyne ether formulations

High monomer reactivity raises the question of shelf-life stability, as thiol-based formulations are known for their rather poor storage stability.<sup>51</sup> It was recently reported that pyrogallol in combination with appropriate phosphonic acids sufficiently suppresses occurring dark reactions in thiol-based resins.<sup>79</sup> Therefore, accelerated stability tests at 50 °C, monitoring the resin viscosity, were carried out with BuBE/TMPMP and BuVE/TMPMP serving as a reference. While BuVE/TMPMP containing 0.5 wt% of pyrogallol and 2 wt% of decylphosphonic acid as stabilizers, completely gelled after 4 h, BuBE/TMPMP, containing the same stabilizers, showed only a viscosity increase of 22% after one week of storage under the same conditions. The higher stability of alkyne monomers can be attributed to their absent reactivity towards Michael donors which is another advantage of thiol-yne systems.

### 2.2.6.2 Investigation of different stabilizers in alkyne carbonate formulations

Additionally, different stabilizers were tested in a DBC/PETMP formulation. Due to toxicological aspects stabilizers have been chosen that can also be found in the food industry including propyl gallate,<sup>80</sup> lauryl gallate,<sup>81</sup> 4-hexylresorcinol,<sup>82</sup>  $\alpha$ -tocopherol<sup>83</sup> and butylated hydroxytoluene (BHT)<sup>84</sup> (see Scheme 6).



Scheme 6: Investigated stabilizers.

To compare their stabilization efficiency in a DBC/PETMP formulation (containing concentrations of 0.25 wt% or 0.5 wt% stabilizer) the viscosity of each formulation was monitored on a cone-plate rheometer under continuous rotation at 50 °C (accelerated stability tests). The stabilizer efficiency was compared to the hetero-synergistic system pyrogallol/diisooctylphosphinic acid (DIOPA) and hydroquinone monomethyl ether (MEHQ). For comparison, the viscosity increase after 20 h is depicted in Table 4.

Table 4: Viscosity increase after 20 h of investigated stabilizers.

	<b>Concentration / wt%</b>	<b>Viscosity increase after 20 h / %</b>
<b>non stabilized</b>	-	278
<b>Propyl gallate</b>	0.25	121
<b>Propyl gallate</b>	0.5	76
<b>Lauryl gallate</b>	0.25	42
<b>Lauryl gallate</b>	0.5	38
<b>4-Hexylresorcinol</b>	0.5	80
<b>BHT</b>	0.5	49
<b>α-Tocopherol</b>	0.5	995
<b>MEHQ</b>	0.5	36
<b>Pyrogallol</b>	0.5	43
<b>Pyrogallol / DIOPA</b>	0.5 / 2.5	42

While the viscosity of the non-stabilized formulation increased by 278%, the investigated additives showed significant stabilizing effects with exception of α-tocopherol which lead to an viscosity increase by 995%. Lauryl gallate (+38% for 0.5 wt% and +42% for 0.25 wt%) clearly showed the best stabilizing effect at both investigated concentrations, comparable to the reference MEHQ (+36% for 0.5 wt%) and pyrogallol (+43% for 0.5 wt%). The effect was slightly less pronounced for BHT (+49% for 0.5 wt%), while decreased stability could be observed by propyl gallate and 4-hexylresorcinol. Mentionable, the acidic co-stabilizer did not show any beneficial effect in combination with pyrogallol.

## 2.2.7 Network structure and thermo-mechanical properties

### 2.2.7.1 Alkyne ethers networks

Thiol-ene derived photopolymers from vinyl ethers are known for their good biocompatibility, however, one major limitation is their poor mechanical properties due to their low glass transition temperatures ( $T_g$ ) compared to thiol-yne networks.<sup>85,65</sup> For polymers intended for hard tissue engineering the glass transition temperature has to be above body temperature, thus, the polymer has to be in its glassy state to provide desired mechanical properties. Major factors influencing the  $T_g$  are the structure of the polymer backbone and the crosslink density. Dynamic mechanical analysis (DMA) measures the temperature dependent storage and loss moduli and therefore gives access to the glass transition temperature. However, getting detailed information about the crosslink density is much more difficult. For slightly crosslinked polymers equilibrium swelling is reported,<sup>86,87,88</sup> while homogenous networks can be studied by correlating the network density with the  $T_g$  and the storage modulus in the rubbery state.<sup>65</sup>

However, to get quantitative access to the network density and also the fraction of non-network-bound chains (e.g. residual monomers, photoinitiators or their cleavage products), double quantum (DQ) solid state NMR represents a unique and versatile method.<sup>89,90</sup> Hereby the residual dipolar couplings ( $D_{res}$ ) of neighboring  $^1H$ - $^1H$  pairs are measured which describe the orientational anisotropy of polymeric chains caused by restricted motion in the polymer, resulting from e.g. crosslinks.  $D_{res}$  is, therefore, direct proportional to the crosslink density. The measuring temperature has to be more than 50°C above the  $T_g$ , enabling unrestricted motion of polymeric segments, thus avoiding artifacts by reducing their conformal space.<sup>91</sup> Using appropriate pulse sequences and fitting parameters for the resulting build-up curve (e.g. Gaussian fit, second momentum approximation),<sup>92</sup>  $D_{res}$  and the defect fraction (DF), describing non-network chains can be obtained.

For a better understanding of the network behavior of thiol-yne photopolymers, DQ NMR was used to compare the network density of a thiol-ene derived polymer with thiol-yne derived polymers based on the same backbone structure. Therefore 1,4-butanediol divinyl ether (BuVE) was compared with BuPE and BuBE in combination with TMPS. Comparison of the  $D_{res}$  values in Table 5 shows that the crosslink density of thiol-yne derived photopolymers is six-times higher compared to thiol-ene photopolymers. This confirms the observations of Fairbanks et al.<sup>65</sup> The fraction of non-network chains is in accordance with the expected



amount and can be explained by residual photoinitiator or its fragments and residual, unreacted monomers in the sample.

Table 5: Analysis of the normalized DQ curves obtained for the different samples at 100 °C.

Sample	$D_{res}/2\pi$ / kHz	$\sigma_{res}/2\pi$ / kHz	non-network chains / %
BuBE/TMPS	9.0	1.4	4.3
BuPE/TMPS	8.4	2.0	4.6
BuVE/TMPS (Gaussian distribution)	1.4	1.3	2.5

The much higher crosslink density of thiol-yne derived photopolymers results in a higher  $T_g$  and thus, in an improvement of their mechanical properties as it is confirmed by DMA measurements. While BuVE/TMPS exhibits a  $T_g$  of only -35 °C, its analogous alkyne ethers BuPE/TMPS and BuBE/TMPS show  $T_g$ s between 34 - 36 °C as it is shown in Table 6.

Table 6: Results of DMA measurements of alkyne ethers.

Monomer	$T_g$ / °C	$E'$ at 37 °C / MPa	FWHM / °C
BuVE	-35±0 <sup>b</sup>	17±1 <sup>b</sup>	10±0 <sup>b</sup>
BuMAc	50±38	1650±20	-
BuAc	80±6	1420±30	-
BuPE	34±1 <sup>b</sup>	255±30 <sup>b</sup>	42±0 <sup>b</sup>
BuBE	36±0 <sup>b</sup>	230±5 <sup>b</sup>	34±1 <sup>b</sup>
BisAEPE	58±0 <sup>b,c</sup>	1200±75 <sup>b,c</sup>	20±0 <sup>b,c</sup>
BisAPE	100±1 <sup>b,c</sup>	1860±10 <sup>b,c</sup>	59±0 <sup>b,c</sup>

<sup>b</sup> Corresponds to a formulation with a stoichiometric amount of TMPS

<sup>c</sup> Measured after post-curing at 100 °C

However, their thermo-mechanical properties are still inferior compared to the (meth)acrylates which show a  $T_g$  of 50 °C (BuMAc) and even 80 °C (BuAc) and much higher moduli at 37 °C of 1400 – 1600 MPa compared to 230 – 250 MPa of BuPE and BuBE. This fact that can be attributed to the high flexibility of thioether linkages.<sup>93</sup> The full width at half-

maximum of tan delta (FWHM) which is a measure of network homogeneity of BuVE is much lower than for BuPE and BuBE indicating a homogeneous network structure. Nevertheless, alkyne ethers still show a much narrower glass transition than the (meth)acrylates as it can be seen for BuAC, BuPE and BuBE in Figure 7 (left).

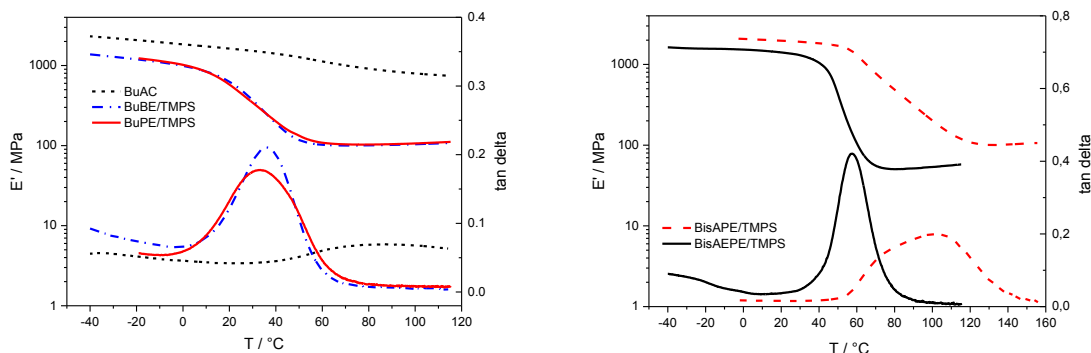


Figure 7: Storage modulus and tan delta versus temperature. Left: BuAc. (dotted) and the stoichiometrically balanced polymerization of BuBE/TMPS (chain-dotted) and BuPE/TMPS (solid). Right: BisAepe/TMPS (solid) and BisAepe/TMPS (dashed).

The use of rigid backbone structures significantly enhances the thermo-mechanical properties as it is shown by the example of the bisphenol A derivatives in Table 6 and Figure 7 (right). Therefore, photopolymers can be obtained with a  $T_g$  well above body temperature, allowing the fabrication of biomedical materials.

### 2.2.7.2 Alkyne carbonates networks

Similar DMA results were obtained for alkyne carbonates which were polymerized with PETMP. Although the  $T_g$  of C4 based monomers is above 37 °C, the storage moduli for 4PC/PETMP and 4BC/PETMP were still too low as it is shown in Table 7 and Figure 8 (left).

A slight improvement in modulus was achieved by the additional methyl group in 4MPC, however, appropriate storage moduli and significantly higher  $T_g$ s were only obtained by rigid backbone structures (BABC or TCBC) or the use of multifunctional alkynes as shown for TMPC in Figure 8 (right).

Table 7: Results of the DMA measurements of alkyne carbonate/PETMP photopolymers.

Monomer	$T_g$ [tan(delta)] / °C	$E'$ (37 °C)	FWHM / °C
4PC/PETMP	45±1	509±33	19±1
4PC/20TMPS	48±1	1134±216	14±1
4BC/PETMP	41±1	257±1	15±1
4MPC/PETMP	49±3	1107±112	14±5
TMPC/PETMP	59±1	1629±126	28±1
BABC/PETMP	60±1	2155±10	17±2
TCBC/PETMP	56±1	1720±141	19±1
TCBC/DiPETMP	72±1	2346±34	17±1

Again the network homogeneity of the presented thiol-yne photopolymers is much higher than for (meth)acrylates as reflected by their lower FWHMs in Table 7 and the weakly defined maximum of tan delta of BuAc in Figure 8.

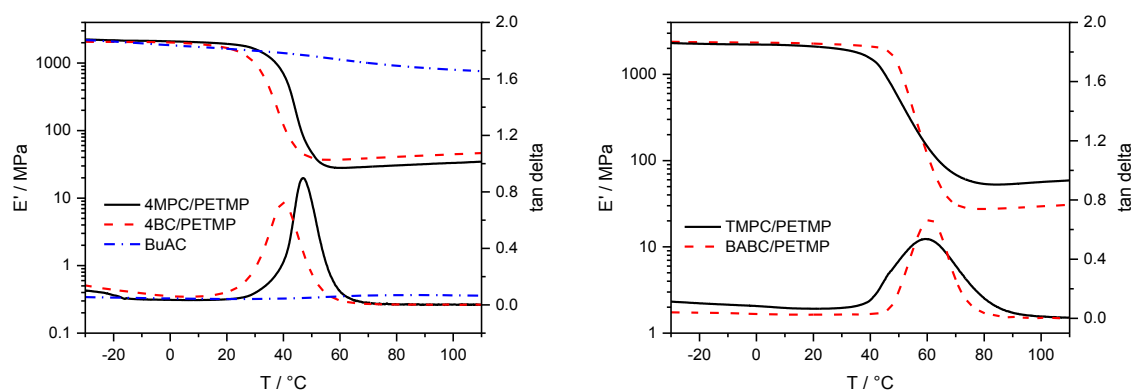


Figure 8: Storage modulus and tan delta from DMA measurements of investigated polymer samples. Left: 4MPC/PETMP (solid), 4BC/PETMP (dashed), BuAc (chain dotted). Right: TMPC/PETMP (solid), BABC/PETMP (dashed).

Replacing 20% of PETMP by TMPS in a 4PC/PETMP formulation already lead to an increase of 3 °C of the  $T_g$  and a narrower glass transition, resulting in a higher storage modulus at 37 °C as depicted in Table 7 (4PC/20TMPS) and Figure 9 (left). Replacing PETMP with DiPETMP as it is shown for TCBC in Figure 9 (right) lead to an increase of 17 °C for the  $T_g$  and an increase in modulus by 600 MPa.

These observations can be compared to thiol-ene derived photopolymers. DMA measurements of cured samples of TATT in combination with TMPS and PETMP revealed that TMPS leads to slightly improved mechanical behavior compared to PETMP in terms of  $T_g$ .

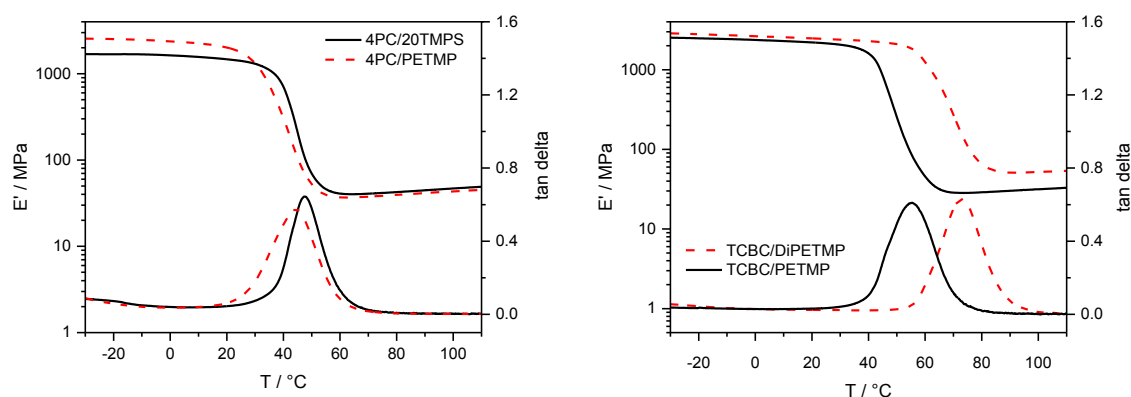


Figure 9: Storage modulus and tan delta from DMA measurements of investigated polymer samples. Left: 4PC/20TMPS (solid), 4PC/PETMP (dashed). Right: TCBC/DiPETMP (dashed) and TCBC/PETMP (solid).

Most mentionable, the mechanical properties of cured TATT/TMPS were mostly unaffected by water uptake as shown in Table 8. It can be seen that the  $T_g$  and the storage modulus of polymer samples after immersion in water for 24 h remained constant. This was not the case for PETMP-derived thiol-ene samples which showed a significant decrease in their  $T_g$  and their storage modulus after water storage.

Table 8: Storage moduli and  $T_g$ s of photocured TATT/TMPS, DBC/PETMP and DBC/DiPETMP resins before and after storage in water for 24 h.

Thiol Monomer	$T_g / ^\circ\text{C}^a$ before	$T_g / ^\circ\text{C}^a$ after	$E' / \text{GPa}$ before	$E' / \text{GPa}$ after
TATT/TMPS	67±1	67±1	1.5 <sup>b</sup>	1.3 <sup>b</sup>
TATT/PETMP	61±1	42±1	2.0 <sup>b</sup>	1.4 <sup>b</sup>
DBC/PETMP	50±1	47±1	1180 <sup>c</sup>	1050 <sup>c</sup>
DBC/DiPETMP	61±1	57±1	1710 <sup>c</sup>	1590 <sup>c</sup>

<sup>a</sup> determined at the maximum of tan delta

<sup>b</sup> storage modulus ( $E'$ ) measured at 25 °C

<sup>c</sup> storage modulus ( $E'$ ) measured at 37 °C

In contrast thiol-yne derived photopolymers with ester-bearing thiols were much less affected by water absorption. This was shown by the example of DBC/PETMP and DBC/DiPETMP in Table 8 where the  $T_g$  and the storage modulus (measured at 37 °C) remained almost constant after immersing samples in water for 70 days. An explanation can be found in the higher crosslink density of thiol-yne photopolymers. Monitoring the water uptake over time (shown in Figure 10) revealed that DBC/PETMP showed higher water absorption compared to DBC/DiPETMP due to its looser network structure. The water absorption capacity is known to increase with the ester content in the polymer.<sup>56,62</sup> This was confirmed by the fact that DBC/TMPS clearly showed the lowest water absorption.

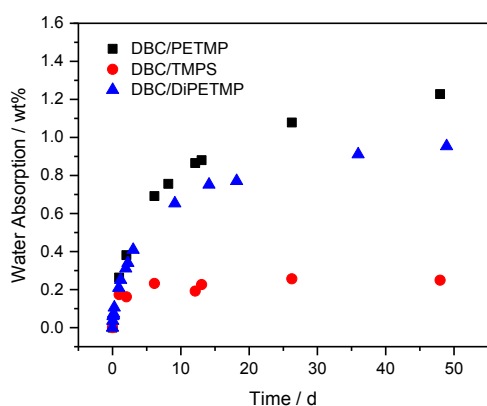


Figure 10: Water absorption of DBC/PETMP, DBC/DiPETMP and DBC/TMPS.

### 2.2.7.3 Impact properties of thiol-yne photopolymers

Dependent on their application, medical devices (e.g. implants) need to withstand external impact forces and they need to show toughness under load-bearing situations. Therefore, impact strength is an important parameter that has to be considered. As a consequence, the impact properties as a measure of polymer toughness of TCBC derived photopolymers were investigated by Charpy impact testing. It was discovered that polymers with high toughness were obtained which showed impact strengths that were much higher (TCBC/PETMP) or comparable (TCBC/DiPETMP) to PLA. As it is shown in Figure 11, these photopolymers significantly outperformed the comparable acrylate in terms of impact strength and provide thermo-mechanical properties sufficiently high for the production of biomedical devices.

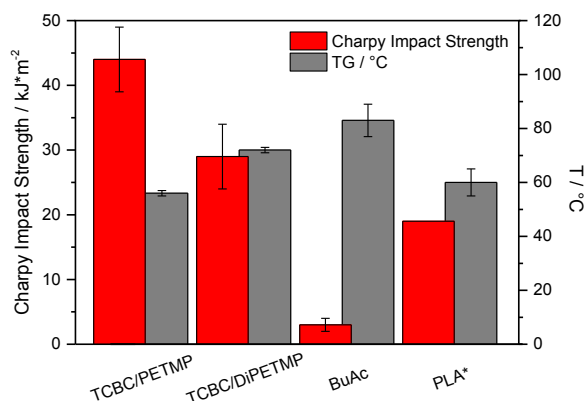


Figure 11: Charpy impact strength and  $T_g$  of DBC/PETMP, DBC/DiPETMP, BuAc and PLA.\*

\*for Charpy impact strength of PLA review Mautner et al.<sup>49</sup>; for  $T_g$  of PLA review Middleton et al.<sup>44</sup> and Hassan et al.<sup>94</sup>

### 2.2.7.4 In-depth investigations on the network formation

In the following chapter, DBC was used and investigated in combination with the three different thiols, TMPMP, PETMP and DiPETMP in order to further study the network formation and its correlation with the functionality of the thiol and trying to link it with the resulting mechanical properties in order to generate tough polymers.

The mechanical properties and the curing speed of photopolymers are strongly influenced by the time to reach gelation ( $t_{gel}$ ), the conversion at the gel point ( $MC_g$ ), the overall monomer conversion (MC) and the shrinkage force ( $F_N$ ). Real-time Near Infrared (RT-NIR) Photorheology is capable of investigating all these parameters within one single measurement.<sup>95</sup> While thiol-yne photopolymers react in a step-growth mechanism they are known for a higher conversion at the gel point compared to (meth)acrylates which react via a chain growth mechanism.<sup>51</sup> Due to a higher mobility of monomers and radicals below the gel point, this results in higher overall monomer conversion. While in (meth)acrylic systems the gel point is reached a low conversion, hindered monomer mobility above the gel point is responsible for the lower overall conversion and the evolution of shrinkage stress.

In photorheology the time of gelation  $t_{gel}$  is reached when the storage modulus ( $G'$ ) intersects the loss modulus ( $G''$ ), hence  $G'/G'' = 1$ , which is displayed in Figure 12 (left) for DBC/TMPMP, DBC/PETMP, DBC/DiPETMP and BuAc as the reference. While BuAc reaches gelation already after 1.7 s, it is significantly delayed in an increasing order starting from DBC/DiPETMP to DBC/PETMP to DBC/TMPMP (compare Table 9), while  $t_{gel}$  increases

with decreasing thiol functionality which is explained by the faster network formation and the higher resin viscosity when applying multifunctional thiols. The shrinkage stress, expressed by the normal force  $F_N$  behaves diametrical to the  $t_{gel}$ , as seen in Figure 12, with BuAc exhibiting the highest shrinkage stress ( $F_N = 32.7$  N), followed by DBC/DiPETMP ( $F_N = 26$  N), DBC/PETMP ( $F_N = 24.7$  N) and DBC/TMPMP ( $F_N = 22.1$  N).

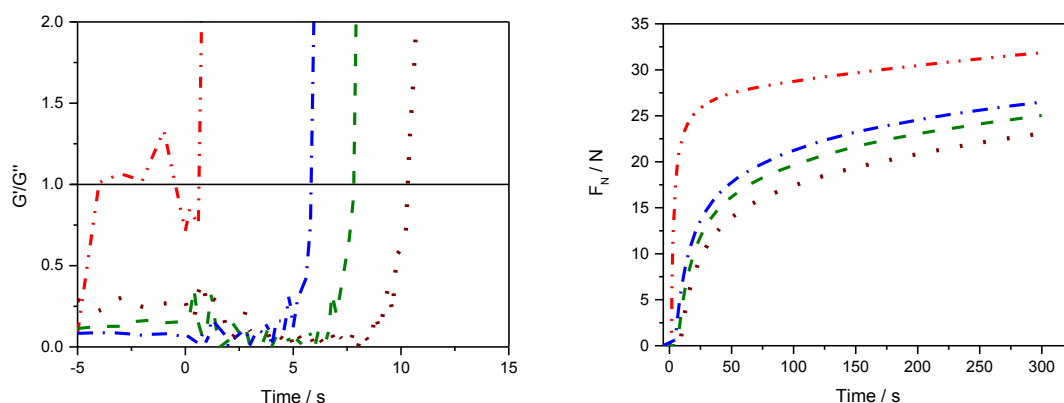


Figure 12: Left: Determination of the gelpoint ( $G'/G'' = 1$ , —). Right: Measurement of the normal force  $F_N$ . BuAc (chain double dotted), DBC/TMPMP (dotted), DBC/PETMP (dashed), DBC/DiPETMP (chain dotted). Light starts at 0 s.

$MC_g$  which was obtained by monitoring the decreasing signals in the NIR region of the triple or double bonds of alkynes or the acrylate, respectively, increases with decreasing thiol functionality while being significantly higher for all thiols compared to BuAc. Although all thiol-ene resins show much higher viscosities ( $\eta$ ) than BuAc, they still reached similar high  $MC_g$ s.

Table 9: Investigated parameters of DBC/thiol formulations and their corresponding photopolymers including reference sample BuAc.

Formulation	$\eta$ / mPa*s	$t_{gel}$ / s	$MC_g$ / %	MC / %	DF / %	Rel. $D_{res}$	Rel. $E'(100^\circ C)$	$T_g$ / °C	$E'$ at 20 °C / MPa
<b>DBC/TMPMP</b>	66	10.3±0.2	55±2	95	5	1	1	37±0	2048±20
<b>DBC/PETMP</b>	114	8.1±0.2	46±1	92	11	1.5	1.3	50±0	1937±266
<b>DBC/DiPETMP</b>	298	5.6±0.3	35±1	90	12	1.8	1.6	61±0	1939±88
<b>BuAc</b>	4	1.7±0.1	18±2	89	---	---	---	83±6	1612±22

Studies of the network properties by DQ NMR showed a direct correlation of the crosslink density (expressed by the relative (Rel.)  $D_{res}$  values in Table 9) with the thiol functionality while the amount of non-network chains (DF) correlated with the expected amount of unreacted monomers and photoinitiator or its cleavage products. Estimating the crosslink density by comparing the storage moduli in the rubbery state (Rel.  $E'(100^\circ\text{C})$  in Table 9), as proposed by Fairbanks et al.<sup>65</sup> lead to only slight deviations to those results. This fact clearly underlines the advantages of DQ NMR where detailed information about the crosslink density and the fraction of non-network chains can be obtained by a single measurement.

As a result of the increasing crosslink density by increasing thiol functionality, the  $T_g$  (at tan delta max) measured by DMA increased steadily from  $37^\circ\text{C}$  (DBC/TMPMP) to  $61^\circ\text{C}$  (DBC/DiPETMP), while the FWHM remained between  $10^\circ\text{C}$  -  $22^\circ\text{C}$ , reflecting highly homogenous networks (compare Figure 13, left). The storage moduli ranged from 1900 - 2100 MPa. Measuring the impact resistance (Charpy impact testing) as an indicator for polymer toughness, high values of  $16 - 38 \text{ kJ}\cdot\text{m}^{-2}$ , as depicted in Figure 13 (right) were obtained which are comparable to TCBC, as discussed previously (vide supra). Especially DBC/DiPETMP can outperform the reference acrylate BuAc in terms of storage modulus and impact resistance (BuAc:  $3 \text{ kJ}\cdot\text{m}^{-2}$  v.s. DBC/DiPETMP:  $16 \text{ kJ}\cdot\text{m}^{-2}$ ) while offering reasonable  $T_g$  of  $61^\circ\text{C}$ . The fact that the observed shrinkage forces only slightly deviated, suggests that not only shrinkage stress, but also network homogeneity is playing a role for the higher impact strength for the investigated alkynes in comparison to the acrylate.

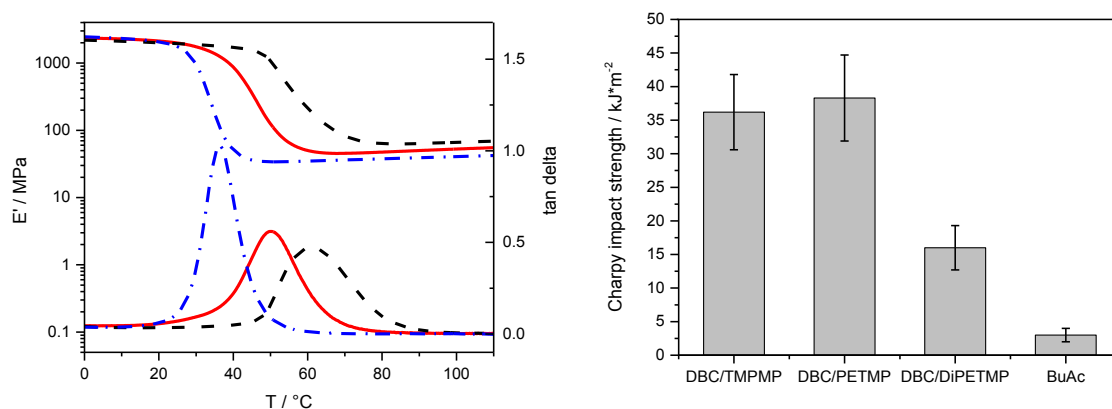


Figure 13: Left: DMA plots of DBC/TMPMP (chain dotted), DBC/PETMP (solid) and DBC/DiPETMP (dashed). Right: Measured Charpy impact strengths for DBC derived polymers and BuAc.



## 2.2.8 Degradation of alkyne carbonates derived photopolymers

For several medical applications as e.g. scaffolds for bone regeneration therapies, hydrolytic polymer degradation can be desired.<sup>35</sup> While degradation products of (meth)acrylates are known for their potentially adverse effects, step-growth derived polymers containing degradable linkers are expected to degrade to low molecular weight degradation products which are easily removed from the degradation site in the human body.<sup>33,49,46</sup>

Therefore, the degradation behavior of alkyne carbonates in alkaline and acidic solution was investigated and it was demonstrated that it is possible to tune the degradation times by combining degradable (PETMP) and non-degradable thiols (TMPS, EDT). While hydrolytically stable polymers were obtained using EDT (g-i in Figure 14), it was possible to significantly slow down degradation in alkaline and acid solution by replacing 5 to 20% of PETMP by the silane-based thiol TMPS (d-f in Figure 14). Mentionable the thermo-mechanical properties were not negatively influenced by TMPS as it was presented in Figure 9 (left). Degradation in alkaline media was expectedly faster than under acidic conditions due to the higher sensitivity of ester groups towards alkaline hydrolysis.<sup>96</sup> In alkaline medium, 4PC/PETMP and 4BC/PETMP showed similar degradation behavior as PLA and fully degraded within 7.6 days. Enhanced hydrophobicity, derived from the additional methyl groups of MPC/PETMP (Figure 14, c) significantly decreased the degradation rate, leading to (extrapolated) full degradation after 34 days. While EDT derived polymers tended to swell as a result of the low network density, all other polymers degraded in a surface erosion manner, which is desired for degradable polymers as bulk erosion leads to a premature loss and non-linear decrease of the mechanical properties.<sup>47</sup>

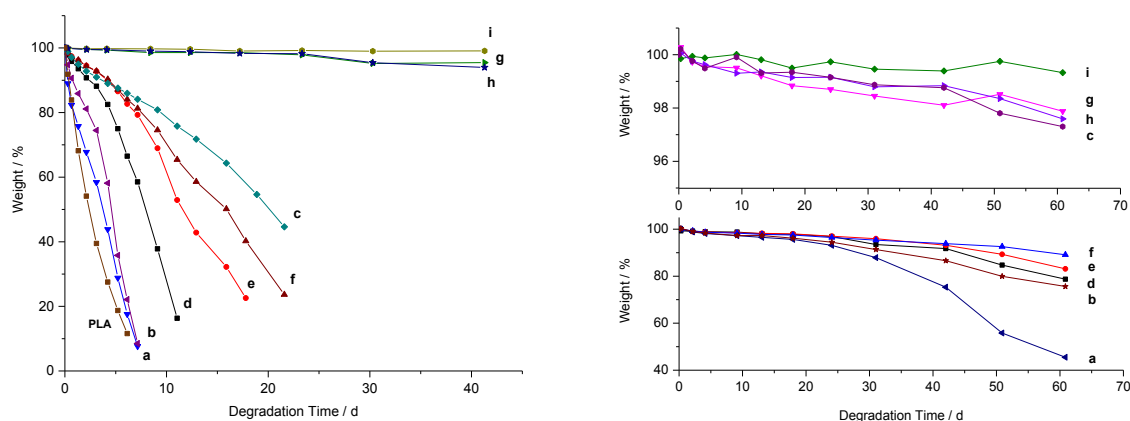


Figure 14: Weight losses during degradation for the formulations a) 4PC/PETMP, b) 4BC/PETMP, c) 4MPC/PETMP d) 4PC/5TMPS, e) 4PC/10TMPS, f) 4PC/20TMPS, g) 4PC/EDT, h) BC/EDT, i) MPC/EDT and PLA (left only) in 1 M NaOH (left) and 1 M HCl (right) at 45 °C.

## 2.2.9 3D printing of tough thiol-yne derived photopolymers

TCBC demonstrated excellent curing rates, conversion and low cytotoxicity, as well as excellent mechanical and impact properties in combination with DiPETMP. Its printability was evaluated using a blue light (peak at 460 nm) DLP printer. Using Sudan II as a light absorber and Ivocerin<sup>®</sup> as a photoinitiator, test patterns (shown in Figure 15) were successfully printed. The achieved accuracy of 40\*40 μm represented a resolution that is high enough for the production of bone scaffolds where pore sizes of 50 – 1000 μm are known to allow optimal bone ingrowth.<sup>32,33,34</sup>

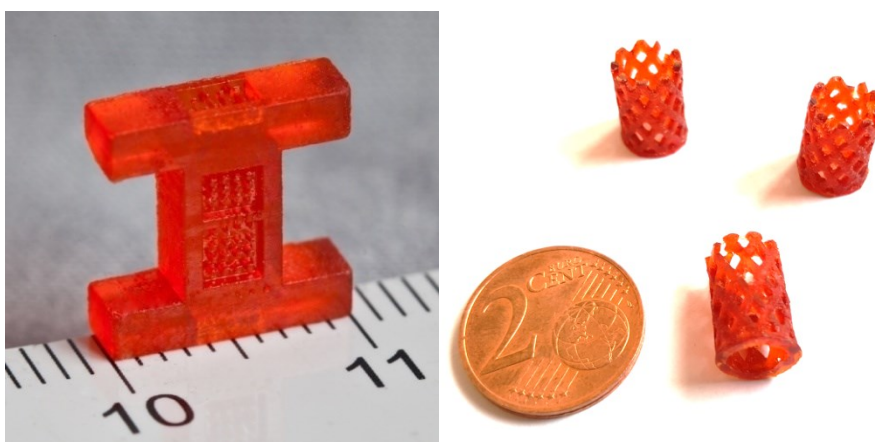


Figure 15: 3D printed test patterns from a TCBC/DiPETMP formulation (scale on the left shown in cm).

***Alkyne ethers, alkyne carbonates and new a thiol in thiol-yne resins are presented as alternatives to (meth)acrylates for the AMT-based production of medical devices. These monomers show significantly lower cytotoxicity and higher monomer conversion, but comparable photoreactivity to acrylates. Studies on their network properties revealed their superiority in terms of network homogeneity and crosslink density, leading to materials with high glass transition temperatures, high storage modulus and toughness, offering tunable degradability and good 3D printability in a DLP process.***

### 3 Low Migration Type I Photoinitiators for Thiol-based Resins

*The following results have been published in European Polymer Journal and submitted to Journal of Material Engineering.*<sup>97,23</sup>

#### 3.1 State of the art

Photoinitiators (PIs) are essential components in photoreactive resins. While the toxicity of the commonly used (meth)acrylate monomers has already been discussed in the previous chapter, the migration of photoinitiators or their cleavage products is an important issue which has to be addressed for the development of new biocompatible materials. To date only a few studies can be found in the literature that deal with the toxicity of commonly used photoinitiators or their migration potential in 3D printed medical materials.<sup>98,99</sup> Williams et al. investigated the toxicity of different photoinitiators using a various cell types and concluded that Irgacure 2959 (I2959) shows biocompatibility and low cellular toxicity.<sup>98</sup> The superiority of I2959 in terms of low cytotoxicity was confirmed very recently by Liska and co-workers who studied water-soluble hydroxyl ketone and acylphosphine oxide based photoinitiators.<sup>99</sup> However, the toxicity of cleavage or side products of photoinitiators was not considered, which is surprising due to the fact that the toxicity of the main cleavage product of I2959, the 4-(2-hydroxyethoxy)benzaldehyde has not been evaluated to our knowledge.<sup>100</sup> Addressing low photoinitiator migration, polymers carrying photoinitiating units or oligomeric photoinitiators have been studied. However, due to their reduced mobility resulting from a strong viscosity increase due to the high molecular weight of applied PIs, only poor reactivity and sometimes poor resin compatibility were observed.<sup>101,102</sup> Another interesting approach to achieve low PI migration are polymerizable photoinitiators as published in the patent literature by DuPont.<sup>103</sup> This concept describes a polymerizable group being attached to a photoinitiator. Upon photopolymerization, the photoinitiating unit gets immobilized by covalent linking to the polymer matrix inhibiting its diffusion and thus, migration. While this concept is rather simple, most studies dealing with this type of photoinitiators only focused on the photochemical performance, ignoring their migration behavior.<sup>104,105</sup> In most cases reduced reactivity could be observed during polymerization as the diffusion of radicals and excited groups is being reduced due to the subsequent photoinitiator immobilization.

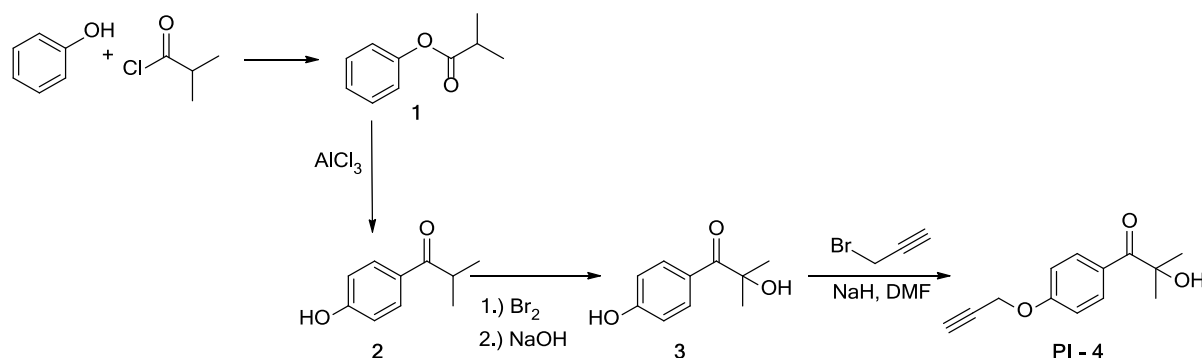
While studying the photoreactive behavior and the migration potential of benzophenone derivatives, carrying polymerizable alkynyl ester and vinyl carbonate groups, we observed high migration stability with decent initiation performance of these PIs in 1,4-butanediol divinyl carbonate BuVC/TMPMP formulations.<sup>106</sup> In this thiol-ene system, due to the step-growth mechanism, a high mobility of benzophenone and the formed radicals is enabled below the gel point. However, the Norrish type II initiation mechanism of benzophenone is known for its inferior initiation performance compared to type I initiators.<sup>107</sup> This behavior is explained by the fact that the cleavage reaction of type I photoinitiators proceeds much faster than the electron and proton transfer of type II photoinitiators.

Expecting a consequently higher photoreactivity of type I photoinitiators, derivatives of I2959 and Irgacure TPO-L (TPO-L), carrying a photoreactive propargyl ether group, respectively, were synthesized. Their absorption characteristics and performance in a low cytotoxic thiol-ene resin (BuVC/TMPMP) was investigated. Furthermore, their migration behavior was studied and compared to their non-polymerizable references. The photoreactivity and the migration behavior of I2969 and its polymerizable derivative were additionally studied in a thiol-yne resin (DBC/PETMP) to show the versatility of these types of PIs.

## 3.2 Results and Discussion

### 3.2.1 Synthesis

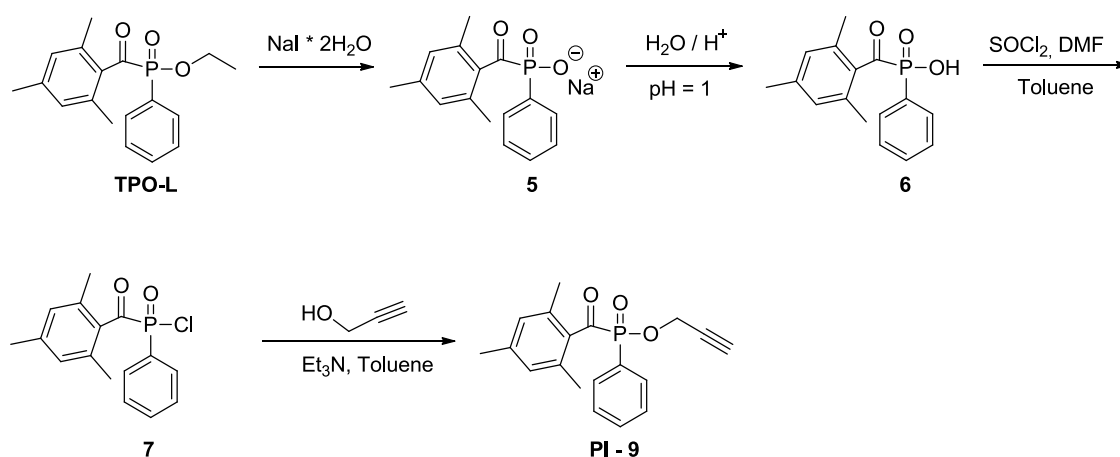
The synthesis of the modified I2959, PI-4, was carried out by an esterification of phenol followed a subsequent Fries rearrangement using catalytic amounts of  $\text{AlCl}_3$  as described in the literature (see Scheme 7).<sup>108</sup>



Scheme 7: Synthesis of photoinitiator PI - 4.

Bromination of 2 and subsequent reaction with NaOH lead to the hydroxy ketone 3 which was further reacted with NaH and propargyl bromide to the desired PI - 4.

The modified TPO-L was synthesized according to Scheme 8. The commercially available TPO-L was reacted with sodium iodide to its corresponding salt which was converted to 6 under acidic conditions. Further reaction of 6 with SOCl<sub>2</sub> under elevated temperatures (110 °C) and catalytic amounts of DMF lead to its corresponding acid chloride 7 which was subsequently converted to PI - 9 under alkaline conditions with propargyl alcohol.



Scheme 8: Synthesis of the photoinitiator PI – 9.

### 3.2.2 Absorption by UV-Vis Spectroscopy

UV-Vis spectroscopy was used in order to investigate the absorption behavior of light which is an essential factor for photocurable resins as the absorption maximum has to match with the emission spectrum of the light source. The absorption characteristics of both PIs did not significantly deviate from their references as shown in Figure 16. The modified PIs show only slightly higher absorptions.

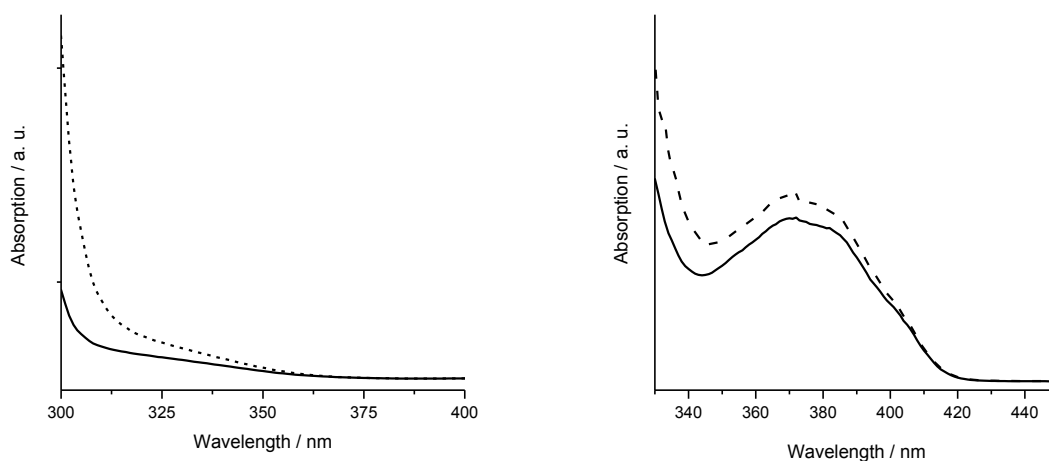


Figure 16: Absorption spectra of the synthesized photoinitiators and the commercially available reference substances (1.0 mM in acetonitrile). Left: I2959 (solid line), PI – 4 (dotted line); right: TPO-L (solid line), PI – 9 (dashed line).

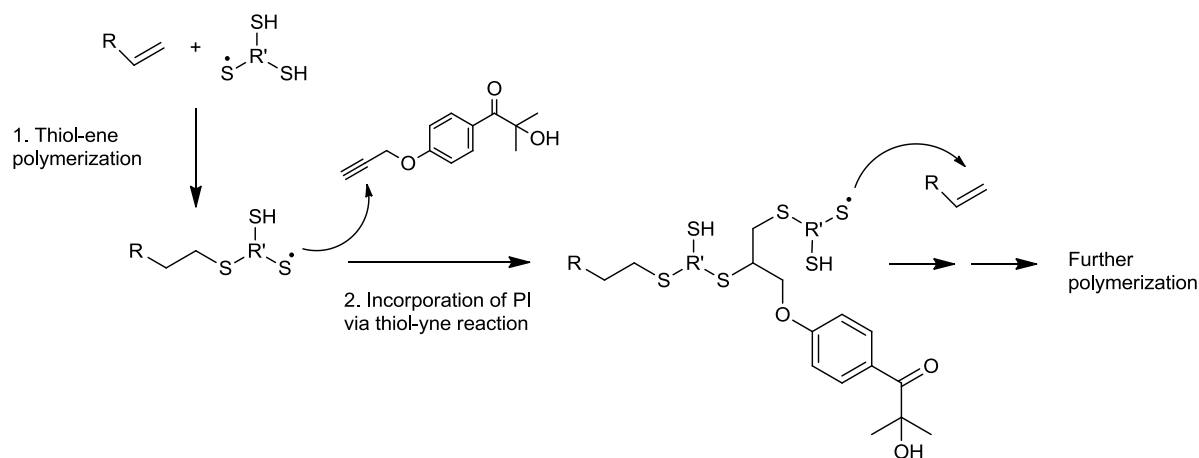
### 3.2.3 Photoreactivity

The photoreactivity which was characterized by photo-DSC revealed similar values for PI – 9 compared to TPO-L (compare Table 10) at both investigated concentrations of 1 mol% and 5 mol% in a BuVC/TMPMP resin. This was not the case for PI - 4. Here, significantly lower values regarding peak height and conversion ( $\Delta H$ ) and higher  $t_{\max}$  values were obtained. This indicates its lower reactivity compared to I2959 as shown in Table 10.

Table 10: Photopolymerization parameters obtained by photo-DSC.

Photoinitiator	$t_{\max}$ / s	Peak height / $\text{mW}\cdot\text{mg}^{-1}$	$\Delta H$ / $\text{J}\cdot\text{g}^{-1}$
I2959 (5 mol%)	1.9	52	280
PI - 4 (5 mol%)	2.5	23	190
TPO-L (5 mol%)	2.0	51	285
TPO-L (1 mol%)	1.9	48	320
PI – 9 (5 mol%)	2.2	51	310
PI – 9 (1 mol%)	2.1	48	300

RT-FT-IR spectroscopy was used to observe the incorporation of the newly synthesized PIs into the polymer matrix that are expected to follow the mechanistic principles shown in Scheme 9.



Scheme 9: Incorporation of PI - 4 into the thiol-ene network during photopolymerization.

By studying the conversion of the triple bond of the alkyne functionality at  $3250 - 3330 \text{ cm}^{-1}$  a quantitative conversion of both polymerizable PIs was confirmed as shown in Figure 17 (left). Thus, non-reacted PI molecules but also their functionalized fragmentation products are immobilized in the polymer matrix. Mentionable, as studied by Jokusch et al. and Kolczak et al., who studied the fragmentation of the reference PIs, I2959 and TPO-L, the formation of leachable acetone (PI - 4) and 2,4,6-trimethylbenzaldehyde (PI - 9) can be expected.<sup>109,110</sup>

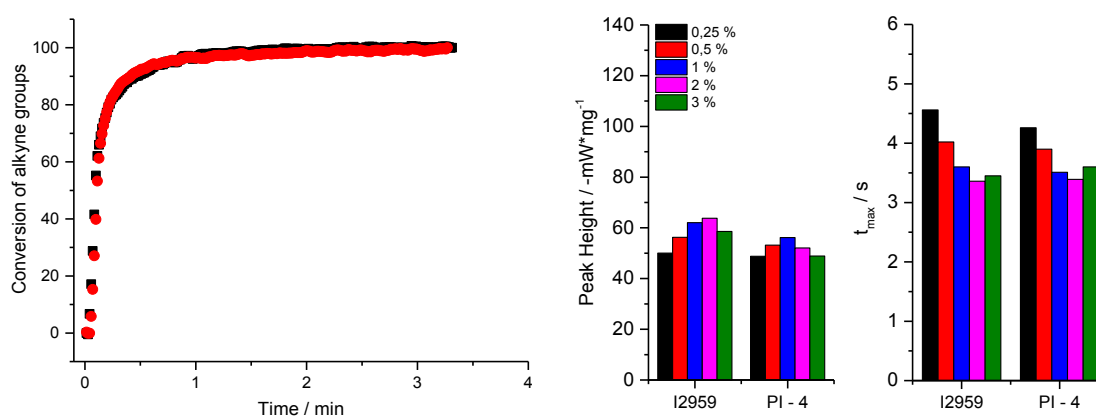


Figure 17: Conversion of alkyne ether groups of PI - 4 (red circle) and PI - 9 (black square) during UV illumination (left) and results of photo-DSC measurements ( $t_{\text{max}}$  and peak height) of different concentrations (shown in wt%) of PI - 4 and I2959 in a DBC/PETMP resin formulation (right).

The photoreactivity of PI – 4 was also studied in a thiol-yne resin at different applied concentrations and compared to I2959 as shown in Figure 17 (right). The results of PI – 4 and its reference do not significantly deviate. Mentionable, a minimum concentration of 1 wt% seems to be necessary for an optimal curing performance. However, both PIs show similar peak heights and  $t_{\max}$  values at all investigated concentrations and also no significant changes in  $\Delta H$  were observed. This is in contrast to the observations in a thiol-ene resin. The difference in photoreactivity of this PI in both systems cannot be explained by its immobilization in the polymer matrix. It is therefore subject of current research.

### 3.2.4 Migration Studies

For quantification of the amount of leachable photoinitiator and their cleavage products in order to characterize their overall migration behavior, cured resin samples were immersed in ethanol at 50 °C for 96 h. Using GC-MS it was possible to analyze the amount of I2959 and PI – 4 in the extracts.

In the extracts of the thiol-ene resin, BuVC/TMPMP, approximately 27% of the initially applied amount of I2959 was detected, while the amount of PI – 4 was below the detection limit of the applied method ( $0.15 \mu\text{g}\cdot\text{mL}^{-1}$ ) as shown in Figure 18 (left). Mentionable, none of its cleavage products were detected.

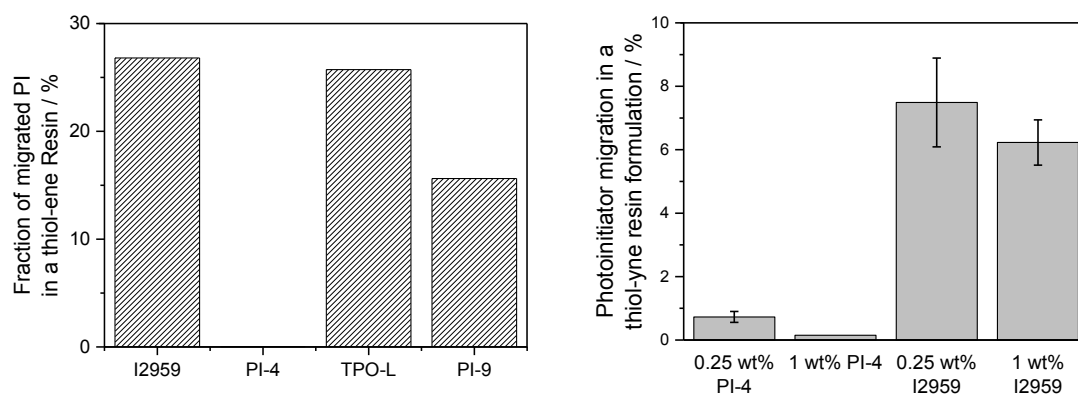


Figure 18: Results of migration studies of PI - 4 and P - 9 and their references in a thiol-ene (BuVC/TMPMP) resin (left) and PI – 4 and its reference at two different concentrations, respectively, in a thiol-yne resin (DBC/PETMP) (right).

These results confirm the observations of the RT-FT-IR measurements in Figure 17 (left) and reveal the beneficial effect of PI -4 in terms of migration. In order to determine the amount of



leachable PI – 9 and its reference TPO-L in the thiol-ene resin, ICP-MS measurements were performed which allow the quantification of these phosphorous containing PIs and also potential, phosphorous-containing fragmentation products in the extracts. Surprisingly, a rather high amount of phosphorous could be detected in the extract of PI – 9 (which corresponds to approximately 16% of its applied amount). Due to RT-FT-IR measurements, much lower values would have been expected. Presumably, a partial fragmentation of the P-O bond can explain this observation, which had not been reported for TPO-L so far. Nevertheless, the migration behavior was still reduced compared to TPO-L.

GC-MS studies on the extracts of thiol-yne (DBC/PETMP) resins with different concentrations of PI – 4 and its reference I2959, respectively, revealed that the detected amount of PI – 4 at an initially applied concentration of 0.25 wt% was approximately ten times lower compared to its reference. At an applied concentration of 1 wt%, the amount of PI – 4 in the extracts was even below the detection limit (LOD) ( $0.5 \mu\text{g}\cdot\text{mL}^{-1}$ ) of the used method, while about 6.5% of I2959 were extracted. The higher extracted amounts at lower applied concentrations is explained by the reduced photoreactivity as shown in Figure 17 (right) which might have led to insufficiently cured samples, thus higher PI mobility. Additional focus was set on the migration of the cleavage product of PI – 4. Besides acetone, which was not considered in these studies due to its low toxicity, 4-(2-hydroxyethoxy)benzaldehyde is the main cleavage product of I2959 as reported in the literature.<sup>111</sup> Assuming an analogous cleavage behavior for PI – 4, 4-(prop-2-yn-1-yloxy)benzaldehyde was expected as the major cleavage product. However, this cleavage product was not detected in any of the extracts of PI – 4, which underlines the superiority of PI – 4 as a highly efficient, low migration PI for thiol-yne resins, making this type of polymerizable PI a promising candidate for biocompatible applications.

***Two propargyl ether-functionalized photoinitiators were synthesized and their absorption behavior was characterized. While PI – 9 showed excellent photoreactivity in a thiol-ene resin, PI – 4 is particularly suitable for thiol-yne resins. This was confirmed by migration studies, where this type of PI showed almost quantitative incorporation into the polymer network, reducing the amount of migration products to a minimum below the detection limit of the applied GC-MS analysis method.***

## 4 Summary

The present work highlights the potential of thiol-yne photopolymers as biocompatible alternatives to (meth)acrylates for the AMT-based production of medical devices. Alkyne ethers and alkyne carbonates have been synthesized in facile reaction pathways with high yields. As it was proven by real-time NMR studies, molecules bearing terminal alkyne groups show no significant reaction towards Michael donors under simulated physiological conditions in contrast to (meth)acrylates. Thus, a low cellular toxicity of alkyne-based monomers was predicted which could be confirmed by in-vitro cell culture tests. Photo-DSC revealed very high photoreactivities of these monomers in combination with multifunctional thiols, which were in the range of acrylates, especially for but-1-yn-4-yl ethers and carbonates. Most importantly, it was demonstrated by real-time FT-IR spectroscopy that these investigated thiol-yne formulations show very high monomer conversions. Additionally, it could be shown, that the overall conversion can be increased by UV post-curing under elevated temperature, making these polymers interesting for the production of medical devices, where low migration of unreacted monomers is essential. Investigations of different stabilizers in a DBC/PETMP formulation revealed that the storage stability was significantly enhanced by the use of food-compatible additives.

Investigations on the network density of 1,4-butanediol based alkyne ether derived thiol-yne photopolymers showed a six times higher crosslink density compared to an analogous thiol-ene (vinyl ether) derived photopolymer as it was studied by DQ solid state NMR spectroscopy. As a result,  $T_g$ s and storage moduli are significantly increased as confirmed by DMA measurements. Additionally, the studied networks appeared very homogenous as it was indicated by the narrow FWHMs of tan delta. The use of rigid backbone structures as shown by the example of bisphenol A derivatives further improved the storage moduli and lead to  $T_g$ s that were significantly above body temperature.

A similar behavior was observed for alkyne carbonates. 1,4-butanediol based alkynes lead to photopolymers with insufficiently high glass transition temperatures for internal body applications. In contrast, multifunctional alkynes or rigid backbone structures yield photopolymers with high  $T_g$ s and also very high impact strengths (Charpy impact) that are in the range or even higher than it is reported in the literature for PLA.

In-depth investigations on the network formation by photorheology of DBC in combination with the three different thiols (TMPMP, PETMP and DiPETMP) revealed that gelation is significantly delayed for thiol-yne derived photopolymer compared to the reference acrylate. This lead to high conversions at the gel point and high overall monomer conversions with

slightly lower shrinkage stress values. Expectably, the crosslink densities and the  $T_g$ s of these thiol-yne photopolymers increases with increasing thiol functionality as studied by DQ NMR and DMA. As the measured shrinkage stress value of the acrylate only slightly deviates from the investigated thiol-yne polymers, the increased impact strength can be attributed to their high network homogeneity.

Thiol-yne formulations also showed excellent printing behavior with high accuracy in a DLP process, as it was demonstrated on the example of a TCBC/DiPETMP formulation. It was also shown that thiol-yne polymers were able to undergo controlled degradation under alkaline or acidic conditions. Studies on alkyne carbonates revealed that the degradation rate can be easily tuned by combining the hydrolytically unstable PETMP with the hydrolytically stable thiol TMPS, without significantly reducing the thermo-mechanical properties. While TMPS was synthesized in a two-step process, it showed much lower viscosity than PETMP. Most importantly, the thermo-mechanical properties of thiol-based photopolymers containing TMPS were slightly improved and not negatively influenced by water absorption.

Using alkyne functionalized PIs, low migration of PIs or their cleavage products was achieved in thiol-based resins. This was demonstrated in biocompatible thiol-ene and thiol-yne formulations with propargyl ether functionalized derivatives of I2959 (see PI – 4) and TPO-L (see PI – 9). While these PIs can be accessed via facile multi-step reactions, they showed similar absorption behavior as their non-polymerizable references.

Both PIs showed quantitative triple bond conversions and high photoreactivities in thiol-ene or thiol-yne resins. GC-MS analysis of the extracts of PI – 4 containing samples revealed that the amount of leachable PI and its cleavage products in thiol-ene and thiol-yne photopolymers, respectively, was below the detection limit of the GC-MS method. Much higher amounts of phosphorous-containing fragments were detected by ICP-MS for PI – 9 in thiol-ene samples. However, its concentration was still lower than for the reference PI. Especially, their low PI migration but also their high initiation performance in thiol-based resins makes these PIs interesting candidates for low migration applications as for example medical materials.

Due to the versatile properties of the presented thiol-yne photopolymers including low monomer cytotoxicity, high photoreactivity and monomer conversion, together with excellent thermo-mechanical and impact properties, while revealing good printability, this material show very high potential for the 3D printing of medical devices.

## 5 List of Enclosed Publications

### Publication I (Ref.<sup>19</sup>)

#### **Exploring Thiol-yne Based Monomers as Low Cytotoxic Building Blocks for Radical Photopolymerization**

Oesterreicher, Andreas; Ayalur-Karunakaran, Santhosh; Moser, Andreas; Mostegel, Florian H.; Edler, Matthias; Kaschnitz, Petra; Pinter, Gerald; Trimmel, Gregor; Schlögl, Sandra; Griesser, Thomas

*Journal of Polymer Science Part A: Polymer Chemistry* **2016**, 54, 3484–3494.

Author's Contribution: 70%

Alkyne ethers and their cured thiol-yne derived resins are presented as biocompatible alternatives to (meth)acrylates. The synthetic work and the investigation of the photoreactivity by photo-DSC and FT-IR spectroscopy were performed by Oesterreicher Andreas. DMA measurements were made by Moser Andreas under the supervision of Prof. Pinter Gerald. Ayalur-Karunakaran Santhosh and Schlögl Sandra were responsible for the DQ-NMR studies. RT-NMR studies were performed by Kaschnitz Petra under supervision of Prof. Gregor Trimmel and Oesterreicher Andreas. The publication was written by Oesterreicher Andreas in accordance with input and corrections from Prof. Griesser Thomas, who supervised this project.

### Publication II (Ref.<sup>20</sup>)

#### **Tough and Degradable Photopolymers Derived from Alkyne Monomers for 3D Printing of Biomedical Materials**

Oesterreicher, Andreas; Wiener, Johannes; Roth, Meinhart; Moser, Andreas; Gmeiner, Robert; Edler, Matthias; Pinter, Gerald; Griesser, Thomas

*Polymer Chemistry* **2016**, 7, 5169–5180.

Author Contribution: 75%

Thiol-yne resins based on alkyne carbonates are studied for the 3D printing of medical devices. A particular focus was set on their synthesis, cytotoxicity and the mechanical performance of cured resins, as well as their 3D printability. The synthetic work was done by Oesterreicher Andreas with helpful support from Wiener Johannes. DMA and Charpy impact

measurements were performed by Moser Andreas under the supervision of Prof. Pinter Gerald. FT-IR, photo-DSC and viscosity measurements, as well as degradation studies as well as sample preparations, were done by Oesterreicher Andreas with kind support from Roth Meinhart and Edler Matthias. Gmeiner Robert with support of Oesterreicher Andreas was responsible for the 3D printing experiments. The publication was written by Oesterreicher Andreas in accordance with input and corrections from Prof. Griesser Thomas, who supervised this project.

### Publication III (Ref.<sup>21</sup>)

#### **Exploring Network Formation of Tough and Biocompatible Thiol-yne Based Photopolymers**

Oesterreicher, Andreas; Gorsche, Christian; Ayalur-Karunakaran, Santhosh; Moser, Andreas; Edler, Matthias; Pinter, Gerald; Schlögl, Sandra; Liska, Robert; Griesser, Thomas  
*Macromolecular Rapid Communication* **2016**, 37, 1701-1706.

Author's Contribution: 65%

An in-depth investigation of the network generation of di(but-1-yn-4-yl)carbonate (DBC) in combination with different thiols is presented. Synthetic work, preliminary studies and sample preparation was performed by Oesterreicher Andreas who also supported Gorsche Christian under the supervision of Prof. Liska Robert with the photorheology measurements. DMA measurements and Charpy impact tests were performed by Moser Andreas under the supervision of Prof. Pinter Gerald. Ayalur-Karunakaran Santhosh and Schlögl Sandra were responsible for the DQ-NMR measurements. The publication was written by Oesterreicher Andreas in accordance with input and corrections from Prof. Griesser Thomas, who supervised this project.

### Publication IV (Ref.<sup>22</sup>)

#### **Silicon-based Mercaptans: High-Performance Monomers for Thiol-ene Photopolymerization**

Roth, Meinhart; Oesterreicher, Andreas; Mostegel, Florian H.; Moser, Andreas; Pinter, Gerald; Edler, Matthias; Piock, Richard; Griesser, Thomas

*J. Polym. Sci. Part A: Polym. Chem.* **2016**, 54, 418–424

Coauthor's Contribution: 30 %

New silicon-based thiol monomers and their application and investigation in thiol-ene photopolymers are presented. Major parts of this work were performed by Roth Meinhart. DMA measurements were performed by Moser Andreas under the supervision of Prof. Pinter Gerald. Oesterreicher Andreas assisted at the upscaling of the thiol synthesis and the purification by Kugelrohr distillation. Furthermore, he performed the degradation studies and the DMA sample preparation.

## Publication V (Ref.<sup>97</sup>)

### **Low Migration Type I Photoinitiators for Biocompatible Thiol-Ene Formulations**

Oesterreicher, Andreas; Roth, Meinhart; Hennen, Daniel; Mostegel, Florian H., Edler, Matthias; Kappaun, Stefan; Griesser, Thomas

*Eur. Polym. J.* **2016**, *accepted and in press*

DOI: 10.1016/j.eurpolymj.2016.10.040

Author's Contribution: 55 %

Two new type-I photoinitiators bearing polymerizable groups are investigated in a biocompatible thiol-ene formulation. Roth Meinhart investigated the synthetic strategies, Oesterreicher Andreas assisted with Hennen Daniel and performed the optimization and upscaling of the synthetic process. Oesterreicher Andreas also performed photo-DSC measurements and supported Edler Matthias at the migration studies. The publication was written by Oesterreicher Andreas in accordance with input and corrections from Prof. Griesser Thomas, who supervised this project.

## Publication VI (Ref.<sup>23</sup>)

### **Investigating Photo-curable Thiol-yne Resins for Biomedical Materials**

Oesterreicher, Andreas; Moser, Andreas; Edler, Matthias; Griesser, Heidi; Schlögl, Sandra; Pichelmayer, Margit; Griesser, Thomas

submitted to: *Macromolecular Materials and Engineering*, on October 14, 2016.

Author's Contribution: 75 %

Low-toxic photoinitiators and stabilizers are evaluated in a thiol-yne resin taking into account their effect on the photoreactivity. Furthermore PI migration and the water absorption behavior in cured polymer samples were studied. Sample preparation, photo-DSC measurements, stabilization and water absorption and degradation tests were performed by Oesterreicher Andreas and Griesser Heidi, who was under supervision of Schlögl Sandra. DMA measurements were performed by Moser Andreas. GC-MS measurements were carried out by Edler Matthias. The publication was written by Oesterreicher Andreas in accordance with input and corrections from Prof. Griesser Thomas, who supervised this project.

## Publication I

Oesterreicher, Andreas; Ayalur-Karunakaran, Santhosh; Moser, Andreas; Mostegel, Florian H.; Edler, Matthias; Kaschnitz, Petra; Pinter, Gerald; Trimmel, Gregor; Schlögl, Sandra; Griesser, Thomas: Exploring Thiol-yne Based Monomers as Low Cytotoxic Building Blocks for Radical Photopolymerization *J. Polym. Sci. Part A: Polym. Chem.* **2016**, 54, 3484–3494.



## Exploring Thiol-Yne Based Monomers as Low Cytotoxic Building Blocks for Radical Photopolymerization

Andreas Oesterreicher,<sup>1</sup> Santhosh Ayalur-Karunakaran,<sup>2</sup> Andreas Moser,<sup>3</sup>  
Florian H. Mostegel,<sup>1</sup> Matthias Edler,<sup>1</sup> Petra Kaschnitz,<sup>4</sup> Gerald Pinter,<sup>3</sup> Gregor Trimmel,<sup>4</sup>  
Sandra Schlägl,<sup>2</sup> Thomas Griesser<sup>1</sup>

<sup>1</sup>Chair of Chemistry of Polymeric Materials & Christian Doppler Laboratory for Functional and Polymer Based Ink-Jet Inks, University of Leoben, Otto-Glöckel-Strasse 2, Leoben, 8700, Austria

<sup>2</sup>Polymer Competence Center Leoben GmbH, Roseggerstrasse 12, Leoben, 8700, Austria

<sup>3</sup>Chair of Material Science and Testing of Polymers, University of Leoben, Otto-Glöckel-Strasse 2, Leoben, 8700, Austria

<sup>4</sup>Institute for Chemistry and Technology of Materials (ICTM), NAWI Graz, University of Technology, Stremayrgasse 9, Graz, 8010, Austria

Correspondence to: T. Griesser (E-mail: thomas.griesser@unileoben.ac.at)

Received 28 April 2016; accepted 18 July 2016; published online 2 August 2016

DOI: 10.1002/pola.28239

**ABSTRACT:** The last decade has seen a remarkable interest in the development of biocompatible monomers for the realization of patient specific medical devices by means of UV-based additive manufacturing technologies. This contribution deals with the synthesis and investigation of novel thiol-yne based monomers with a focus on their biocompatibility and also the mechanical properties in their cured state. It could be successfully shown that propargyl and but-1-yne-4-yl ether derivatives have a significant lower cytotoxicity than the corresponding (meth)acrylates with similar backbones. Together with appropriate thiol monomers, these compounds show reactivities in the range of (meth)acrylates and almost quantitative triple

bond conversions. A particular highlight is the investigation of the network properties of photo cured alkynyl ether/thiol resins by means of low field solid state nuclear magnetic resonance spectroscopy. Additionally, dynamic mechanical analysis of those polymers revealed that monomers containing rigid backbones lead to moduli and glass transition temperatures ( $T_g$ 's), sufficiently high for the fabrication of medical devices by UV based additive manufacturing methods. © 2016 Wiley Periodicals, Inc. *J. Polym. Sci., Part A: Polym. Chem.* **2016**, *54*, 3484–3494

**KEYWORDS:** low cytotoxicity; photopolymers; thiol-yne

**INTRODUCTION** Recent years have seen an increasing interest in the development of biocompatible, UV curable monomers for medical applications.<sup>1</sup> This fact can mainly be explained by the rapid progress in UV-based additive manufacturing technologies (AMTs), such as stereolithography, digital light processing, or three-dimensional (3D) ink-jet printing, which enable fast, accurate, and individual fabrication of biocompatible structures.<sup>2</sup>

Currently, monomers based on (meth)acrylates are the state-of-the-art UV curable materials for protective and decorative coatings.<sup>3–5</sup> These building blocks are characterized by their excellent storage stability and fast curing rates. Moreover, the mechanical properties of the resulting polymers can easily be adjusted by the choice of different spacers in photopolymerizable oligomers and by using different types of low molecular mono-, di-, and multifunctional (meth)acrylates as

reactive diluents. One considerable drawback of this class of chemical compounds is their comparably high irritancy and even cytotoxicity in their uncured state.<sup>6,7</sup> This disadvantageous behavior can be mainly attributed to the reactivity of the acrylate double bond toward Michael addition reactions with amino- or thiol-groups of proteins or DNA.<sup>8</sup> This fact, together with the incomplete curing behavior of (meth)acrylates (double bond conversions in the range of 60%–90% can usually be obtained) prevents their usability for medical purposes, that is, for materials which remain in contact with or within the human body.

Recently, several alternative radical curable functionalities, such as vinylcarbonates, vinylesters, and vinylcarbamates have been introduced as interesting alternatives to (meth)acrylate based resins providing a significant lower cytotoxicity.<sup>1,2,9</sup> However, the need of expensive reagents for the synthesis of

Additional Supporting Information may be found in the online version of this article.

© 2016 Wiley Periodicals, Inc.

those monomers along with their comparably low homopolymerization rates may explain why such resins have not entered the market so far.<sup>1</sup> In particular, compounds bearing easily abstractable hydrogens as, for example, in oligo ethylene glycol units are far less reactive than the corresponding acrylates. Although the addition of multifunctional thiols, which also provide very low cytotoxicity, accelerates the curing rates of those monomers toward values of acrylates, the Young's modulus and the glass transition temperature are lowered significantly. This fact can be attributed to a decrease in the cross-link density and also to the flexibility of the commonly used thiol compounds, that is, mercapto propionic ester derivatives, and the formed thioether bonds.<sup>9</sup>

In general, the addition of thiols to ene-monomers results in reduced resin stability (shelf-life) due to occurring dark polymerization reactions.<sup>10</sup> Another mentionable drawback is the characteristic odor of thiol monomers. Due to the limited network properties, thiol-ene photopolymers do not fulfill the demands of medical applications, such as dental restoratives or hard tissue replacements.<sup>11</sup> This fundamental limitation of the thiol-ene step growth polymerization is explained by the fact that each ene functional group reacts only once with a thiol, whereas in chain growth polymerization, each ene group becomes part of a polymer chain leading to higher network densities. Numerous approaches have been undertaken to increase the mechanical properties of thiol-ene polymers by using rigid ene and thiol compounds or monomers which are capable to form hydrogen bonds.<sup>10,12–15</sup>

Another possibility to enhance the network properties is to increase the network density of such photopolymers. An elegant approach is to use multifunctional alkynes instead of ene monomers.<sup>16–19</sup> In this so called thiol-yne polymerization an yne functional group reacts with a thiol to form a vinylsulfide, which can subsequently react with another thiol. Outside of the dual reactivity that offers a significant increase in the cross-link density, all other characteristics of the thiol-yne photopolymerization follow the ideal click reaction paradigm of thiol-ene systems. The polymerization is highly efficient and relatively unaffected by oxygen, ensuring the formed network being nearly ideal in homogeneity.

Fairbanks et al. studied systematically the relative reactivities of a range of different yne monomers revealing high reaction rates for terminal alkynes and propargyl esters.<sup>20</sup> Only moderate polymerization rates were found for propargylethers and internal alkynes. Cyclooctyne, methylpropargylamine and ethyl propiolate do not show this bireactive character.

Very recently, Pretzel et al. investigated the cytotoxic potential of internal alkynes. It was found that besides the type of the polymerizable moiety, also the spacer group of photo-reactive building blocks exerts significant influence on the curing and cytotoxic behavior.<sup>21</sup> Moreover, the network properties of the cured monomers strongly depend on the type and flexibility of the spacer. For example, monomers containing rigid structures such as bisphenol A moieties,

which are known to offer high moduli and high  $T_g$ 's, lead to comparably low curing rates and double bond conversions.<sup>22</sup>

Taking those facts into account, in the present article, the curing and cytotoxic behavior of propargyl and but-1-yne-4-yl monomers containing butyl (C4) spacers, that is, butanediol dipropargyl ether (BuPE) and butanediol di-1-butynyl ether (BuBE), were investigated and compared with the corresponding (meth)acrylate based compounds butanediol dimethacrylate (BuMAc) and butanediol diacrylate (BuAc). The network properties (cross-link density, glass transition temperature, and storage modulus) of these thiol-yne polymers were studied by solid state nuclear magnetic resonance (NMR) and dynamic mechanical analysis (DMA) measurements. Additionally, a second class of alkynyl ether based monomers bearing rigid spacers was investigated considering reactivity and network properties after UV polymerization. This study reveals the versatility of those monomers for the individual and patient customized fabrication of medical devices by UV-based additive manufacturing methods.

## EXPERIMENTAL

### NMR Studies

<sup>1</sup>H-NMR and <sup>13</sup>C-NMR spectra were recorded on a Varian 400-NMR spectrometer operating at 399.66 and 100.5 MHz, respectively, and were referenced to Si(CH<sub>3</sub>)<sub>4</sub>. For the acquisition of the <sup>1</sup>H-NMR spectra a relaxation delay of 10 s and a 45° pulse were used. The NMR spectra were referenced to solvent residual peaks according to values given in the literature.<sup>23</sup>

<sup>1</sup>H-NMR spectra for real-time experiments were recorded on a Varian INOVA 500 MHz spectrometer operating at 499.803 MHz and were referenced to Si(CH<sub>3</sub>)<sub>4</sub>. A relaxation delay of 1 s and 45° pulse were used for acquisition of the <sup>1</sup>H-NMR spectra. The measurements were performed at 37 °C.

Low field NMR measurements were recorded on a Bruker minispec mq20 NF series spectrometer equipped with a 0.47 T magnet (<sup>1</sup>H resonance frequency of 20 MHz) and a ratio probe. The 90°, 180° pulse lengths and the receiver dead time were 2.8, 5.7, and 9 μs, respectively. The sample was cut into stripes, which were vertically stacked into the sample tube to fill a cylindrical volume of 8 mm diameter and 8 mm height. Measurements were carried out at 100 °C after an equilibration time of about 45 min. The sample was heated by dry air and the temperature regulated with a BVT3000 variable temperature controller.

DQ NMR measurements were carried out with the so-called 5-pulse segment<sup>24</sup> and the modified Baum-pines sequence. Further details of the measurement principle are given in the Supporting Information and were reviewed elsewhere.<sup>25</sup>

### Real-Time FT-IR Measurements

Kinetic real-time FT-IR measurements were conducted on a VERTEX 70 (Bruker, Billerica) in reflection mode with the unit A513. About 1 μL of the resin of investigation was

placed in between two CaF<sub>2</sub> windows (8 mm diameter, 1 mm thickness) and illuminated with an Omnicure s1000 (Lumen Dynamics, Mississauga) with 9 cm gap between the sample and light guide ( $P = 22 \text{ mW/cm}^2$  at the sample surface). For real-time FT-IR measurements the corresponding monomers were mixed with 5 wt % of the photoinitiator blend, diphenyl(2,4,6-trimethylbenzoyl)phosphine oxide/2-hydroxy-2-methylpropiophenone and a stoichiometric amount of trimethylolpropane tris(3-mercaptopropionate) (TMPMP). The corresponding (meth)acrylates were prepared without any thiol component. For thermal post-curing the sample was placed on a 100 °C heated plate and illuminated stepwise with the same intensity as described above.

#### Photo-DSC

The photo-DSC experiments were performed on a NETZSCH photo-DSC 204 F1 Phoenix. All measurements were conducted at 50 °C in aluminum crucibles under nitrogen atmosphere. Sample quantity was 8 mg of resin, which was prepared in the same way as being described for real-time FT-IR measurements [5 wt % of the photoinitiator blend, diphenyl(2,4,6-trimethylbenzoyl)phosphine oxide/2-hydroxy-2-methylpropiophenone and a stoichiometric amount of TMPMP]. The Omnicure s2000 was used as the light source at  $1 \text{ W/cm}^2$  resulting in an intensity of  $80 \text{ mW/cm}^2$  at the surface of the sample (range of wavelength was 250–445 nm). For the determination of the reaction enthalpy and  $t_{\text{max}}$  the samples were illuminated twice for 10 min each with an idle time of 2 min in between. For the analysis, the second run was subtracted from the first one to obtain the reaction enthalpy curve.

#### Sample Preparation

For the determination of the thermomechanical properties of derived photopolymers sample specimens with  $2 \times 5 \times 20 \text{ mm}$  rectangular dimensions, respectively, were fabricated in PTFE molds. The resin samples were photocured by a Lighthammer 6 (Fusion UV Systems) with a Hg bulb (4 passes each side, belt speed of 4 m/min, 40% light intensity,  $E = 4.7 \text{ J/cm}^2$ ). The resin contained the corresponding alkyne with a stoichiometric amount of silanetetratyltetrakis(propene-1-thiol) and 3 wt % of the photoinitiator Irgacure® TPO-L. The  $T_g$  was determined at the maximum of  $\tan \delta$ .

#### Dynamic Mechanical Thermal Analysis (DMA)

The thermomechanical properties were measured in tension mode using a DMA/SDTA 861 (Mettler Toledo) with a heating rate of 2 K/min in the temperature range from  $-40 \text{ °C}$  to  $115 \text{ °C}$ . The operating frequency was determined at 1 Hz. For comparison of the alkyne ether formulations, the storage modulus was evaluated at room temperature (37 °C) and the glass transition temperature was determined at the maximum of  $\tan \delta$ .

#### Viscosity Measurements

The viscosities of the monomers were determined using an Anton Paar rheometer (MCR-102, Graz, Austria) in a cone-plate system setup with titanium cone (MK 22/60 mm, 0.58°) with an opening angle of 0.58° and a diameter of

60 mm at a shear rate of  $300 \text{ s}^{-1}$ . The viscosity was measured at 25 °C.

#### Cytotoxicity

The cytotoxicity experiments were conducted at Cytox biologische Sicherheitsprüfungen (Bayreuth, Germany) according to ISO 10993-5:2009. For these tests mouse fibroblast cells (L929) were used. Cells were cultured for 24 h in Dulbecco's modified Eagle's medium (DMEM) with added antibiotics, supplemented with 10% fetal calf serum at 37 °C in an incubator with 5% CO<sub>2</sub>. Four different concentrations of the examined substance (dissolved in DMSO) were applied onto the cells and incubated for 48 h at 37 °C with 5% CO<sub>2</sub>. The final concentration of DMSO in all cavities in the cell culture medium was 1% (v/v). Triton X 100 was used as toxic positive control [final concentration 1% (v/v)] and the cell culture medium was used as non-toxic negative control. All experiments were conducted four times simultaneously. After the incubation the L929-cells were washed with phosphate buffered saline (PBS), and after an alkaline lysis step the protein concentration was determined via the Bradford method. Graphical illustrations of the protein content in dependence of the monomer concentration can be found in the Supporting Information.

#### Materials

2-Hydroxyethyl acrylate (Sigma Aldrich, 96%), 2-hydroxyethyl methacrylate (Sigma Aldrich, 99%), ethanolamine hydrochloride (Sigma Aldrich, 99%), 2-(2-methoxyethoxy)ethanethiol (97%), 1,4-dibromobutane (Sigma Aldrich, 99%), 2-propyn-1-ol (Sigma Aldrich, 99%), 3-butyn-1-ol (Sigma Aldrich, 97%), sodium hydride (Sigma Aldrich, 60% dispersion), tetrabutylammonium iodide (Sigma Aldrich, 98%), bisphenol A (Sigma Aldrich, 99%), ethylene carbonate (Sigma Aldrich, 99%), 3-bromo-1-propyne (Sigma Aldrich, 80 wt % in toluene), tetrachlorosilane (Sigma Aldrich, 99%), magnesium (Sigma Aldrich, 99.9%), 3-chloro-1-propene (Sigma Aldrich, 99%), 2,2'-azobis(2-methylpropanionitrile) (Fluka), thioacetic acid (Sigma Aldrich, 96%), ethyl(2,4,6-trimethylbenzoyl)phenylphosphinate (Irgacure® TPO-L, BASF), diphenyl(2,4,6-trimethylbenzoyl)phosphine oxide/2-hydroxy-2-methylpropiophenone, blend (Sigma Aldrich), pentaerythritol tetra(3-mercaptopropionate) (PETMP) (Sigma Aldrich, 99%), and trimethylolpropane tri(3-mercaptopropionate) (TMPMP) (Bruno Bock Chemische Fabrik GmbH & Co. KG) were used as received. 1,4-Butanediol diacrylate (abcr GmbH) and 1,4-butanediol dimethacrylate (abcr GmbH, 90%) have been purified by flash chromatography prior usage. Tetra(3-mercaptopropyl)silane (TMPS) was synthesized according to literature.<sup>26</sup>

#### Synthesis

##### 1,4-Butanediol dipropargyl Ether (BuPE)

In a three-neck round-bottom flask 2.4 g (100.0 mmol, 2.7 eq) sodium hydride was washed two times with n-hexane and afterward suspended in 50 mL DMF. The mixture was purged with nitrogen and cooled down to  $-10 \text{ °C}$  in an ethanol cooling bath. About 5.4 g (96.3 mmol, 2.6 eq) 2-propyn-

1-ol in 50 mL DMF was added dropwise over 30 min. The mixture was stirred for 2 h. Eight grams of (37.1 mmol) 1,4-dibromobutane in 50 mL DMF was added dropwise over a time span of 30 min. The reaction mixture was kept at 0 °C for further 3 h and quenched afterward with a saturated ammonium chloride solution. Afterward the mixture was extracted three times with diethyl ether and dried over Na<sub>2</sub>SO<sub>4</sub>. The combined organic extracts were concentrated under reduced pressure at elevated temperature to remove the excess of 2-propyn-1-ol and residual DMF. The crude product was further purified by flash column chromatography (ethyl acetate:cyclohexane 1:10) leading to 5.3 g (yield: 86%) of BuPE as a transparent and colorless liquid.

<sup>1</sup>H-NMR (δ, 400 MHz, 25 °C, CDCl<sub>3</sub>): 4.11 (d, 4H, CH<sub>2</sub>-C≡C); 3.52 (m, 4H, CH<sub>2</sub>-O); 2.52 (t, 2H, C≡CH); 1.66 (m, 4H, CH<sub>2</sub>-CH<sub>2</sub>-O) ppm.

<sup>13</sup>C-NMR: (δ, 100 MHz, 25 °C, CDCl<sub>3</sub>): 79.92 (s, 2C, -C≡C); 74.01 (s, 2C, -C≡C); 69.68 (s, 2C, C-O); 57.93 (s, 2C, C-C≡C); 26.08 (s, 2C, C-C-O) ppm.

#### 1,4-Butanediol dibut-3-yn-1-yl Ether (BuBE)

In a 500 mL three-neck round-bottom flask 3.00 g (12.5 mmol, 2.5 eq.) sodium hydride was washed two times with n-hexane and afterward suspended in 150 mL DMF. The mixture was purged with nitrogen and cooled down to -10 °C in an ethanol cooling bath. About 21.20 g 3-butyne-1-ol (300 mmol, 6 eq.) in 50 mL DMF was added dropwise over 30 min. The mixture was stirred for 2.5 h while the temperature was kept around 0 °C. About 1.30 g tetrabutylammonium iodide (3.5 mmol; 0.07 eq.) was added to the mixture before a solution of 10.80 g 1,4-dibromobutane (50 mmol) in 40 mL DMF was added dropwise over a time span of 30 min. The reaction mixture was kept at 0 °C for 4 h and quenched with a saturated solution ammonium chloride. Afterward the mixture was extracted three times with diethyl ether and dried over Na<sub>2</sub>SO<sub>4</sub>. The combined organic extracts were concentrated under reduced pressure at elevated temperature to remove the excess of 3-butyne-1-ol and residual DMF. The crude product was further purified by flash column chromatography (ethyl acetate:cyclohexane 1:20 → 1:10) leading to 3.3 g (yield: 34%) of BuBE as a transparent and colorless liquid.

<sup>1</sup>H-NMR (δ, 400 MHz, 25 °C, CDCl<sub>3</sub>): 3.55–3.48 (m, 8H, CH<sub>2</sub>-O-CH<sub>2</sub>); 2.45 (t, 4H, CH<sub>2</sub>-C≡C); 1.97 (t, 2H, C≡C-H); 1.65 (m, 4H, O-CH<sub>2</sub>-CH<sub>2</sub>) ppm.

<sup>13</sup>C-NMR: (δ, 100 MHz, 25 °C, CDCl<sub>3</sub>): 81.4 (s, 2C, -C≡C); 70.7 (s, 2C, O-C); 69.2 (s, 2C, -C≡C); 68.7 (s, 2C, C-C≡C); 26.2 (s, 2C, C-C-C); 19.8 (s, 2C, C-C≡C) ppm.

#### 2,2-Bis[4-(2-hydroxy)ethoxyphenyl]propane (BisAE)

The product was synthesized according to a modified literature procedure.<sup>27</sup> In a three-neck round-bottom flask equipped with a reflux condenser 20 g (87.6 mmol) bisphenol A and 17.7 g (201.5 mmol, 2.3 eq.) ethylene carbonate were added to 24.2 g (175 mmol, 2 eq.) K<sub>2</sub>CO<sub>3</sub> in 300 mL

DMF and refluxed at 145 °C for 3 h. The reaction mixture was then poured into 1.5 L deionized water. The resulting white precipitate was filtered and washed with water, with methanol and afterward with a small amount of cold THF. The remaining white powder was dried under vacuum at 70 °C to yield 18.0 g (65%) of BisAE.

<sup>1</sup>H-NMR (δ, 400 MHz, 25 °C, CDCl<sub>3</sub>): 7.15–7.13 (d, 4H, Ar-H); 6.83–6.81 (d, 4H, Ar-H); 4.07 (t, 4H, -CH<sub>2</sub>-O-); 3.95 (m, 4H, -CH<sub>2</sub>-OH); 1.64 (s, 6H, -CH<sub>3</sub>) ppm.

<sup>13</sup>C-NMR: (δ, 100 MHz, 25 °C, CDCl<sub>3</sub>): 156.42 (2C, Ar-C-O), 143.57 (2C, Ar-C), 127.78 (4C, Ar-C), 113.92 (4C, Ar-C), 69.09 (2C, O-C), 61.53 (2C, C-OH), 41.72 (1C, C-CH<sub>3</sub>), 31.02 (2C, CH<sub>3</sub>); ppm

#### 2,2-Bis[4-(2-(prop-2-yn-1-yloxy)ethoxyphenyl)]propane (BisAEPE)

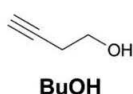
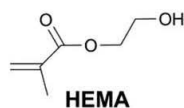
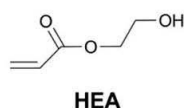
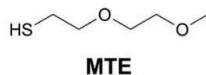
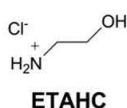
In a 250 mL three-neck round-bottom flask 0.9 g (37.9 mmol, 2.4 eq.) sodium hydride was washed with n-hexane and afterward suspended in 30 mL DMF. The mixture was purged with nitrogen and cooled down to -10 °C in an ethanol cooling bath. Five grams (15.8 mmol) of BisAE were dissolved in 30 mL DMF and added dropwise over 30 min. The mixture was stirred for 1 h while the temperature was kept around 0 °C. A solution of 4.7 g (39.5 mmol, 2.5 eq.) 3-bromo-1-propyne in 30 mL DMF was added dropwise over a time span of 30 min. The reaction mixture was stirred for 2 h while the mixture was allowed to reach room temperature. It was then quenched with a saturated solution of ammonium chloride, extracted with diethyl ether and dried over Na<sub>2</sub>SO<sub>4</sub>. The combined organic extracts were concentrated under reduced pressure to receive the crude product, which was further purified by flash column chromatography (ethyl acetate:cyclohexane 1:3) to yield 5.4 g (87%) of BisAEPE as a transparent, yellowish liquid.

<sup>1</sup>H-NMR (δ, 400 MHz, 25 °C, CDCl<sub>3</sub>): 7.13–7.11 (d, 4H, Ar-H); 6.83–6.81 (d, 4H, Ar-H); 4.27 (d, 4H, CH<sub>2</sub>-C≡C); 4.13 (t, 4H, CH<sub>2</sub>-O-Ar); 3.89 (t, 4H, CH<sub>2</sub>-O); 2.45 (t, 2H, C≡C-H); 1.63 (s, 6H, CH<sub>3</sub>) ppm.

<sup>13</sup>C-NMR: (δ, 100 MHz, 25 °C, CDCl<sub>3</sub>): 156.47 (s, 2C, Ar-C-O); 143.41 (s, 2C, Ar-C); 127.69 (s, 4C, Ar-C); 113.94 (s, 4C, Ar-C); 79.49 (s, 2C, -C≡C); 74.69 (s, 2C, -C≡C); 68.26 (s, 2C, O-C); 67.11 (s, 2C, Ar-O-C); 58.53 (s, 2C, C-C≡C); 41.68 (s, 1C, Cq); 31.03 (s, 2C, CH<sub>3</sub>) ppm.

#### 2,2-Bis[4-(prop-2-yn-1-yloxy)phenyl]propane (BisAPE)

In a 250 mL three-neck round-bottom flask 1.3 g (52.6 mmol, 2.4 eq.) sodium hydride was washed with n-hexane and afterward suspended in 50 mL DMF. The mixture was purged with nitrogen and cooled down to -10 °C in an ethanol cooling bath. Five grams (21.9 mmol) of bisphenol A was dissolved in 50 mL DMF and added dropwise over 30 min. The mixture was stirred for 1 h while the temperature was kept around 0 °C. A solution of 6.8 g (57.2 mmol, 2.6 eq.) 3-bromo-1-propyne in 30 mL DMF was added dropwise over a time span of 30 min. The reaction mixture was stirred for

**Michael acceptors****Michael donors**

**SCHEME 1** Water soluble model compounds [HEA, 2-hydroxyethyl acrylate; HEMA, 2-hydroxymethyl acrylate; BuOH, 3-butyne-1-ol; ETAHC, ethanolamine hydrochloride; MTE, 2-(2-methoxyethoxy)ethanethiol] used for the evaluation of the reactivity of unsaturated functional groups.

2 h while the mixture was allowed to reach room temperature. It was then quenched with a saturated solution of ammonium chloride, extracted with diethyl ether and dried over  $\text{Na}_2\text{SO}_4$ . The combined organic extracts were concentrated under reduced pressure to receive the crude product, which was further purified by flash column chromatography (ethyl acetate:cyclohexane 1:5) to yield 6.1 g (92%) of BisAPE as a transparent and yellow liquid.

$^1\text{H-NMR}$  ( $\delta$ , 400 MHz, 25 °C,  $\text{CDCl}_3$ ): 7.17–7.15 (d, 4H, Ar-H); 6.89–6.87 (d, 4H, Ar-H); 4.67 (d, 4H, C=C-H); 2.52 (t, 2H, C=C-H); 1.64 (s, 6H,  $\text{CH}_3$ ) ppm.

$^{13}\text{C-NMR}$ : ( $\delta$ , 100 MHz, 25 °C,  $\text{CDCl}_3$ ): 155.4 (s, 2C, Ar-C); 143.9 (s, 2C, Ar-C); 127.7 (s, 4C, Ar-C), 114.2 (s, 4C, Ar-C); 78.8 (s, 2C, C=C); 75.35 (s, 2C, C=C); 55.8 (s, 2C, O-C); 41.8 (s, 1C, Cq.); 30.9 (s, 2C,  $\text{CH}_3$ ) ppm.

**RESULTS AND DISCUSSION****Reactivity of Monomer Model Compounds Under Physiological Conditions**

The cytotoxicity of state-of-the-art building blocks can be attributed to their reactivity toward amino- or thiol-groups of proteins or DNA.<sup>8</sup> In general, the electron density of unsaturated compounds, that is, the Michael acceptor, strongly determines the reactivity with (hetero) Michael donors.<sup>28,29</sup> Both facts can explain the lower cytotoxicity of methacrylates compared with their acrylate counterparts due to the higher electron density induced by the additional methyl group. Moreover, it is well reported that terminal alkyne groups, without electron withdrawing moieties in

their neighborhood, are mostly inert in the thiol Michael reaction even under basic conditions.<sup>30</sup>

The reactivity of radically polymerizable moieties toward amino and mercapto groups under physiological conditions was studied by  $^1\text{H-NMR}$  spectroscopy using  $\text{D}_2\text{O}$  soluble model compounds (as shown in Scheme 1). Taking into Account the pH-Value (pH  $\sim$  7.4) and the puffer capacity of blood, as well as the comparably high  $\text{pK}_b$  value of primary amines, it can be assumed that the majority of protein or DNA related amino groups exist in their protonated state. Considering this fact and the lower nucleophilicity of protonated amines, ethanolamine hydrochloride was chosen as model compound in the following experiments. For the exclusion of radical mediated reactions (e.g., thiol-ene) 0.1 wt % of pyrogallol was added as radical scavenger in all samples. Figure 1 shows the double bond conversion (DBC) of the (meth)acrylate model compounds during storage determined by kinetic NMR measurements at body temperature (37 °C). As expected, the acrylate, that is, HEA, shows the highest reactivity toward both nucleophiles. While the reaction with the mercapto group proceeds quantitatively within several minutes, a conversion of 30% was reached with ETAHC after 30 h.

Detailed NMR spectra confirmed the formation of the thiol Michael adduct, whereas the reaction with ETAHC lead to several by-products. Presumably, the formed secondary amine undergoes a subsequent Michael addition; furthermore, hydrolytic cleavage reactions of present ester groups are conceivable.

In contrast, HEMA shows a significant lower reactivity in both cases. Although it also provides full conversion in the reaction with MTE after 19 h, no formation of the aza Michael adduct could be observed, which can be assigned to the higher electron density of the C=C double bond (vide

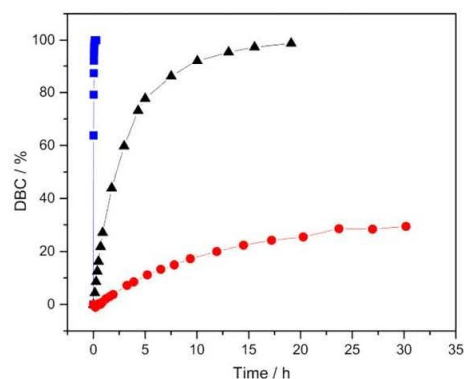
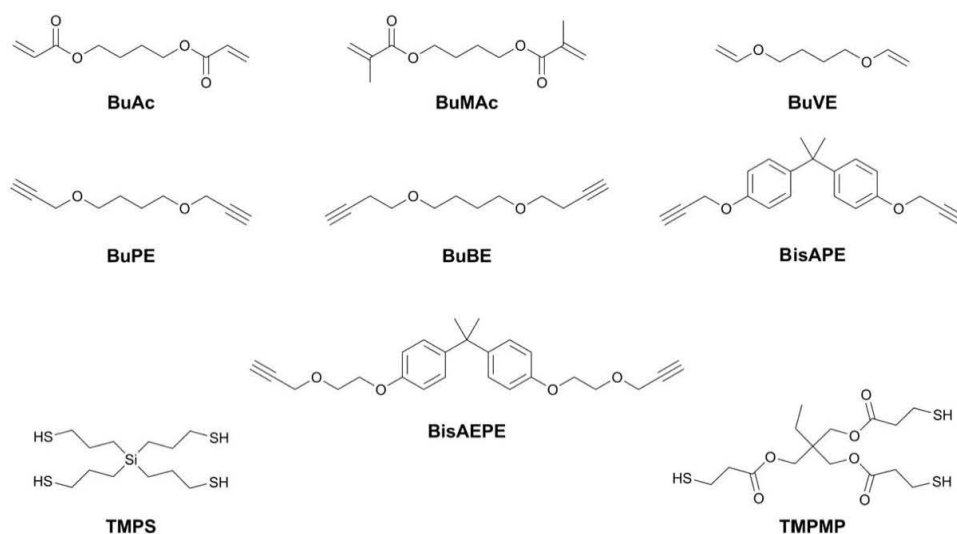


**FIGURE 1** Double bond conversion (DBC) of HEA/MTE (squares), HEMA/MTE (triangles), and HEA/ETAHC (circles) under simulated physiological conditions. [Color figure can be viewed in the online issue, which is available at [wileyonlinelibrary.com](http://wileyonlinelibrary.com).]



**SCHEME 2** Structures of the investigated monomers.

supra). Importantly, under these conditions, the terminal alkyne group undergoes no reaction with any of the two Michael donors, neither with mercapto, nor with amino hydrochloride groups.

#### Synthesis of Alkynyl Ether Monomers

An overview of the synthesized alkynyl ether based monomers is given in Scheme 2. A straightforward procedure for the preparation of those bifunctional ether derivatives, that is, BuPE, BuBE, BisAPE, and BisAEPE, represents the well described Williamson etherification reaction using hydroxyl- and bromo-functionalized starting compounds. For the synthesis of BisAEPE, the intermediate 2,2-bis[4-(2-hydroxy)ethoxyphenyl]propane was obtained by a reaction of bisphenol A with ethylene carbonate as described elsewhere.<sup>12</sup> In a first step, the hydroxyl terminated bifunctional spacers were converted with sodium hydride to the corresponding sodium alkoxylates, which were subsequently reacted with propargyl bromide to give BuPE, BisAPE, and BisAEPE in appropriate yields of 86%, 92%, and 87%. This reaction strategy, however, failed for the synthesis of the but-1-yne-4-yl ether derivatives leading to an isomerization of the triple bond and the formation of internal 2-yne. Alternatively, but-1-yne-4-yl ether monomers could be synthesized by the reaction of the sodium 3-butyne-1-olate with brominated bifunctional compounds as reported previously.<sup>31</sup> BuBE was obtained in moderate yields of 34% after purification by column chromatography. The synthesized monomers were characterized by <sup>1</sup>H- and <sup>13</sup>C-NMR spectroscopy. The obtained data are in good agreement with the proposed structures.

#### Monomers with C4 Spacer

Besides the type of unsaturated polymerizable moiety and its reactivity toward the thiol and aza Michael reaction, also the group of photoreactive building blocks exerts significant influence on the cytotoxic behavior, which is a key requirement for UV curable resins for biomedical applications. For that reason the cytotoxic potential of the synthesized alkyne ether monomers with aliphatic C4 spacer, that is, BuPE and BuBE, was determined by *in-vitro* tests using mouse fibroblast cells (L929, ISO 10993-5:2009) and compared with the cytotoxicity of BuAc and BuMAc. Consequently, L929 cells were incubated in a defined media with increasing concentrations of the monomers for 48 h at 37 °C. The concentration at which the half of the cells remained alive compared with the negative control (cell culture medium, see Supporting Information) was assessed as cell viability (EC50). The (meth)acrylate based compounds (BuAc and BuMAc) exhibit a significant higher cytotoxicity than the alkynyl ethers BuPE and BuBE by at least a factor of 12 (as shown in Table 1). This finding is in good accordance with the observed inertia of terminal alkyne groups toward the thiol and aza Michael reaction. Thus, it could be demonstrated that alkynyl ether derivatives are a potential alternative to common (meth)acrylate based monomer systems.

Further important key factors for the fabrication of medical devices by photolithographic AMT techniques, are the rate and yield of photopolymerization, as both determine the amount of leachable monomers in the build device. Besides health considerations, residual monomers can also reduce the network properties, that is, mechanical properties and glass transition temperature, of the cured materials. The curing behavior of resins based on propargyl and but-1-yne-4-yl

**TABLE 1** Cell Viability of Investigated Monomers From Cytotoxicity Tests

Monomer	Viability (EC50)/mM
BuMAc	<0.16
BuAc	<0.16
BuPE	3
BuBE	2

monomers containing butyl (C4) spacers and the commercially available multifunctional thiol TMPMP were investigated by means of photo-DSC and FT-IR spectroscopy and compared with the corresponding (meth)acrylate based compounds BuMAc and BuAc. One important parameter, which can be obtained by photo-DSC, is the time to reach the maximum of polymerization enthalpy ( $t_{max}$ ) revealing information about the curing speed of the investigated system. Alternatively, real-time FT-IR spectroscopy provides detailed information on changes in the molecular structure of the monomers during the curing reaction, enabling the precise monitoring of the conversion of polymerizable groups with increasing illumination time.

Although, it has been reported that propargyl ether derivatives offer moderate rates of polymerization compared with aliphatic terminal alkynes and propargyl esters,<sup>20</sup> BuPE can easily compete with the methacrylate based monomer BuMAc which is reflected by the significant lower  $t_{max}$  as depicted in Table 2. Interestingly, the but-1-yne-4-yl ether derivative BuBE outperforms BuPE and BuMAc considerably and reacts only slightly slower than the structurally related aliphatic acrylate BuAc. The superiority of the but-1-yne-4-yl ether derivative might be explained by the additional CH<sub>2</sub> group between the alkyne and ether group reducing the influence of the ether moiety (+I-effect) on the electronic density of the yne triple bond. This hypothesis is supported by the outstanding reactivity of aliphatic terminal alkynes, which react significantly faster than propargyl ethers in the

thiol-yne reaction. However, a general prediction of reactivities based on the electronic density of polymerizable groups, as possible for the thiol-ene reaction, is problematic in case of the thiol-yne polymerization, which was shown by Fairbanks et al. at the example of propargyl acetate, methyl propargyl amine and ethyl propiolate.<sup>20</sup>

Figure 2 (above) shows the thiol and alkyne conversions for 2:1 stoichiometric reactions of BuPE/TMPMP and BuBE/TMPMP determined by real-time FT-IR spectroscopy, confirming the findings in the photo-DSC measurements and underlining the superiority of the but-1-yne-4-yl derivative in terms of reaction rate. It has to be mentioned that each alkyne and thiol monomer is consumed simultaneously and at the same extend, indicating the absence of side reactions such as the homopolymerization of vinylsulfide intermediates or the formation of stable vinylsulfide compounds. Importantly, both alkyne based systems provide a significant higher conversion of polymerizable groups than the curing of the corresponding (meth)acrylates as revealed in Figure 2 (below). While the photopolymerization of BuAc and BuMAc lead to a double bond conversion of 79% and 74% after 2 min of illumination ( $P = 22 \text{ mW/cm}^2$ ), respectively, an almost quantitative consumption of alkyne and thiol groups were obtained for resins of BuPE/TMPMP (94%) and BuBE/TMPMP (99%).

One limitation of thiol based photopolymers can mainly be attributed to specific characteristics of the used multifunctional thiols. The predominantly applied and studied thiols are esters of mercapto propionates and thio glycolates, which can be explained by their facile synthesis from readily available precursors. However, the polarity of the ester group and its affinity to water favors water absorption which decreases the mechanical performance by lowering the modulus, glass transition temperature and strength, all factors that are detrimental for medical applications such as implants. One strategy, to overcome this limitation is to use ester-free silane based mercaptanes providing an appropriate curing behavior and good mechanical

**TABLE 2** Summary of Materials Properties for Alkyne Monomers and Their Photocured Alkyne/Thiol Networks Including Reference Samples (BuAc and BuMAc)

Monomer	Viscosity (25 °C)/ mPa*s	$t_{max}$ /s	Conversion (2 min)/ %	$T_g$ /°C	$E'$ at 37 °C/MPa	FWHM/°C
BuVE	–	1.0 <sup>a</sup>	–	–35 ± 0 <sup>b</sup>	17 ± 1 <sup>b</sup>	10 ± 0 <sup>b</sup>
BuMAc	4.7	6.7	74	50 ± 38	1,650 ± 20	–
BuAc	4.4	1.8	79	80 ± 6	1,420 ± 30	–
BuPE	4.7	5.2 <sup>a</sup>	94 <sup>a</sup>	34 ± 1 <sup>b</sup>	255 ± 30 <sup>b</sup>	42 ± 0 <sup>b</sup>
BuBE	6.2	2.3 <sup>a</sup>	99 <sup>a</sup>	36 ± 0 <sup>b</sup>	230 ± 5 <sup>b</sup>	34 ± 1 <sup>b</sup>
BisAEPE	949	6.2 <sup>a</sup>	65 <sup>b</sup> (98) <sup>b,c</sup>	58 ± 0 <sup>b,c</sup>	1,200 ± 75 <sup>b,c</sup>	20 ± 0 <sup>b,c</sup>
BisAPE	596	8.1 <sup>a</sup>	62 <sup>b</sup> (92) <sup>b,c</sup>	100 ± 1 <sup>b,c</sup>	1,860 ± 10 <sup>b,c</sup>	59 ± 0 <sup>b,c</sup>

<sup>a</sup> Corresponds to a formulation with a stoichiometric amount of TMPMP.

<sup>b</sup> Corresponds to a formulation with a stoichiometric amount of TMPMP.

<sup>c</sup> Measured after post-curing at 100 °C.

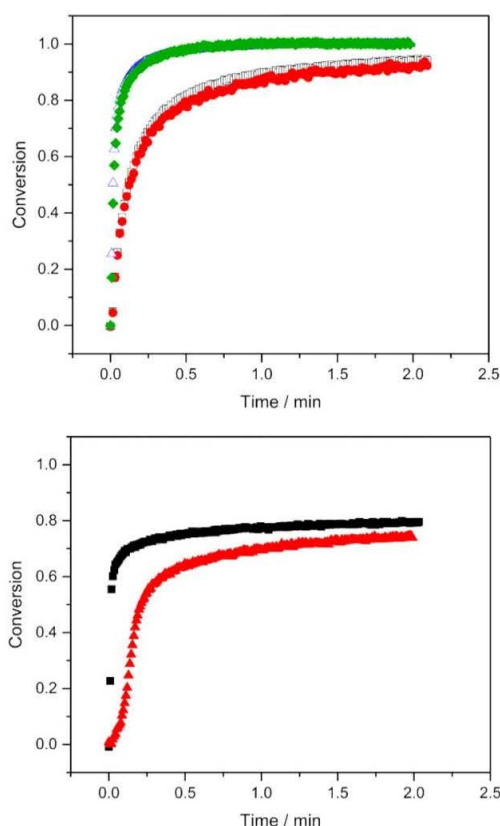


**FIGURE 2** Real-time FT-IR measurements: Conversion of alkyne and thiol moieties [above: BuBE (open triangle)/TMPMP (diamond), BuPE (open square)/TMPMP (circle)], and the (meth)acrylate groups [below: BuAc (square) and BuMAC (triangle)]. [Color figure can be viewed in the online issue, which is available at [wileyonlinelibrary.com](http://wileyonlinelibrary.com).]

properties in the cured state even after water storage as recently demonstrated.<sup>26,32</sup> Consequently, formulations containing the multifunctional thiol tetra(3-mercaptopropyl)silane (TMPS) instead of TMPMP were used for the characterization of the network properties. The synthesis of TMPS has previously been described in a patent dealing with novel biocompatible thiol-ene based materials for augmentation of hard tissues.<sup>33</sup> As shown recently, this thiol compound offers a comparable reactivity as mercapto propionic acid derivatives.<sup>26</sup>

It has to be mentioned that similar high conversions have been reported for thiol-ene polymerization reactions of vinyl ethers, which are also known to provide good biocompatibility due to their electron rich double bond.<sup>34</sup> However, the comparably low cross-link densities of such thiol-ene networks lead to mechanical properties which are inferior compared with thiol-yne polymers.<sup>17</sup> Besides the mechanical

properties, the cross-link density, together with the structure of the polymer backbone, determines the glass transition temperature of the network, which has to be above body temperature for polymers intended for hard tissue engineering. There are only a few methods reported, which allow for the investigation of the network density of photopolymers. For several reasons some of them, for example, equilibrium swelling, can only be applied to slightly cross-linked polymers.<sup>35–37</sup> For very homogeneous networks, the cross-link density correlates with the glass transition temperature and the storage modulus in the rubbery state.<sup>17</sup>

An alternative method to study network characteristics is the DQ build-up NMR method<sup>38,39</sup> which gives quantitative access to network density as well as the fraction of non-network chains (in this case unreacted monomers, photoinitiator or its cleavage products which are not incorporated in the polymeric network). In simple terms, the residual dipolar couplings ( $D_{res}$ ) measured through this method are influenced by the orientational anisotropy of the chains which is in turn directly proportional to the cross-link density, that is, the molecular weight between the network points, and chain stiffness. The ability of this method to exclusively access  $D_{res}$ , allows a quantitative description of the network, assuming a physically appropriate model is used for analysis.

In this study, DQ NMR has been used to investigate and to compare the cross-link density of a vinyl ether based thiol-ene network with the highly cross-linked alkynyl ether networks. Consequently, butanediol divinylether (BuVE), BuPE, and BuBE (in combination with TMPS) were used as model compounds as these monomers provide a C4 backbone leading to a similar stiffness.

Considering that (a) the network chain length is near-homogenous and (b) any heterogeneity appears only due to the spin-system heterogeneity and/or the different mobility of the two component chains between network points, an analytical model assuming Gaussian distribution of residual dipolar couplings with an average value  $D_{res}$  and its standard deviation  $\sigma_{res}$  accounting for the aforementioned heterogeneity was used (see eq. 1).

Analytical fitting equation assuming Gaussian distribution

$$I_{nDQ}(\tau_{DQ}, D_{res}, \sigma_{res}) = 0.5 \left\{ 1 - \frac{\exp\left(-\frac{2D_{res}^2 \tau_{DQ}^2}{1 + \frac{4}{5}\sigma_{res}^2 \tau_{DQ}^2}\right)}{\sqrt{1 + \frac{4}{5}\sigma_{res}^2 \tau_{DQ}^2}} \right\} \quad (1)$$

The  $D_{res}$  values (which relates to the cross-link density) and the fraction of non-network chains determined for samples BuBE/TMPS and BuPE/TMPS are given in Table 3. For comparison, measurements were also carried out on BuVE/TMPS and for consistency analyzed with the same model. It should be noted for the latter sample, however, that with  $\sigma_{res} \approx D_{res}$  (in other words a too high standard deviation), the limits of applicability of this fit becomes unrealistic. Therefore, the



**TABLE 3** Analysis of the Normalized DQ Curves Obtained for the Different Samples at 100 °C

Sample	$D_{res}/2\pi$ [kHz]	$\sigma_{res}/2\pi$ [kHz]	% Non-Network Chains
BuBE/TMPS	9.0	1.4	4.3
BuPE/TMPS	8.4	2.0	4.6
BuVE/TMPS (Gaussian distribution)	1.4	1.3	2.5

curve was also analyzed with a simple two-component Gaussian fit (see Supporting Information eq. S2).

The analysis (see Table 3) shows an increase in cross-link density by about the factor of six for samples BuBE/TMPS and BuPE/TMPS compared with sample BuVE/TMPS which is in good accordance with the findings of Bowman and co-workers for networks formed of bifunctional ynones and tetrafunctional thiols.<sup>17</sup> The fraction of non-network chains corresponds to the expected amount of unbound species (monomer, photoinitiator, cleavage products). Further details of the analysis and interpretation of the data for sample BuVE/TMPS are given in Supporting Information.

Moreover, the thermo-mechanical properties, that is, the glass transition temperature and the storage modulus in the rubbery state, of the thiol-yne networks are significantly higher than the BuVE network (shown in Fig. 3), which can be directly attributed to the higher cross-link density. The alkynyl ether/TMPS based polymers exhibit significant lower network properties than the corresponding (meth)acrylates BuAc and BuMAc (Table 2 and Fig. 3). While BuAc provides a  $T_g$  (~80 °C) well above the body temperature together with an appropriate storage modulus ( $E' = 1420$  MPa), the glass transition temperature of BuPE/TMPS (34 °C) and BuBE/TMPS (36 °C) is only in the range of body temperature explaining the comparably low moduli (BuBE:  $E' = 230$  MPa; BuPE:  $E' = 260$  MPa) at 37 °C. This fact can be attributed to the rather flexible (thio)ether linkage of the thiol-yne polymers.<sup>40</sup> Interestingly, there is only a slight difference, in the thermo-mechanical properties of BuBE and BuPE, despite two additional carbon atoms per molecule.

The full width at half-maxima (FWHM) of tan delta of the BuBE/TMPS and the BuPE/TMPS networks are approximately three times higher than the one of the BuVE/TMPS network. However, this transition is still narrow compared with chain growth networks, such as BuAc (see Fig. 3). However, materials that offer glass transition temperatures in the range or even below body temperature are not suitable for hard tissue engineering.

#### Monomers Containing Rigid Spacers

One possibility to increase the network properties of photopolymers is to introduce rigid spacers such as biphenyl, isocyanurate,<sup>12</sup> bisphenol A,<sup>41</sup> bisphenol S,<sup>42</sup> etc., in the used

building blocks. This concept is commonly applied for high performance resins such as dental restoratives or automotive and aerospace resins; for example, 2,2-bis-[4-(2-hydroxy-3-methacryloyloxypropoxy)phenyl]-propane (Bis-GMA), is a widely applied monomer in dental practice. Although the stiff molecular structure of Bis-GMA is responsible for the excellent mechanical properties and low polymerization shrinkage, it also leads to an extremely high viscosity and to a comparably low degree of conversion.<sup>22</sup>

However, in these systems the gel point is reached very quickly, which significantly reduces the mobility of the unreacted functional monomers. An additional decrease in mobility can be observed when the  $T_g$  exceeds the polymerization reaction temperature. Both effects limit the final conversion of high viscous monomers containing rigid spacer.<sup>17</sup>

In principle, a similar behavior can also be observed for BisAPE/TMPS and BisAEPE/TMPS formulations as shown in Figure 4. While these bisphenol A based monomers exhibit curing rates in the range of BuPE, which seems to be typical

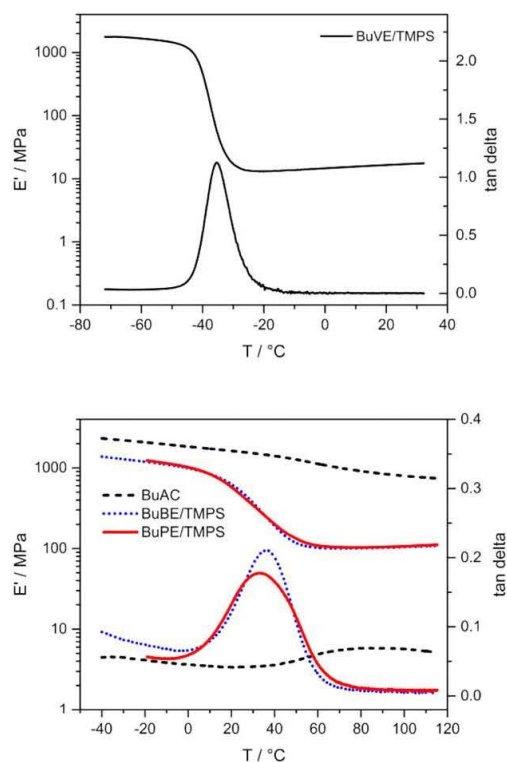


**FIGURE 3** Storage modulus and tan delta versus temperature for the stoichiometrically balanced polymerization of BuVE/TMPS (above), as well as BuAc (below: dashed), BuBE (below: dotted), and BuPE/TMPS (below: solid). [Color figure can be viewed in the online issue, which is available at [wileyonlinelibrary.com](http://wileyonlinelibrary.com).]

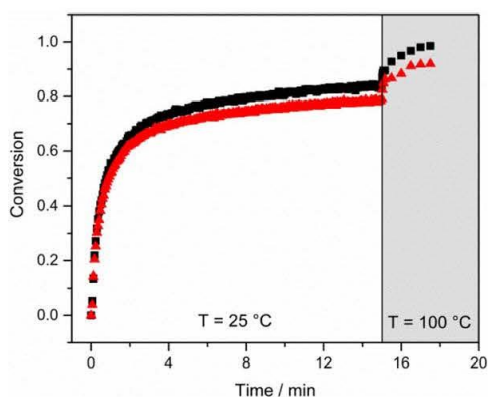


**FIGURE 4** Conversion of the alkyne monomers [BisAEPE (square), BisAPE (triangle)] in alkyne/TMPS formulations versus illumination time. [Color figure can be viewed in the online issue, which is available at [wileyonlinelibrary.com](http://wileyonlinelibrary.com).]

for propargyl ethers, the degree of conversion is comparably low for BisAPE/TMPS (62%) and BisAEPE/TMPS (65%).

However, it can be shown that a post curing of BisAPE and BisAEPE based resins above the  $T_g$  (in this case 100 °C were chosen) significantly increases the degree of conversion of both systems toward 92% (BisAPE) and 98% (BisAEPE), respectively, as demonstrated in Figure 4. This behavior is fully compatible with photolithographic AMT techniques, in which post curing of the printed structures is commonly performed, enabling the fabrication of biomedical devices with a low content of leachable monomeric residues.

As expected the networks formed of monomers with rigid spacers provide a significantly higher  $T_g$  as the corresponding C4 based polymers resulting in  $T_g$ 's which are well above the body temperature as depicted in Figure 5.

In particular, bisphenol A based monomers (with TMPS as thiol component) offer decent storage moduli (comparable to those of the C4 (meth)acrylic monomers) making these materials interesting for biocompatible AMT resins. Additionally, the comparably low FWHM of tan delta of BisAEPE/TMPS has to be highlighted, indicating a very homogeneous network and also providing almost constant mechanical properties over a long range up to 40 °C (=onset temperature of the glass transition; compare Fig. 5).

Another limiting factor of thiol based formulations is their poor shelf-life stability preventing a broad application in the UV curing and coating industry so far.<sup>10</sup> While formulations of BuVE/TMPMP (containing 0.5 wt % of pyrogallol and 2 wt % decylphosphonic acid as stabilizer) showed gelation after 4 h at 50 °C storage temperature, the corresponding thiol-yne resin, that is, BuBE/TMPMP (with the same stabilizer), increased in viscosity by only 22% after 1 week of storage under equal conditions. Presumably, the inertia of the alkyne triple bond toward Michael addition reactions

explains the superiority of the alkyne ether/TMPMP formulation in this accelerated shelf-life tests, which represents another important advantage of the presented thiol-yne system.

## CONCLUSIONS

This contribution deals with the development of new biocompatible monomers based on the thiol-yne reaction for the fabrication of medical devices by UV-based additive manufacturing technologies. It could be successfully shown that propargyl and but-1-yne-4-yl ether derivatives offer a significant lower cytotoxicity than the corresponding (meth)acrylates with similar backbones. Together with appropriate thiol monomers, these compounds show reactivities in the range of acrylates (but-1-yne-4-yl ether) and methacrylates (propargyl ether), respectively, and almost quantitative triple bond conversions. Besides the reaction behavior, also the thermo-mechanical properties as well as the cross-link density of photo cured samples of alkyne ether/thiol networks were investigated by DMA and solid state NMR and compared with those of BuVE/TMPS formulations. Although the BuPE/TMPS and BuBE/TMPS networks provide a six times higher cross-link density and thermo-mechanical properties, which are far above of the corresponding vinyl ether based network (BuVE/TMPS), these polymers show glass transition temperatures which are in the range of the body temperature. By using monomers that contain rigid bisphenol A spacers comparably high triple bond conversions after a post-curing step at elevated temperatures were obtained. The derived polymers show decent storage moduli and  $T_g$ 's which seems to be sufficiently high for the fabrication of medical devices.

Even though, the cytotoxicity of C4 alkyne ethers is far lower than the one of the corresponding (meth)acrylates, the long term toxicity of such compounds, in particular of monomers containing bisphenol A moieties, has to be investigated in

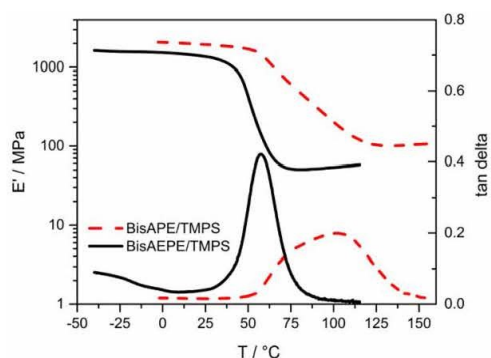


**FIGURE 5** Storage modulus and tan delta versus temperature for stoichiometrically balanced polymerization of BisAEPE/TMPS (solid) and BisAPE/TMPS (dashed). [Color figure can be viewed in the online issue, which is available at [wileyonlinelibrary.com](http://wileyonlinelibrary.com).]

further studies. However, the almost quantitative conversion of the investigated alkynyl ether/thiol resins significantly reduces the migration of potential harmful compounds to a level which cannot be reached by (meth)acrylate monomers.

This study reveals the versatility of this class of monomers paving the way toward the individual and patient specific fabrication of medical devices by UV-based additive manufacturing methods.

#### ACKNOWLEDGMENTS

Financial support by the Christian Doppler Research Association, the Austrian Federal Ministry of Science, Research and Economy (BMWFW), and Durst Phototechnik GmbH is gratefully acknowledged. Part of the research work of this paper was performed at the Polymer Competence Center Leoben GmbH (PCCL, Austria) within the framework of the COMET-program of the Federal Ministry for Transport, Innovation, and Technology and Federal Ministry for Economy, Family and Youth.

#### REFERENCES

- 1 B. Husar, R. Liska, *Chem. Soc. Rev.* **2012**, *41*, 2395.
- 2 C. Heller, M. Schwentenwein, G. Russmüller, T. Koch, D. Moser, C. Schopper, F. Varga, J. Stampfl, R. Liska, *J. Polym. Sci. Part A: Polym. Chem.* **2011**, *49*, 650–661.
- 3 A. B. Scranton, C. N. Bowman, R. W. Peiffer, *Photopolymerization: Fundamentals and Applications*; American Chemical Society: Washington DC, **1997**, vol. 673.
- 4 N. S. Allen, *Photopolymerization and Photoimaging Science and Technology*, 1st ed.; Elsevier Applied Science: London, **1989**.
- 5 J. P. Fouassier, *Photoinitiation, Photopolymerization, and Photocuring: Fundamentals and Applications*; Hanser Publisher: New York, **1995**.
- 6 C. D. Calnan, *Contact Dermatitis* **1980**, *6*, 53–54.
- 7 L. S. Andrews, J. J. Clary, *J. Toxicol. Environ. Health.* **1986**, *19*, 149–164.
- 8 M. Friedman, J. F. Cavins, J. S. Wall, *J. Am. Chem. Soc.* **1965**, *87*, 3672–3682.
- 9 A. Mautner, X. Qin, G. Kapeller, G. Russmüller, T. Koch, J. Stampfl, R. Liska, *Macromol. Rapid Commun.* **2012**, *33*, 2046–2052.
- 10 C. E. Hoyle, T. Y. Lee, T. Roper, *J. Polym. Sci. Part A: Polym. Chem.* **2004**, *42*, 5301–5338.
- 11 A. Lowe, C. Bowman, *Thiol-X Chemistries in Polymer and Materials Science*, RSC Publishing: Cambridge, **2013**.
- 12 S. Reinelt, M. Tabatabai, N. Moszner, U. K. Fischer, A. Utterodt, H. Ritter, *Macromol. Chem. Phys.* **2014**, *215*, 1415–1425.
- 13 J. A. Carioscia, J. W. Stansbury, C. N. Bowman, *Polymer* **2007**, *48*, 1526–1532.
- 14 Q. Li, H. Zhou, D. A. Wicks, C. E. Hoyle, *J. Polym. Sci. Part A: Polym. Chem.* **2007**, *45*, 5103–5111.
- 15 S. Parker, R. Reit, H. Abitz, G. Ellson, K. Yang, B. Lund, W. E. Voit, *Macromol. Rapid Commun.* **2016**, *37*, 1027–1032.
- 16 A. B. Lowe, *Polymer* **2014**, *55*, 5517–5549.
- 17 B. D. Fairbanks, T. F. Scott, C. J. Kloxin, K. S. Anseth, C. N. Bowman, *Macromolecules* **2009**, *42*, 211–217.
- 18 J. W. Chan, J. Shin, C. E. Hoyle, C. N. Bowman, A. B. Lowe, *Macromolecules* **2010**, *43*, 4937–4942.
- 19 J. W. Chan, H. Zhou, C. E. Hoyle, A. B. Lowe, *Chem. Mater.* **2009**, *21*, 1579–1585.
- 20 B. D. Fairbanks, E. A. Sims, K. S. Anseth, C. N. Bowman, *Macromolecules* **2010**, *43*, 4113–4119.
- 21 D. Pretzel, B. Sandmann, M. Hartlieb, J. Vitz, S. Hölzer, N. Fritz, N. Moszner, U. S. Schubert, *J. Polym. Sci. Part A: Polym. Chem.* **2015**, *53*, 1843–1847.
- 22 F. Goncalves, Y. Kawano, C. Pfeifer, J. W. Stansbury, R. R. Braga, *Eur. J. Oral Sci.* **2009**, *117*, 442–446.
- 23 H. E. Gottlieb, V. Kotlyar, A. Nudelman, *J. Org. Chem.* **1997**, *62*, 7512–7515.
- 24 M. A. Voda, D. E. Demco, J. Perlo, R. A. Orza, B. Blümich, *J. Magn. Reson.* **2005**, *172*, 98–109.
- 25 K. Saalwächter, *Prog. Nucl. Magn. Reson. Spectrosc.* **2007**, *51*, 1–35.
- 26 M. Roth, A. Oesterreicher, F. H. Mostegel, A. Moser, G. Pinter, M. Edler, R. Piock, T. Griesser, *J. Polym. Sci. Part A: Polym. Chem.* **2016**, *54*, 418–424.
- 27 S. A. Caldarelli, S. El Fangour, S. Wein, C. van Tran Ba, C. Perigaud, A. Pellet, H. J. Vial, S. Peyrottes, *J. Med. Chem.* **2013**, *56*, 496–509.
- 28 E. D. Bergmann, D. Ginsburg, R. Pappo, *Org. React.* **1959**, *10*, 179–556.
- 29 D. P. Nair, M. Podgórski, S. Chatani, T. Gong, W. Xi, C. R. Fenoli, C. N. Bowman, *Chem. Mater.* **2014**, *26*, 724–744.
- 30 H. Peng, C. Wang, W. Xi, B. A. Kowalski, T. Gong, X. Xie, W. Wang, D. P. Nair, R. R. McLeod, C. N. Bowman, *Chem. Mater.* **2014**, *26*, 6819–6826.
- 31 I. N. Michaelides, B. Darses, D. J. Dixon, *Org. Lett.* **2011**, *13*, 664–667.
- 32 M. Podgórski, E. Becka, S. Chatani, M. Claudino, C. N. Bowman, *Polym. Chem.* **2015**, *6*, 2234–2240.
- 33 A. R. Molenberg, E. Zamparo, L. Rapillard, S. Cerritelli, WO 2011004255, Compositions for Tissue Augmentation, **2011**.
- 34 M. Sangermano, *Pure Appl. Chem.* **2012**, *84*, 2089–2101.
- 35 P. J. Flory, *Principles of Polymer Chemistry*; Cornell University Press: Ithaca, NY, **1953**.
- 36 P. J. Flory, J. Rehner, *J. Chem. Phys.* **1943**, *11*, 521.
- 37 P. J. Flory, *J. Chem. Phys.* **1950**, *18*, 108.
- 38 R. Graf, D. E. Demco, S. Hafner, H. W. Spiess, *Solid State Nucl. Magn. Reson.* **1998**, *12*, 139–152.
- 39 M. Schneider, L. Gasper, D. E. Demco, B. Blümich, *J. Chem. Phys.* **1999**, *111*, 402.
- 40 N. Moszner, W. Schöb, V. Rheinberger, *Polym. Bull.* **1996**, *37*, 289–295.
- 41 N. Moszner, U. Salz, *Macromol. Mater. Eng.* **2007**, *292*, 245–271.
- 42 S. Reinelt, M. Tabatabai, U. K. Fischer, N. Moszner, A. Utterodt, H. Ritter, *Beilstein J. Org.* **2014**, *10*, 1733–1740.

## Publication II

Oesterreicher, Andreas; Wiener, Johannes; Roth, Meinhard; Moser, Andreas; Gmeiner, Robert; Edler, Matthias; Pinter, Gerald; Griesser, Thomas: Tough and Degradable Photopolymers Derived from Alkyne Monomers for 3D Printing of Biomedical Materials *Polym. Chem.* **2016**, 7, 5169–5180.

Cite this: *Polym. Chem.*, 2016, **7**,  
5169

## Tough and degradable photopolymers derived from alkyne monomers for 3D printing of biomedical materials†

Andreas Oesterreicher,<sup>a</sup> Johannes Wiener,<sup>a</sup> Meinhard Roth,<sup>a</sup> Andreas Moser,<sup>b</sup> Robert Gmeiner,<sup>c</sup> Matthias Edler,<sup>a</sup> Gerald Pinter<sup>b</sup> and Thomas Griesser<sup>\*a</sup>

This contribution deals with the synthesis and exploration of alkyne carbonate derivatives as biocompatible building blocks in the thiol–yne photopolymerisation reaction with the aim to facilitate the fabrication of tailor made medical devices by UV based additive manufacturing technologies. It turned out that the investigated alkyne carbonates offer curing rates similar to comparable acrylates, while providing much higher conversion and lower monomer cytotoxicity. Curing the synthesized building blocks in combination with the commercially available thiol pentaerythritol tetra(3-mercaptopropionate) (PETMP) leads to networks that degrade in aqueous alkaline and acidic media in a surface erosion manner. Additionally, a selective adjustment of the degradability is feasible by the choice and content of thiol monomers. Notably, monomers containing a tricyclo[5.2.1.0<sup>2,6</sup>]decane-4,8-dimethanol backbone provide decent thermo-mechanical properties and appropriate impact strengths similar to polylactic acid (PLA). Most importantly, selected thiol–yne formulations were printed successfully with an accuracy of 40 × 40 μm, which seems to be sufficiently high to print medical devices in appropriate resolution.

Received 29th June 2016

Accepted 20th July 2016

DOI: 10.1039/c6py01132b

www.rsc.org/polymers

### Introduction

The production of medical devices by additive manufacturing technologies (AMT) has become a popular field of research in the last few years as it allows the fabrication of complex and individually shaped geometries in short production times from 3D models that can be directly obtained from the patients' X-ray, MRI or CT scans.<sup>1,2</sup> There is a vast amount of applications reaching from dental to surgical devices including implants, prosthetics and tissue engineering scaffolds which are 3D printed from different materials like metals, ceramics and polymers.<sup>2–4</sup> Polymers shaped by fused deposition modelling (FDM) have been successfully implanted already.<sup>3,5</sup> However, limitations of this technology are its low feature resolution, the weak layer adhesion and its restriction in material selection as only thermoplastic polymers can be used.<sup>6</sup>

In contrast, AMTs based on the photopolymerisation of light sensitive resins, *e.g.* stereolithography (SLA), digital light processing (DLP) or 3D inkjet printing (3-DP), allow the fast and very precise production of complex structures with high surface quality and tuneable mechanical properties.<sup>7,8</sup> State-of-the-art resins are mainly based on acrylate and methacrylate building blocks which are well established in the decorative and protecting coating industry.<sup>9,10</sup> They show fast curing rates, excellent storage behaviour as well as tuneable mechanical properties.<sup>11</sup> One considerable drawback of this class of chemical compounds is their low biocompatibility. Although biocompatible dimethacrylates can be found *e.g.* in dental materials,<sup>12</sup> many (meth)acrylates show high irritancy levels or even cytotoxicity in the uncured state.<sup>13,14</sup> As double bond conversions are usually rather low (in the of range between 60 to 90%) unreacted monomers (leachables) can state health risks when cured resin is in direct contact with the human body. Another negative aspect is the hydrolytic degradation of the (meth)acrylate network within the human body resulting in high molecular (meth)acrylic acid that can lead to a local decrease of pH and, therefore, tissue necrosis might occur in the worst case.<sup>15–17</sup>

Another drawback of radical cured photopolymers is their insufficient polymer toughness, which explains the brittleness of 3D manufactured parts. This behaviour can be attributed to the evolution of shrinkage stress during the fast radical chain

<sup>a</sup>Chair of Chemistry of Polymeric Materials & Christian Doppler Laboratory for Functional and Polymer Based Ink-Jet Inks, University of Leoben, Otto-Glöckel-Strasse 2, A-8700 Leoben, Austria. E-mail: thomas.griesser@unileoben.ac.at; Tel: +43-3842-402-2358

<sup>b</sup>Chair of Material Science and Testing of Polymers, University of Leoben, Otto-Glöckel-Strasse 2, A-8700 Leoben, Austria

<sup>c</sup>Cubicure GmbH, Photopolymer development, Getreidemarkt 9, 1060 Vienna, Austria

† Electronic supplementary information (ESI) available. See DOI: 10.1039/c6py01132b

growth polymerization and to an inhomogeneous polymeric architecture.<sup>18–20</sup> Besides an appropriate Young's modulus and tensile strength, a high toughness in terms of impact resistance is a key requirement for medical devices used for hard tissue engineering such as bone scaffolds, cranial or sternum implants.

Recently, the group of Liska *et al.* reported on alternative photopolymerizable building blocks based on vinylcarbonates, vinylesters and vinylcarbamates and demonstrated their biocompatibility and also biodegradability by *in vitro* as well as *in vivo* tests.<sup>8,21</sup> Moreover, they successfully showed that the introduction of cyclic structures and urethane groups can enhance the impact strengths of such networks significantly.<sup>22</sup> The rather low photoreactivities and homopolymerisation rates of these monomers can be accelerated by the addition of multifunctional thiols that, however, lowers the network properties, *i.e.* modulus and glass transition temperature. This fact can be attributed to a decrease of the crosslink density and also to the flexibility of the formed thioether bonds.<sup>17,23</sup> Additionally, economic aspects might hinder this group of building blocks to enter the market, as the synthesis of vinylcarbonates, vinylesters and vinylcarbamates requires expensive reagents and multi-step synthesis routes.<sup>21</sup>

One possibility to generate highly crosslinked thioether based networks is to use multifunctional alkynes instead of vinyl monomers. This so called thiol-yne reaction leads to homogeneous networks that offer the well reported advantageous aspects of thiol chemistry such as low oxygen inhibition and low shrinkage.<sup>24,25</sup> Moreover, thiols exhibit a comparably low cytotoxic behaviour as recently demonstrated by Mautner *et al.*<sup>22</sup> The concept of thiol-yne polymerization was first described in the 1930 and has undergone a resurgence of interest in the field of photopolymerisation during the last few years.<sup>26,27</sup> Particularly, the highly crosslinked and uniform networks formed in this polymerization reaction provide unique thermo-mechanical properties and promise enhanced toughness compared to (meth)acrylate photopolymers.<sup>26</sup>

The aim of this contribution is to synthesize and study alkyne derivatives as biocompatible building blocks, which are capable to provide both, biodegradability and impact strength similar or even higher than thermoplastic biopolymers such as polylactic acid, the most commonly used polymeric bioresorbable implant material. Consequently, novel monomers based on terminal alkyne carbonates were synthesized and evaluated with respect to their cytotoxicity, curing rate and triple bond conversion. The degradability of thiol-yne derived polymers in acidic and alkaline media was investigated and the influence of the choice of monomer on the degradation behaviour was studied. The mechanical properties were analysed by dynamic mechanical thermal analysis (DMA) and Charpy impact testing for selected polymers. Importantly, the 3D printability of such resins could be successfully shown by means of DLP, whereby basic biocompatible 3D structures were obtained.

This study reveals the huge potential of alkyne carbonate based monomers for the fabrication of patient customized medical devices by UV based AMTs.

## Experimental

### <sup>1</sup>H-NMR and <sup>13</sup>C-NMR spectroscopy

<sup>1</sup>H-NMR and <sup>13</sup>C-NMR spectra were recorded on a Varian 400-NMR spectrometer operating at 399.66 MHz and 100.5 MHz, respectively, and were referenced to Si(CH<sub>3</sub>)<sub>4</sub>. For the acquisition of the <sup>1</sup>H-NMR spectra a relaxation delay of 10 s and a 45° pulse were used. The NMR spectra were referenced to solvent residual peaks according to values given in the literature.<sup>28</sup>

### FT-IR (RT) measurements

FT-IR (RT) measurements were conducted on a VERTEX 70 (Bruker, Billerica, USA) in reflection mode with the unit A513. 1 μL of the resin of investigation was placed in between two CaF<sub>2</sub> windows (8 mm diameter, 1 mm thickness) and illuminated with an Omnicure s1000 (Lumen Dynamics, Missis-sauga, USA) with 9 cm gap between the sample and light guide ( $P = 22 \text{ mW cm}^{-2}$  at the sample surface). For real-time FT-IR measurements the corresponding monomers were mixed with 5 wt% of the photoinitiator blend, diphenyl(2,4,6-trimethylbenzoyl)phosphine oxide and 2-hydroxy-2-methylpropio-phenone and a stoichiometric amount of trimethylol-propane-tris(3-mercaptopropionate) (TMPMP). The corresponding (meth)acrylates were prepared without any thiol component.

### Photo-DSC

The Photo-DSC experiments were performed on a NETZSCH Photo-DSC 204 F1 Phoenix. All measurements were conducted at 50 °C in aluminium crucibles under nitrogen flow (20 mL min<sup>-1</sup>). Omnicure s2000 was used as light source at 1 W cm<sup>-2</sup> resulting in an intensity of 80 mW cm<sup>-2</sup> at the surface of the sample (range of wavelength was 250–445 nm). For the determination of the reaction enthalpy and  $t_{\text{max}}$ , the samples were illuminated twice for 10 min each with an idle time of 2 min in between (sample quantity: 8 ± 0.05 mg resin, containing 3 wt% of Irgacure TPO-L and stoichiometric amounts of PETMP). For the analysis, the second run was subtracted from the first one to obtain the reaction enthalpy curve.

### Sample preparation

For the determination of the thermomechanical properties and the impact properties of the photopolymers, sample specimens with 1 × 4 × 25 mm<sup>3</sup> (DMA) and 150 × 100 × 4 mm<sup>3</sup> (Charpy) rectangular dimensions were fabricated in PTFE moulds covered with a glass slide (DMA) or between two glass plates (Charpy). The resin samples were photocured by a Light hammer 6 (Fusion UV Systems) with a Hg bulb (specimen for DMA: 5 passes each side, belt speed of 4 m min<sup>-1</sup>, 40% light intensity ( $E = 3.8 \text{ J cm}^{-2}$ ) specimen for Charpy: first run: 4 passes each side, belt speed of 8 m min<sup>-1</sup>, 40% light intensity ( $E = 1.6 \text{ J cm}^{-2}$ ). Second run: 10 passes each side, belt speed 4 m min<sup>-1</sup>, 40% light intensity ( $E = 7.5 \text{ J cm}^{-2}$ ). Third run: 5 passes each side, belt speed 4 m min<sup>-1</sup>, 40% light intensity after removing glass plates and sample heated to 90 °C

( $E = 13.3 \text{ J cm}^{-2}$ ). The resins contained 3 wt% of the photoinitiator Irgacure® TPO-L.

#### Dynamic mechanical thermal analysis (DMA)

The thermomechanical properties were measured in tension mode using a DMA/SDTA 861 (Mettler Toledo) with a heating rate of  $2 \text{ K min}^{-1}$  in the temperature range from  $-40$  to  $120 \text{ }^\circ\text{C}$ . The operating frequency was determined at 1 Hz. For comparison of the alkyne carbonate formulations, the storage modulus was evaluated at room temperature ( $37 \text{ }^\circ\text{C}$ ). The glass transition temperature was determined at the maximum of  $\tan \delta$ .

#### Charpy impact tests

Charpy impact tests were performed on a CEAST RESIL 25 testing machine on unnotched samples in an edgewise arrangement with the dimensions  $80 \times 10 \times 4 \text{ mm}^3$ . The drive hammer energy was 2.0 J. Samples were tested at  $20 \text{ }^\circ\text{C}$ . Obtained results were corrected for machine parameters.

#### Viscosity measurements

Viscosity measurements were conducted on an Anton Paar rheometer (MCR-102, Graz, Austria) with a cone-plate system setup with a titanium cone (MK 22/60 mm,  $0.58^\circ$ ) having an opening angle of  $0.58^\circ$  and a diameter of 60 mm. The viscosity was measured at  $25 \text{ }^\circ\text{C}$  at a constant shear rate of  $300 \text{ s}^{-1}$ .

#### Cytotoxicity

The cytotoxicity experiments were conducted at Cytoxbiologische Sicherheitsprüfungen (Bayreuth, Germany) according to ISO 10993-5:2009. For these tests mouse fibroblast cells (L929) were used. Cells were cultured for 24 h in Dulbecco's modified Eagle's medium (DMEM) with added antibiotics, supplemented with 10% fetal calf serum at  $37 \text{ }^\circ\text{C}$  in an incubator with 5%  $\text{CO}_2$ . Four different concentrations of the examined substance (dissolved in DMSO) were applied onto the cells and incubated for 48 h at  $37 \text{ }^\circ\text{C}$  with 5%  $\text{CO}_2$ . The final concentration of DMSO in all cavities in the cell culture medium was 1% (v/v). Triton X 100 was used as toxic positive control (final concentration 1% (v/v)) and the cell culture medium was used as non-toxic negative control. All experiments were conducted four times simultaneously. After the incubation the L929-cells were washed with phosphate buffered saline (PBS), and after an alkaline lysis step the protein concentration was determined *via* the Bradford method. Graphical illustrations of the protein content in dependence of the monomer concentration can be found in the ESL.†

#### In vitro degradation

For the evaluation of the hydrolytic degradation behaviour the corresponding specimen were prepared according to the procedure described for DMA samples. The specimen with the dimensions  $4 \times 4 \times 1 \text{ mm}^3$  were extracted in ethanol for 48 h and subsequently immersed in 1 M NaOH or in 1 M HCl, respectively, at  $45 \text{ }^\circ\text{C}$  under continuous shaking. For PLA as a reference substance spherical shaped samples with a diameter

of 4 mm were used. The sample dry weight was monitored over the test period. To estimate the time to reach full degradation the experimental curves were extrapolated.

#### Digital light processing

Printing experiments were performed by Cubicure GmbH and conducted on a digital light processing (DLP) prototype printer. Formulation TCBC/DiPETMP with 0.2 wt% Ivocerin®, 0.1 wt% Sudan II and 0.5 wt% lauryl gallate was used. The test patterns were generated with a layer thickness of  $25 \text{ } \mu\text{m}$  (test pattern – Fig. 6, left) and  $50 \text{ } \mu\text{m}$  (stents – Fig. 6, right). Backward illumination was 25 s. Illumination time was 50 s per layer at an intensity of  $30 \text{ mW cm}^{-2}$  (test pattern) and  $100 \text{ mW cm}^{-2}$  (stents). The total build time was 100 min (test pattern) and 6.5 h (stents). After the structuring process the sample was rinsed with isopropanol, followed by post-curing for three times 120 s in an Intelli-Ray 400 UV Curing System set to maximum power.

#### Materials

1,4-Butanediol (Sigma Aldrich, 99%), 2-propyn-1-ol, (Sigma Aldrich, 99%), 3-butyn-1-ol (Sigma Aldrich, 97%), 4-pentyn-2-ol (Sigma Aldrich, >98%), 1,1'-carbonyldiimidazole (CDI) (Sigma Aldrich, reagent grade), 1,1,1-tris(hydroxymethyl)propane (Sigma Aldrich, 97%), bisphenol A (Sigma Aldrich, 99%), ethylene carbonate (Sigma Aldrich, 99%), tricyclo[5.2.1.0<sup>2,6</sup>]decane-4,8-dimethanol (Sigma Aldrich, 96%), ethyl(2,4,6-trimethylbenzoyl)phenylphosphinate (Irgacure® TPO-L, BASF), diphenyl (2,4,6-trimethylbenzoyl)phosphine oxide/2-hydroxy-2-methylpropiophenone, blend (Sigma Aldrich), dipentaerythritol hexa(3-mercaptopropionate) (DiPETMP) (Bruno Bock Chemische Fabrik GmbH & Co. KG), pentaerythritol tetra(3-mercaptopropionate) (PETMP) (Bruno Bock Chemische Fabrik GmbH & Co. KG), trimethylolpropane tri(3-mercaptopropionate) (TMPMP) (Bruno Bock Chemische Fabrik GmbH & Co. KG), and 2,2'-(ethylenedioxy)diethanethiol (Sigma Aldrich, 95%) were used as received. 1,4-Butanediol diacrylate (abcr GmbH) and 1,4-butanediol dimethacrylate (abcr GmbH, 90%) have been purified by flash chromatography prior usage. Ivocerin® was provided with kind support from Ivoclar Vivadent AG. Tetra(3-mercaptopropyl)silane (TMPS) was synthesized according to literature.<sup>29</sup> L929 cells were obtained from Leibniz Institute DSMZ-German Collection of Microorganisms and Cell Cultures. Dulbecco's modified Eagle's medium (DMEM), fetal calf serum, penicillin/streptomycin solution, accutase enzyme solution and phosphate buffered saline (PBS) was purchased from PAA Laboratories GmbH, Austria (GE Healthcare Europe GmbH).

#### Synthesis

**Butane-1,4-diyl bis(1H-imidazole-1-carboxylate) (4-CDI).** In a three-neck round-bottom flask 15.0 g (166.5 mmol) 1,4-butanediol with 62.1 g (382.8 mmol, 2.3 eq.) 1,1'-carbonyldiimidazole (CDI) and catalytic amounts of KOH were added to 400 mL dry toluene and stirred for 20 h at  $60 \text{ }^\circ\text{C}$ . The mixture was then diluted with dichloromethane and washed three times with

deionized water. The combined organic extracts were dried over  $\text{Na}_2\text{SO}_4$  and then concentrated under reduced pressure. The crude product (white solid) showed quantitative conversion (monitored by  $^1\text{H}$ - and  $^{13}\text{C}$ -NMR).

$^1\text{H}$ -NMR ( $\delta$ , 400 MHz,  $\text{CDCl}_3$ , 25 °C): 8.14 (s, 2H,  $-\text{N}-\text{CH}=\text{N}-$ ); 7.43 (s, 2H,  $-\text{N}-\text{CH}=\text{CH}-$ ); 7.07 (s, 2H,  $-\text{CH}=\text{N}-\text{CH}$ ); 4.49 (m, 4H,  $-\text{CH}_2-\text{O}$ ); 1.97 (m, 4H,  $-\text{CH}_2-\text{CH}_2-\text{O}$ ) ppm.  $^{13}\text{C}$ -NMR ( $\delta$ , 100 MHz,  $\text{CDCl}_3$ , 25 °C): 148.58 (s, 2C,  $\text{C}=\text{O}$ ); 137.00 (s, 2C,  $-\text{C}=\text{N}-\text{C}$ ); 130.74 (s, 2C,  $-\text{C}=\text{N}-\text{C}$ ); 117.03 (s, 2C,  $-\text{N}-\text{C}=\text{C}$ ); 67.36 (s, 2C,  $-\text{O}-\text{C}$ ); 25.04 (s, 2C,  $-\text{C}-\text{C}-\text{O}$ ) ppm.

**1,4-Butanediol dipropargyl carbonate (4PC).** In a three-neck round-bottom flask 7.0 g (25.2 mmol) of 4-CDI with 3.4 g (60.4 mmol, 2.4 eq.) 2-propyn-1-ol and catalytic amounts of KOH were added to 200 mL dry toluene and stirred for 15 h at 60 °C. The mixture was diluted with dichloromethane and washed three times with deionized water. The combined organic extracts were dried over  $\text{Na}_2\text{SO}_4$  and concentrated under reduced pressure. The crude product was purified with flash column chromatography (cyclohexane:ethyl acetate = 8:1) to yield 6 g (94%) of 4PC as a colourless, transparent liquid.

$^1\text{H}$ -NMR ( $\delta$ , 400 MHz,  $\text{CDCl}_3$ , 25 °C): 4.71 (d, 4H,  $-\text{CH}_2-\text{C}=\text{C}$ ); 4.20 (m, 4H,  $-\text{CH}_2-\text{O}$ ); 2.52 (t, 2H,  $-\text{C}=\text{CH}$ ); 1.79 (m, 4H,  $-\text{CH}_2-\text{CH}_2-\text{O}$ ) ppm.  $^{13}\text{C}$ -NMR ( $\delta$ , 100 MHz,  $\text{CDCl}_3$ , 25 °C): 154.42 (s, 2C,  $\text{C}=\text{O}$ ); 76.91 (s, 2C,  $-\text{C}=\text{CH}$ ); 75.62 (s, 2C,  $-\text{C}=\text{CH}$ ); 67.73 (s, 2C,  $-\text{C}-\text{O}$ ); 55.12 (s, 2C,  $-\text{C}-\text{C}=\text{C}$ ); 24.97 (s, 2C,  $-\text{C}-\text{C}-\text{O}$ ) ppm.

**1,4-Butanediol dibut-3-yn-1-yl carbonate (4BC).** 4BC was prepared according to the procedure described for 4PC. 5.3 g (19.0 mmol) of 4-CDI with 3.2 g (45.7 mmol, 2.4 eq.) 3-butyne-1-ol and catalytic amounts of KOH in 150 mL dry toluene were used. The crude product was recrystallized in a mixture of cyclohexane and ethyl acetate (5:1) to yield 4.2 g (78%) of 4BC as white crystals.

$^1\text{H}$ -NMR ( $\delta$ , 400 MHz,  $\text{CDCl}_3$ , 25 °C): 4.24 (t, 4H,  $-\text{CH}_2-\text{CH}_2-\text{C}=\text{CH}$ ); 4.18 (m, 4H,  $-\text{CH}_2-\text{O}$ ), 2.57 (m, 4H,  $-\text{CH}_2-\text{C}=\text{CH}$ ); 2.02 (t, 2H,  $-\text{C}=\text{CH}$ ); 1.78 (m, 4H,  $-\text{CH}_2-\text{CH}_2-\text{O}$ ) ppm.  $^{13}\text{C}$ -NMR ( $\delta$ , 100 MHz,  $\text{CDCl}_3$ , 25 °C): 154.82 (s, 2C,  $\text{C}=\text{O}$ ); 79.38 (s, 2C,  $-\text{C}=\text{CH}$ ); 70.23 (s, 2C,  $-\text{C}=\text{CH}$ ); 67.44 (s, 2C,  $-\text{C}-\text{O}$ ); 65.31 (s, 2C,  $-\text{C}-\text{C}=\text{C}$ ); 25.01 (s, 2C,  $-\text{C}-\text{C}-\text{O}$ ); 19.00 (s, 2C,  $-\text{C}-\text{C}=\text{CH}$ ) ppm.

**1,4-Butanediol dipent-4-yn-2-yl carbonate (4MPC).** *Step 1:* Pent-4-yn-2-yl 1H-imidazole-1-carboxylate (P-CDI) was synthesized according to the procedure described for 4-CDI. 5.0 g (59.4 mmol) 4-pentyne-2-ol with 11.57 g (71.3 mmol, 1.2 eq.) CDI and catalytic amounts of KOH were used. The crude product was used in the following reaction without further purification. *Step 2:* 4MPC was synthesized according to the procedure described for 4PC. 9.0 g (51.6 mmol, 2.3 eq.) of P-CDI and 2.0 g (22.2 mmol) 1,4-butanediol with catalytic amounts of KOH were used. The crude product was purified by flash column chromatography (cyclohexane:ethyl acetate = 4:1) to yield 6.0 g (87%) of 4MPC as a transparent, colourless liquid.

$^1\text{H}$ -NMR ( $\delta$ , 400 MHz,  $\text{CDCl}_3$ , 25 °C): 4.86 (m, 2H,  $-\text{CH}-\text{CH}_3$ ); 4.16 (m, 4H,  $-\text{CH}_2-\text{O}$ ); 2.52 (m, 4H,  $-\text{CH}_2-\text{C}=\text{CH}$ );

2.03 (t, 2H,  $-\text{C}=\text{CH}$ ); 1.77 (t, 4H,  $-\text{CH}_2-\text{CH}_2-\text{O}$ ); 1.39–1.37 (d, 6H,  $-\text{CH}_3$ ) ppm.

$^{13}\text{C}$ -NMR ( $\delta$ , 100 MHz,  $\text{CDCl}_3$ , 25 °C): 154.45 (s, 2C,  $\text{C}=\text{O}$ ); 79.21 (s, 2C,  $-\text{C}=\text{CH}$ ); 72.55 (s, 2C,  $-\text{C}-\text{CH}_3$ ); 70.23 (s, 2C,  $-\text{C}=\text{CH}$ ); 67.25 (s, 2C,  $-\text{C}-\text{O}$ ); 25.58 (s, 2C,  $-\text{C}-\text{C}=\text{C}$ ); 25.12 (s, 2C,  $-\text{C}-\text{C}-\text{O}$ ); 19.02 (s, 2C,  $-\text{C}-\text{CH}_3$ ) ppm.

**1,1,1-Tris(hydroxymethyl)propane tripropargyl carbonate (TMPC).** *Step 1:* 1,1,1-Tris(hydroxymethyl)propane 1H-imidazole-1-carboxylate (TMP-CDI) was synthesized according to the procedure described for 4-CDI. 5.0 g (37.3 mmol) 1,1,1-Tris(hydroxymethyl)propane with 19.9 g (123.0 mmol, 3.3 eq.) CDI and catalytic amounts of KOH were used. The crude product was used in the following reaction without further purification.

*Step 2:* TMPC was synthesized according to the procedure described for 4PC. 15.5 g (37.2 mmol) TMP-CDI and 6.7 g (11.9 mmol, 3.2 eq.) 2-propyne-1-ol were used. The crude product was purified with flash column chromatography (cyclohexane:ethyl acetate = 4:1) to yield 13.2 g (93%) of TMPC as a transparent, colourless, viscous liquid.

$^1\text{H}$ -NMR ( $\delta$ , 400 MHz,  $\text{CDCl}_3$ , 25 °C): 4.73 (d, 6H,  $-\text{CH}_2-\text{C}=\text{CH}$ ); 4.16 (s, 6H,  $-\text{CH}_2-\text{O}$ ); 2.54 (t, 3H,  $-\text{C}=\text{CH}$ ); 1.53 (m, 2H,  $-\text{CH}_2-\text{CH}_3$ ); 0.91 (t, 3H,  $-\text{CH}_3$ ) ppm.

$^{13}\text{C}$ -NMR ( $\delta$ , 100 MHz,  $\text{CDCl}_3$ , 25 °C): 154.18 (s, 3C,  $\text{C}=\text{O}$ ); 76.76 (s, 3C,  $-\text{C}=\text{CH}$ ); 75.89 (s, 3C,  $-\text{C}=\text{CH}$ ); 67.37 (s, 3C,  $-\text{C}-\text{O}$ ); 55.52 (s, 3C,  $-\text{C}-\text{C}=\text{C}$ ); 41.27 (s, 1C,  $\text{C}_q$ ); 22.34 (s, 1C,  $-\text{C}-\text{CH}_3$ ); 7.22 (s, 1C,  $-\text{CH}_3$ ) ppm.

**2,2-Bis[4-(2-hydroxy)ethoxyphenyl]propane (BisAE).** The product was synthesized according to a modified literature procedure.<sup>30</sup>

In a three-neck round-bottom flask equipped with a reflux condenser 20 g (87.6 mmol) bisphenol A and 17.7 g (201.5 mmol, 2.3 eq.) ethylene carbonate were added to 24.2 g (175 mmol, 2.0 eq.)  $\text{K}_2\text{CO}_3$  in 300 mL DMF and refluxed at 145 °C for 3 h. The reaction mixture was poured into 1.5 L deionized water. The resulting white precipitate was filtered and washed with water, with methanol and afterwards with a small amount of cold THF. The remaining white powder was dried under vacuum at 70 °C to yield 18.0 g (65%) of BisAE.

$^1\text{H}$ -NMR ( $\delta$ , 400 MHz,  $\text{CDCl}_3$ , 25 °C): 7.15–7.13 (d, 4H, Ar-H); 6.83–6.81 (d, 4H, Ar-H); 4.07 (t, 4H,  $-\text{CH}_2-\text{O}$ ); 3.95 (m, 4H,  $-\text{CH}_2-\text{OH}$ ); 1.64 (s, 6H,  $-\text{CH}_3$ ) ppm.

$^{13}\text{C}$ -NMR ( $\delta$ , 100 MHz,  $\text{CDCl}_3$ , 25 °C): 156.42 (2C, Ar-C-O), 143.57 (2C, Ar-C), 127.78 (4C, Ar-C), 113.92 (4C, Ar-C), 69.09 (2C, O-C), 61.53 (2C,  $-\text{C}-\text{OH}$ ), 41.72 (1C,  $-\text{C}-\text{CH}_3$ ), 31.02 (2C,  $-\text{CH}_3$ ) ppm.

**2,2-Bis[4-(2-hydroxy)ethoxyphenyl]propane dibut-3-yn-1-yl carbonate (BABC).** *Step 1:* 2,2-Bis[4-(2-hydroxy)ethoxyphenyl]propane bis(1H-imidazole-1-carboxylate) (BA-CDI) was synthesized according to the procedure described for 4-CDI. 6.2 g (19.6 mmol) BisAE with 7.9 g (49.0 mmol, 2.5 eq.) CDI and catalytic amounts of KOH were used. The crude product was used in the following reaction without further purification.

*Step 2:* BABC was synthesized according to the procedure described for 4BC. 5.0 g (9.9 mmol) BA-CDI with 1.7 g (23.8 mmol, 2.4 eq.) 3-butyne-1-ol and catalytic amounts of KOH were used. The crude product was purified by flash column chromatography (cyclohexane:ethyl acetate =



5 : 1) to yield 4.3 g (85%) of BABC as a colourless, transparent liquid.

<sup>1</sup>H-NMR ( $\delta$ , 400 MHz, CDCl<sub>3</sub>, 25 °C): 7.14–7.10 (d, 4H, Ar-H); 6.82–6.79 (d, 4H, Ar-H); 4.48 (t, 4H, Ar-O-CH<sub>2</sub>-CH<sub>2</sub>); 4.26 (t, 4H, -O-CH<sub>2</sub>-); 4.17 (t, 4H, -CH<sub>2</sub>-O-Ar); 2.58 (m, 4H, -CH<sub>2</sub>-C≡C); 2.01 (t, 2H, -C≡CH); 1.63 (s, 6H, -CH<sub>3</sub>) ppm.

<sup>13</sup>C-NMR ( $\delta$ , 100 MHz, CDCl<sub>3</sub>, 25 °C): 156.16 (s, 2C, Ar-C-O); 154.79 (s, 2C, C=O); 143.66 (s, 2C, Ar-C-Cq.); 127.76 (s, 4C, Ar-C); 113.97 (s, 4C, Ar-C); 79.31 (s, 2C, -C≡C); 70.28 (s, 2C, -C≡C-H); 66.30 (s, 2C, -O-CH<sub>2</sub>-); 65.55 (s, 4C, -O-CH<sub>2</sub>); 41.72 (s, 1C, Cq.); 30.99 (s, 2C, -CH<sub>3</sub>); 18.99 (s, 2C, -CH-C≡C) ppm.

**Tricyclo[5.2.1.0<sup>2,6</sup>]decane-4,8-dimethanol dibut-3-yn-1-yl carbonate (TCBC).** *Step 1:* Tricyclo[5.2.1.0<sup>2,6</sup>]decane-4,8-dimethylbis(1H-imidazole-1-carboxylate) (TCBC-CDI) was synthesized according to the procedure described for 4-CDI. 79.4 g (404.5 mmol) tricyclo[5.2.1.0<sup>2,6</sup>]decane-4,8-dimethanol with 164.0 g (1011 mmol, 2.5 eq.) CDI and catalytic amounts of KOH were used in 1000 mL toluene. The crude product was used in the following reaction without further purification. *Step 2:* TCBC was synthesized according to the procedure described in entry 4BC. 155.5 g (404.5 mmol) TCBC-CDI with 73.7 g (1052 mmol, 2.6 eq.) 3-butyne-1-ol and catalytic amounts of KOH were used in 700 mL toluene. 156 g (99%) of TCBC was received as a colourless, transparent liquid. The product was used without further purification.

<sup>1</sup>H-NMR ( $\delta$ , 400 MHz, CDCl<sub>3</sub>, 25 °C): 4.23 (t, 4H, -O-CH<sub>2</sub>-), 3.96 (m, 4H, -CH<sub>2</sub>-O-), 2.58 (m, 4H, -CH<sub>2</sub>-C≡C), 2.02 (s, 2H, -C≡CH); 2.58–0.90 (m, 14H, -CH-, -CH<sub>2</sub>-; isomers of backbone) ppm.

<sup>13</sup>C-NMR ( $\delta$ , 100 MHz, CDCl<sub>3</sub>, 25 °C): 155.02 (s, 2C, C=O); 79.44 (s, 2C, -C≡C); 72.53, 71.73, 71.67, 71.54, 71.47 (multiple s, -C-O-, isomers); 70.21 (s, 2C, -C≡C-H); 65.26 (s, 2C, -O-CH<sub>2</sub>-CH<sub>2</sub>-C≡C); 49.05, 48.60, 45.44, 44.83, 44.80, 43.68, 42.87, 42.61, 41.45, 40.17, 38.86, 38.31, 34.27, 34.18, 33.34, 32.42, 32.16, 30.60, 30.33, 28.09, 27.70, 27.27, 25.17, 24.45 (multiple s, -CH-, -CH<sub>2</sub>-; isomers of backbone); 19.04 (s, 2C, -CH-C≡C) ppm.

## Results and discussion

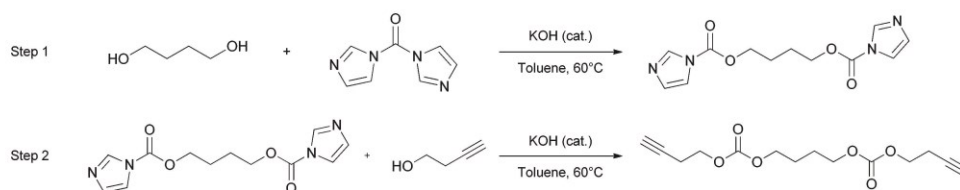
### Synthesis

In this contribution, bifunctional alkyne carbonate building blocks with different alkynyl functionalities and spacer mole-

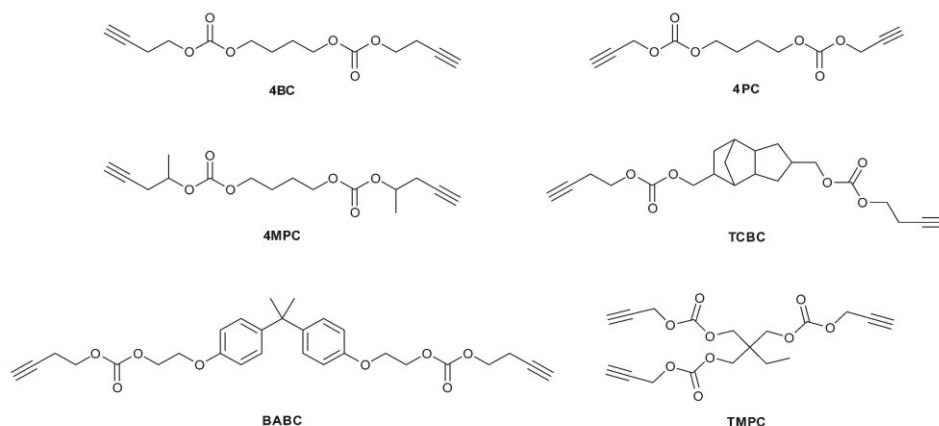
cules were synthesized. The conventional synthesis of functional carbonates is mainly based on highly toxic compounds such as phosgene, triphosgene or chloroformate derivatives.<sup>31</sup> For the preparation of these building blocks an alternative synthetic pathway has been chosen involving less toxic reagents and very mild reaction conditions. As illustrated in Scheme 1 the reaction of the hydroxyl functionalized backbone molecule with a slight excess of 1,1'-carbonyldiimidazole (CDI) and catalytic amounts of KOH in toluene at elevated temperatures leads to an imidazole carboxylic ester derivative. This intermediate was reacted with propargyl alcohol and 3-butyne-1-ol, respectively, to give the corresponding monomers in decent yields (65–98%).<sup>32</sup> The molecular structures of these monomers are depicted in Scheme 2. One particular feature of this reaction is the fact that excess of CDI and the resulting imidazole can be easily removed during aqueous workup, as CDI is hydrolytically unstable and the formed imidazole is water soluble. Extraction of the reaction mixture with water leads to products that in some cases did not even require additional purification. Since imidazole carboxylic ester provide only sufficiently high reactivity towards primary hydroxyl groups, the synthesis of 4MPC was performed by the reaction of 4-pentyne-2-ol with CDI and a subsequent conversion of the formed imidazole carboxylic ester with 1,4-butanediol. The synthesized monomers were characterized by <sup>1</sup>H- and <sup>13</sup>C-NMR spectroscopy. The obtained data are in good agreement with the proposed structures. All monomers were in their liquid state at room temperature, except for 4BC that formed solid crystals that are soluble in the used thiols at slightly elevated temperature.

### Photoreactivity and monomer conversion

The curing rate and the conversion of UV curable monomers are two very important parameters that have to be considered for biomedical applications as they determine the 3D printing speed and the amount of leachable monomers in the built medical device. The polymerization behaviour of the synthesized monomers was investigated by photo-DSC, using PETMP as co-monomer. The obtained data were compared to the (meth)acrylate based compounds BuMac and BuAc. Photo-DSC represents a unique method for the fast and accurate evaluation of kinetic parameters of UV induced polymerizations. The reaction time  $t_{\max}$  is the time to reach the maximum of polymerization enthalpy. Together with the peak shape, it reveals information about the overall photoreactivity.



**Scheme 1** Synthesis of butyne-1-yl carbonates from alcohols in a two-step reaction involving carbonyldiimidazole (CDI).



Scheme 2 Synthesized propargyl and butyne-1-yl carbonates.

Fig. 1 displays the photo-DSC plots of the investigated thiol-yne formulations and the reference substances BuAc and BuMAc. All investigated alkyne carbonate monomers, bearing C4 spacer, *i.e.* 4PC, 4BC, 4MPC, offer photoreactivities that are comparable with the corresponding acrylate BuAc which is

reflected by their similar  $t_{\max}$  values (see Table 1) and the time (approximately 30 s) to reach their overall polymerization heat (see Fig. 1). However, a slight difference between propargyl and but-3-yne-1-yl derivatives can be observed. Although propargyl carbonates react much faster than the reference methacrylate, 4MAC, they show a tendency of lower  $t_{\max}$  values than the but-3-yne-1-yl and pent-4-yne-2-yl carbonates. The superiority of the but-3-yne-1-yl and pent-4-yne-2-yl derivatives might be explained by the additional  $\text{CH}_2$  group between the alkyne and carbonate group that reduces the influence of the carbonate group on the electronic density of the yne triple bond. This hypothesis is supported by the outstanding reactivity of aliphatic terminal alkynes, which react significantly faster than other alkyne derivatives.<sup>33</sup>

Besides the kinetics of photopolymerisations, photo-DSC can also be used to determine monomer conversion (MC), as it is directly proportional to the developed reaction heat. However, due to different theoretical heats of polymerization of (meth)acrylates and propargyl and but-3-yne-1-yl and pent-4-yne-2-yl carbonates, respectively, MC was determined by infrared spectroscopy (Table 1). Detailed results of the real-time FT-IR spectroscopy measurements can be found in the ESI.† Most importantly, alkyne carbonates bearing a C4 spacer, *i.e.*

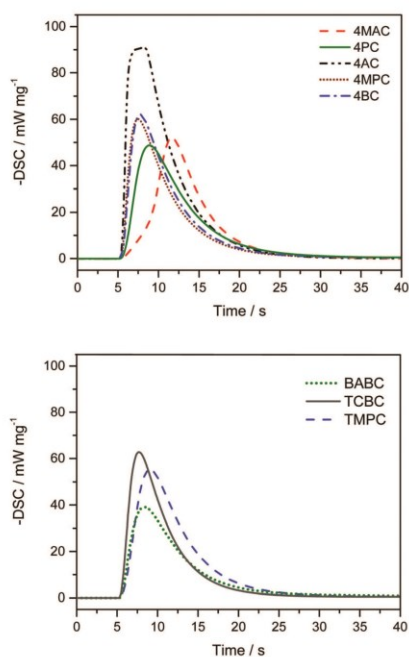


Fig. 1 P-DSC plots of investigated monomers. Upper: 4PC (solid), 4BC (chain dotted), 4MPC (dotted), 4AC (chain double dotted) and 4MAC (dashed). Lower: BABC (dotted), TCBC (solid) and TMPC (dashed). Illumination starts at 5.1 s.

Table 1 Obtained parameters from photo-DSC ( $t_{\max}$ ) and real-time FT-IR (MC) measurements, as well as EC50 values from *in vitro* cytotoxicity tests

Monomer	$t_{\max}/\text{s}$	MC/%	EC50/mM
4PC	3.8	98	0.55
4BC	2.8	98	2.00
4MPC	2.5	96	10.0
TCBC	2.6	94	2.40
TMPC	3.7	91	—
BABC	3.5	84	—
4AC	2.7	79	<0.16
4MAC	6.5	75	<0.16

4PC, 4BC and 4MPC, show significantly higher monomer conversions than their corresponding meth(acrylates). These monomers provide almost quantitative conversion (see Table 1), while 4AC and 4MAC reaches only 79% and 75%, respectively. Monomers bearing multiple alkyne carbonate groups (TMPC) or rigid backbones (BABC, TCBC) show slightly lower conversions (84–94%) and curing rates (see Table 1). This can be attributed to their higher viscosity. While for example 4PC has a measured viscosity of 44 mPa s, TCBC shows a viscosity of 2330 mPa s, however, they still outperform 4MAC in terms of MC (see Table 1).

### *In vitro* cytotoxicity

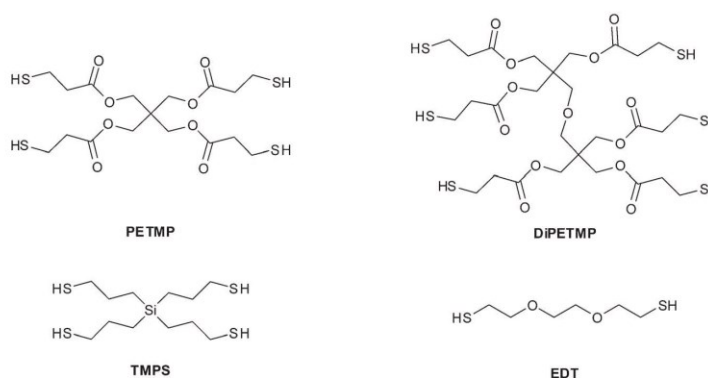
Although the conversion of the investigated alkyne carbonates is comparably high, there is still an amount of leachable monomer present in the cured polymer. This fact explains why cytotoxicity of monomers is a detrimental factor that has to be considered for applications where photopolymers are in contact with human body fluids or tissue. The cytotoxicity of (meth)acrylates can be attributed to their reactivity towards amino- or thiol-groups of proteins or DNA.<sup>6,34</sup> It is well known that terminal alkyne groups, without electron withdrawing moieties in their neighbourhood, are mostly inert in the thiol Michael reaction even under basic conditions, which suggests a higher biocompatibility of the synthesized monomers compared to (meth)acrylate building blocks. In order to prove this hypothesis, the cytotoxic potential of the alkyne carbonate and (meth)acrylate monomers was evaluated by vitro tests using L929 mouse fibroblast cells (ISO 10993-5:2009). The concentration where 50% of the cells were still viable was denoted as EC50. Besides the unsaturated groups, also the spacer moiety can exert influence on the cytotoxic behaviour. Consequently, these tests were performed with alkyne carbonate and (meth)acrylate monomers bearing C4 spacer, *i.e.* 4PC, 4BC, 4MPC. Additionally, TCBC was also evaluated, as it was used in the 3D printing experiments (*vide infra*). Compared to the tested (meth)acrylates 4AC and 4MAC, cells show much higher tolerance towards alkyne carbonates, reflected by at least the factor

of three higher EC50 values (see Table 1). Interestingly, the cytotoxicity of the tested alkyne carbonates is strongly influenced by the alkyne functionality, whereby the pent-4-yne-2-yl derivative (4MPC) offers the highest EC50 value of 10.0 mM, followed by both but-3-yne-1-yl carbonates (4BC: 2.00 mM; TCBC: 2.40 mM) and the propargyl based compound (4PC: 0.55 mM). More details on the testing results can be found in the ESI.†

### Characterization of the network properties

Since medical implants have to withstand or even absorb mechanical forces, appropriate thermo-mechanical properties at body temperature are crucial requirements, which determine the choice of the building material. Besides the network density of photopolymers also the type of the monomer backbone exerts significant influence on the modulus and toughness.<sup>22,30,35</sup> While flexible spacer such as alkyl or oligo glycol chains are known to result in rather flexible and soft materials with low glass transition temperatures, molecules with rigid ring systems are anticipated to be responsible for good mechanical properties at even higher temperatures.<sup>22</sup> In thiol-yne resins, the structure and functionality of both types of monomers, *i.e.* yne and thiol, determine the network properties. Consequently, alkyne carbonate building blocks (see Scheme 2) with different spacer groups and alkyne functionalities were polymerized in combination with the multifunctional thiols PETMP, DiPETMP and TMPS (Scheme 3) that differ in their functionality and backbone structure.

It is well reported that the thiol-yne reaction leads to a uniform network formation, which is responsible for a narrow glass transition resulting in a rapid loss in storage modulus above the  $T_g$ .<sup>26,36</sup> For hard tissue replacements the storage modulus ( $E'$ ) must be sufficiently high, thus the polymer needs to be in the glassy state at body temperature. Table 2 shows the storage moduli, the  $T_g$  at the maximum of tan delta and the full width at half-maxima (FWHM) of tan delta of the investigated thiol-yne networks.



Scheme 3 Thiols used in photopolymers.

**Table 2**  $T_g$ , storage modulus ( $E'$  at 37 °C) and FWHM of polymerized alkyne carbonate formulations and 4AC and 4MAC as references

Monomer	$T_g$ [tan( $\delta$ )]/°C	$E'$ (37 °C)	FWHM/°C
4AC	83 ± 6	1422 ± 30	—
4MAC	—	1649 ± 20	—
4PC(PETMP)	45 ± 1	509 ± 33	19 ± 1
4PC(20TMPs)	48 ± 1	1134 ± 216	14 ± 1
4BC(PETMP)	41 ± 1	257 ± 1	15 ± 1
4MPC(PETMP)	49 ± 3	1107 ± 112	14 ± 5
TMPC(PETMP)	59 ± 1	1629 ± 126	28 ± 1
BABC(PETMP)	60 ± 1	2155 ± 10	17 ± 2
TCBC(PETMP)	56 ± 1	1720 ± 141	19 ± 1
TCBC(DiPETMP)	72 ± 1	2346 ± 34	17 ± 1

Comparing the properties of cured alkyne monomers with same spacer length, only a slight difference in the  $T_g$  of 8 °C can be observed for 4PC/PETMP ( $T_g = 45$  °C), 4BC/PETMP ( $T_g = 41$  °C) and 4MPC/PETMP ( $T_g = 49$  °C) as shown in Table 2. This effect can be explained by the different length and substitution of the terminal alkynyl chain. Accordingly, the additional methyl groups of 4MPC/PETMP result in an increase in  $T_g$  of about 8 °C compared to 4BC/PETMP. While both networks of 4BC and 4PC are in the transition region at body temperature, which results in lower moduli, 4MPC provides a reasonable storage modulus at 37 °C. The generally lower thermo-mechanical properties of these thiol-yne photopolymer compared to homopolymers of the corresponding (meth)acrylates can be attributed to the rather flexible thioether linkages. The DMA plot of 4MAC can be found in the ESI.† While the moduli of 4AC and 4MAC steadily decrease over the measured temperature range, the moduli of 4PC, 4BC and 4MPC decline significantly after reaching the onset temperature of tan delta, which can be assigned to the narrow glass transitions (FWHMs of 15–20 °C) in these photopolymers. Besides the terminal alkynyl chain of the carbonate monomers also the type of thiol exerts influence on the network properties of the cured resins. For example, the substitution of 20 mol% PETMP by TMPS in a 4PC based thiol-yne resin leads to a 3 °C higher glass transition temperature and a more homogenous network formation (reduction of FWHM by 5 °C). As expected, the monomers BABC and TCBC which contain a bisphenol A or tricyclo[5.2.1.0<sup>2,6</sup>]decane-4,8-dimethanol backbone and the three functional monomer TMPC provide enhanced thermo-mechanical properties. In combination with PETMP these monomers lead to photopolymers with glass transition temperatures between 56°–60 °C (see Table 2) and to storage moduli that are well above 1600 MPa. It is worth mentioning that the usage of the hexafunctional DiPETMP instead of PETMP further increases the glass transition temperature and the modulus in TCBC based networks, which is explained by the higher crosslinking density (Fig. 2 and 3).

Besides a high modulus at body temperature, medical implants, in particular bone replacements, need to have appropriate impact strengths, in other words material toughness. State-of-the-art photopolymers obtained by radical curing of (meth)acrylates are rather brittle due to the evolution of

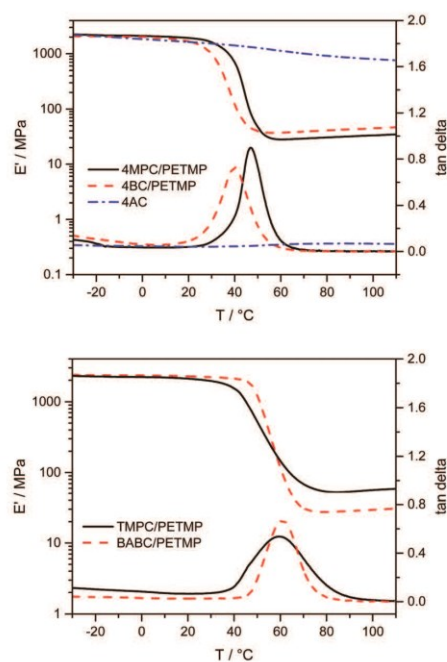


**Fig. 2** Storage modulus and tan delta from DMA measurements of investigated polymer samples. Upper: 4MPC/PETMP (solid), 4BC/PETMP (dashed), 4AC (chain dotted). Lower: TMPC/PETMP (solid), BABC/PETMP (dashed).

shrinkage stress during the fast radical chain growth polymerization and the inhomogeneous polymeric architecture, respectively. For example, 4AC offers a comparably high glass transition temperature of 83 °C and an appropriate modulus (1422 MPa), however, it exhibits a Charpy impact strength of only  $a_{CU} = 3 \pm 1$  kJ m<sup>-2</sup>, (see Fig. 4) which is far too low for an application as hard tissue replacements.

Since the thiol-yne polymerization yields networks with unique homogeneity and reduced shrinkage stress, these polymeric materials are expected to possess increased toughness.

This assumption could be confirmed for TCBC/PETMP and TCBC/DiPETMP providing Charpy impacts strengths of  $a_{CU} = 44 \pm 5$  kJ m<sup>-2</sup> and  $a_{CU} = 29 \pm 5$  kJ m<sup>-2</sup>. Although the combination TCBC/DiPETMP shows lower impact strength than TCBC/PETMP, it offers similar properties to PLA ( $a_{CU} \approx 19$  kJ m<sup>-2</sup>,  $T_g \approx 55$ –65 °C,  $E' \approx 3000$  MPa).<sup>16,22,37</sup> One explanation for the lower impact strength of TCBC/DiPETMP compared to TCBC/PETMP is its higher crosslinking density that is known to behave diametrically to the impact properties.

### Degradation

Hydrolytic degradation of polymers can be one desired material property of medical devices, as it is the case for scaffolds required for bone regeneration therapies.<sup>38</sup>

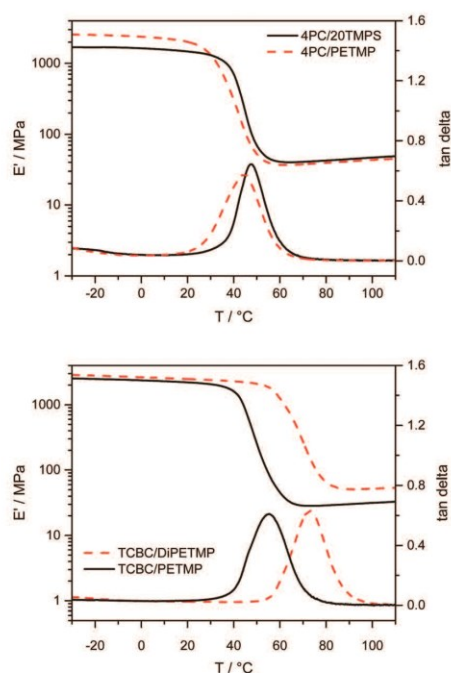


Fig. 3 Storage modulus and tan delta from DMA measurements of investigated polymer samples. Upper: 4PC/20TMPS (solid), 4PC/PETMP (dashed). Lower: TCBC/DIPETMP (dashed) and TCBC/PETMP (solid).

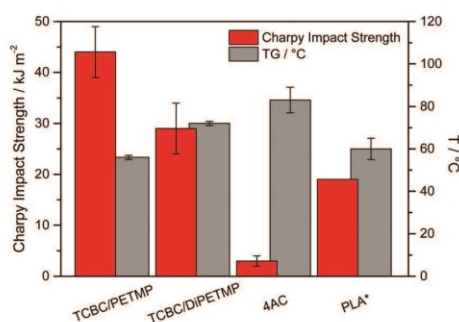


Fig. 4 Charpy impact strength and  $T_g$  of TCBC/PETMP, TCBC/DIPETMP, 4AC and PLA (\* for Charpy impact strength of PLA review Mautner *et al.*; for  $T_g$  of PLA review Middleton *et al.* and Hassan *et al.*<sup>16,22,37</sup>).

(Meth)acrylate networks provide, however, only very limited biodegradability and the resulting high molecular weight (meth)acrylic acid can lead to adverse effects like tissue necrosis.<sup>6</sup> In contrast, polymers made from step-growth reaction that contain degradable linkers are expected to degrade in low molecular fragments that can be easily transported within the human body allowing frequent reduction of undesired degradation products from the degradation site.<sup>22,39</sup> Although there

are several procedures and media described for the *in vitro* evaluation of the biodegradability of polymeric materials, *e.g.* phosphate-buffered saline with a pH of 7.4 at 37 °C, a proper simulation of *in vivo* bio resorption can hardly be accomplished as factors like polymer-cell interactions cannot be simulated easily.<sup>8</sup> Since degradation times can take up to several years, it is common to perform accelerated tests at higher temperatures and/or pH.<sup>16,40,41</sup> Considering the fact that medical devices could also be exposed to regions with a lower pH value as of blood (pH = 7.4), for example to the buccal mucosa, accelerated degradation test were performed under both, alkaline (1 M NaOH) and acidic conditions (1 M HCl) at 45 °C. The herein investigated alkyne and thiol building blocks contain carbonate and ester moieties, which are capable to undergo hydrolytic degradation under these conditions. Firstly, the degradability of the carbonate group and the impact of the alkyne chain functionality were studied using 4PC, 4BC and 4MPC in combination with the bifunctional thiol 2,2'-(ethylenedioxy)diethanethiol (EDT), which bears glycol ether groups, known to be chemically inert in both basic and acid aqueous media. Moreover, it can be expected that EDT supports the hydrolysis of these polymers, as it decreases the cross-link density (compared to tetrafunctional thiols) and the polar ether groups facilitate swelling. Interestingly, these networks show only minor degradation (1–7% decrease in mass) after 40 days of storage in both media (as shown in Fig. 5) revealing the comparably high stability of carbonate moieties under these conditions. In contrast, alkyne carbonates that were photo-crosslinked with PETMP showed a considerable high degradation that can be attributed to hydrolytic sensitivity of the ester groups. Importantly, the rate strongly depends on the alkynyl chain functionality and on the pH of the simulant. Table 3 shows the extrapolated time to reach full degradation in NaOH for formulations crosslinked with PETMP and/or TMPS. For comparison reasons these values are an extrapolation of the presented curves in Fig. 5. While 4PC/PETMP and 4BC/PETMP show full degradation within 7.6 days in 1 M NaOH, which behave similar to PLA (7.5 d), the rate of degradation is much lower for 4MPC/PETMP (34.6 d). This finding can be attributed to the additional methyl group of 4MPC that enhances the hydrophobicity of the network and can sterically decelerate hydrolytic cleavage reactions. Not surprisingly, the degradation rate in 1 M HCl is significantly lower, as ester moieties are more sensitive towards alkaline hydrolysis.<sup>42</sup> Following the concept that the content on ester moieties in polymeric networks determines the degradation rate,<sup>43</sup> 4PC was photo-cured with two different thiols, PETMP and the non-degradable, tetrafunctional thiol TMPS. Both thiols were mixed in different molar ratios, upholding the overall stoichiometry (alkyne groups : mercapto groups = 1 : 2). The replacement of only 5 mol% of PETMP by TMPS leads to a clear reduction of the degradation velocity (12.6 d) as clearly revealed in Fig. 5. The degradation rate could be further reduced by substitution of 10 mol% (21.7 d) and 20 mol% (28.0 d) PETMP, respectively. These results clearly indicate that it is possible to selectively adjust the

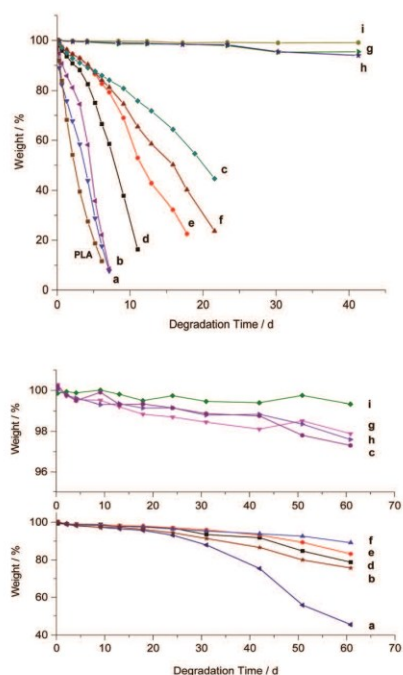


Fig. 5 Weight loss during degradation for the formulations (a) 4PC/PETMP, (b) 4BC/PETMP, (c) 4MPC/PETMP, (d) 4PC/5TMPS, (e) 4PC/10TMPS, (f) 4PC/20TMPS, (g) 4PC/EDT, (h) BC/EDT, (i) MPC/EDT and PLA (upper only) in 1 M NaOH (upper) and 1 M HCl at 45 °C (lower).

Table 3 Time to reach full degradation (extrapolated values)

Formulation	Estimated full degradation/d
4PC/PETMP	7.6
4BC/PETMP	7.7
MPC/PETMP	34.6
4PC/5TMPS	12.6
4PC/10TMPS	21.7
4PC/20TMPS	28.0
PLA	7.5

degradation time of such materials by the choice of the selected monomers. In this context, it has to be mentioned that the substitution of 20% PETMP by TMPS does not negatively influence the thermo-mechanical properties (*vide supra*). Importantly, it turned out that networks made from tetrafunctional thiols, *i.e.* PETMP and TMPS, show surface erosion, while polymers containing the bifunctional thiol EDT tend to swelling and bulk erosion. For bioresorbable medical implants surface erosion is favoured because swelling in combination with bulk degradation leads to a premature and non-linear decrease in the mechanical properties.<sup>44</sup> Based on the presented results alkyne carbonates seem to be appropriate candidates for bioresorbable hard tissue replacements, although

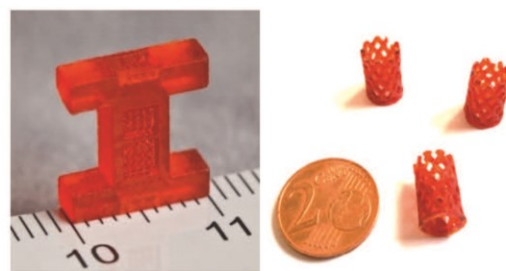


Fig. 6 3D printed test patterns from a TCBC/DiPETMP formulation (scale on the left shown in cm).

further detailed studies on the *in vivo* degradation behaviour are necessary.

### 3D printing of tough resin formulation

Since TCBC based resins showed excellent performances regarding curing rate and conversion together with low cytotoxicity and their networks provide decent mechanical properties in terms of modulus and impact strength, this monomer was chosen for the evaluation of its 3D printability by a DLP printer, offering the advantage of low material consumption, short production times and sufficiently high resolution. As the used DLP system is based on blue light (peak at 465 nm) an appropriate light absorber (Sudan II) and photoinitiator (Ivocerin®) has to be added. Formulation of TCBC/DiPETMP could be printed successfully with an accuracy of  $40 \times 40 \mu\text{m}$  as shown on the test structures illustrated in Fig. 6. This resolution is high enough to print medical devices with smooth surfaces or bone scaffolds, where textures with pore sizes of 50–1000  $\mu\text{m}$  are known to allow optimal bone ingrowth.<sup>6,45</sup>

## Conclusion

This contribution deals with the synthesis of new biocompatible monomers based on the thiol-yne reaction with the aim to facilitate the fabrication of tailor made medical devices by UV based additive manufacturing technologies. A particular focus was set on the investigation of the cytotoxicity of the monomers, the mechanical properties of the obtained networks and their biodegradability. While the curing rates of the investigated alkyne carbonate/thiol formulation are in the range of acrylates, they offer significantly higher conversions between 84–98%. Moreover, it could be successfully shown that the synthesized alkyne carbonate based compounds provide considerably lower cytotoxicity as the corresponding (meth)acrylates. Interestingly, the cytotoxicity of the tested alkyne carbonates is strongly influenced by the alkynyl functionality, whereby the pent-4-yn-2-yl derivative (4MPC) offers the highest EC50 value. Although the long term toxicity of such compounds has to be investigated in further studies, these alkyne carbonate/thiol

resins provide almost quantitative conversions that reduces the migration of potential harmful compounds to a level that cannot be reached by (meth)acrylate monomers. Curing the synthesized building blocks in combination with PETMP, networks which contain cleavable ester moieties were obtained that provide degradability in aqueous alkaline and acidic media. Through the substitution of PETMP by 5 to 20 mol% TMPS, a selective adjustment of the degradation rate is feasible, which does not negatively influence the thermo-mechanical properties. Moreover, it turned out that networks made from the tetrafunctional thiols PETMP and TMPS showed surface erosion with an almost linear decrease in mass during storage in 1 M NaOH and 1 M HCl at 45 °C, respectively. Most importantly, monomers that contain a tricyclo[5.2.1.0<sup>2,6</sup>]decane-4,8-dimethanol spacer provide decent thermo-mechanical properties together with appropriate impact strength in the range of PLA. These findings can be attributed to the network homogeneity and the reduced shrinkage stress which occur during thiol-yne photopolymerisation. Formulations of TCBC/DiPETMP were printed successfully with an accuracy of 40 × 40 μm, which seems to be high enough to print medical devices with smooth surfaces or bone scaffolds, where textures with pore sizes of 50–1000 μm are known to support bone ingrowth.

Alkyne carbonate based resins seem to be appropriate candidates for the 3D fabrication of bioresorbable hard tissue replacements, even though further detailed studies on the *in vivo* degradation behaviour and on the tissue compatibility are necessary.

## Acknowledgements

Financial support by the Christian Doppler Research Association, the Austrian Federal Ministry of Science, Research and Economy (BMWFW), and Durst Phototechnik GmbH is gratefully acknowledged.

## References

- J. Banks, *IEEE Pulse*, 2013, 4, 22–26.
- B. C. Gross, J. L. Erkal, S. Y. Lockwood, C. Chen and D. M. Spence, *Anal. Chem.*, 2014, 86, 3240–3253.
- G. T. Klein, Y. Lu and M. Y. Wang, *World Neurosurg.*, 2013, 80, 233–235.
- A. Dawood, B. M. Marti, V. Sauret-Jackson and A. Darwood, *Br. Dent. J.*, 2015, 219, 521–529.
- E. Farré-Guasch, J. Wolff, M. N. Helder, E. A. Schulten, T. Forouzanfar and J. Klein-Nulend, *J. Oral Maxillofac. Surg.*, 2015, 73, 2408–2418.
- B. Husár, C. Heller, M. Schwentenwein, A. Mautner, F. Varga, T. Koch, J. Stampfl and R. Liska, *J. Polym. Sci., Part A: Polym. Chem.*, 2011, 49, 4927–4934.
- R. Liska, M. Schuster, R. Inführ, C. Turecek, C. Fritscher, B. Seidl, V. Schmidt, L. Kuna, A. Haase, F. Varga, H. Lichtenegger and J. Stampfl, *J. Coat. Technol. Res.*, 2007, 4, 505–510.
- C. Heller, M. Schwentenwein, G. Russmüller, T. Koch, D. Moser, C. Schopper, F. Varga, J. Stampfl and R. Liska, *J. Polym. Sci., Part A: Polym. Chem.*, 2011, 49, 650–661.
- Photopolymerization and Photoimaging Science and Technology*, ed. N. S. Allen, Elsevier Applied Science, London, 1st edn, 1989.
- Photoinitiation, Photopolymerization, and Photocuring: Fundamentals and applications*, ed. J. P. Fouassier, Hanser Publisher, New York, NY, USA, 1995.
- M. Schuster, C. Turecek, B. Kaiser, J. Stampfl, R. Liska and F. Varga, *J. Polym. Sci., Part A: Polym. Chem.*, 2007, 44, 547–557.
- N. Moszner and U. Salz, *Macromol. Mater. Eng.*, 2007, 292, 245–271.
- L. S. Andrews and J. J. Clary, *J. Toxicol. Environ. Health*, 1986, 19, 149–164.
- E. A. Emmett, *Contact Dermatitis*, 1977, 3, 245–248.
- I. Vroman and L. Tighzert, *Materials*, 2009, 2, 307–344.
- J. C. Middleton and A. J. Tipton, *Biomaterials*, 2000, 21, 2335–2346.
- A. Mautner, X. Qin, G. Kapeller, G. Russmüller, T. Koch, J. Stampfl and R. Liska, *Macromol. Rapid Commun.*, 2012, 33, 2046–2052.
- C. Gorsche, K. Seidler, P. Knaack, P. Dörfinger, T. Koch, J. Stampfl, N. Moszner and R. Liska, *Polym. Chem.*, 2016, 7, 2009–2014.
- P. Dörfinger, J. Stampfl and R. Liska, *MSF*, 2015, 825–826, 53–59.
- S. C. Ligon-Auer, M. Schwentenwein, C. Gorsche, J. Stampfl and R. Liska, *Polym. Chem.*, 2016, 7, 257–286.
- B. Husar and R. Liska, *Chem. Soc. Rev.*, 2012, 41, 2395.
- A. Mautner, B. Steinbauer, S. Orman, G. Russmüller, K. Macfelda, T. Koch, J. Stampfl and R. Liska, *J. Polym. Sci., Part A: Polym. Chem.*, 2016, 54, 1987–1997.
- A. Mautner, X. Qin, H. Wutzel, S. C. Ligon, B. Kapeller, D. Moser, G. Russmüller, J. Stampfl and R. Liska, *J. Polym. Sci., Part A: Polym. Chem.*, 2013, 51, 203–212.
- A. B. Lowe, *Polymer*, 2014, 55, 5517–5549.
- A. Lowe and C. Bowman, *Thiol-X Chemistries in Polymer and Materials Science*, Royal Society of Chemistry, Cambridge, 2013.
- B. D. Fairbanks, T. F. Scott, C. J. Kloxin, K. S. Anseth and C. N. Bowman, *Macromolecules*, 2009, 42, 211–217.
- J. W. Chan, J. Shin, C. E. Hoyle, C. N. Bowman and A. B. Lowe, *Macromolecules*, 2010, 43, 4937–4942.
- H. E. Gottlieb, V. Kotlyar and A. Nudelman, *J. Org. Chem.*, 1997, 62, 7512–7515.
- M. Roth, A. Oesterreicher, F. H. Mostegel, A. Moser, G. Pinter, M. Edler, R. Piock and T. Griesser, *J. Polym. Sci., Part A: Polym. Chem.*, 2016, 54, 418–424.
- S. Reinelt, M. Tabatabai, N. Moszner, U. K. Fischer, A. Utterodt and H. Ritter, *Macromol. Chem. Phys.*, 2014, 215, 1415–1425.
- L. Cotarca, P. Delogu, A. Nardelli and V. Šunjić, *Synthesis*, 1996, 553–576.

- 32 S. P. Rannard and N. J. Davis, *Org. Lett.*, 1999, **1**, 933–936.
- 33 B. D. Fairbanks, E. A. Sims, K. S. Anseth and C. N. Bowman, *Macromolecules*, 2010, **43**, 4113–4119.
- 34 C. D. Calnan, *Contact Dermatitis*, 1980, **6**, 53–54.
- 35 S. Reinelt, M. Tabatabai, U. K. Fischer, N. Moszner, A. Utterodt and H. Ritter, *Beilstein J. Org. Chem.*, 2014, **10**, 1733–1740.
- 36 J. W. Chan, H. Zhou, C. E. Hoyle and A. B. Lowe, *Chem. Mater.*, 2009, **21**, 1579–1585.
- 37 E. Hassan, Y. Wei, H. Jiao and M. Yu, *JFBI*, 2013, **6**, 85–94.
- 38 T. Weigel, G. Schinkel and A. Lendlein, *Expert Rev. Med. Devices*, 2014, **3**, 835–851.
- 39 C. Heller, M. Schwentenwein, G. Russmueller, F. Varga, J. Stampfl and R. Liska, *J. Polym. Sci., Part A: Polym. Chem.*, 2009, **47**, 6941–6954.
- 40 Y. Ikada, *J. R. Soc., Interface*, 2006, **3**, 589–601.
- 41 X. Yuan, A. F. Mak and K. Yao, *Polym. Degrad. Stab.*, 2002, **75**, 45–53.
- 42 R. M. Ginde and R. K. Gupta, *J. Appl. Polym. Sci.*, 1987, **33**, 2411–2429.
- 43 M. Podgórski, E. Becka, S. Chatani, M. Claudino and C. N. Bowman, *Polym. Chem.*, 2015, **6**, 2234–2240.
- 44 C. Heller, M. Schwentenwein, G. Russmüller, T. Koch, D. Moser, C. Schopper, F. Varga, J. Stampfl and R. Liska, *J. Polym. Sci., Part A: Polym. Chem.*, 2011, **49**, 650–661.
- 45 A. Curodeau, E. Sachs and S. Caldarise, *J. Biomed. Mater. Res.*, 2000, **53**, 525–535.



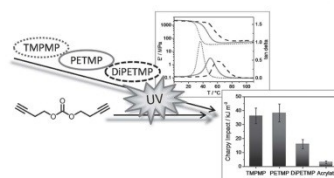
## Publication III

Oesterreicher, Andreas; Gorsche, Christian; Ayalur-Karunakaran, Santhosh; Moser, Andreas; Edler, Matthias; Pinter, Gerald; Schlögl, Sandra; Liska, Robert; Griesser, Thomas: Exploring Network Formation of Tough and Biocompatible Thiol-yne Based Photopolymers *Macromol. Rapid Commun.* **2016**, 37, 1701-1706.

# Exploring Network Formation of Tough and Biocompatible Thiol-yne Based Photopolymers

Andreas Oesterreicher, Christian Gorsche, Santhosh Ayalur-Karunakaran, Andreas Moser, Matthias Edler, Gerald Pinter, Sandra Schlögl, Robert Liska, Thomas Griesser\*

This work deals with the in-depth investigation of thiol-yne based network formation and its effect on thermomechanical properties and impact strength. The results show that the bifunctional alkyne monomer di(but-1-yne-4-yl)carbonate (**DBC**) provides significantly lower cytotoxicity than the comparable acrylate, 1,4-butanediol diacrylate (**BDA**). Real-time near infrared photorheology measurements reveal that gel formation is shifted to higher conversions for **DBC**/thiol resins leading to lower shrinkage stress and higher overall monomer conversion than **BDA**. Glass transition temperature ( $T_g$ ), shrinkage stress, as well as network density determined by double quantum solid state NMR, increase proportionally with the thiol functionality. Most importantly, highly cross-linked **DBC**/dipentaerythritol hexa(3-mercaptopropionate) networks ( $T_g \approx 61$  °C) provide a 5.3 times higher impact strength than **BDA**, which is explained by the unique network homogeneity of thiol-yne photopolymers.



## 1. Introduction

Photopolymers are well established in industry, reaching from coatings and paintings to lithographic resins for the production of microelectronics or optical materials.<sup>[1]</sup> The

last decade has seen a remarkable increase in the development of lithography based additive manufacturing techniques for polymeric materials.<sup>[2–4]</sup> Compared to other 3D printing methods these light-based techniques offer several advantages, including higher writing speed and better resolutions.<sup>[5]</sup> However, state of the art UV curable resins are limited to (meth)acrylate based monomers and their resulting polymeric networks. These building blocks are characterized by high curing rates, which can be ascribed to a fast radical chain growth polymerization that can form highly cross-linked networks within seconds.<sup>[1]</sup> Considerable drawbacks of (meth)acrylate building blocks are their remarkably high irritancy potential and cytotoxicity, which can be attributed to their reactivity toward Michael addition reactions with amino- or thiol-groups of proteins or DNA.<sup>[6–8]</sup> These drawbacks in addition to the nonquantitative curing behavior of this class of monomers prevents them from being considered usable for the individual fabrication of medical devices by additive manufacturing methods where the final product is meant to be in contact or even within the human body.<sup>[9,10]</sup> Another disadvantage of radically cured photopolymers is their comparably low polymer toughness which drastically limits their applicability. This behavior can be attributed to the

A. Oesterreicher, Dr. M. Edler, Prof. T. Griesser  
Chair of Chemistry of Polymeric Materials & Christian  
Doppler Laboratory for Functional and Polymer  
Based Ink-Jet Inks  
University of Leoben  
Otto-Glöckel-Strasse 2, A-8700 Leoben, Austria  
E-mail: thomas.griesser@unileoben.ac.at  
Dr. C. Gorsche, Prof. R. Liska  
Institute of Applied Synthetic Chemistry &  
Christian-Doppler-Laboratory for Photopolymers  
in Digital and Restorative Dentistry  
TU Wien, Getreidemarkt 9/163-MC 1060, Vienna, Austria  
Dr. S. Ayalur-Karunakaran, Dr. S. Schlögl  
Polymer Competence Center Leoben GmbH  
Roseggerstrasse 12, 8700 Leoben, Austria  
A. Moser, Prof. G. Pinter  
Chair of Material Science and Testing of Polymers  
University of Leoben  
Otto-Glöckel-Strasse 2, A-8700 Leoben, Austria

evolution of shrinkage stress during the fast radical chain growth polymerization and the formation of an inhomogeneous polymeric network structure.<sup>[11,12]</sup> Besides an appropriate Young's modulus and glass transition temperature, high toughness in terms of impact resistance is a key requirement for many applications that have to withstand and absorb mechanical forces.

Subsequently, numerous approaches have been proposed to overcome these drawbacks.<sup>[12]</sup> Very recently, it could be shown that the use of addition fragmentation chain transfer reagents in (meth)acrylate resins provides a precise regulation of the network formation, thus improving thermal and mechanical properties.<sup>[11]</sup> Another possibility offered through thiol-ene chemistry is the generation of highly uniform networks via a radical step growth mechanism.<sup>[13]</sup> However, the addition of multifunctional thiols to (meth)acrylates significantly lowers the thermomechanical properties, i.e., modulus and glass transition temperature, of these photopolymers. This fact can be attributed to a decrease of the cross-link density and also to the flexibility of the formed thioether bonds.<sup>[14]</sup>

Highly cross-linked thioether based networks that provide similar thermomechanical properties to those of poly(meth)acrylates can be obtained by using multifunctional alkynes instead of vinyl monomers.<sup>[15–17]</sup> This so-called thiol-yne reaction leads to homogeneous networks and offers the well reported advantageous aspects of thiol based chemistry, including the formation of low shrinkage stress during polymerization which promises photopolymers with decent toughness.<sup>[18]</sup> It is well known that terminal alkyne groups, without electron withdrawing moieties in their neighborhood, are mostly inert toward thiols (thiol Michael reaction), even under basic conditions.<sup>[19]</sup> This suggests a higher biocompatibility of alkyne based building blocks. Moreover, it was shown that thiols based on mercapto propionic acid derivatives provide low monomer cytotoxicity.<sup>[20]</sup>

Herein, we study the formation of thiol-yne networks from di(but-1-yne-4-yl)carbonate (**DBC**) and selected multifunctional thiols (see Scheme 1) with the aim to facilitate photoreactive systems, which combine low cytotoxicity and high photoreactivity with appropriate thermomechanical properties and decent toughness in the cured state.

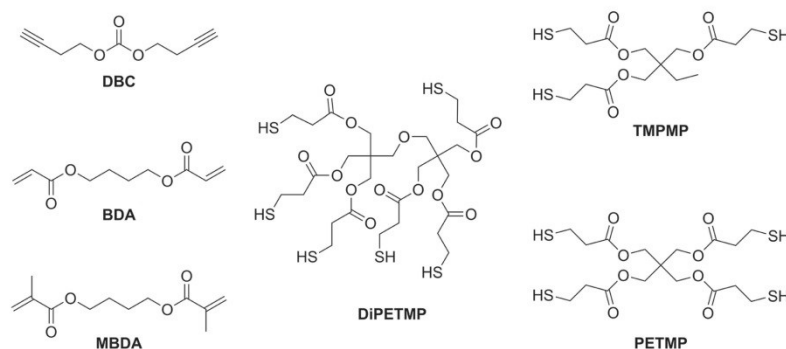
## 2. Results and Discussion

### 2.1. Cell Culture Experiments

The cytotoxic potential of **DBC** (synthesis see Supporting Information) was evaluated and compared to **BDA** and 1,4-butanediol dimethacrylate (**MBDA**). The bifunctional (meth)acrylate model compounds **BDA** and **MBDA**, respectively, were chosen because they provide a similar structure and molecular mass as **DBC**. The results are that **DBC** shows significant higher EC50 values ( $1.6 \times 10^{-3}$  M; concentration where 50% of the cells were still viable) than **BDA** ( $<0.16 \times 10^{-3}$  M) and the corresponding methacrylate **MBDA** ( $<0.16 \times 10^{-3}$  M).

### 2.2. Exploration of the Photoreactivity Via Photo-Differential Scanning Calorimetry (Photo-DSC)

Photo-DSC represents a unique method for the fast and accurate evaluation of kinetic parameters of UV induced polymerizations. The reaction time  $t_{\max}$  is the time to reach the maximum of polymerization enthalpy. Together with the peak shape, it reveals information about the overall photoreactivity. Figure 1 (left) displays the photo-DSC plots of the investigated **DBC**/thiol formulations, **BDA** and **MBDA**. While the thiol-yne formulations provide reactivities similar to **BDA** ( $t_{\max} = 2.4\text{--}2.7$  s), the methacrylate based monomer **MBDA** shows only moderate curing performance ( $t_{\max} = 6.5$  s), thus it was not considered in further investigations. **BDA** and the thiol-yne formulations reach



Scheme 1. Structures of the investigated monomers.

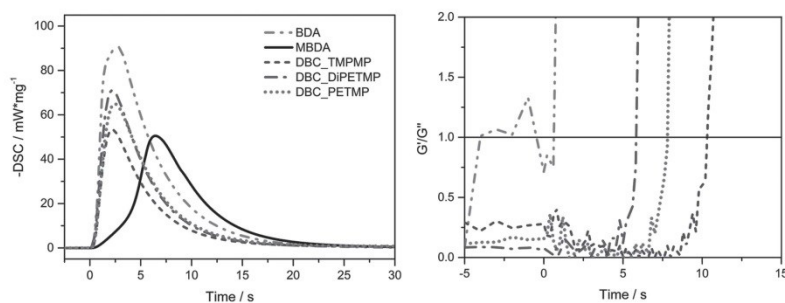


**Figure 1.** Photo-DSC plots (left) and determination of the gel point ( $G'/G'' = 1$ , -) (right) of **BDA** (chain double dotted), **MBDA** (solid, left only), **DBC/TMPMP** (dashed), **DBC/PETMP** (dotted), **DBC/DiPETMP** (chain dotted). Light starts at 0 s.

full polymerization heat after  $\approx 30$  s, which also indicates similar reactivity. Besides the kinetics of photopolymerizations, photo-DSC can also be used to determine monomer conversion (MC), as it is directly proportional to the developed reaction heat. However, due to different theoretical heats of polymerization for (meth)acrylates and thiol-yne resins, respectively, MC was determined by real-time near infrared photorheology (RT-NIR photorheology; vide infra).

### 2.3. In Situ Investigation of Network Formation by RT-NIR-Photorheology

Other important parameters of photopolymerization that strongly influence the curing speed, as well as the mechanical properties of obtained photopolymers, are the time to reach gelation ( $t_{\text{gel}}$ ), the conversion at the gel point ( $\text{MC}_g$ ), the overall conversion (MC), and the shrinkage stress. A unique method to determine all of those parameters provides RT-NIR photorheology.<sup>[21]</sup>

It is well reported that thiol-based step growth polymerization reactions exhibit higher monomer conversions at the gel point compared to the homopolymerization of (meth)acrylates.<sup>[13]</sup> This causes a higher overall conversion, which can be assigned to the higher mobility of monomers and formed radicals below the gel point. The difference in the reaction mechanism also explains the reduced evolution of shrinkage stress during thiol-based polymerization reactions. In acrylate polymerizations, the gel point is reached at low conversions. Further conversion in the gel state induces shrinkage stress, as the material is no longer able to flow and compensate the shrinkage. Consequently, high conversion at the gel point significantly reduces shrinkage stress in the final material.

In photorheology,  $t_{\text{gel}}$  corresponds to the time until the intersection of storage and loss modulus ( $G'/G'' = 1$ ) is reached.<sup>[21]</sup> Figure 1 displays the ratio of  $G'/G''$  in dependence of curing time of the investigated monomers. While **BDA** gels already after 1.7 s, the thiol-yne resins provide significantly delayed gel formation. It was also found that

$t_{\text{gel}}$  decreases with increasing functionality of the thiol used in the formulation. For comparison, resins based on the trifunctional thiol **TMPMP** reach the gel point within 10.3 s, while the resin with the hexafunctional **DiPETMP** requires only approximately half as long (5.3 s). The higher network formation velocity and the higher viscosity of multifunctional monomers explain this behavior.

Furthermore, the conversion at the gel point ( $\text{MC}_g$ ) was evaluated by monitoring the decrease of the peak areas of alkyne and acrylate groups in the NIR region. The results of these measurements (shown in Table 1) reveal considerably higher  $\text{MC}_g$ s at the gel point for the **DBC**/thiol formulations (35%–55%) compared to **BDA** (18%). Accordingly, a decrease in  $\text{MC}_g$  is observed, alongside an increasing thiol functionality. Taking into account that the studied thiol-yne formulations provide similar photoreactivity, lower  $t_{\text{gel}}$  values explain the decrease of  $\text{MC}_g$  with increasing thiol functionality. Beside  $\text{MC}_g$ , the overall conversion is also significantly influenced by  $t_{\text{gel}}$  and the photoreactivity. The step growth mechanism of thiol-yne reactions facilitates delayed gel formation, thus monomers and formed radicals can interact much longer as in the case of **BDA**. Although **DBC**/thiol formulations show significantly higher viscosities (Table 1) than **BDA**, they provide MCs of 90%–95%.

The network formation during curing exerts a strong impact on the properties of the final material. Monitoring the normal force  $F_N$  during photorheology gives an indication of the developed shrinkage stress. As shown in Figure S5 of the Supporting Information, **BDA** shows an  $F_N$  of 32.7 N, whereas the thiol-yne based resins provide lower values of  $F_N$  after 300 s of illumination, as seen for **DBC/TMPMP** (22.1 N), followed by **DBC/PETMP** (24.7 N) and **DBC/DiPETMP** (26.0 N).

### 2.4. Characterization of Network Properties

While the modulus and glass transition temperature of polymers can be measured by dynamic mechanical

**Table 1.** Investigated parameters of alkyne/thiol formulations and their corresponding photopolymers including reference sample **BDA**. ( $\eta$ : viscosity;  $t_{\text{gel}}$ : time to reach gelation;  $MC_{\text{g}}$ : conversion at the gel point;  $MC$ : overall monomer conversion;  $DF$ : defect fraction;  $Rel. D_{\text{res}}$ : relative residual dipolar coupling;  $Rel. E'(100\text{ }^{\circ}\text{C})$ : relative storage modulus at  $T=100\text{ }^{\circ}\text{C}$ ;  $T_{\text{g}}$ : glass transition temperature;  $E'$  at  $20\text{ }^{\circ}\text{C}$ : storage modulus at  $20\text{ }^{\circ}\text{C}$ ).

Formulation	$\eta$ [mPas]	$t_{\text{gel}}$ [s]	$MC_{\text{g}}$ [%]	$MC$ [%]	$DF$ [%]	Rel. $D_{\text{res}}$	Rel. $E'$ ( $100\text{ }^{\circ}\text{C}$ )	$T_{\text{g}}$ [ $^{\circ}\text{C}$ ]	$E'$ at $20\text{ }^{\circ}\text{C}$ [MPa]
DBC/TMPMP	66	$10.3 \pm 0.2$	$55 \pm 2$	95	5	1.0	1.0	37	$2048 \pm 20$
DBC/PETMP	114	$8.1 \pm 0.2$	$46 \pm 1$	92	11	1.5	1.3	50	$1937 \pm 266$
DBC/DiPETMP	298	$5.6 \pm 0.3$	$35 \pm 1$	90	12	1.8	1.6	61	$1939 \pm 88$
BDA	4	$1.7 \pm 0.1$	$18 \pm 2$	89	–	–	–	$83 \pm 6$	$1612 \pm 22$

analysis (DMA), the investigation of the network density of highly cross-linked photopolymers is difficult. For example, equilibrium swelling tests can only be applied to slightly cross-linked polymers.<sup>[22]</sup> For very homogeneous networks, the cross-link density correlates with the glass transition temperature and the storage modulus in the rubbery state.<sup>[15]</sup>

A unique method to study network characteristics is the double quantum (DQ) build-up NMR method.<sup>[23]</sup> This gives quantitative access to network density as well as the fraction of non-network chains (DF), which are a measure for nonreacted monomers, photoinitiator or its cleavage products. Further details can be found in the Supporting Information. In this study, DQ NMR has been used to investigate the cross-link density of the thiol-yne based photopolymers. It can be assumed that the network density directly correlates with the functionality of the applied thiol building blocks. The  $D_{\text{res}}$  values (which relate to the cross-link density) and the fraction of non-network chains determined for samples **DBC/TMPMP**, **DBC/PETMP**, and **DBC/DiPETMP** are given in Table 1. The network of **DBC/TMPMP** shows the lowest cross-link density (4.6) followed by **DBC/PETMP** (7.0) and **DBC/DiPETMP** (8.4). As these networks offer comparably high homogeneity, reflected by their narrow glass transitions indicated by full widths at half maxima (FWHM) of  $10\text{--}22\text{ }^{\circ}\text{C}$  (Figure 2, left), the network density can also be estimated

using the storage moduli in the rubbery state.<sup>[15]</sup> Considering the relative values of  $D_{\text{res}}$  and the relative storage modulus at  $100\text{ }^{\circ}\text{C}$  [Rel.  $E'(100\text{ }^{\circ}\text{C})$ ] (related to **DBC/TMPMP** as shown in Table 1), only slight deviations between both measurements can be found. In addition, the values of the non-network fraction also correlate with the amount of unreacted monomer, including photoinitiator residues and cleavage products. These results clearly reveal the advantage of DQ-NMR that allows the determination of network density as well as the fraction of non-network molecules in one single measurement. Interestingly, the cross-link density exerts only minor influence on the storage modulus (see Table 1). While all investigated polymers exhibit storage moduli in the range of  $1900\text{--}2100$  MPa at  $20\text{ }^{\circ}\text{C}$ , the glass transition temperature increases steadily from  $37\text{ }^{\circ}\text{C}$  (**DBC/TMPMP**) to  $61\text{ }^{\circ}\text{C}$  (**DBC/DiPETMP**) with increasing cross-link density. In comparison, cured **BDA** shows a broad glass transition that is explained by the comparably inhomogeneous network showing its maximum of  $\tan\delta$  at  $83\text{ }^{\circ}\text{C}$  and a storage modulus of  $1612$  MPa at  $20\text{ }^{\circ}\text{C}$  (see Figure S4, Supporting Information).

Moreover, it can be observed that the homogeneity of the thiol-yne networks decreases with higher thiol functionality as reflected by broader glass transitions. Presumably, this behavior can be directly attributed to the decrease in  $MC_{\text{g}}$ . Polymerization above the gel point seems to lead to a decrease in homogeneity.

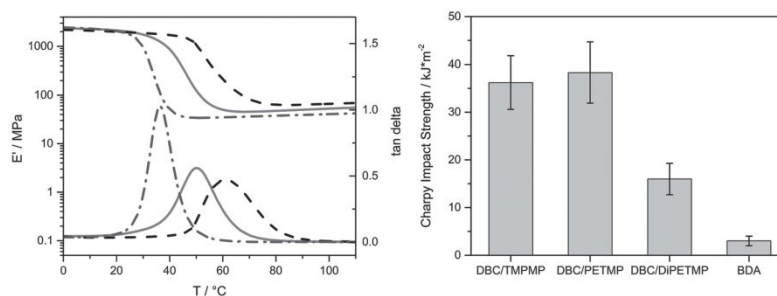


**Figure 2.** (Left) DMA plots of **DBC/TMPMP** (chain dotted), **DBC/PETMP** (solid), and **DBC/DiPETMP** (dashed); (Right) Charpy impact strengths.

Besides a high modulus and glass transition temperature, an appropriate impact resistance that can be seen as an indicator for toughness is an important prerequisite for high performance polymeric materials. State of the art photopolymers are rather brittle due to the evolution of shrinkage stress during the fast radical chain growth polymerization and their inhomogeneous polymeric architecture, respectively. For example, **BDA** exhibits a Charpy impact strength of only  $3 \text{ kJ m}^{-2}$ , which seems to be insufficient for applications that have to be capable of absorbing a certain amount of energy. It is well documented that the addition of thiols to (meth)acrylates results in an increase in toughness by changing the polymerization mechanism from a radical chain growth reaction to a mixed chain growth/step growth-like radical polymerization.<sup>[13]</sup> However, this change goes along with a decrease in cross-link density leading to a significant reduction in the glass transition temperature. In contrast, the thiol-yne networks provide impact strengths between  $16\text{--}38 \text{ kJ m}^{-2}$  (see Figure 2, right) maintaining reasonable glass-transition temperatures ( $37\text{--}61 \text{ }^\circ\text{C}$ ). Notably, highly cross-linked **DBC/DiPETMP** outperforms **BDA** significantly in terms of modulus (**BDA**:  $1612 \text{ MPa}$ , **DBC/DiPETMP**:  $1939 \text{ MPa}$ ) and impact strength (**BDA**:  $3 \text{ kJ m}^{-2}$ , **DBC/DiPETMP**:  $16 \text{ kJ m}^{-2}$ ) and also offers a reasonable  $T_g$  of  $61 \text{ }^\circ\text{C}$ . Interestingly, the polymerization of both resins leads to comparable shrinkage stress values expressed in  $F_N$  (**BDA**:  $33 \text{ N}$ , **DBC/DiPETMP**:  $26 \text{ N}$ ). This fact suggests that the difference in impact strength (factor of 5.3) is not only caused by shrinkage stress, but rather through network homogeneity playing an important role.

### 3. Conclusion

In conclusion, the network formation of thiol-yne resins and their properties in the cured state were studied, aiming for polymers that combine high thermomechanical properties with appropriate toughness. The low-cytotoxic alkyne monomer **DBC** was copolymerized with different multifunctional thiol building blocks and the network properties of resulting polymers were compared with the corresponding acrylate **BDA**. RT-NIR photorheology measurements revealed high  $MC_g$  for thiol-yne resins compared to **BDA**, resulting in high monomer conversions and low shrinkage stress, respectively. Important to note is that the  $t_{gel}$  decreases while shrinkage stress increases with the functionality of the applied thiol. The photoreactivity of the thiol-yne resins in terms of  $t_{max}$  is in the range of **BDA**. High photoreactivity and the delayed gel formation explain the obtained high values of the overall conversion ( $90\text{--}95\%$ ). The  $T_g$  of cured **DBC**/thiol formulations increases proportionally with the network density, which was studied by DQ solid state NMR spectroscopy,

although the storage modulus remains at a similar level. Most importantly, **DBC**/thiol based polymers outperform **BDA** significantly in terms of impact strength. Despite similar shrinkage stress, high cross-link density, and a glass transition temperature above  $60 \text{ }^\circ\text{C}$ , **DBC/DiPETMP** provides a 5.3 times higher impact strength than **BDA**, which can be explained by the unique network homogeneity of thiol-yne photopolymers.

### Supporting Information

Supporting Information is available from the Wiley Online Library or from the author.

**Acknowledgements:** Financial support by the Christian Doppler Research Association, the Austrian Federal Ministry of Science, Research and Economy (BMWFW), and Durst Phototechnik GmbH is gratefully acknowledged. Part of the research work of this paper was performed at the Polymer Competence Center Leoben GmbH (PCCL, Austria) within the framework of the COMET-program of the Federal Ministry for Transport, Innovation, and Technology and Federal Ministry for Economy, Family and Youth.

Received: June 21, 2016; Revised: July 18, 2016;  
Published online: August 30, 2016; DOI: 10.1002/marc.201600369

**Keywords:** network formation; photopolymers; thiol-yne; double quantum solid state NMR

- [1] *Photoinitiation, Photopolymerization, and Photocuring: Fundamentals and Applications*, 1st ed. (Ed: J.-P. Fouassier), Hanser Publishers, Munich, Germany 1995.
- [2] R. Liska, M. Schuster, R. Infuehr, C. Turecek, C. Fritscher, B. Seidl, V. Schmidt, L. Kuna, A. Haase, F. Varga, H. Lichtenegger, J. Stampfl, *J. Coat. Technol. Res.* **2007**, *4*, 505.
- [3] P. Tesavibul, R. Felzmann, S. Gruber, R. Liska, I. Thompson, A. R. Boccaccini, J. Stampfl, *Mater. Lett.* **2012**, *74*, 81.
- [4] M. Schwentenwein, J. Homa, *Int. J. Appl. Ceram. Technol.* **2015**, *12*, 1.
- [5] J. R. Tumbleston, D. Shirvanyants, N. Ermoshkin, R. Januszewicz, A. R. Johnson, D. Kelly, K. Chen, R. Pinschmidt, J. P. Rolland, A. Ermoshkin, E. T. Samulski, J. M. DeSimone, *Science* **2015**, *347*, 1349.
- [6] C. D. Calnan, *Contact Dermatitis* **1980**, *6*, 53.
- [7] L. S. Andrews, J. J. Clary, *J. Toxicol. Environ. Health* **1986**, *19*, 149.
- [8] M. Friedman, J. F. Cavins, J. S. Wall, *J. Am. Chem. Soc.* **1965**, *87*, 3672.
- [9] G. T. Klein, Y. Lu, M. Y. Wang, *World Neurosurg.* **2013**, *80*, 233.
- [10] E. Farré-Guasch, J. Wolff, M. N. Helder, E. A. Schulten, T. Forouzanfar, J. Klein-Nulend, *J. Oral Maxillofacial Surg.* **2015**, *73*, 2408.
- [11] C. Gorsche, K. Seidler, P. Knaack, P. Dorfinger, T. Koch, J. Stampfl, N. Moszner, R. Liska, *Polym. Chem.* **2016**, *7*, 2009.
- [12] S. C. Ligon-Auer, M. Schwentenwein, C. Gorsche, J. Stampfl, R. Liska, *Polym. Chem.* **2016**, *7*, 257.

- [13] C. E. Hoyle, T. Y. Lee, T. Roper, *J. Polym. Sci., Part A: Polym. Chem.* **2004**, *42*, 5301.
- [14] N. Moszner, U. Salz, *Macromol. Mater. Eng.* **2007**, *292*, 245.
- [15] B. D. Fairbanks, T. F. Scott, C. J. Kloxin, K. S. Anseth, C. N. Bowman, *Macromolecules* **2009**, *42*, 211.
- [16] A. B. Lowe, *Polymer* **2014**, *55*, 5517.
- [17] J. W. Chan, J. Shin, C. E. Hoyle, C. N. Bowman, A. B. Lowe, *Macromolecules* **2010**, *43*, 4937.
- [18] A. Lowe, C. Bowman, *Thiol-X Chemistries in Polymer and Materials Science*, Royal Society of Chemistry, Cambridge **2013**.
- [19] H. Peng, C. Wang, W. Xi, B. A. Kowalski, T. Gong, X. Xie, W. Wang, D. P. Nair, R. R. McLeod, C. N. Bowman, *Chem. Mater.* **2014**, *26*, 6819.
- [20] A. Mautner, B. Steinbauer, S. Orman, G. Russmüller, K. Macfelda, T. Koch, J. Stampfl, R. Liska, *J. Polym. Sci., Part A: Polym. Chem.* **2016**, *54*, 1987.
- [21] C. Gorsche, T. Koch, N. Moszner, R. Liska, *Polym. Chem.* **2015**, *6*, 2038.
- [22] R. Graf, D. E. Demco, S. Hafner, H. W. Spiess, *Solid State Nucl. Magn. Reson.* **1998**, *12*, 139.
- [23] M. Schneider, L. Gasper, D. E. Demco, B. Blümich, *J. Chem. Phys.* **1999**, *111*, 402.

## Publication IV

Roth, Meinhart; Oesterreicher, Andreas; Mostegel, Florian H.; Moser, Andreas; Pinter, Gerald; Edler, Matthias; Piock, Richard; Griesser, Thomas: Silicon-based Mercaptans: High-Performance Monomers for Thiol-ene Photopolymerization *J. Polym. Sci. Part A: Polym. Chem.* **2016**, 54, 418–424.



## Silicon-Based Mercaptans: High-Performance Monomers for Thiol-ene Photopolymerization

Meinhart Roth,<sup>1</sup> Andreas Oesterreicher,<sup>1</sup> Florian H. Mostegel,<sup>1</sup> Andreas Moser,<sup>2</sup> Gerald Pinter,<sup>2</sup> Matthias Edler,<sup>1</sup> Richard Piock,<sup>3</sup> Thomas Griesser<sup>1</sup>

<sup>1</sup>Chair of Chemistry of Polymeric Materials and Christian Doppler Laboratory for Functional and Polymer Based Ink-Jet Inks, University of Leoben, Otto-Glöckel-Strasse 2, Leoben, A-8700, Austria

<sup>2</sup>Institute of Material Science and Testing of Polymers, University of Leoben, Otto-Glöckel-Strasse 2, Leoben, A-8700, Austria

<sup>3</sup>Durst Phototechnik DIT, Julius-Durst-Strasse 11, Lienz, A-9900, Austria

Correspondence to: T. Griesser (E-mail: thomas.griesser@unileoben.ac.at)

Received 2 June 2015; accepted 9 July 2015; published online 17 August 2015

DOI: 10.1002/pola.27792

**ABSTRACT:** Ester-free silane and siloxane-based thiol monomers were successfully synthesized and evaluated for application in thiol-ene resins. Polymerization reaction rates, conversion, network properties as well as degradation experiments of those thiol monomers in combination with triallyl-1,3,5-triazine-2,4,6(1H,3H,5H)-trione (TATT) as ene component were performed and compared with formulations containing the commercially available mercaptopropionic ester-based thiol pentaerythritol tetra-3-mercaptopropionate. Kinetic analysis revealed appropriate reaction rates and conversions reaching 90% and higher. Importantly, storage stability tests of those formulations clearly indicate the superiority of the synthesized mercaptans compared with pentaerythritol tetra-3-mercaptopropionate/TATT resins. Moreover, photocured samples containing silane-based mercaptans provide higher glass transition temperatures and withstand water storage without a significant loss in their network properties. This behavior together with the observed excellent degradation resistance of photocured silane-based thiol/TATT formulations make these multifunctional mercaptans interesting candidates for high-performance applications, such as dental restoratives and automotive resins. © 2015 Wiley Periodicals, Inc. *J. Polym. Sci., Part A: Polym. Chem.* **2016**, *54*, 418–424

**KEYWORDS:** mercaptans; monomers; photopolymerization; step-growth polymerization; thiol-ene

**INTRODUCTION** Although the reaction of thiols with enes has already been observed in 1905, it was not until the beginning of the 1930s that this reaction was used for the fabrication of polymeric materials.<sup>1,2</sup> Thiol-ene polymers are formed by the stoichiometric reaction of multifunctional enes and thiols via a multiple step radical mechanism after thermal<sup>3</sup> or photochemical initiation.<sup>4</sup> In contrast to acrylate polymerization, the thiol-ene polymerization follows a step growth mechanism bringing unique properties to this interesting class of materials.<sup>5</sup> Polymerization shrinkage is low, and high-impact strength materials can be achieved due to the homogenous network structure. However, the most salient feature of thiol-ene photopolymerization is that almost any type of ene can be applied in this photoreaction. Furthermore, it is important to note that oxygen inhibition plays only a minor role due to efficient hydrogen abstraction of peroxy radicals from thiols under the simultaneous formation of highly reactive thiyl radicals.<sup>6</sup> Besides these advantages, two important issues have to be considered for thiol-

ene systems. First, the characteristic odor of thiol monomers and second, the generally low glass transition temperature ( $T_g$ ) of thiol-ene-based polymers, which can be attributed to the rather flexible thioether linkages.<sup>7</sup> For applications that desire high moduli and high  $T_g$ 's such as dental restoratives and automotive and aerospace resins, the low  $T_g$  of thiol-ene networks is a detriment.

One strategy to overcome this limitation is to use rigid ene structures such as triallyl-1,3,5-triazine-2,4,6(1H,3H,5H)-trione (TATT) or norbornene derivatives.<sup>2,8,9</sup> Also monomers that are capable to form hydrogen bonds in the thiol-ene network provide reasonable glass transition temperatures together with excellent hardness and impact properties.<sup>10</sup>

Another method for producing thiol-ene networks with high  $T_g$ 's is to use multifunctional (meth)acrylate (co)monomers, which can on the one hand copolymerize with the thiol (step growth thiyl addition) and also homopolymerize (chain growth mechanism).<sup>2</sup> However, the corresponding high

Additional Supporting Information may be found in the online version of this article.

© 2015 Wiley Periodicals, Inc.

temperature glass transition regions of these systems are broad compared with that of thiol-ene networks obtained by pure step growth polymerization.

Besides the mechanical properties, other limitations of the thiol-ene photopolymerization can mainly be attributed to specific characteristics of the used multifunctional thiols. The predominantly applied and studied thiols for thiol-ene curing are esters of mercapto propionic acid, for example, trimethylolpropane tri(3-mercaptopropionate) and pentaerythritol tetra-3-mercaptopropionate (PETMP), and thioglycolates, which are commercially available and offer superior reactivity compared with that of alkylthiols.<sup>11</sup>

The hydrolytic sensitivity of the ester groups reduces the resistance of the cured polymeric materials toward acidic and basic media, which is detrimental for high-performance applications, such as dental restoratives and automotive resins. The hydrolysis process deteriorates the mechanical properties over time and ultimately leads to mechanical failure.<sup>12,13</sup> Further, the polarity of the ester group and its affinity to water favor water absorption, which decreases the mechanical performance by lowering the modulus, glass transition, and strength.<sup>14</sup> In principle, the formed thioether groups in thiol-ene polymers are rather stable, and, therefore, it can be expected that formulations that contain persistent monomers, that is, enes and thiols without hydrolytic sensitive groups, lead to stable polymeric materials similar to cationic cured epoxy resins.

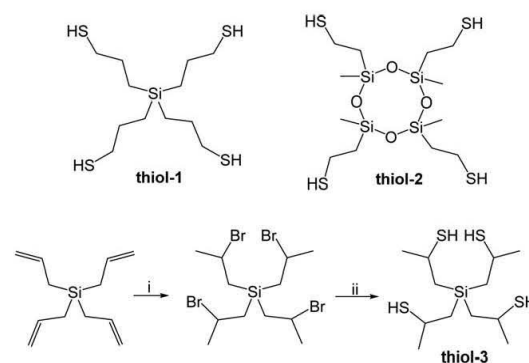
Although there is a vast number of studies describing the effect of different enes on the physicochemical properties of thiol-ene polymers,<sup>15–17</sup> there are only a few reports, which deal with alternative thiol compounds and their impact on the polymeric properties.<sup>18,19</sup> Very recently, the group of Bowman and coworkers<sup>14</sup> successfully demonstrated the beneficial behavior of ester-free thiols based on the example of tetra(2-mercaptopropyl)silane.

In this article, we studied several ester-free silane and siloxane-based thiol monomers for thiol-ene photopolymerization. A particular focus was set on the synthesis and application of a multifunctional monomer bearing secondary thiol groups. It is well reported that resins prepared from such steric hindered mercaptans show improved shelf life stability.<sup>18</sup> In this context, the photoreactivity and storage stability of these monomers, in combination with TATT as ene component were investigated and compared with those of PETMP/TATT formulations. Moreover, also the mechanical properties as well as the degradation behavior of the cured formulations were determined, revealing the versatility of this class of monomers.

## RESULTS AND DISCUSSION

### Synthesis

For the preparation of functional thiol compounds, several reaction strategies are described in the literature.<sup>20–22</sup> One elegant and straightforward procedure exploits the radical



**SCHEME 1** Overview of the synthesized thiol monomers: (i) HBr,  $-3\text{ }^{\circ}\text{C}$ , 2 h. (ii) (1) thiourea, RT, 24 h; (2) aqueous NaOH, RT, 1 h.

induced thiol-ene reaction of thioacetic acid with functional alkenes to give thioester derivatives that can be hydrolyzed under alkaline or acidic conditions, yielding the corresponding thiol compounds. This method has been applied for the preparation of thiol-1 and thiol-2 (Scheme 1) starting from tetraallylsilane and 2,4,6,8-tetramethyl-2,4,6,8-tetravinylcyclotetrasiloxane, which gives reasonable yields of 75% and 45%, respectively. This reaction procedure is not suitable for the synthesis of secondary thiol compounds because of the anti-Markovnikov behavior of the radical induced addition of thioacetic acid.

Consequently, a multistep reaction route has to be chosen for the synthesis of thiol-3. In the first step, the ionic addition reaction of hydrogen bromide to tetraallylsilane was exploited to give tetrakis(2-bromopropyl)silane in a good yield of 84%. Subsequently, this intermediate was converted with thiourea to the corresponding isothiuronium salt, which can be hydrolyzed with aqueous sodium hydroxide to give thiol-3 in a moderate yield of 10%. The conversion of alkylhalogenides to thiols by the aid of thiourea is well known and represents a versatile alternative to the thioacetic-based reaction route.<sup>22</sup>

The synthesized thiol was characterized by  $^1\text{H}$ ,  $^{13}\text{C}$ , and  $^{29}\text{Si}$  NMR spectroscopies. The obtained data are in good agreement with the proposed structures. The chemophysical properties of these compounds compared with PETMP are depicted in Table 1. The silicon-based mercaptans exhibit much lower viscosities as the commercially available PETMP, making these monomers interesting candidates for the formulation of UV-curable thiol-ene resins for low viscosity applications in the printing and coating industry (e.g., ink-jet printing). Although, thiol-2 shows a significant lower surface tension ( $\sigma = 27\text{ mN m}^{-1}$ ) than the other measured mercaptans, which is mainly explained by the apolar siloxane ring, no negative effect on the miscibility with the utilized ene components, that is, TATT and triethyleneglycol divinylether (TEGDVE), was observed. Furthermore, it has to be

**TABLE 1** Density ( $\rho$ ), Surface Tension ( $\sigma$ ), Viscosity ( $\eta$ ), Time to Reach the Maximum Heat of Polymerization ( $t_{\max}$ ), Reaction Enthalpy ( $\Delta H$ ), and Calculated Double Bond Conversion (DBC)

Thiol Monomer	$\rho$ (g cm <sup>-3</sup> )	$\sigma$ (mN m <sup>-1</sup> )	$\eta$ (25 °C) (mPa s) ( $\dot{\gamma} = 300$ s <sup>-1</sup> )	$t_{\max}^a$ (s)	$\Delta H^a$ (J g <sup>-1</sup> )	DBC <sup>a</sup> (%)
Thiol-1	1.10	44	50	1.6	420	99
Thiol-2	1.02	27	38	1.7	350	99
Thiol-3	1.07	36	52	2.5	380	93
PETMP	1.28	48	450	1.0	330	90

<sup>a</sup> Corresponds to a formulation of 50 mol % of thiol and 50 mol % of TATT.

mentioned that the secondary thiol-3 had only little odor compared with the other mercapto compounds.

#### Photoreactivity

It is well reported that thiols based on propionate esters and glycolate esters result in higher reaction rates than conventional alkyl thiols because of a weakening of the sulfur-hydrogen bond by hydrogen bonding of the thiol hydrogen group with the ester carbonyl. Rates of addition almost six times greater have been found for the free radical addition of methyl mercaptopropionate to 1-heptene than for pentanethiol to 1-heptene.<sup>2</sup>

The reactivity of the synthesized thiol monomers (in combination with TATT) toward polymerization after photoinitiation has been investigated by photo-DSC, which represents a unique method for the fast and accurate evaluation of the curing behavior of UV-polymerizable resins.<sup>23</sup> Using photo-DSC, various important parameters can be obtained with one single measurement. The reaction time  $t_{\max}$  is the time to reach the maximum of polymerization enthalpy and reveals information about the curing speed of the investigated system. Furthermore, the double bond conversion (DBC) can be calculated from the overall reaction enthalpy  $\Delta H$  (peak area) providing that the theoretical heat of polymerization ( $\Delta H_0$ , p) is known. A straightforward method to obtain  $\Delta H_0$ , p is to determine the DBC of photo-DSC cured samples by means of ATR-IR and correlate this value to the heat released during the photo-DSC experiment.<sup>24</sup> In general, the determination of the DBC by means of photo-DSC is restricted to enes that show no homopolymerization, which can be observed in (meth)acrylate-based thiol-ene formulations.

Because of overlapping IR signals and the fact that the reaction enthalpy for thiol-ene systems strongly depends on the structure of the ene (electron density), monofunctional model thiol compounds, that is, octane thiol and butylmercaptopropionate, were used to estimate  $\Delta H_0$ , p of the thiol addition to TATT. In these experiments, the DBC was determined by means of NMR spectroscopy after dissolving the non-cross-linked thiol-ene adducts in CDCl<sub>3</sub>. For the photoinduced addition of octanethiol and butylmercaptopropionate to TATT, the theoretical reaction enthalpy ( $\Delta H_0$ , p) was found to be 203 and 228 kJ mol<sup>-1</sup>, respectively. Interestingly, the structure of the thiol compound (alkyl thiol vs. mercaptopropionic ester derivative)

also influences the overall reaction enthalpy. This fact was considered for the calculation of the DBC of the synthesized mercaptans thiol-1, thiol-2, and thiol-3.

It was found that thiol-1 and thiol-2 react almost quantitatively (see Table 1), whereas thiol-3 and PETMP yield conversions of 93% and 90%, respectively. Although, the multifunctional mercapto propionic ester derivative PETMP leads to the lowest measured DBC, it reached the maximum of polymerization heat within 1 s. In comparison, the monomers containing primary thiol moieties, that is, thiol-1 and thiol-2, show  $t_{\max}$  values of 1.6 and 1.7 s, respectively, whereas thiol-3 exhibits the slowest reaction rate ( $t_{\max} = 2.5$  s). These measured values are in good accordance with previously described reaction behaviors of thiol derivatives.<sup>2</sup> The moderate reaction rate of thiol-3 can be explained by the sterically hindered secondary mercapto groups.

One possible explanation for the higher conversions of the silicon-based thiols is their comparable low viscosities. Although PETMP exhibits a viscosity of 450 mPa s, the viscosity of the synthesized mercaptans is in the range between 40 and 50 mPa s. A lower viscosity leads to a higher mobility of the monomers during polymerization, which may explain the superiority in terms of DBC despite lower reactivity.

#### Storage Stability

One limiting factor of thiol-ene formulations is their poor shelf life stability, preventing a broad application in the UV curing and coating industry so far. The limited stability of such resins may be due to a variety of reasons, including (1) a base catalyzed addition of thiol to the ene double bond, (2) the decomposition of peroxide impurities and subsequent initiation of a thermal free-radical reaction, or (3) the spontaneous initiation of polymerization via the generation of radicals through a ground-state charge-transfer complex formed between the thiol and ene components in the mixture.<sup>2</sup> However, it is well reported that resins prepared from steric hindered mercaptans, for example, secondary thiols such as thiol-3, are superior in terms of shelf life stability.<sup>10</sup>

Figure 1 shows the viscosity increase of resins containing the synthesized thiols in combination with TATT as a function of time at a storage temperature of 50 °C. This

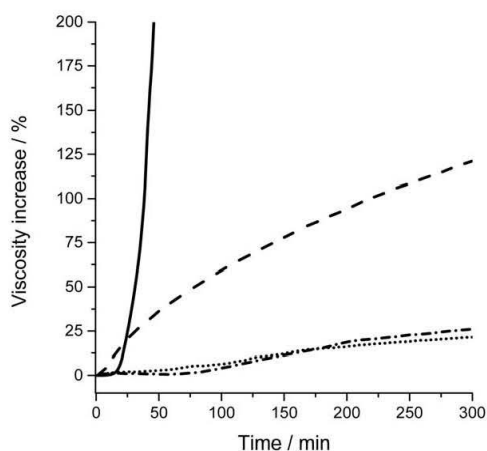


**FIGURE 1** Increase in viscosity of the investigated resins during time of storage (50 °C). Solid line: PETMP/TATT, dashed line: thiol-2/TATT, dotted line: thiol-3/TATT, and dot-dashed line: thiol-1/TATT.

accelerated shelf life tests clearly reveal the inferiority of the PETMP/TATT system, in which a viscosity increase of 100% can be observed after 40 min of storage (50 °C). Interestingly, the secondary (thiol-3) as well as the primary thiol monomer (thiol-1) exhibit similar good stability under these conditions, which is reflected by a minor viscosity increase of approximately 25% after 300 min of storage time for both thiol compounds. In contrast, formulations containing thiol-2 lead to an increase of 125% after 300 min. Although, the observed stability behavior is, as expected, inversely proportional to the measured reactivities (*vide supra*) of the investigated thiol monomers, the absolute values clearly indicate the superiority of the silane-based thiols, that is, thiol-1 and thiol-3, over PETMP. Although the resin with thiol-1 shows only a slightly lower  $t_{\max}$  value (only a difference of 0.6 s, see Table 1), the storage stability is far better than the formulation prepared with PETMP.

#### Mechanical Properties

The characterization of photocured thiol-ene networks has mainly been focused on the structural parameters related to ene flexibility in the past.<sup>2,5,25</sup> Although there are some reports describing the effect of different thiol monomers on the cured network,<sup>8,14,19</sup> most of them deal with mercapto propionic acid derivatives such as PETMP, TMPMP, or pentaerythritol tetrakis (mercaptobutylate).<sup>2,5,10</sup> Basically, it is well documented that thermal and mechanical properties directly correspond to features inherent to the chemical structure of the ene and thiol monomer. Furthermore, it has been shown that the functionality of both types of monomers influence the cross-link density and glass transition temperature.<sup>2</sup>

For a detailed investigation of the effect of the different mercaptane compounds on the network properties, a DMA analy-

sis of cured resins prepared from TATT and the synthesized thiols (1:1 ratio of molar functional groups) were performed and compared with the network properties of a PETMP/TATT-based polymer as shown in Table 2. The corresponding storage moduli and tan delta versus temperature plots are shown in the Supporting Information. In general, all cured formulations show rather narrow tan delta peak widths ( $T_g$  1/2 width  $\sim$  20–40 °C), which are characteristic for step-growth systems.<sup>2</sup>

The networks containing thiol-1 and thiol-3 achieved noticeable higher glass transition temperatures of 67 ( $\pm$ 1) °C and 67 ( $\pm$ 5) °C, respectively, compared with cured PETMP/TATT samples ( $T_g$  = 61 ( $\pm$ 1) °C). This result is in good accordance with the findings of Podgorski et al. for a photocured tetra(2-mercaptoethyl)silane/TATT formulation exhibiting also a higher glass transition temperature than the corresponding PETMP/TATT sample. This behavior is explained by the good cross-linking capability of silane-based multifunctional thiols as well as the absence of ester moieties in the formulations.<sup>14</sup>

Furthermore, thiol-3 provides also the highest storage modulus (thiol-3: 2.2 GPa and PETMP: 2.0 GPa at 25 °C) of the investigated thiols in the glassy state.

The superiority of thiol-3-based networks can be assigned to the hindered rotation of thiol-ether linkages afforded by the additional  $\alpha$ -methyl group of thiol-3. This behavior has also been reported for secondary mercapto propionic ester-based mercaptans previously.<sup>10</sup> It is worth mentioning that this outstanding performance of the investigated networks was achieved without the use of excessively viscous resin mixtures.

For many industrial and medical applications, the mechanical performance of the materials after water storage is of significant importance. Several studies of acrylate-based photopolymers have shown a clear dependency between strength, stiffness, hydrophilicity, and water uptake of the polymer. In Table 2, the effect of water storage at room temperature of the photocured samples on the moduli and the  $T_g$ s is shown. This treatment strongly deteriorates the network properties

**TABLE 2** Storage Moduli and  $T_g$ 's of Photocured Thiol/TATT Resins Before and After Storage in Water for 24 h

Thiol Monomer	$T_g$ (°C) <sup>a</sup>		$E$ (GPa) <sup>b</sup>	
	Before	After	Before	After
Thiol-1	67 ( $\pm$ 1)	67 ( $\pm$ 1)	1.5	1.3
Thiol-2	58 ( $\pm$ 1)	60 ( $\pm$ 2)	1.5	1.6
Thiol-3	67 ( $\pm$ 5)	63 ( $\pm$ 3)	2.2	2.1
PETMP	61 ( $\pm$ 1)	42 ( $\pm$ 1)	2.0	1.4

Values in brackets are standard deviations values.

<sup>a</sup> Determined at  $\tan \delta_{\max}$ .

<sup>b</sup> Storage modulus ( $E$ ) measured at 25 °C.

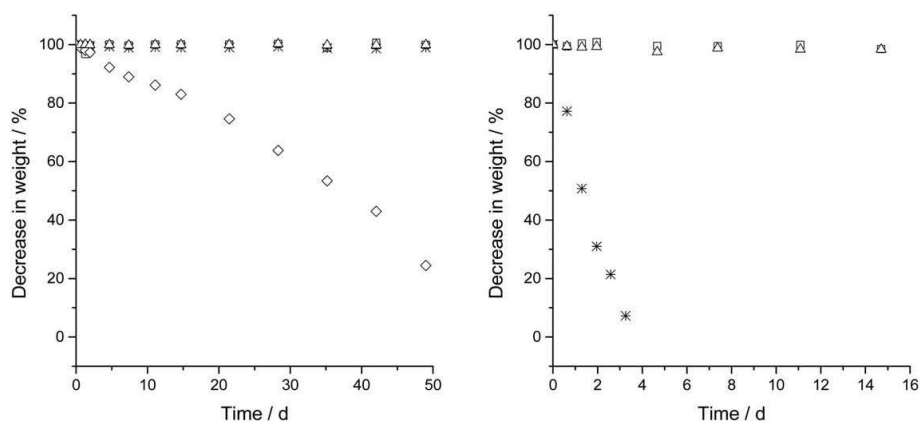


**FIGURE 2** Decrease in weight of the cured polymer samples during the immersion in 1 M NaOH solution (50 °C). Left: thiol/TATT resins (square: thiol-1/TATT; star: thiol-2/TATT; triangle: thiol-3/TATT; and diamond: PETMP/TATT). Right: thiol/TEGDVE resins (square: thiol-1/TEGDVE; star: thiol-2/TEGDVE; and triangle: thiol-3/TEGDVE).

of the PETMP-based polymers, whereas silane and siloxane-based samples are only slightly influenced. The performance of the PETMP/TATT significantly decreased after storage in water. The storage modulus was lowered from 2.0 to 1.4 GPa, as well as the glass transition temperature dropped from 61 ( $\pm 1$ ) to 42 ( $\pm 1$ ) °C. Very recently, a similar deterioration after water treatment has also been reported for PETMP/TATT-based dental composite materials.<sup>8</sup>

#### Degradation Behavior

To investigate the hydrolytic stability of the synthesized thiol monomers, the degradation behavior of cured polymer samples were evaluated under alkaline conditions (1 M NaOH) at a storage temperature of 37 °C and compared with that of the PETMP-based thiol-ene polymer. For that purpose, TATT and TEGDVE were used as ene components. It is expected that the hydrophilic ethylene glycol groups of TEGDVE facilitate a good penetration of water into the polymeric network, which should increase the degradation rate of the thiol component toward reasonable time scales.

In Figure 2, the decrease in weight of the cured polymer samples during the immersion in 1 M NaOH solution (50 °C) is depicted. Although samples of cured PETMP/TEGDVE fully degrade within 15 h (not shown in Fig. 2), owing to the hydrolytic sensitivity of the ester groups in PETMP, both silane-based polymers show no significant loss of weight even after a storage time of 15 days. Accordingly, cured PETMP/TATT formulations also show a significant degradation of approximately 80 wt % after 50 days of storage, whereas cured blends of TATT with thiol-1, thiol-2, and thiol-3 remained stable. Interestingly, the thiol-2/TEGDVE network also fully degrades under storage in sodium hydroxide solution within 4 days, which is presumably caused by the hydrolytic sensitivity of the Si—O bond. In general,

siloxane-based polymers such as PDMS are known to readily undergo degradation reactions under alkaline conditions.<sup>26</sup>

#### CONCLUSION

In this contribution, several ester-free silane and siloxane-based thiol monomers were successfully synthesized and evaluated for an application in thiol-ene resins. Besides the reaction behavior, that is, reaction rate and yield, of these monomers in combination with TATT as ene component, also the mechanical properties as well as the degradation behavior of photocured samples were investigated and compared with those of PETMP/TATT formulations. PETMP and thiol-2 yield conversions of 90% and 93%, respectively, whereas the silane-based thiol monomers, that is, thiol-1 and thiol-2, react almost quantitatively. Moreover, the synthesized thiols showed also appropriate reaction rates with reaction times ( $t_{\text{max}}$ ) in the range of 1.6–2.5 s. The observed storage stability of the thiol/TATT formulations is indirectly proportional to the measured reactivities. However, a comparison of the stability with the reaction behavior of the synthesized thiols with PETMP clearly indicates the superiority of the silane-based mercaptans. Although the resin with thiol-1 shows only a slightly lower  $t_{\text{max}}$  value (0.6 s slower), the storage stability is far better than the stability formulation prepared with PETMP. Moreover, photocured samples containing thiol-1 and 3 provide higher glass transition temperatures compared with that of PETMP/TATT resins. Thiol-3 offers the highest storage modulus of the investigated thiols in the glassy state, which can be assigned to the hindered rotation of thiol-ether linkages afforded by the additional  $\alpha$ -methyl group. In addition, ester-free thiol-ene networks were shown to withstand water storage without a significant loss in the network properties and also basic treatment for an extended amount of time. This behavior, together with the excellent mechanical properties, makes silane-based thiol-ene formulations interesting

candidates for high-performance applications, such as dental restoratives and automotive resins.

## EXPERIMENTAL

### Materials

All reagents were purchased from commercial sources and were used without further purification. Irgacure TPO-L was obtained from BASF. PETMP was donated by Bruno Bock.

### Characterization

$^1\text{H}$  NMR and  $^{13}\text{C}$  NMR spectra were recorded with a Varian 400-NMR spectrometer operating at 399.66 MHz and 100.5 MHz, respectively, and were referenced to  $\text{Si}(\text{CH}_3)_4$ . A relaxation delay of 10 s and  $45^\circ$  pulse were used for acquisition of the  $^1\text{H}$ -NMR spectra. Solvent residual peaks were used for referencing the NMR spectra to the corresponding values given in the literature.<sup>27</sup>  $^{29}\text{Si}$ -NMR spectra were recorded on a Varian INOVA 300 spectrometer (59.3 MHz).

The Photo-DSC experiments were performed on a NETZSCH Photo-DSC 204 F1 Phoenix. All measurements were conducted at  $50^\circ\text{C}$  in aluminum crucibles under nitrogen atmosphere. The Omnicure s2000 was used as the light source at  $1\text{ W cm}^{-2}$ . For the determination of the reaction enthalpy and  $t_{\text{max}}$  the samples (sample quantity: 8 mg resin containing 3 wt % of Irgacure TPO-L) were illuminated twice for 10 min each. For the analysis, the second run was subtracted from the first one to give the reaction enthalpy curve.

For the determination of the thermomechanical properties and the degradation behavior of the photopolymers, sample specimens with  $2 \times 4 \times 19\text{ mm}$  and  $2 \times 4 \times 5\text{ mm}$  rectangular dimensions, respectively, were fabricated by curing the corresponding resins (3 wt % of Irgacure TPO-L,  $E = 4.5\text{ J cm}^{-\text{m}}$ ) in glass molds. The thermomechanical properties were measured in tension mode using a DMA/SDTA 861 (Mettler Toledo) with a heating rate of  $2\text{ K min}^{-1}$  in the temperature range from  $-20$  to  $110^\circ\text{C}$ . The operating frequency was determined at 1 Hz. For comparison of the thiol formulations, the storage modulus was evaluated at room temperature ( $25^\circ\text{C}$ ), and the glass transition temperature was determined at the maximum of the  $\tan \delta$  curve for each measurement.

Degradation tests were performed by immersion of the sample specimens in 1 M NaOH at  $50^\circ\text{C}$ . During this test, the sample dry weight was monitored.

The viscosity of the formulations was determined using an Anton Paar rheometer (MCR-102, Graz, Austria) in a cone-plate system setup with Titan cone (MK 22/60 mm,  $0.5^\circ$ ) with an opening angle of  $0.5^\circ$  and a diameter of 60 mm at a shear rate of  $300\text{ s}^{-1}$ .

### Synthesis

#### *Silanetetrayltetrakis(propane-3,1-diyli) tetraethanethioate (1)*

An amount of 100 g (1314 mmol, 10 Äq.) thioacetic acid and 25.25 g (131.3 mmol) tetraallylsilane were dissolved in 200 mL THF. After the addition of 1.08 g (6.6 mmol,

0.05 Äq.) 2,2'-azobis(2-methylpropionitrile), the mixture was heated to  $65^\circ\text{C}$  and stirred overnight. The solvent was evaporated, and the residue was dissolved in ethyl acetate and extracted with 200 mL water, sodium hydrogen carbonate, and brine. Afterward, the solvent was removed under reduced pressure and the product was dried by azeotropic distillation with toluene. The crude product was used for the next reaction step without further purification.

#### *Silanetetrayltetrakis(propane-1-thiol) (Thiol-1)*

65.28 g (148.1 mmol) of **1** was dissolved in EtOH and cooled to  $0^\circ\text{C}$ . To this, 32 mL of 25% NaOH solution was added and stirred overnight until complete conversion of the educt (reaction progress by TLC ethyl acetate/cyclohexane 1:5). The mixture was neutralized with HCl and extracted three times with 200 mL toluene. The combined organic layers were washed three times with 200 mL water and dried over  $\text{Na}_2\text{SO}_4$ . The solvent was removed under reduced pressure, and the crude product was purified by Kugelrohr vacuum distillation ( $300^\circ\text{C}$ , 2 mbar) to obtain the colorless liquid product (24 g, 60%).

$^1\text{H}$ -NMR ( $\delta$ , 400 MHz,  $\text{CDCl}_3$ ,  $25^\circ\text{C}$ ): 2.51 (m, 8H, C-SH); 1.58 (m, 8H, C-C-SH); 0.63 (m, 8H, Si-C) ppm.

$^{13}\text{C}$ -NMR ( $\delta$ , 100 MHz,  $\text{CDCl}_3$ ,  $25^\circ\text{C}$ ): 28.65 (d, 4C, C-C-SH); 28.27 (s, 4C, C-SH), 11.45 (s, 4C, Si-C) ppm.

$^{29}\text{Si}$ -NMR ( $\delta$ , 59.3 MHz  $\text{CDCl}_3$ ,  $25^\circ\text{C}$ ): 3.64 (s, Si) ppm.

#### *Ethanethioic acid, -[(2,4,6,8-tetramethylcyclotetrasiloxane-2,4,6,8-tetrayl)tetrakis(2,1-ethanediyl)] ester*

*2,4,6,8-tetramethyl-2,4,6,8-tetravinyl-cyclotetrasiloxane* 23.7 g (0.069 mmol) of 2,4,6,8-tetravinyl-2,4,6,8-tetramethyl-cyclotetrasiloxane, 26.2 g (0.343 mol, 5 Äq) thioacetic acid, and 1.13 g 2,2'-azobis(2-methylpropionitrile) (6.88 mmol, 0.1 Äq) were dissolved in 110 mL anhydrous THF. The mixture was refluxed under inert gas for 18 h until it was cooled down to room temperature. The excess of solvent and thioacetic acid was removed under reduced pressure. The crude product was used for the next reaction step without further purification.

$^1\text{H}$ -NMR: ( $\delta$ , 400 MHz,  $25^\circ\text{C}$ ,  $\text{CDCl}_3$ ): 2.88 (m, 8H,  $\text{CH}_2$ ); 2.26 (m, 12H,  $-\text{CH}_3$ ); 0.89 (m, 8H,  $-\text{CH}_2$ ); 0.14 (m, 12H,  $-\text{CH}_3$ ) ppm.

#### *2,4,6,8-Tetramethylcyclotetrasiloxane-2,4,6,8-tetraethanethiol*

**2** was dissolved in 100 mL methanol and mixed with 16 mL concentrated hydrochloric acid, degassed by bubbling with nitrogen for 30 min, and hold on  $60^\circ\text{C}$  for 10 h. In the next step, 100 mL of water was added, and the mixture was extracted three times with  $\text{CH}_2\text{Cl}_2$ . The combined organic layers were washed with saturated  $\text{NaHCO}_3$  solution and dried over  $\text{Na}_2\text{SO}_4$ . The crude product was purified by column chromatography (hexane:diethylether 3:2) and activated carbon filtration to give a slight yellow liquid. Further a Kugelrohr vacuum distillation was performed ( $300^\circ\text{C}$ , 2

mbar) to obtain the slightly yellow liquid product (20 g, 60%).

$^1\text{H-NMR}$  ( $\delta$ , 400 MHz, 25 °C,  $\text{CDCl}_3$ ): 2.62 (m, 8H,  $\text{CH}_2$ ); 1.54 (m, 4H, -SH); 0.99 (m, 8H, - $\text{CH}_2$ ); 0.14 (m, 12H, - $\text{CH}_3$ ) ppm.

$^{13}\text{C-NMR}$  ( $\delta$ , 100 MHz,  $\text{CDCl}_3$ , 25 °C): 31.05 (d, 4C, C-Br); 27.92 (s, 4C, Si-C), 31.05 (s, 4C, C- $\text{CH}_3$ ) ppm.

$^{29}\text{Si-NMR}$  ( $\delta$ , 59.3 MHz,  $\text{CDCl}_3$ , 25 °C): 22.20 (s, Si) ppm.

#### **Tetrakis(2-bromopropyl)silane (3)**

21.5 g (111.8 mmol) tetraallylsilane was dissolved in *n*-hexane and cooled to -3 °C. Under constant stirring, 38.0 g (469.7 mmol, 4.2 Äq.) gaseous HBr was introduced into the flask, which was tightly sealed for 2 h. The excess of solvent was removed under reduced pressure to obtain 54 g of the product as a white solid, which was recrystallized from *n*-hexane (50 g, 84%).

$^1\text{H-NMR}$  ( $\delta$ , 400 MHz,  $\text{CDCl}_3$ , 25 °C): 4.52 (m, 4H, C-Br); 1.82 (m, 12H, C- $\text{CH}_3$ ); 1.66 (m, 8H, Si-C) ppm.

$^{13}\text{C-NMR}$  ( $\delta$ , 100 MHz,  $\text{CDCl}_3$ , 25 °C): 31.05 (d, 4C, C-Br); 27.92 (s, 4C, Si-C), 31.05 (s, 4C, C- $\text{CH}_3$ ) ppm.

#### **Silane tetrayltetrakis(propane-2-thiol) (Thiol-3)**

25.0 g (48.4 mmol) **3** and 25.4 g (333.96 mmol, 6.9 Äq.) thiourea were dissolved in 400 mL dry THF and refluxed for 24 h. Afterward, the reaction was cooled to room temperature and quenched with 50% NaOH. The mixture was stirred for 1 h, neutralized with 5% HCl, extracted with 2-methoxy-2-methylpropane, and dried over  $\text{Na}_2\text{SO}_4$ . The crude product was purified by column chromatography (cyclohexane:ethyl acetate 5:1) to give a colorless liquid (2.5 g, 10%).

$^1\text{H-NMR}$  ( $\delta$ , 400 MHz,  $\text{CDCl}_3$ , 25 °C): 4.52 (m, 4H, C-Br); 1.82 (m, 12H, C- $\text{CH}_3$ ); 1.66 (m, 8H, Si-C) ppm.

$^{13}\text{C-NMR}$  ( $\delta$ , 100 MHz,  $\text{CDCl}_3$ , 25 °C): 31.05 (d, 4C, C-Br); 27.92 (s, 4C, Si-C); 31.05 (s, 4C, C- $\text{CH}_3$ ) ppm.

$^{29}\text{Si-NMR}$  ( $\delta$ , 59.3 MHz,  $\text{CDCl}_3$ , 25 °C): -1.49 (s, Si); 0.18 (s, Si); 1.22 (s, Si) ppm.

#### **ACKNOWLEDGMENTS**

Financial support by the Christian Doppler Research Association, the Austrian Federal Ministry of Economy, Family, and Youth (BMWFF), and Durst Phototechnik GmbH is gratefully acknowledged.

#### **REFERENCES AND NOTES**

- 1 M. S. Karasch, F. R. Mayo, *Chem. Ind.* **1938**, 57, 752–754.
- 2 C. E. Hoyle, T. Y. Lee, T. Roper, *J. Polym. Sci., Part A: Polym. Chem.* **2004**, 42, 5301–5338.
- 3 L. M. Campos, K. L. Killups, R. Sakai, J. M. J. Paulusse, D. Damiron, E. Drockenmuller, B. W. Messmore, C. J. Hawker, *Macromolecules* **2008**, 41, 7063–7070.
- 4 C. R. Morgan, A. D. Ketley, *J. Radiat. Curing* **1980**, 7, 10–13.
- 5 C. N. Bowman, C. E. Hoyle, *Angew. Chem. Int. Ed.* **2010**, 49, 1540–1573.
- 6 D. P. Gush, A. D. Ketley, *Mod. Paint Coat.* **1978**, 68, 58–66.
- 7 N. Mosner, W. Schoeb, V. Reinberger, *Polym. Bull.* **1996**, 37, 289–295.
- 8 S. Reinelt, M. Tabatabai, N. Moszner, U. K. Fischer, A. Utterodt, H. Ritter, *Macromol. Chem. Phys.* **2014**, 215, 1415–1425.
- 9 J. A. Carioscia, L. Schneidewind, C. O'Brien, R. Ely, C. Feeser, N. Cramer, C. N. Bowman, *J. Polym. Sci., Part A: Polym. Chem.* **2007**, 45, 5686–5696.
- 10 Q. Li, H. Zhou, D. A. Wicks, C. E. Hoyle, *J. Polym. Sci., Part A: Polym. Chem.* **2007**, 45, 5103–5111.
- 11 N. B. Cramer, C. N. Bowman, *J. Polym. Sci., Part A: Polym. Chem.* **2001**, 39, 3311–3319.
- 12 J. L. Ferracane, *Dent. Mater.* **2006**, 22, 211–222.
- 13 A. E. Rydholm, C. N. Bowman, K. S. Anseth, *Biomaterials* **2005**, 26, 4495–4506.
- 14 M. Podgorski, E. Becka, S. Chantani, M. Claudino, C. N. Bowman, *Polym. Chem.* **2015**, 2, 2234–2240.
- 15 T. M. Roper, C. E. Hoyle, A. C. Guymon, *Polym. Prepr.* **2003**, 44, 111–112.
- 16 M. Podgorski, S. Chantani, C. N. Bowman, *Macromol. Rapid Commun.* **2014**, 35, 1497–1502.
- 17 A. A. Oswald, W. Naegele, *Makromol Chem* **1966**, 97, 258–266.
- 18 Q. Li, H. Zhou, C. E. Hoyle, *Polymer* **2009**, 50, 2237–2245.
- 19 S. Reinelt, M. Tabatabai, U. K. Fischer, N. Moszner, A. Utterodt, H. Ritter, *Beilstein J. Org. Chem.* **2014**, 10, 1733–1740.
- 20 E. I. Miranda, M. J. Diaz, L. Rosado, J. A. Soderquist, *Tetrahedron Lett.* **1994**, 35, 3221–3224.
- 21 A. R. Jennings, D. Y. Son, *Chem. Commun.* **2013**, 49, 3467–3469.
- 22 I. V. Koval, *Russ. J. Org. Chem.* **2005**, 41, 631–648.
- 23 D. S. Esen, F. Karasu, N. Arsu, D. S. Esen, F. Karasu, N. Arsu, *Prog. Org. Coat.* **2011**, 70, 102–107.
- 24 C. Heller, M. Schwentenwein, G. Russmüller, T. Koch, D. Moser, C. Schopper, F. Varga, J. Stampfl, R. Liska, *J. Polym. Sci., Part A: Polym. Chem.* **2011**, 49, 650–661.
- 25 J. A. Carioscia, L. Schneidewind, C. O. Brien, R. Ely, C. Feeser, N. Cramer, C. N. Bowman, *J. Polym. Sci., Part A: Polym. Chem.* **2007**, 45, 5686–5696.
- 26 G. Ducom, B. Laubie, A. Ohannessian, C. Chottier, P. Germain, V. Chatain, *Water Sci. Technol.* **2013**, 68, 813–820.
- 27 H. E. Gottlieb, V. Kotlyarand, A. Nudelman, *J. Org. Chem.* **1997**, 62, 7512–7515.

## Publication V

Oesterreicher, Andreas; Roth, Meinhart; Hennen, Daniel; Mostegel, Florian H.; Edler, Matthias; Kappaun, Stefan; Griesser, Thomas: Low Migration Type I Photoinitiators for Biocompatible Thiol-Ene Formulations *European Polymer Journal* **2016**, *accepted and in press* DOI: 10.1016/j.eurpolymj.2016.10.040.



## Accepted Manuscript

Low Migration Type I Photoinitiators for Biocompatible Thiol-Ene Formulations

Andreas Oesterreicher, Meinhart Roth, Daniel Hennen, Florian H. Mostegel, Matthias Edler, Stefan Kappaun, Thomas Griesser

PII: S0014-3057(16)31179-X  
DOI: <http://dx.doi.org/10.1016/j.eurpolymj.2016.10.040>  
Reference: EPJ 7577

To appear in: *European Polymer Journal*

Received Date: 27 September 2016  
Revised Date: 25 October 2016  
Accepted Date: 26 October 2016

Please cite this article as: Oesterreicher, A., Roth, M., Hennen, D., Mostegel, F.H., Edler, M., Kappaun, S., Griesser, T., Low Migration Type I Photoinitiators for Biocompatible Thiol-Ene Formulations, *European Polymer Journal* (2016), doi: <http://dx.doi.org/10.1016/j.eurpolymj.2016.10.040>

This is a PDF file of an unedited manuscript that has been accepted for publication. As a service to our customers we are providing this early version of the manuscript. The manuscript will undergo copyediting, typesetting, and review of the resulting proof before it is published in its final form. Please note that during the production process errors may be discovered which could affect the content, and all legal disclaimers that apply to the journal pertain.



## Low Migration Type I Photoinitiators for Biocompatible Thiol-Ene

### Formulations

*Andreas Oesterreicher<sup>1</sup>, Meinhart Roth<sup>1</sup>, Daniel Hennen<sup>1</sup>, Florian H. Mostegel<sup>1</sup>, Matthias Edler<sup>1</sup>, Stefan Kappaun<sup>2</sup>, Thomas Griesser<sup>1</sup>*

<sup>1</sup> Chair of Chemistry of Polymeric Materials & Christian Doppler Laboratory for Functional and Polymer Based Ink-Jet Inks, University of Leoben, Otto-Glöckel-Strasse 2, A-8700 Leoben, Austria

<sup>2</sup> Durst Phototechnik DIT, Julius-Durst-Strasse 11, A-9900 Lienz, Austria

\* corresponding author: Thomas Griesser, email: thomas.griesser@unileoben.ac.at, Tel. +43-3842-402-2358

Keywords: photoinitiator, low-migration, thiol-ene

### Abstract

In this contribution, polymerizable hydroxyalkyl phenone (**PI-4**) and monoacylphosphine oxide (**PI-9**) based photoinitiators (PIs) bearing alkyne groups were synthesized with the aim to realize low PI migration together with high photoactivity in biocompatible vinyl carbonate/thiol resins. Although, photo-DSC measurements showed that the initiation performance of **PI-4** in the present formulation is lower than the photoactivity of the reference PI Irgacure 2959 (**I2959**), it turned out that its migration is significantly reduced compared to **I2959**. This fact is explained by the copolymerization of the alkyne functionality via a thiol/yne reaction as revealed by real-time FT-IR measurements, leading to a covalent immobilization of this PI in the polymeric network. Most importantly, the alkyne functionalized monoacylphosphine oxide based PI provides almost similar initiation activity as its reference PI Irgacure TPO-L (**TPO-L**) while exhibiting 40% lower migration than the non-functionalized **TPO-L**. These findings

make PI-4 and PI-9 promising candidates for their application in biocompatible vinyl carbonate/thiol formulations, in which low migration of the PI is desired.

ACCEPTED MANUSCRIPT

## Introduction

Photopolymerization is a well-established and highly efficient method for curing of coatings and printing inks. Over the last decade, the topic of UV-based 3D-printing has attracted the public interest, which is obviously a result of its fascinating approach for smart manufacturing on demand.[1, 2] Its potential for the design of patient-specific individualized implants, scaffolds or tissue engineering applications will certainly change the future of modern implantology.[3–5] However, before UV light based 3D-printing processes can be used routinely in reconstructive surgery, it is essential to overcome several limitations. Beside the well-documented toxicity of commonly used acrylates,[6–8] also the migration of the applied photoinitiators is a non-neglectable topic for the design of biocompatible materials. Although, there are several reports on low-cytotoxic thiol-based monomer systems including vinyl carbonates/PETMP[9], vinyl esters/PETMP[10] and alkynes/PETMP[2, 8, 11], only a limited number of publications deals with the toxicity of commonly used photoinitiators[12,13] and their migration from 3D-printed medical devices. C. G. Williams et al. reported on the biocompatibility of I2959 who investigated its tolerance over a wide range of cell types and initiator concentrations, concluding that the hydroxy ketone photoinitiator shows low cellular toxicity.[12] Very recently, Liska and co-workers investigated the biocompatibility of water soluble hydroxy ketone and acylphosphine oxide based PIs, respectively. In these studies, they could confirm the superiority of I2959 in terms of cell compatibility.[13] However, it must be emphasized that cleavage or side products, which are generated during the illumination process, were not taken into consideration. It is well known that the 4-(2-hydroxyethoxy)benzaldehyde, which is one of the main cleavage products of I2959, is labeled as an irritant substance.[14] Based on these findings, the necessity of the development of low migration derivatives of this type of photoinitiator is the next logical step towards biocompatible materials for 3D-printing. There are only a few strategies to prevent unfavored migration of non-reacted PIs or their cleavage products. Among these, polymeric systems containing photoinitiating groups that are covalently bound to a

macromolecular backbone are proposed exhibiting improved migration stability. Nevertheless, in most cases, they suffer from low reactivity and poor compatibility with many resin systems.[15] Another approach uses oligomeric photoinitiators which reduce the mobility of the noxious compounds by an elevated molecular weight of the reactive species. Unfortunately, they usually lead to a significant increase of the resin viscosity, which subsequently reduces the photochemical performance of the investigated formulation.[16] Alternatively, an interesting approach is the introduction of polymerizable photoreactive species to realize low migration behavior. The concept of these types of photoinitiators is rather simple and it was published for the first time in the patent literature in 1961 by Du Pont.[17] In general, the photoinitiating unit gets immobilized by its chemical linking to the polymer matrix. [14] Consequently, the unwanted migration is reduced as the photoreactive species is covalently bound to the polymer network and its diffusion processes are inhibited. Only a few scientific publications deal with the topic of polymerizable photoinitiators and they mainly focused on the photochemical performance, whereas the migration behavior is only discussed superficially.[18, 19] Most of these studies found that polymerizable PIs show reduced photoreactivity, which can also be attributed to a reduced diffusion of radicals or excited groups, as during polymerization the photoinitiator is immobilized on the growing polymer chain.

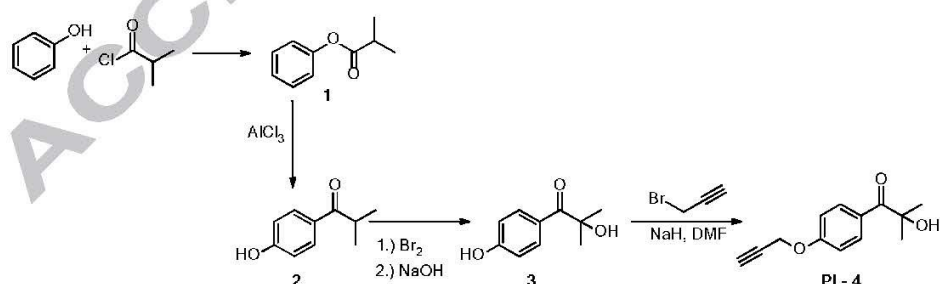
Very recently, we studied the performance and migration behavior of benzophenone derivatives bearing vinyl carbonate and alkynyl ester moieties in a low-cytotoxic butanediol divinyl carbonate/TMPMP resin.[20] It turned out that these PIs offer high migration stability together with a decent initiation performance in this thiol-ene system. This finding is explained by the step growth based network formation that facilitates a high mobility of the excited benzophenones and the formed radicals below the gel point, despite their functionalization with polymerizable groups. However, one general limitation of benzophenone based PIs is their Norrish type II initiation mechanism, which explains their lower initiation performance compared to type I initiators. The cleavage of type I systems is much faster than the electron and/or proton transfer of type II systems.[21]

Consequently, in this contribution we synthesized derivatives of the highly reactive type I PIs I-2959 and Irgacure TPO-L (TPO-L) bearing polymerizable vinyl carbonate and propargyl ether groups and evaluated their performance in vinyl carbonate/thiol formulations with the aim to realize biocompatible, UV curable resins with low PI migration in the cured state. Beside the provided synthetic pathways of these novel substances the photochemical reactivity as well as the migration behavior of these compounds is discussed extensively.

## Results and Discussion

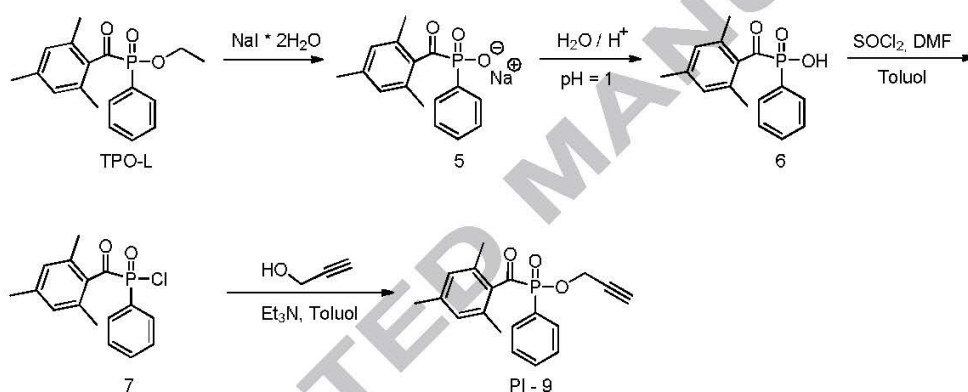
### Synthesis

The photoinitiator PI - 4 was synthesized via a multi-step reaction as shown in Scheme 1. In the first step, an esterification of the phenol was performed to obtain **1** in good yields (97%). Afterwards, **1** was converted to **2** (83%) by a Fries rearrangement [22] using  $\text{AlCl}_3$  as a catalyst. The hydroxyketone derivative **3** was obtained by the bromination of **2** and subsequent reaction with NaOH in decent yield of 61%. [23] This compound was used as a precursor molecule for the synthesis of the photoinitiators PI - 4, which could be obtained by an etherification of **3** under basic conditions with propargyl bromide in a yield of 68%.



Scheme 1: Synthesis of the photoinitiator PI - 4.

The phosphine oxide derivative **PI-9** was synthesized in a straightforward four-step procedure as depicted in Scheme 2. As a starting point, the commercially available Irgacure TPO-L was converted with sodium iodide to the corresponding salt **5**, which was isolated by filtration in an excellent yield of 90%. This reaction step was followed by the generation of the phosphine acid derivative **6** under acidic conditions, which was dried by an azeotropic distillation before the crude product was purified by recrystallization in toluene (78%). The obtained phosphine acid derivative was reacted at elevated temperatures (110°C) with  $\text{SOCl}_2$  in the presence of a catalytic amount of DMF to the corresponding acid chloride,<sup>[24]</sup> which was converted into the alkyne derivative **PI-9** (63%).



Scheme 2: Synthesis of the photoinitiator **PI-9**.

### UV-Vis Spectroscopy

The absorption of electromagnetic radiation is a key factor for the reactivity of photo initiating systems. To achieve satisfying curing behavior of an investigated resin and to obtain high quantum yields the emission spectrum of the applied light source has to match the absorption maximum of the photoinitiator. Especially in the case of pigmented systems or the presence of photoactive additives phenomena like an inner filter effect, light scattering or photo quenching reactions have to be taken into consideration.<sup>[25]</sup>

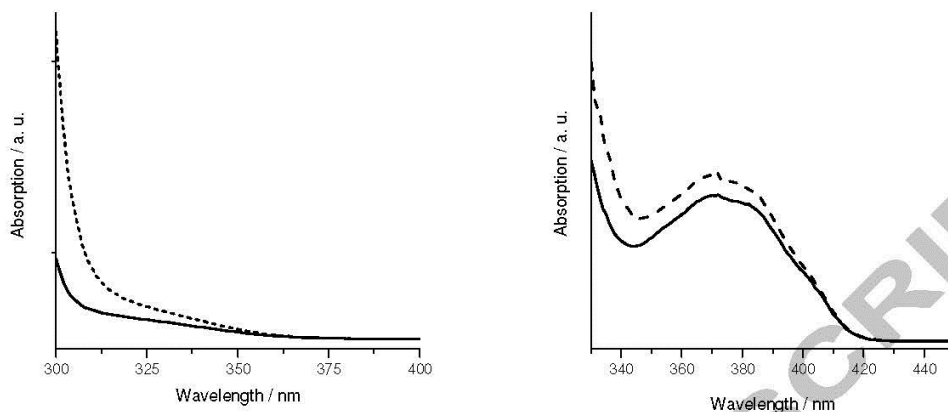


Figure 1: Absorption spectra of the synthesized photoinitiators and the commercially available reference substances (1.0 mM in acetonitrile); left: **I2959** (solid line), **PI – 4** (dotted line); right: **TPO-L** (solid line), **PI – 9** (dashed line).

The UV-VIS absorption behavior of the synthesized PIs was determined by UV-VIS spectroscopy and compared to **I2959** and **TPO-L**. It is well known that the  $\alpha$ -cleavage occurs mainly from the triplet state of the excited  $n-\pi^*$  transition and that **I2959** shows a maximum for this transition in the range of 325 nm. As shown in Figure 1 (left) **PI-4** provides a similar absorption behavior in this region. Interestingly, the alkyne functionalized PI offers an appreciably higher molar extinction coefficient than **I2959** at 325 nm ( $\epsilon$ , shown in Table 1). The monoacylphosphine oxide based PIs **TPO-L** and **I2959** show the maxima of the  $n-\pi^*$  transition of the carbonyl moiety at  $\sim 372$  nm. Compared to **PI – 4** and **I2959**, a strong shift of the  $n-\pi^*$  transition can be observed, which can be explained by the overlap of the d-orbitals of phosphorus with the  $\pi^*$ -orbitals of the C=O group, thus reducing the necessary energy for the  $n-\pi^*$  transition, which is responsible for the radical generation.[26] It has to be mentioned that the derivatization of **TPO-L** also leads to a slightly increased  $\epsilon$  for the  $n-\pi^*$  transition as shown in Table 1.



Table 1: Molar extinction coefficients of maxima of the synthesized PIs.

PI	$\lambda_{\max}$ [nm]	$\epsilon$ [dm <sup>3</sup> mol <sup>-1</sup> cm <sup>-1</sup> ]
I2959	325	2912 ± 70
PI-4	325	1953 ± 56
TPO-L	372	2215 ± 62
PI-9	372	2538 ± 63

### Photoreactivity

The photochemical performance of the synthesized photoinitiators was characterized by means of photo differential scanning calorimetry (photo-DSC) measurements. Important parameters which can be obtained by photo-DSC measurements are the time to reach the maximum heat of polymerization ( $t_{\max}$ ) and the maximum heat flow ( $\text{Peak}_{\max}$ ). In combination, these parameters give information about the curing speed of the investigated system.[4] Furthermore the overall reaction enthalpy ( $\Delta H$ , peak area) is proportional to the monomer conversion. Due to the fact that homopolymerization reactions cannot be excluded in these BuVC/TMPMP formulations, an exact calculation of the monomer conversion exploiting the standard reaction enthalpy of the thiol-vinyl carbonate addition reaction is not feasible. However, assuming that the degree of homopolymerization is independent of the used PI, the overall reaction enthalpy provides a relative measure for the monomer conversion for the tested PIs in this thiol-ene system. Within the group of the hydroxy ketone photoinitiators, a reduced reactivity of the alkyne functionalized PI was observed as revealed from the photo-DSC plots as shown in Figure 2.

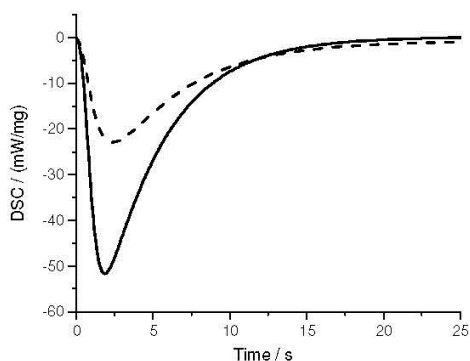


Figure 2: Photo-DSC plots of BuVC/TMPMP containing 5 mol% of **I2959** (solid) and 5 mol% of **PI-4** (dashed).

Besides the curing performance ( $t_{\max}$  +32%; peak height -56%), also the conversion (-32%) is noticeable decreased compared to a formulation containing **I2959** (as shown in Table 1). Presumably, the additional propargyl ether moiety in the proximity of the aromatic system of **PI-4** influences the efficiency of radical generation upon UV irradiation.

Most importantly, the alkyne functionalized monoacylphosphine oxide based PI provides almost identical initiation performance in terms of  $t_{\max}$  (+10%) and  $\text{Peak}_{\max}$  as the reference PI **TPO-L** (Figure 3 and Table 2). Interestingly, **PI-9** (310 J/g) exhibits an even slightly higher  $\Delta H$  than **TPO-L** (285 J/g). Apart from a higher monomer conversion, the heat of polymerization of the additional alkyne functionality has to be considered for **PI-9**.

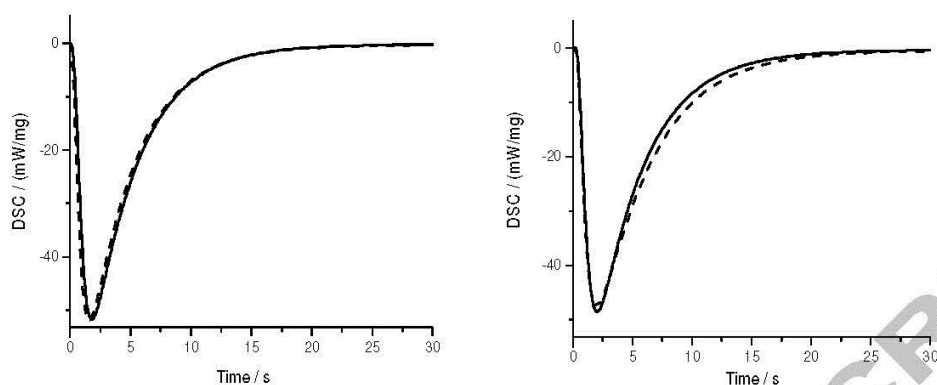


Figure 3: left: Photo-DSC plots of BuVC/TMPMP containing 5 mol% of TPO-L (solid) and 5 mol% of PI-9 (dashed). Right: Photo-DSC plots of BuVC/TMPMP containing 1 mol% of TPO-L (solid) and 1 mol% of PI-9 (dashed).

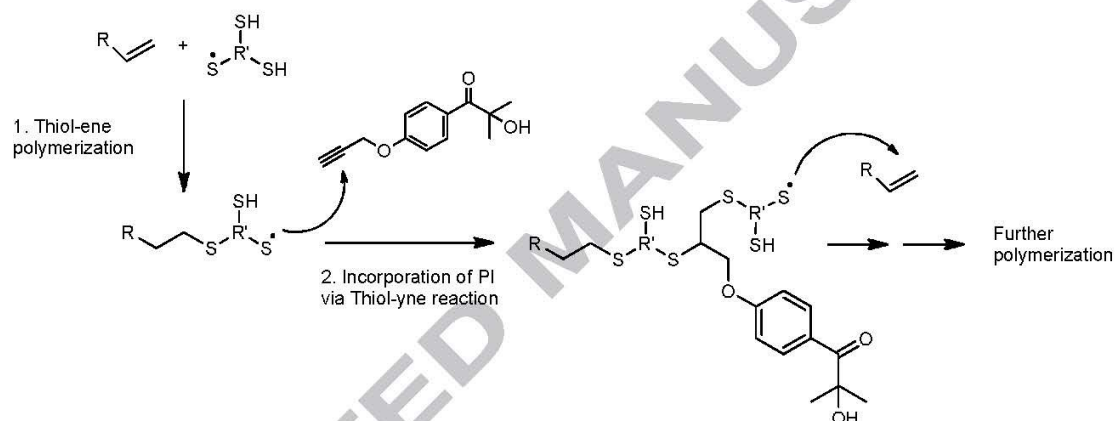
In Figure 3, the polymerization heat evolution of BuVC/TMPMP containing 1 mol% of PI-9 and TPO-L, respectively, is shown. Also at lower concentrations, PI-9 provides a similar photoactivity as TPO-L. Moreover, at this concentration, both initiators offer an only slightly decreased curing performance ( $t_{\max}$ ,  $\text{Peak}_{\max}$ , see Table 2) compared to in the concentration of 5 mol%.

Table 2: Photopolymerization parameters obtained by Photo-DSC.

Photoinitiator	$t_{\max}$ [s]	$\text{Peak}_{\max}$ [mW/mg]	$\Delta H$ [J/g]
I2959 (5 mol%)	1.9	52	280
PI-4 (5 mol%)	2.5	23	190
TPO-L (5 mol%)	2.0	51	285
TPO-L (1 mol%)	1.9	48	320
PI-9 (5 mol%)	2.2	51	310
PI-9 (1 mol%)	2.1	48	300

### Investigation of alkyne group conversion by RT-FT-IR spectroscopy

Real-time Fourier transformed IR spectroscopy (RT-FT-IR), a versatile tool to follow chemical group transformations during UV illumination, enables comprehensive kinetic studies of photopolymerization reactions. Consequently, the conversion of the alkyne functionality of **PI-4** and **PI-9** was investigated to prove the incorporation of those PIs into the polymer network during the photochemical reaction as shown in Scheme 3 on the example of **PI-4**.



Scheme 3: Incorporation of **PI-4** into the thiol-ene network during photopolymerization.

These kinetic studies were facilitated by the distinctive and isolated signal of the terminal alkyne groups (C-H stretching) which appears in the region of 3250-3330  $\text{cm}^{-1}$ . As shown in Figure 4, the alkyne functionalities of both PIs, i.e. **PI-4** and **PI-9**, show similar reaction rates and almost quantitative conversion. The chemical linking of the PIs leads to an immobilization of non-reacted **PI-4** and **PI-9** and also its alkyne functionalized PI fragments in the polymeric network. The fragmentation of the reference PIs **I2959** and **TPO-L** was studied in detail by Jockusch[27] as well as Kolczak[28] and coworkers. It is

worth mentioning that due to the fragmentation mechanism of these type I PIs, the formation of leachable acetone (PI-4) and 2,4,6-trimethylbenzaldehyde (PI-9) can be expected.

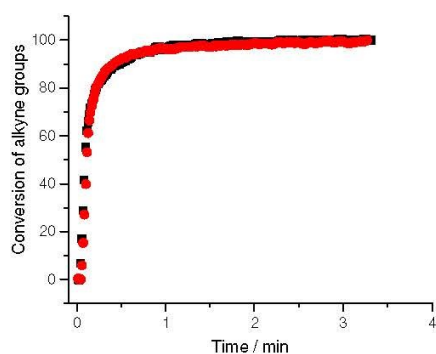


Figure 4: Conversion of alkyne ether groups of **4a** (red circle) and **9b** (black square) during UV illumination.

### Migration studies

To characterize the migration behavior of non-converted photoinitiators, samples of cured resin were immersed in ethanol at 50°C for 96h. The quantification of I2959 and PI-4 was performed using GC-MS analysis. Using this technique a significant concentration of I2959 (26.8% of the applied PI, as shown in Figure 5) was found in the ethanolic extract. In contrast, the concentration of PI-4 is below the detection limit (0.15 µg/ml) of this method and also none of its cleavage products could be detected. These findings are in good accordance with the performed RT-FT-IR measurements (vide supra), which revealed an almost quantitative incorporation of PI-4 in the polymeric network. In order to determine phosphorus containing leachables in the ethanolic extract, ICP-MS measurements were performed, which enable the quantification of the monoacylphosphine oxide based PIs TPO-L and PI-9. Besides both compounds, also possible phosphorus containing cleavage products are detected by this method. Interestingly, the

amount of the measured phosphorus in the sample derived from **PI-9** (depicted in Figure 5) was significantly higher (corresponding to 15.6% of applied **PI-9**), than it was expected from FT-IR measurements. This finding might be attributed to a partial fragmentation of the P-O bond in **PI-9**, which has not been reported for **TPO-L** so far and which is currently a topic of further investigations. However, compared to the sample derived from **TPO-L**, in which 25.7% of the applied phosphorus in **TPO-L** was detected, a considerable lower migration of phosphorus-containing compounds could be found.

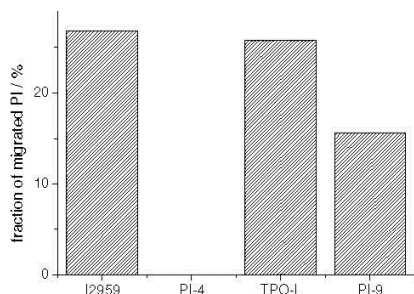


Figure 5: Results of migration studies.

### Conclusion

In this contribution, alkyne functionalized hydroxyalkylphenone (**PI-4**) and monoacylphosphine oxide (**PI-9**) based PIs, respectively, were synthesized and their photoinitiation performance and migration stability were evaluated in a vinyl carbonate/thiol formulation. Although, photo-DSC measurements showed that the curing performance ( $t_{max}$  +32%; peak height -56%), as well as the conversion (-32%) of vinyl carbonate/thiol mixtures containing **PI-4**, are lower than those of formulations containing the reference PI **I2959**, it turned out that the migration of this PI is significantly reduced compared to **I2959**. The concentration of this **PI-4** in the extract was found to be below the detection limit (0.15  $\mu\text{g/ml}$ ), while 26.8% of the applied **I2959** could be detected after extraction. Most importantly, the alkyne functionalized monoacylphosphineoxide based PI provides almost identical initiation activity in terms of

$t_{\max}$  and  $\text{Peak}_{\max}$  as the reference PI **TPO-L**. The quantification of **PI-9** and its reference **TPO-L** in the ethanolic extract was performed by the determination of the overall phosphorus content using ICP-MS, which does not only detect the PI, but also its cleavage products. From these measurements, it was found that 15.7% (including phosphorus containing cleavage products) of the applied **PI-9** were extracted. Since FT-IR measurements showed an almost quantitative conversion of the alkyne bond during photopolymerization and thus an immobilization of **PI-9** can be expected, the detected amount of extracted **PI-9** and its cleavage products might be attributed to a cleavage of the P-O bond during photopolymerization or extraction. In comparison, 25.7% of the applied non-functionalized **TPO-L** could be found in the extract. This fact, together with the high initiation activity of **PI-9** makes this monoacylphosphine oxide based PI a promising candidate for an application in biocompatible vinyl carbonate/thiol formulations, in which low migration of the PI is desired.

#### **Acknowledgements**

Financial support by the Durst Phototechnik GmbH is gratefully acknowledged. Furthermore, the authors thank the Christian Doppler research association and the Austrian Ministry of Science, Research and Economy (BMWFV) for financial support.

#### **Materials**

All chemicals were purchased from commercial sources (Sigma Aldrich, TCI Europe, VWR International, Acros Organics, Bruno-Bock Thiochemicals or Carl Roth) and used without further purification.

#### **Characterization**

## NMR

$^1\text{H}$  NMR and  $^{13}\text{C}$  NMR spectra were recorded with a Varian 400-NMR spectrometer operating at 399.66 MHz and 100.5 MHz, respectively, and were referenced to  $\text{Si}(\text{CH}_3)_4$ . A relaxation delay of 10 s and  $45^\circ$  pulse were used for the acquisition of the  $^1\text{H}$ -NMR spectra. Solvent residual peaks were used for referencing the NMR spectra to the corresponding values given in the literature.[29]

## UV-Vis

UV-Vis spectra were recorded in absorbance mode, in the range of 200 nm - 800 nm with a Varian Cary 50 conc.-spectrophotometer. All substances were dissolved in MeCN and measured in Hellma QS 10.00 mm absorption cells with a spectral transmission between 200 nm and 2500 nm. All provided spectra were measured at a concentration of 1.0 mM, except for the phosphine oxide initiators, which were characterized at a concentration of 1.0 mM.

## Photo-DSC

The Photo-DSC experiments were performed on a NETZSCH Photo-DSC 204 F1 Phoenix. All measurements were conducted at  $50^\circ\text{C}$  in aluminum crucibles under nitrogen atmosphere. The Omnicure s2000 was used as a light source providing an intensity of  $0.5\text{ W/cm}^2$  at the tip of the light guide. This correlates to a light intensity of approximately  $40\text{ mW/cm}^2$  at the sample surface (measured in the wavelength range from 250 to 445 nm using a Power Puck II, EIT LLC, Sterling, Virginia, USA). For the determination of the reaction enthalpy and  $t_{\text{max}}$  the samples (sample quantity: 8 mg resin containing 5 mol% of the evaluated photoinitiator related to the monomers (this corresponds to 3.8 w% of I2959, 3.7 w% of PI-4, 5.5 w% of TPO-L and 5.3 w% of PI-9) or 1 mol% (corresponds to 0.76 w% of I2959, 0.74 w% of PI-4, 1.1 w% of PI TPO-L and 1.1 w% of PI-9) were illuminated twice for 10 min each with an idle



time of 2 min in between. For the analysis, the second run was subtracted from the first one to give the reaction enthalpy curve.

#### **Sample preparation GC-MS and ICP-MS**

To obtain representative and reproducible values for the migration of the polymerizable photoinitiators and to reduce the observational error of inhomogeneous illumination and inconsistent curing conditions (oxygen inhibition, curing temperature etc.), 20 mg of all resin formulations were cured by Photo-DSC under N<sub>2</sub> atmosphere and with a radiation intensity of 5 W/cm<sup>2</sup>. The increased illumination intensity was chosen to reach the highest possible monomer conversion of the investigated resins. The resulting polymers were extracted with ethanol at 50°C for 96 h and continuous shaking. In a subsequent step, the solvent was evaporated and the residue re-dissolved in a defined volume of ethanol for the GC-MS measurements. For the ICP-MS measurements, an acidic digestion of the extracts after solvent evaporation was performed in a High Pressure Asher (HPA-S, Anton Paar), with concentrated HNO<sub>3</sub> at 240°C and a pressure of 120 bar for 60 minutes in an aqueous medium. For each photoinitiator, a fourfold determination was performed.

#### **GC-MS**

##### **Gas chromatography mass spectroscopy (GC-MS)**

Analyses were performed using a Shimadzu QP2010 plus gas chromatography equipped with a mass spectroscopy unit. The mass calibrations were performed according to the manufacturer recommendation before sample analysis. The capillary column was an Optima 5-Accent (MS-5) (30 m × 0.25-mm i.d., 0.25-μm film thickness). Helium was used as the carrier gas with a flow velocity of 47.2 cm/s. The initial oven temperature was 50°C for 1 min followed by a temperature-programmed increase

of 10°C/min to 300°C. Split ratio (1:0) was used for sample injection of 1 µL volume at an injection temperature of 300°C. The samples were analysed using both full scan and SIM modes. In SIM mode, the characteristic ions of 121 and 181 were used for quantification of Irgacure 2959. For PI-4 the focus was set on the ions 131, 159, 175.

#### ICP-MS

The phosphorus-containing samples were characterized by an Agilent 8800 Triple-quadrupole-ICP-MS, after acidic digestion. The measurements were performed in a MS/MS-mode with oxygen as a reactive gas. For external calibration 1000 mg/L<sup>-1</sup> CertiPur standards from Merck were diluted with water to the desired concentration.

#### Synthesis:

##### Phenylisobutyrate (1)

50.00 g (1 eq., 0.531 mol) phenol was cooled in a flask to 0°C and 70.73 g (1.25 eEq, 0.664 mol) isobutyl acid chloride was added dropwise. The mixture was held at 0°C for one hour and after that, it was allowed to warm to room temperature. After two hours, remaining isobutyl acid chloride was removed under reduced pressure to obtain the product as a yellow liquid (97.4% yield).

<sup>1</sup>H-NMR (δ, 400 MHz, 25°C, CDCl<sub>3</sub>): 7.28 (d, 2H, Ar); 7.22 (d, 1H, Ar); 7.09 (d, 1H, Ar); 2.81 (d, 1H, CH); 1.33 (s, 6H, -CH<sub>3</sub>) ppm.

<sup>13</sup>C-NMR (δ, 100 MHz, CDCl<sub>3</sub>, 25 °C): 175.51 (1C, C=O); 150.94 (1C, Ar); 129.35 (2C, Ar); 125.63 (1C, Ar); 121.51 (2C, Ar); 34.17 (1C, C); 18.93 (2C, CH<sub>3</sub>) ppm.

##### 1-(4-Hydroxyphenyl)-2-methylpropan-1-one (2)

38.98 g (2.4 eq, 0.292 mol)  $\text{AlCl}_3$  were suspended in chlorobenzene at  $0^\circ\text{C}$  and was stirred at room temperature for 45 min. 20.00 g (1 eq., 0.121 mol) of **1** were added dropwise and the reaction mixture was stirred for two days. The reaction was stopped by the addition of ice and HCl and was extracted with toluene. In the next step, the combined organic layers were extracted with saturated NaCl and the solvent was removed under reduced pressure. The residue was suspended in 300 mL  $\text{H}_2\text{O}$  and the pH was adjusted to 14 by the addition of 30% NaOH. The mixture was extracted with ethyl acetate and the water phase was acidulated to a pH of 0 by the addition of HCl. After an extraction step with ethyl acetate, the combined organic layers were dried over  $\text{Na}_2\text{SO}_4$  and the solvent was removed under reduced pressure to obtain the product as a white solid (82.5% yield).

$^1\text{H-NMR}$ : ( $\delta$ , 400 MHz,  $25^\circ\text{C}$ ,  $\text{CDCl}_3$ ): 8.1 (d, 2H, Ar); 6.7 (d, 2H, Ar); 5.35 (d, 1H, OH) 2.81 (d, 1H, CH); 1.33 (s, 6H,  $-\text{CH}_3$ ) ppm.

$^{13}\text{C-NMR}$  ( $\delta$ , 100 MHz,  $\text{CDCl}_3$ ,  $25^\circ\text{C}$ ): 202.20 (1C, C=O); 162.54 (1C, Ar); 130.29 (2C, Ar); 129.4 (1C, Ar); 115.8 (2C, Ar); 35.00 (1C, C); 18.01 (2C,  $\text{CH}_3$ ) ppm.

### **2-Hydroxy-1-(4-hydroxyphenyl)-2-methylpropan-1-one (3)**

21 g (1 Eq., 0.127 mol) of **2** were dissolved in dioxane and cooled to  $0^\circ\text{C}$ . 22.48 g (1.1 eq., 0.140 mol)  $\text{Br}_2$  were added and the mixture was stirred for 2h at room temperature. The reaction was poured into 500 mL water and extracted two times with ethyl acetate. In the next step, the solvent was removed under reduced pressure and the brownish oil was suspended in 400 mL water. The pH of 14 was adjusted by the addition of 20 mL NaOH (30%). The mixture was stirred at room temperature for 3h and subsequently neutralized by the addition of HCl. The slightly yellow crystals were filtered off and recrystallized from toluene to obtain the pure product as white crystals (60.8% yield).

$^1\text{H-NMR}$ : ( $\delta$ , 400 MHz,  $25^\circ\text{C}$ ,  $\text{CDCl}_3$ ): 8.1 (d, 2H, Ar); 6.7 (d, 2H, Ar); 5.35 (s, 1H, OH) 3.28 (s, 1H, OH); 1.33 (s, 6H,  $-\text{CH}_3$ ) ppm

<sup>13</sup>C-NMR: ( $\delta$ , 100 MHz, 25°C, CDCl<sub>3</sub>): 198.59 (1C, C=O); 162.54 (1C, Ar); 132.69 (2C, Ar); 126.8 (1C, Ar); 115.25 (2C, Ar); 81.00 (1C, C); 28.70 (2C, CH<sub>3</sub>) ppm

#### **2-Hydroxy-2-methyl-1-(4-(prop-2-yn-1-yloxy)phenyl)propan-1-one (PI – 4)**

0.21 g (2 eq., 23.99 mmol) NaH were added to a three necked round bottom flask and washed three times with dry THF to remove the mineral oil. Afterwards, the NaH was suspended in DMF and the reaction was cooled to -40 °C. The dissolved **3** (1.1 eq., 13.19 mmol) was added dropwise and the mixture was stirred for one additional hour while the temperature was held between -40°C and -10°C. Propargyl bromide (80% in toluene) (1 eq., 0.68 g) was added, the cooling bath was removed and the reaction was stopped after 5h by the addition of ice cubes. Subsequently, the solvent was evaporated under reduced pressure and the residue was redissolved in water and extracted three times with CH<sub>2</sub>Cl<sub>2</sub>. The combined organic layers were dried over Na<sub>2</sub>SO<sub>4</sub>, to obtain the title compound as a white solid after purification by flash chromatography (silica gel, cyclohexane / ethyl acetate=3:1) (68.1% yield).

<sup>1</sup>H-NMR: ( $\delta$ , 400 MHz, 25°C, CDCl<sub>3</sub>): 8.08 (d, 2H, Ar); 7.04 (d, 2H, Ar); 4.77 (s, 2H, CH<sub>2</sub>); 4.18 (s, 1H, OH); 2.56 (s, 1H, CH); 1.64 (s, 6H, CH<sub>3</sub>).

<sup>13</sup>C-NMR: ( $\delta$ , 100 MHz, 25°C, CDCl<sub>3</sub>): 202.60 (1C, C=O); 161.19 (1C, Ar); 132.27 (2C, Ar); 126.68 (1C, Ar); 114.48 (2C, Ar); 77.63 (1C, C); 76.30 (1C,  $\equiv$ C); 75.93 (1C,  $\equiv$ CH); 28.61 (2C, CH<sub>3</sub>).

#### **Sodium phenyl(2,4,6-trimethylbenzoyl)phosphinate (5)**

10 g of TPO-L (31.61 mmol) were dissolved in methyl ethyl ketone and NaI\*2H<sub>2</sub>O (5.9 g, 31.61mmol) was added over a period of 15 min. The mixture was stirred overnight at 65°C. Then the yellow precipitate was filtered off on the next day. It was washed twice with 10 ml n-hexane and dried under vacuum at 60°C for 24 h (90.1% yield). The product was used in the following reaction step without further purification.

**Phenyl(2,4,6-trimethylbenzoyl)phosphinic acid (6)**

5 (7.26 g, 23.3 mmol) was dissolved in H<sub>2</sub>O and acidulated with 0.5 M H<sub>2</sub>SO<sub>4</sub> to pH = 1. After a reaction time of 1h white crystals were filtered off and washed twice with H<sub>2</sub>O. The precipitate was dissolved in toluene and dried by azeotropic distillation, the remaining toluene was evaporated under reduced pressure and the residue was recrystallized in ethyl acetate. Subsequently, the pale yellow crystals were dried under vacuum at 60°C for 16 h (78.1% yield).

<sup>1</sup>H-NMR: (δ, 400 MHz, 25°C, CDCl<sub>3</sub>): 7.71 (m, 2H, Ar); 7.63 (m, 1H, Ar); 7.52 (m, 2H, Ar), 6.85 (m, 2H, Ar), 2.24 (s, 3H, CH<sub>3</sub>), 2.07 (s, 6H, CH<sub>3</sub>).

<sup>13</sup>C-NMR: (δ, 100 MHz, 25°C, CDCl<sub>3</sub>): 215.74 (1C, C=O); 139.61 (1C, Ar); 136.20 (1C, Ar); 134.30 (2C, Ar); 132.96 (1C, Ar); 132.7 (1C, Ar); 128.28 (4C, Ar); 21.02 (1C, CH<sub>3</sub>); 19.13 (2C, CH<sub>3</sub>) ppm.

**Phenyl(2,4,6-trimethylbenzoyl)phosphine chloride (7)**

6 (1 eq., 1.73 mmol) was dissolved in 5 ml toluene. 5 μl DMF and 2.5 ml SOCl<sub>2</sub> (4.13 g, 34.69 mmol) were added. The mixture was heated to 110°C for 16 h and the reaction progress was monitored by <sup>1</sup>H-NMR. After complete conversion of 6 the solvent and the excess of SOCl<sub>2</sub> was removed under reduced pressure (98% yield).

<sup>1</sup>H-NMR: (δ, 400 MHz, 25°C, CDCl<sub>3</sub>): 7.79 (m, 2H, Ar); 7.47 (m, 1H, Ar); 7.37 (m, 2H, Ar), 6.69 (m, 2H, Ar), 2.11 (s, 3H, CH<sub>3</sub>), 1.99 (s, 6H, CH<sub>3</sub>).

**2-Hydroxyethylvinylcarbonate (8)**

Ethylene glycol (6.4 eq, 11.19 g, 180.26 mmol) and pyridine (1 eq., 2.27 mL, 28.17 mmol) were dissolved in CH<sub>2</sub>Cl<sub>2</sub> and cooled to 0 °C. Vinyl chloroformate (3.0 g, 28.17 mmol, 1 Eq.) was added dropwise and

after one hour the reaction was warmed to RT and stirred overnight. The product was extracted three times with 5% HCl and the combined organic layers were dried over Na<sub>2</sub>SO<sub>4</sub>. Subsequently, the solvent was evaporated under reduced pressure and the residue was purified by flash chromatography (silica gel, cyclohexane / ethyl acetate = 4:1), to obtain the title compound **6** as a white viscous oil (54.0% yield).

<sup>1</sup>H-NMR: (δ, 400 MHz, 25°C, CDCl<sub>3</sub>): 7.07 (m, 1H, CH<sub>2</sub>); 4.94 (m, 1H, CH<sub>2</sub>); 4.58 (m, 1H, CH<sub>2</sub>); 4.51 (s, 1H, OH); 4.32 (m, 2H, CH<sub>2</sub>), 3.87 (m, 2H, CH<sub>2</sub>).

<sup>13</sup>C-NMR: (δ, 100 MHz, 25°C, CDCl<sub>3</sub>): 152.82 (1C, C=O); 142.49 (1C, CH=); 98.02 (1C, =CH<sub>2</sub>); 69.78 (1C, CH<sub>2</sub>); 60.50 (1C, CH<sub>2</sub>) ppm.

**Prop-2-yn-1-yl phenyl(2,4,6-trimethylbenzoyl)phosphinate (PI – 9)**

**7** (1 eq., 1.38 mmol) and propargyl alcohol (1 eq., 80 μl, 1.38 mmol) were dissolved in 20 mL CH<sub>2</sub>Cl<sub>2</sub> cooled to 0°C. 190 μl (0.140 g, 1.38 mmol, 1 eq.) triethylamine was added to the mixture and the ice bath was removed after 1 h and the reaction was stirred at RT overnight. On the next day the reaction was stopped by the addition of water, extracted three times with CH<sub>2</sub>Cl<sub>2</sub> and dried with Na<sub>2</sub>SO<sub>4</sub>. Subsequently, the solvent was evaporated under reduced pressure and the residue was purified by flash chromatography (silica gel, cyclohexane / ethyl acetate=4:1) to obtain the title compound **2b** as a brownish viscous oil. (62.5% yield)

<sup>1</sup>H-NMR: (δ, 400 MHz, 25°C, CDCl<sub>3</sub>): 7.85 (m, 2H, Ar); 7.59 (m, 1H, Ar); 7.48 (m, 2H, Ar), 6.81 (m, 2H, Ar), 4.69 (d, 2H, CH<sub>2</sub>), 2.49 (s, 1H, CH), 2.26 (s, 3H, CH<sub>3</sub>), 2.15 (s, 6H, CH<sub>3</sub>).

<sup>13</sup>C-NMR: (δ, 100 MHz, 25°C, CDCl<sub>3</sub>): 214.89 (1C, C=O); 140.29 (1C, AR); 134.66 (1C, AR); 133.66 (2C, Ar); 133.10 (1C, Ar); 128.81 (4C, Ar); 76.44 (1C, ≡CH); 53.39 (1C, CH<sub>2</sub>); 21.29 (1C, CH<sub>3</sub>); 19.56 (2C, CH<sub>3</sub>) ppm

<sup>31</sup>P-NMR: (δ, 100 MHz, 25°C, CDCl<sub>3</sub>): 18.52 (s, P) ppm.

### Acknowledgements

Financial support by the Christian Doppler Research Association, the Austrian Federal Ministry of Science, Research and Economy (BMWFW), and Durst Phototechnik GmbH is gratefully acknowledged.

### References

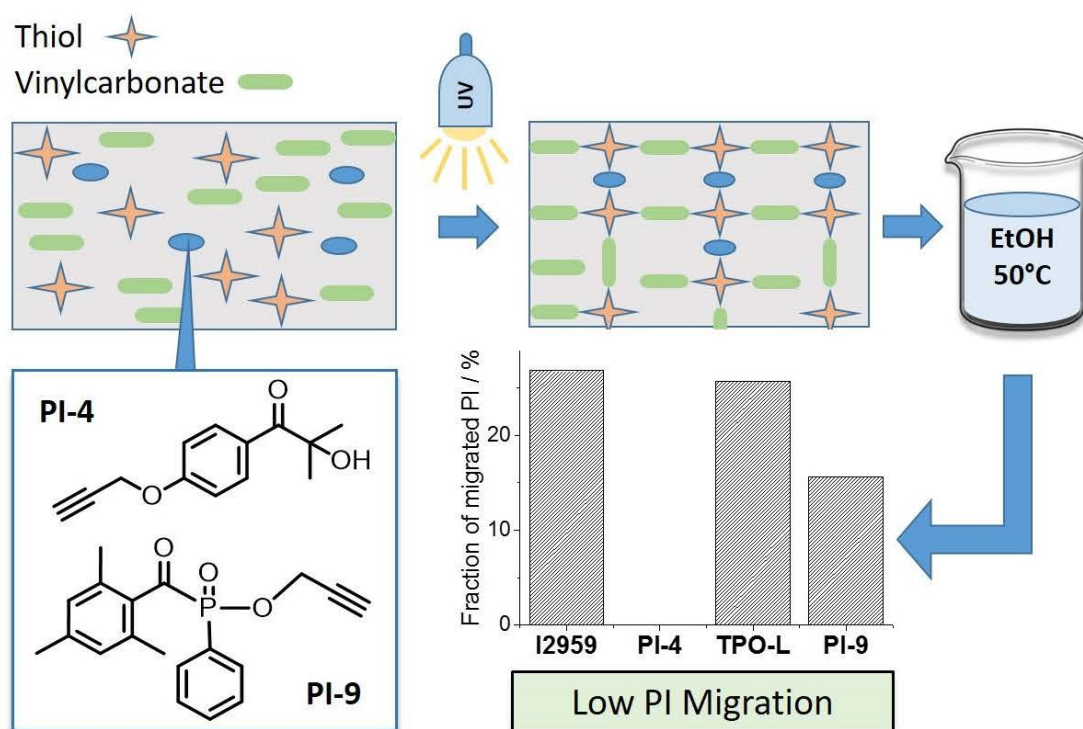
1. Gorsche C, Seidler K, Knaack P et al. (2016) Rapid formation of regulated methacrylate networks yielding tough materials for lithography-based 3D printing. *Polym. Chem.* 7(11): 2009–2014. doi: 10.1039/C5PY02009C
2. Oesterreicher A, Wiener J, Roth M et al. (2016) Tough and degradable photopolymers derived from alkyne monomers for 3D printing of biomedical materials. *Polym. Chem.* 7(32): 5169–5180. doi: 10.1039/C6PY01132B
3. Cooke MN, Fisher JP, Dean D et al. (2003) Use of stereolithography to manufacture critical-sized 3D biodegradable scaffolds for bone ingrowth. *J Biomed Mater Res B Appl Biomater* 64(2): 65–69. doi: 10.1002/jbm.b.10485
4. Heller C, Schwentenwein M, Rusmüller G et al. (2011) Vinylcarbonates and vinylcarbamates: Biocompatible monomers for radical photopolymerization. *J. Polym. Sci. A Polym. Chem* 49(49(3) // 3): 650–661. doi: 10.1002/pola.24476
5. Melchels FPW, Feijen J, Grijpma DW (2010) A review on stereolithography and its applications in biomedical engineering. *Biomaterials* 31(24): 6121–6130. doi: 10.1016/j.biomaterials.2010.04.050
6. Andrews LS, Clary JJ (1986) Review of the toxicity of multifunctional acrylates. *Journal of Toxicology and Environmental Health* 19(2): 149–164. doi: 10.1080/15287398609530916

7. Friedman M, Cavins JF, Wall JS (1965) Relative Nucleophilic Reactivities of Amino Groups and Mercaptide Ions in Addition Reactions with  $\alpha,\beta$ -Unsaturated Compounds<sup>1,2</sup> // Relative Nucleophilic Reactivities of Amino Groups and Mercaptide Ions in Addition Reactions with  $\alpha,\beta$ -Unsaturated Compounds 1,2. *J. Am. Chem. Soc* 87(16): 3672–3682. doi: 10.1021/ja01094a025
8. Oesterreicher A, Ayalur-Karunakaran S, Moser A et al. (2016) Exploring thiol-yne based monomers as low cytotoxic building blocks for radical photopolymerization. *Journal of Polymer Science Part A: Polymer Chemistry*. doi: 10.1002/pola.28239
9. Mautner A, Qin X, Kapeller G et al. (2012) Efficient Curing of Vinyl Carbonates by Thiol-Ene Polymerization. *Macromolecules Rapid Communications* 33(23): 2046–2052. doi: 10.1002/marc.201200502
10. Mautner A, Qin X, Wutzel H et al. (2013) Thiol-ene photopolymerization for efficient curing of vinyl esters. *J. Polym. Sci. A Polym. Chem* 51(1): 203–212. doi: 10.1002/pola.26365
11. Oesterreicher A, Gorsche C, Ayalur-Karunakaran S et al. (2016) Exploring Network Formation of Tough and Biocompatible Thiol-yne Based Photopolymers. *Macromolecular Rapid Communications*. doi: 10.1002/marc.201600369
12. Williams CG, Malik AN, Kim TK et al. (2005) Variable cytocompatibility of six cell lines with photoinitiators used for polymerizing hydrogels and cell encapsulation. *Biomaterials* 26(11): 1211–1218. doi: 10.1016/j.biomaterials.2004.04.024
13. Benedikt S, Wang J, Markovic M et al. (2016) Highly efficient water-soluble visible light photoinitiators. *Journal of Polymer Science Part A: Polymer Chemistry* 54(4): 473–479. doi: 10.1002/pola.27903
14. W.D. Davies, F.D. Jones, J. Garrett et al. (2001) Copolymerisable photoinitiators and water-based UV-curable systems. *Surface coatings international Part B: Coatings Transactions*(84): 169–242



15. Klos R, Gruber H, Greber G (1991) Photoinitiators with Functional Groups. Part I. Polymer Photoinitiators. *Journal of Macromolecular Science: Part A - Chemistry* 28(9):925–947. doi: 10.1080/00222339108054070
16. Lalevée J, Allonas X, Jradi S et al. (2006) Role of the Medium on the Reactivity of Cleavable Photoinitiators in Photopolymerization Reactions. *Macromolecules* 39(5):1872–1879. doi: 10.1021/ma052173k
17. Organic Polymers(GB925117)
18. Xiao P, Zhang H, Dai M et al. (2009) Synthesis and characterization of 4,4'-diacryloyloxybenzophenone. *Progress in Organic Coatings* 64(4): 510–514. doi: 10.1016/j.porgcoat.2008.08.016
19. Yang J, Tang R, Shi S et al. (2013) Synthesis and characterization of polymerizable one-component photoinitiator based on sesamol. *Photochem Photobiol Sci* 12(5): 923–929. doi: 10.1039/c3pp00003f
20. Meinhart Roth, Daniel Hennen, Andreas Oesterreicher, Florian H. Mostegel, Stefan Kappaun, Matthias Edler, Thomas Griesser Exploring Functionalized Benzophenones as Low-migration Photoinitiators for Biocompatible Thiol/Ene Formulations
21. Ullrich G, Burtscher P, Salz U et al. (2006) Phenylglycine derivatives as coinitiators for the radical photopolymerization of acidic aqueous formulations. *Journal of Polymer Science Part A: Polymer Chemistry* 44(1): 115–125. doi: 10.1002/pola.21139
22. Briggs TI, Dutton GGS, Merler E (1956) THE FRIES REARRANGEMENT OF PHENYL ISOBUTYRATE. *Can. J. Chem.* 34(7): 851–855. doi: 10.1139/v56-113
23. E. Meneguzzo, G. Norcini, G. Li Bassi Process for the preparation of aromatic alpha-hydroxy ketons(WO2009135895)
24. R. Noe, E. Beck, M. Maase et al. Mono and Biacylphosphine derivatives(WO03/0678785)

25. Fouassier JP, Lalevée J (2012) Photoinitiators for Polymer Synthesis: Scope, Reactivity and Efficiency. Wiley, Weinheim
26. Fouassier J-P (1995) Photoinitiation, photopolymerization, and photocuring: Fundamentals and applications. Hanser; Distributed by Hanser/Gardner Publications, Munich, New York, Cincinnati
27. Jockusch S, Koptug IV, McGarry PF et al. (1997) A Steady-State and Picosecond Pump-Probe Investigation of the Photophysics of an Acyl and a Bis(acyl)phosphine Oxide. *J. Am. Chem. Soc.* 119(47): 11495–11501. doi: 10.1021/ja971630c
28. Kolczak U, Rist G, Dietliker K et al. (1996) Reaction Mechanism of Monoacyl- and Bisacylphosphine Oxide Photoinitiators Studied by  $^{31}\text{P}$ -,  $^{13}\text{C}$ -, and  $^1\text{H}$ -CIDNP and ESR. *J. Am. Chem. Soc.* 118(27): 6477–6489. doi: 10.1021/ja9534213
29. Gottlieb HE, Kotlyar V, Nudelman A (1997) NMR Chemical Shifts of Common Laboratory Solvents as Trace Impurities. *J. Org. Chem* 62(21): 7512–7515. doi: 10.1021/jo971176v



ACCEPTED

## Publication VI

Oesterreicher, Andreas; Moser, Andreas; Edler, Matthias; Griesser, Heidi; Schlögl, Sandra; Pichelmayer, Margit; Griesser, Thomas: Investigating Photo-curable Thiol-yne Resins for Biomedical Materials submitted to: *Macromolecular Materials and Engineering*, on October 14, 2016.

## Investigating Photo-curable Thiol-yne Resins for Biomedical Materials

Andreas Oesterreicher<sup>1</sup>, Andreas Moser<sup>2</sup>, Matthias Edler<sup>1</sup>, Heidi Griesser<sup>3,4</sup>, Sandra Schlögl<sup>4</sup>, Margit Pichelmayer<sup>3</sup>, Thomas Griesser<sup>1\*</sup>

<sup>1</sup>Chair of Chemistry of Polymeric Materials & Christian Doppler Laboratory for Functional and Polymer Based Ink-Jet Inks, University of Leoben, Otto-Glöckel-Strasse 2, A-8700 Leoben, Austria

<sup>2</sup>Chair of Material Science and Testing of Polymers, University of Leoben, Otto-Glöckel-Strasse 2, A-8700 Leoben, Austria

<sup>3</sup>Division of Oral Surgery and Orthodontics, Department of Dental Medicine and Oral Health, Medical University Graz, Billrothgasse 4, 8010 Graz, Austria.

<sup>4</sup>Polymer Competence Center Leoben GmbH, Roseggerstrasse 12, 8700 Leoben, Austria

\*corresponding author: Thomas Griesser, email: thomas.griesser@unileoben.ac.at, Tel. +43-3842-402-2358

### Abstract

This study deals with the investigation of photocurable thiol-yne resins covering several important aspects for the production of medical devices by UV based manufacturing processes. In this context, the performance of different low-toxic photoinitiators and stabilizers were evaluated in thiol-yne formulations based on di(but-1-yn-4-yl) carbonate (DBC) and various multifunctional thiol monomers. Photo-DSC measurements revealed that the conversion of all resin formulations is mostly independent on the type and concentration of the applied photoinitiator, however, significant differences in their curing speed were observed. It turned out that the migration of an alkyne derivatized photoinitiator is significantly reduced while providing almost similar photoactivity as its non-functionalized reference. Moreover, it was found that lauryl gallate and butylated hydroxytoluene (BHT) lead to significant stabilization without affecting the overall photoreactivity. Notably, the thermo-mechanical properties of the investigated photopolymers are only slightly affected by water absorption. Using ester free thiols, water absorption could be reduced and hydrolytically stable polymers were realized. These results highlight the versatility of the present thiol-yne system for the production of medical materials by photopolymerization.

1

## Introduction

Recent developments of biocompatible photopolymers for UV based 3D printing of medical devices, such as customized surgical and dental implants or prosthetics, have brought up several alternative concepts to overcome the drawbacks of commonly used (meth)acrylates, which are associated with high irritancy or even monomer cytotoxicity and material brittleness.<sup>1,2,3,4</sup> Besides vinyl carbonates and –carbammates,<sup>5,6,7</sup> also vinyl esters,<sup>8,7,9</sup> and several concepts involving thiol-ene chemistry have demonstrated excellent biocompatibility and decent material properties.<sup>10,11,12,13</sup> As recently presented, also thiol-yne photopolymers are potential candidates for the production of medical materials by UV based 3D printing technologies.<sup>14,15</sup> Especially alkyne ethers and alkyne carbonates show low monomer cytotoxicity, appropriate photoreactivity, high monomer conversions, as well as excellent mechanical properties in their cured state.<sup>14,16</sup>

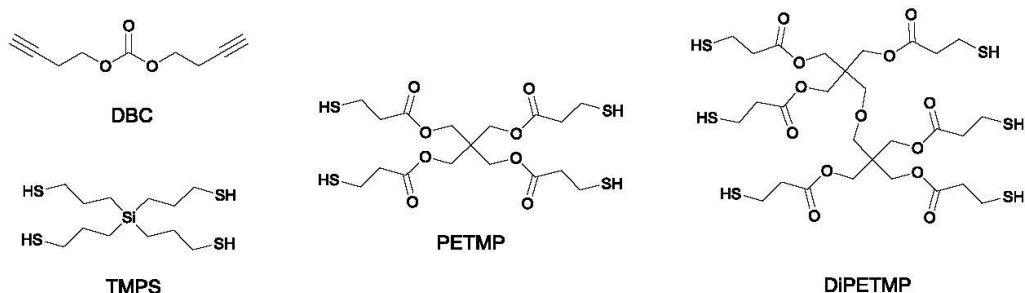
For the production of medical devices, which are in direct contact with human tissue, especially in the case of mucosa or blood, non-network bound components like photoinitiators (PIs) or their cleavage products, but also residual monomers, stabilizers, degradation products or monomer impurities are of major concern.<sup>17</sup> Many of these components state health risks when released to the human body by migration processes. Even when the monomer toxicity is low, migration of PIs can still be a risk. From the wide range of available PIs, only few can be considered as benign in low dose. Prominent examples are camphorquinone or Ivocerin which are used in dental applications.<sup>18,19,20</sup> Also, Irgacure 2959<sup>10,21,22,23</sup> and Irgacure 819<sup>5,24,7</sup> have been used in biocompatible applications. A promising strategy to reduce photoinitiator migration is the use of oligomeric,<sup>25</sup> polymeric<sup>26</sup> or polymerizable photoinitiators.<sup>27,28,29</sup> Unfortunately, oligomeric and polymeric PIs usually lead to a significant increase of the resin viscosity, which subsequently reduces the photochemical performance of the investigated formulation.

Besides the photoreactivity, the shelf-life of photoactive resins for 3D printing applications is of high importance. The limited shelf-life stability of thiol-ene and thiol-yne based resins is one major disadvantage for industrial applications.<sup>11</sup> Reduced shelf-life stability is caused by dark reactions including the spontaneous formation of radicals, peroxide impurities or base-catalyzed nucleophilic

addition of thiols to double and triple bonds.<sup>30</sup> Several attempts have been made to suppress dark reactions in thiol-based resins, which are associated with strong viscosity increase or even premature gelation.<sup>31,32,33,34</sup> The addition of appropriate stabilizers, especially phenolic radical scavengers, with or without the addition of acidic co-stabilizers showed the most promising results in the stabilization of thiol-ene formulations.<sup>30,35</sup> However, for the production of medical devices, also toxicological aspects of those additives have to be taken into consideration.

Another important factor for photo-cured polymeric materials is their water absorption capacity, which is associated with swelling and a decrease in the mechanical properties in terms of  $T_g$ , modulus and strength.<sup>36</sup> Especially polymers with high ester content, as it is the case for (meth)acrylates are known for their high affinity to water.<sup>12</sup> Recent efforts focused on the synthesis of ester free thiols to reduce water susceptibility in thiol-ene photopolymers, in order to maintain their mechanical properties in aqueous surroundings.<sup>13,36,37,38</sup> It has to be mentioned that ester moieties in thiol-yne networks can be exploited for the realization of biodegradable materials as recently shown by our group.<sup>14</sup> In this case, the hydrolytic cleavage of the ester groups, which is triggered by basic or acidic conditions, leads to a degradation of the polymeric materials via a surface erosion process.

In this contribution, we extended the investigations on thiol-yne polymers derived from alkyne carbonate monomers, in order to consider aspects as the choice of the PI and stabilizers as well as the behavior of these polymers in aqueous solution, all of which are crucial factors for the realization of medical devices. Several resin formulations based on di(but-1-yn-4-yl) carbonate (DBC) and the commercially available mercapto propionic ester derivative pentaerythritol tetra(3-mercaptopropionate) (PETMP, monomers are shown in Scheme 1) were prepared to assess the performance of different photoinitiators and stabilizers in the given thiol-yne system. Furthermore, the water absorption and its influence on the thermomechanical properties of cured resin samples containing PETMP, dipentaerythritol hexa(3-mercaptopropionate) (DiPETMP) and tetra(3-mercaptopropyl)silane (TMPS) were investigated.



Scheme 1: Investigated monomers

In addition, the photoinitiator migration of the commercially available photoinitiator Irgacure 2959 and the recently presented polymerizable photoinitiator 2-hydroxy-2-methyl-1-(4-(prop-2-yn-1-yloxy)phenyl)propan-1-one (Irg 2959mod) was studied. (insert DOI when available) Covering these aspects, this paper gives insights into the challenges of the development of photocurable materials for the fabrication of medical devices.

## Experimental

Photo differential scanning calorimetry (Photo-DSC)

Photo-DSC experiments were performed on an NETZSCH Photo-DSC 204 F1 Phoenix. All measurements were conducted at 50 °C in aluminum crucibles under nitrogen flow (20 mL\*min<sup>-1</sup>). The Omnicure s2000 was used as a light source at 1 W\*cm<sup>-2</sup> resulting in an intensity of 80 mW\*cm<sup>-2</sup> at the surface of the sample (range of wavelength was 250 - 445 nm). For the determination of the reaction enthalpy and  $t_{max}$ , the samples were illuminated twice for 10 min, each with an idle time of 2 min in between (sample quantity: 8 ± 0.05 mg resin of DBC and stoichiometric amounts of PETMP including the corresponding photoinitiator). For the analysis, the second run was subtracted from the first one to obtain the reaction enthalpy curve.



### **Viscosity measurements**

Viscosity measurements were conducted on an Anton Paar rheometer (MCR-102, Graz, Austria) with a cone-plate system setup with a titanium cone (MK 22/60 mm, 0.58°) having an opening angle of 0.58° and a diameter of 60 mm. The viscosity was monitored in an accelerated setup at 50 °C over 20 h at a constant shear rate of 300 s<sup>-1</sup>.

### **Sample Preparation**

For the determination of the thermomechanical properties of the photopolymers, sample specimens with 1 x 5 x 25 mm<sup>3</sup> (DMA), 1 x 5 x 50 mm<sup>3</sup> (Water absorption), 1 x 5 x 5 mm<sup>3</sup> (Degradation) and 1 x 50 x 50 mm<sup>3</sup> rectangular (Migration) dimensions were fabricated in PTFE moulds covered with a glass slide or between two glass plates (Migration). The resin samples were photocured by a Lighthammer 6 (Fusion UV Systems) with a Hg bulb (5 passes each side, belt speed of 4 m\*min<sup>-1</sup>, 40% light intensity, E = 3.8 J\*cm<sup>-2</sup> followed by UV/thermal post-curing: 5 passes each side, belt speed of 4 m\*min<sup>-1</sup>, 40% light intensity and sample heated to 90 °C, E = 3.8 J\*cm<sup>-2</sup>).

### **Dynamic mechanical analysis (DMA)**

The thermomechanical properties were measured by DMA in tension mode using a DMA/SDTA 861 (Mettler Toledo) with a heating rate of 2 K\*min<sup>-1</sup> in the temperature range from -40 to 120 °C. The operating frequency was determined at 1 Hz. For comparison of the polymer samples the storage modulus was evaluated at 37 °C. The glass transition temperature was determined at the maximum of tan delta.

### **Sample preparation for migration**

Polymer samples of about 35 mg were extracted in 5 mL ethanol at 50 °C for 96 h. Formulations consisting out of DBC/DiPETMP, containing 0.25 wt% and 1 wt% of either the photoinitiators Irg 2959

or Irg 2959mod and 0.25 wt% of the stabilizer propyl gallate, were used. The extracts of the samples were analyzed by GC-MS after removing the solvent and re-dissolving the residue in 1mL of ethanol.

#### **Gas chromatography – mass spectroscopy (GC-MS)**

The migration studies were performed on a Shimadzu QP2010 plus gas chromatography equipped with a mass spectroscopy unit. The mass calibrations were performed according to the manufacturer recommendation before sample analysis. The capillary column was an Optima 5-Accent (MS-5) (30 m × 0.25-mm I.D., 0.25- $\mu$ m film thickness). Helium was used as the carrier gas with a flow velocity of 47.2 cm/s. The initial oven temperature was 75 °C for 2 min followed by a temperature-programmed increase of 20°C/min to 250°C and subsequently 10°C/min to 300°C. The splitless mode was used for sample injection of 1  $\mu$ L volume at an injection temperature of 300°C. The samples were analyzed using both full scans and SIM modes. In SIM mode, the characteristic ions of 121 for Irg 2959 and 131 for Irg 2959mod respectively cleavage products were used for quantification. MS-Method: Electron energy: -70 eV, Ion Source Temp: 300 °C, Interface Temp: 300 °C.

#### **Water absorption**

For the evaluation of water absorption samples were immersed in deionized water. The sample weight was determined after samples were dried with paper towels.

#### **Degradation**

For the evaluation of the hydrolytic degradation behavior, the corresponding specimens were extracted in ethanol for 48 h and subsequently immersed in 1 M NaOH at 50 °C while the sample vial was continuously rotated. The sample dry weight was monitored over the test period.

## Materials

2-hydroxy-4'-(2-hydroxyethoxy)-2-methylpropiophenone (Irgacure® 2959) (Sigma Aldrich, 98%), 2,6-di-(*tert*-butyl)-4-methylphenol (BHT) (Sigma Aldrich, 99%), 4-methoxyphenol (MEHQ) (Sigma Aldrich, 99%), pyrogallol (Sigma Aldrich, 99%), diisooctylphosphinic acid (DIOPA) (Sigma Aldrich, 90), 4-hexylresorcinol (Sigma Aldrich, 98%), propyl gallate (Sigma Aldrich, 98%), lauryl gallate (Sigma Aldrich, 99%),  $\alpha$ -tocopherol (Sigma Aldrich, 96%) were used as received. Ethyl(2,4,6-trimethylbenzoyl) phenylphosphinate (Irgacure® TPO-L), diphenyl(2,4,6-trimethylbenzoyl)phosphine oxide (Irgacure® TPO), bis(2,4,6-trimethylbenzoyl)phenylphosphine oxide (Irgacure® 819) were donated from BASF. Bis-(4-methoxybenzoyl)diethyl germane (Ivocerin®) was donated from Ivoclar Vivadent AG. Dipentaerythritol hexa(3-mercaptopropionate) (DiPETMP) and pentaerythritol tetra(3-mercaptopropionate) (PETMP) were donated from Bruno Bock Chemische Fabrik GmbH & Co. KG. Tetra(3-mercaptopropyl)silane (TMPS) was synthesized according to the literature.<sup>37</sup> DBC was synthesized as described elsewhere.<sup>39</sup> 2-Hydroxy-2-methyl-1-(4-(prop-2-yn-1-yloxy)phenyl)propan-1-one (Irg 2959mod) was synthesized as recently reported. [\(insert DOI when available\)](#)

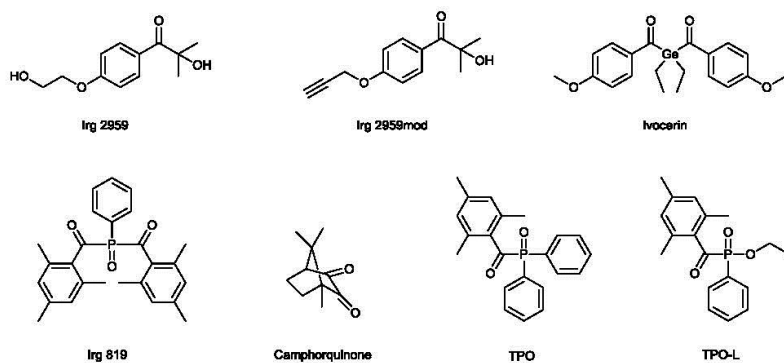
## Results and Discussion

### Investigation of different photoinitiators in a DBC/PETMP formulation

Photoinitiators are an indispensable component of photoreactive resins, which are responsible for the initiation of the polymerization reaction. The activity of photoinitiators in terms of curing speed and obtainable conversion depends on several parameters including the resin viscosity,<sup>25</sup> the structure of the monomers,<sup>25</sup> the ability of UV-light absorption,<sup>40</sup> the triplet lifetime of the excited photoinitiator<sup>41</sup> and the concentration of the PI.

In this study, several low cytotoxic photoinitiators have been evaluated in the biocompatible DBC/PETMP system with the aim to obtain maximum monomer conversion and curing speed, which are two very important parameters that have to be considered for biomedical applications as they

determine the fabrication speed and the amount of leachable monomers in the built medical device. Beside the well-known photoinitiators mono- and bisacylphosphine oxides Irgacure 819, Irgacure TPO and Irgacure TPO-L, also Irgacure 2959, Ivocerin and an alkyne functionalized alpha-hydroxyalkyl phenone based PI (Irg2959mod) were tested in this formulation (see Scheme 2). The alkyne group of Irg2959mod facilitates copolymerization with the resin via a thiol-yne reaction and therefore, immobilization of the photoinitiator or some of its cleavage products in the polymeric network, anticipating reduced migration behavior. Moreover, camphorquinone was evaluated, however, in absence of a coinitiator due to the presences of abstractable hydrogens of thiol groups.



Scheme 2: Investigated photoinitiators

In these experiments, different PI concentrations between 0.25 and 3 wt% were added to the stoichiometric DBC/PETMP resin formulations and their photoactivity was characterized by photo differential scanning calorimetry (photo-DSC). This method has become a prominent tool to characterize photopolymerization reaction by time-dependently measuring of the generated polymerization heat. The time to reach the maximum of the reaction enthalpy ( $t_{max}$ ) in combination with the peak height (h) is a measure of the reaction speed, while the peak area ( $\Delta H$ ) is proportional to the overall monomer conversion.

The results are depicted in Figure 1. It has to be mentioned that Irg 819 was not soluble in concentrations higher than 1 wt%. Camphorquinone is not shown in Figure 1 as it revealed very weak

curing performance, even at 3wt% ( $t_{\max} = 28$  s,  $\Delta H = -375 \text{ J x g}^{-1}$ ,  $h = 3,9$  mW). In general, PIs based on a Norrish type II initiation mechanism show lower initiation performance compared to type I initiators. The cleavage of type I systems is much faster than the electron and/or proton transfer of type II systems.<sup>42</sup>

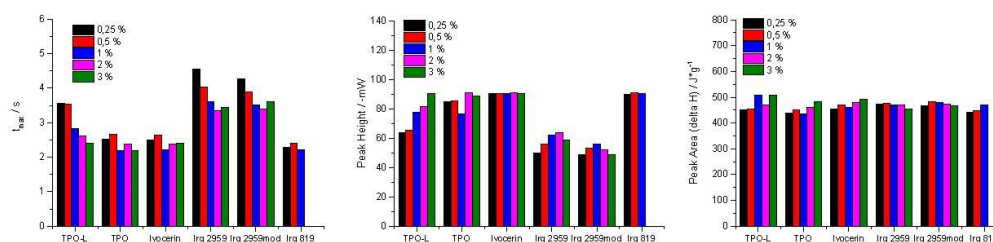
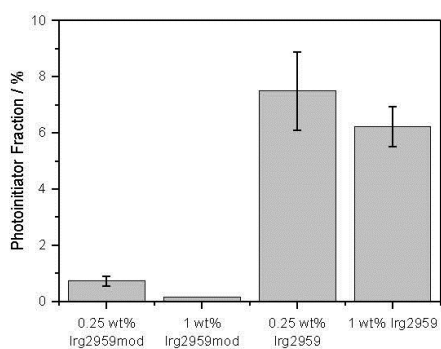


Figure 1:  $t_{\max}$ , peak height  $h$  and peak area ( $\Delta H$ ) of investigated photoinitiators in a DBC/PETMP formulation.

The monomer conversions (expressed by  $\Delta H$ ) did not change significantly for all investigated photoinitiators, nevertheless, differences in their reactivity are evident as seen in Figure 1. The curing speed (expressed by the peak height and  $t_{\max}$ ) of Irg TPO-L, Irg 2959 and Irg 2959mod depend on their employed concentration. A decrease of  $t_{\max}$  and an increase of the peak height  $h$  can be observed for lower concentrations. For all three PIs, a minimum concentration of 1 wt% seems to be appropriate to achieve acceptable performance. In contrast, Ivocerin and Irg 819 showed a high reactivity that was comparable to the acylphosphine oxides and almost no dependency on the applied concentration. Irg 2959 and Irg 2959mod showed the lowest reaction speed (revealed by overall lower peak heights and higher  $t_{\max}$ ) compared to all other investigated photoinitiators, a fact that has been also observed in acrylate systems.<sup>43</sup> Between Irg 2959 and Irg 2959mod no significant difference in terms of photoreactivity was observed.

## Migration Analysis

Although DBC showed low monomer cytotoxicity in previous studies, the toxicity of photoinitiators or their cleavage products must not be neglected.<sup>39</sup> Consequently, the migration behavior of the alkyne functionalized PI Irg 2959mod was studied and compared to its non-derivatized reference Irg 2959. In these experiments, samples of cured resin containing 0.25 wt% and 1wt% PI, respectively, were immersed in ethanol at 50°C for 96h. The quantification of Irg 2959mod and Irg 2959 was performed using GC-MS analysis. Using this technique a significant concentration of Irg 2959 (between 6 - 7.5% of the initial concentration as shown in Figure 2) was found in the ethanolic extract. In contrast, the concentration of Irg 2959mod is approximately ten times lower for 0.25wt% compared to Irg 2959. Most importantly, after extraction of networks containing 1 wt% of Irg 2959mod, its concentration in the extract was below the detection limit (LOD) ( $0.5 \mu\text{g}\cdot\text{mL}^{-1}$ ) of the used method. The higher migration at a concentration of 0.25 wt% can be explained by the reduced photoactivity of these alpha-hydroxyalkyl phenone based PIs at lower concentrations. Reduced initiation performance can lead to a lower conversion (particularly in thick samples) and slighter cross-linked networks in which the diffusion of PI molecules is increased.

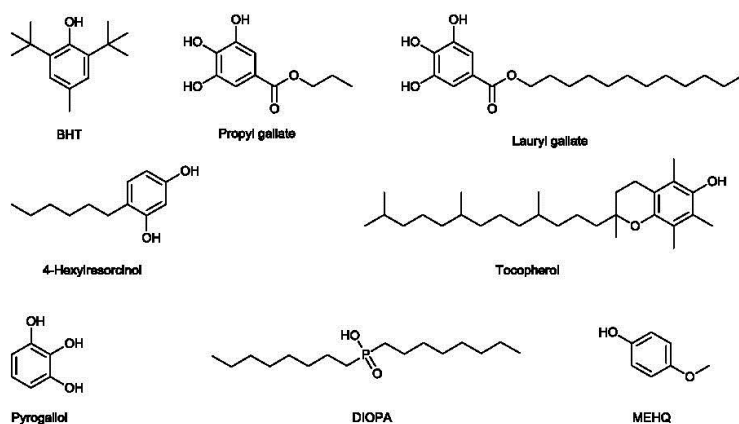


**Figure 2:** Fraction of extracted amounts of photoinitiator Irg 2959 and Irg 2959mod related to initial amounts in DBC/DiPETMP formulations.

Additional focus was set on the detection of PI cleavage products. Besides acetone, which was not considered in these studies due to its low toxicity, 4-(2-hydroxyethoxy)benzaldehyde is the main cleavage product of Irg 2959 as reported in the literature.<sup>41</sup> Assuming only little influence of the propargyl ether substituent on the cleavage behavior, we expected 4-(prop-2-yn-1-yloxy)benzaldehyde as the major cleavage product of Irg 2959mod. To underline this hypothesis, Irg 2959 and Irg 2959mod were illuminated and the obtained products were analyzed by GC-MS. In both cases, signals which correspond to the mass of their expected cleavage products, i.e. 4-(2-hydroxyethoxy)benzaldehyde ( $m/z=121$ ) and 4-(prop-2-yn-1-yloxy)benzaldehyde ( $m/z=131$ ), were detected. Interestingly, both cleavage products could only be found in very low concentration – below the LOQ ( $1.5 \mu\text{g}\cdot\text{mL}^{-1}$ ) of the method - in the corresponding ethanolic extracts.

#### **Storage Stability and Stabilizers**

Shelf-life stability of UV curable resins is a key requirement for many industrial applications. Very recently, it could be shown that the usage of pyrogallol in combination with appropriate phosphonic acids sufficiently suppresses occurring dark reaction in thiol-based resins.<sup>30</sup> For the production of medical devices, however, also toxicological aspects have to be taken into consideration as usually stabilizers are not chemically bound to the polymer matrix and can, therefore, migrate out of the device and interact with the human body. Taking this fact into account, this study focused on hydroxybenzene based stabilizers which are used in the food industry including propyl gallate,<sup>44</sup> lauryl gallate,<sup>45</sup> 4-hexylresorcinol,<sup>46</sup>  $\alpha$ -tocopherol<sup>47</sup> and butylated hydroxytoluene (BHT)<sup>48</sup> (see Scheme 3). The relative stabilization efficiency of these phenolic antioxidants on the DBC/PETMP formulation was evaluated by determining the viscosity increase on a cone-plate rheometer under continuous rotation at 50 °C (accelerated stability tests). Moreover, their efficiency was compared to the hetero-synergistic system pyrogallol/diisooctylphosphinic acid (DIOPA) and hydroquinone monomethyl ether (MEHQ).



Scheme 3: Investigated stabilizers.

In these experiments, the stabilizers (in concentrations of 0.25 or 0.5 wt%) were mixed with a stoichiometric formulation of DBC/PETMP containing 3 wt% TPO-L. For comparison, the viscosity increase after 20 h is depicted in Table 1.

Table 1: Viscosity increase after 20 h of investigated stabilizers including  $t_{max}$ ,  $\Delta H$  and  $h$  from photo-DSC measurements.

	Concentration / wt%	Viscosity increase after 20 h / %	$t_{max}$ / s	$\Delta H$ / J $\cdot$ g $^{-1}$	$h$ / mW
non stabilized	-	278	2.4	-550	-88
Propyl gallate	0.25	121	2.4	-540	-79
Propyl gallate	0.5	76	2.4	-560	-79
Lauryl gallate	0.25	42	2.2	-520	-84
Lauryl gallate	0.5	38	2.4	-500	-75
4-Hexylresorcinol	0.5	80	2.5	-430	-55
BHT	0.5	49	2.3	-540	-78
Tocopherol	0.5	995	3.5	-410	-43
MEHQ	0.5	36	2.0	-440	-74
Pyrogallol	0.5	43	2.8	-580	-62
Pyrogallol / DIOPA	0.5 / 2.5	42	2.5	-510	-64

While the viscosity of the non-stabilized formulation increased by 278%, a stabilizing effect of the investigated additives is clearly visible, except for  $\alpha$ -tocopherol which even lead to an accelerated viscosity increase (+995%). In these experiments, lauryl gallate showed the best stabilizing effect for both investigated concentrations (+38% for 0.5 wt% and +42% for 0.25 wt%), comparable to the



reference system with MEHQ (+36% for 0.5 wt%) and pyrogallol (+43% for 0.5 wt%), followed by BHT (+49% for 0.5wt%). No beneficial effect of the acidic co-stabilizer could be observed for pyrogallol. The stabilizing effect was less pronounced for 4-hexylresorcinol and 0.5wt% propyl gallate. Only moderate stabilization could be achieved by 0.25wt% propyl gallate.

Photo-DSC was used to investigate the influence of the applied stabilizers on the photoreactivity of the DBC/PETMP resin. As shown in Table 1, it turned out that the addition of propyl gallate, BHT and lauryl gallate (in a concentration of 0.25 wt%) results only in a slight decrease in  $\Delta H$  and  $h$ , while  $t_{max}$  is not affected at all. Also, only little influence on the reaction speed could be observed for pyrogallol and its combination with DIOPA, expressed by a slightly lower peak height. While 4-hexylresorcinol and MEHQ led to significantly reduced monomer conversions (lower  $\Delta H$ ), a negative effect on the photoreactivity was mostly pronounced for  $\alpha$ -tocopherol which caused the lowest reaction speed, i.e.  $t_{max}$  and peak height and conversion ( $\Delta H$ ).

#### **Water Absorption and Degradation**

The water absorption capacity of thiol-based photopolymers highly depends on the presence of polar functionalities such as ester groups. In the case of thiol-based photopolymers, ester groups are mainly introduced by the application of commercially available mercaptopropionic acid based monomers. This ester moieties lead to increased water absorption as well as degradation in acidic and basic media, respectively. In order to investigate the influence of different thiol monomers on the water absorption, formulation of DBC/PETMP, DBC/DiPETMP and DBC/TMPS were UV cured and immersed in water for 50 days. As expected DBC/PETMP showed the highest water absorption of about 1.2 % (see Figure 3 left) which is explained by its looser network structure compared to DBC/DiPETMP (~ 1 %). In contrast, the ester free thiol TMPS lead to networks that showed five times lower water absorption (0.2 %).

In Figure 3, the effect of water storage of DBC/PETMP and DBC/DiPETMP networks after 70 days of immersion on the thermomechanical properties, namely the storage moduli and the tan delta, is shown.

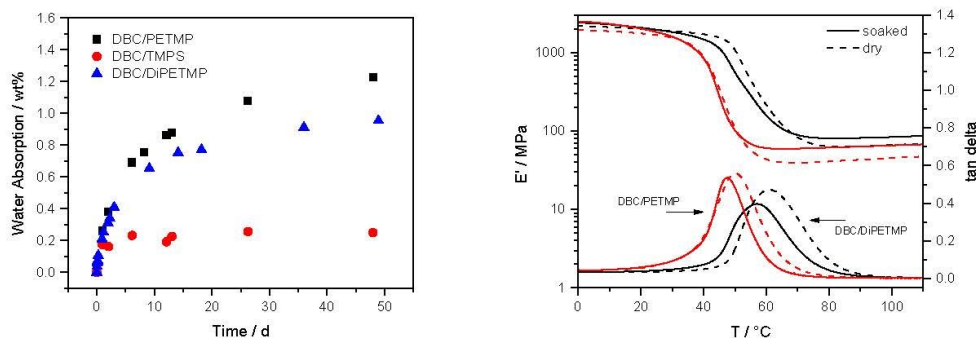


Figure 3: Water absorption of DBC/PETMP, DBC/DiPETMP and DBC/TMPS (left) and DMA measurements ( $E'$  and tan delta) of DBC/PETMP, DBC/DiPETMP before and after immersion in water for 70 days.

Most importantly, the polymer samples did not swell and the thermo-mechanical properties were only slightly influenced as shown in Table 2. It was found that the  $T_{g,s}$  (at the maximum of tan delta) of these networks dropped only by 3-4 °C, the storage modulus ( $E'$ ) at 37 °C did not change significantly and also the full width at the half maxima (FWHMs) of the tan delta remained mostly unaffected. This is in contrast to previously studied thiol-ene networks which showed a significant reduction in their thermo-mechanical properties after water immersion.<sup>37</sup>

Table 2: Obtained results from DMA measurements of DBC/PETMP and DBC/DiPETMP before and after immersion in water.

Formulation	$T_g$ (tan delta) / °C		$E'$ at 37 °C / MPa		FWHM / °C	
	dry	soaked	dry	soaked	dry	soaked
DBC/PETMP	50.2±0.1	47.1±0.7	1177±10	1050±95	18.1±1.3	13.8±1.1
DBC/DiPETMP	61.0±0.1	57.1±0.1	1708±82	1589±12	21.6±0.1	20.5±0.1

However, it has to be mentioned that the ester containing photopolymers are susceptible to alkaline hydrolysis. While the DBC/TMPS polymer showed no degradation after 50 days in 1 M NaOH at 50°C, the DBC/PETMP network fully degrades within 70 h under these conditions.

## Conclusion

In this contribution, several important aspects of thiol-yne photopolymers based on DBC were addressed including the choice of the PI and stabilizers as well as the interaction of these networks with an aqueous solution. Photo-DSC measurements revealed that the conversion (expressed in  $\Delta H$ ) of all resin formulations is mostly independent on the type and concentration of the applied photoinitiator, however, significant differences were observed in their curing speed. While Ivocerin and Irg 819 led to almost similar values of  $t_{max}$  and  $h$  for all investigated concentrations, Irg 2959, Irg 2959mod and the reference Irg TPO-L showed lower reactivity for concentrations below 1 wt%. Additionally, the migration behavior of the alkyne functionalized PI Irg 2959mod was studied and compared with its non-derivatized reference Irg 2959. It turned out that the concentration of Irg 2959mod in the ethanolic extracts is approximately ten times lower compared to Irg 2959 applied in a concentration of 0.25 wt%. Most importantly, after extracting networks containing 1 wt% of Irg 2959mod, its concentration in the extract was even below the detection limit of the used analytic method (GC-MS). This shows the versatility of polymerizable photoinitiators in terms of migration stability in the thiol-yne system. In order to improve the stability of thiol-yne formulations based on DBC, several low-toxic hydroxybenzene based stabilizers were evaluated. In these experiments, lauryl gallate provided the most efficient stabilization, followed by BHT. Only moderate stabilization could be achieved by propyl gallate, while  $\alpha$ -tocopherol led to an even higher viscosity increase than the non-stabilized formulation. It has to be mentioned that  $\alpha$ -tocopherol also negatively influenced the photoreactivity of the resin formulation in terms of reaction speed and conversion. Only little influence on the overall photoreactivity has been detected for lauryl gallate, propyl gallate and BHT, especially at concentrations of 0.25 wt%. The suitable stabilization effect without significantly affecting the curing performance makes lauryl gallate and BHT favored stabilizers in the investigated thiol-yne resin. The water absorption capacity and the degradation stability of these DBC based photopolymers highly depend on the used thiol co-monomer. While the water absorption of DBC/PETMP and DBC/DiPETMP was in the range of 1 to 1.2% after a storage time of 50 days, the ester free thiol TMPS lead to networks that show a five times lower water absorption (0.2 %).

Surprisingly the water absorption only slightly affected the mechanical performance of DBC/PETMP and DBC/DiPTMP samples as DMA measurements revealed. Notably, the ester containing photopolymers are susceptible to alkaline hydrolysis. While the DBC/TMPS polymer showed no degradation after 50 days in 1 M NaOH at 50 °C, the DBC/PETMP network fully degrades within 70 h under these conditions.

### Acknowledgements

Financial support by the Christian Doppler Research Association, the Austrian Federal Ministry of Science, Research and Economy (BMWF) is gratefully acknowledged. Part of the research work of this paper was performed at the Polymer Competence Center Leoben GmbH (PCCL, Austria) within the framework of the COMET-program of the Federal Ministry for Transport, Innovation and Technology and Federal Ministry for Economy, Family and Youth.

### References

- 1 L. S. Andrews and J. J. Clary, *Journal of Toxicology and Environmental Health*, 1986, **19**, 149–164.
- 2 M. Friedman, J. F. Cavins and J. S. Wall, *J. Am. Chem. Soc.*, 1965, **87**, 3672–3682.
- 3 S. C. Ligon-Auer, M. Schwentenwein, C. Gorsche, J. Stampfl and R. Liska, *Polym. Chem.*, 2016, **7**, 257–286.
- 4 C. Gorsche, K. Seidler, P. Knaack, P. Dorfinger, T. Koch, J. Stampfl, N. Moszner and R. Liska, *Polym. Chem.*, 2016, **7**, 2009–2014.
- 5 C. Heller, M. Schwentenwein, G. Russmüller, T. Koch, D. Moser, C. Schopper, F. Varga, J. Stampfl and R. Liska, *J. Polym. Sci. A Polym. Chem.*, 2011, **49**, 650–661.
- 6 B. Husar, R. Liska and B. Husár, *Chem. Soc. Rev.*, 2012, **41**, 2395.
- 7 G. Russmueller, R. Liska, J. Stampfl, C. Heller, A. Mautner, K. Macfelda, B. Kapeller, R. Lieber, A. Haider, K. Mika, C. Schopper, C. Perisanidis, R. Seemann and D. Moser, *Materials*, 2015, **8**, 3685–3700.
- 8 B. Husár, C. Heller, M. Schwentenwein, A. Mautner, F. Varga, T. Koch, J. Stampfl and R. Liska, *J. Polym. Sci. A Polym. Chem.*, 2011, **49**, 4927–4934.
- 9 A. Mautner, B. Steinbauer, S. Orman, G. Russmüller, K. Macfelda, T. Koch, J. Stampfl and R. Liska, *J. Polym. Sci. Part A: Polym. Chem.*, 2016, **54**, 1987–1997.
- 10 A. Mautner, X. Qin, H. Wutzel, S. C. Ligon, B. Kapeller, D. Moser, G. Russmueller, J. Stampfl and R. Liska, *J. Polym. Sci. A Polym. Chem.*, 2013, **51**, 203–212.
- 11 A. Lowe and C. Bowman, *Thiol-X Chemistries in Polymer and Materials Science*, RSC Publishing, Cambridge, 2013.

- 12 M. Podgórski, E. Becka, M. Claudino, A. Flores, P. K. Shah, J. W. Stansbury and C. N. Bowman, *Dent. Mater.*, 2015, **31**, 1255–1262.
- 13 S. Reinelt, M. Tabatabai, N. Moszner, U. K. Fischer, A. Utterodt and H. Ritter, *Macromol. Chem. Phys.*, 2014, **215**, 1415–1425.
- 14 A. Oesterreicher, J. Wiener, M. Roth, A. Moser, R. Gmeiner, M. Edler, G. Pinter and T. Griesser, *Polym. Chem.*, 2016, **7**, 5169–5180.
- 15 A. S. Quick, de los Santos Pereira, Andres, M. Bruns, T. Bückmann, C. Rodriguez-Emmenegger, M. Wegener and C. Barner-Kowollik, *Adv. Funct. Mater.*, 2015, **25**, 3735–3744.
- 16 A. Oesterreicher, S. Ayalur-Karunakaran, A. Moser, F. H. Mostegel, M. Edler, P. Kaschnitz, G. Pinter, G. Trimmel, S. Schlögl and T. Griesser, *J. Polym. Sci. Part A: Polym. Chem.*, 2016.
- 17 J. L. Ferracane, *Dental materials : official publication of the Academy of Dental Materials*, 2006, **22**, 211–222.
- 18 N. Moszner and U. Salz, *Macromol. Mater. Eng.*, 2007, **292**, 245–271.
- 19 B. Ganster, U. K. Fischer, N. Moszner and R. Liska, *Macromolecules*, 2008, **41**, 2394–2400.
- 20 Moszner N., *F&E-Report, IvoclarVivadent AG*, 2013, **19**, July.
- 21 S. J. Bryant, C. R. Nuttelman and K. S. Anseth, *Journal of Biomaterials Science, Polymer Edition*, 2000, **11**, 439–457.
- 22 S. Benedikt, J. Wang, M. Markovic, N. Moszner, K. Dietliker, A. Ovsianikov, H. Grützmacher and R. Liska, *J. Polym. Sci. Part A: Polym. Chem.*, 2016, **54**, 473–479.
- 23 C. G. Williams, A. N. Malik, T. K. Kim, P. N. Manson and J. H. Elisseeff, *Biomaterials*, 2005, **26**, 1211–1218.
- 24 M. Schuster, C. Turecek, B. Kaiser, J. Stampfl, R. Liska and F. Varga, *Journal of Macromolecular Science, Part A*, 2007, **44**, 547–557.
- 25 J. Lalevée, X. Allonas, S. Jradi and J.-P. Fouassier, *Macromolecules*, 2006, **39**, 1872–1879.
- 26 R. Klos, H. Gruber and G. Greber, *Journal of Macromolecular Science: Part A - Chemistry*, 1991, **28**, 925–947.
- 27 W.D. Davies, F.D. Jones, J. Garrett, I. Hutchinson and G. Walton, *Surface coatings international Part B: Coatings Transactions*, 2001, 169–242.
- 28 GB925117.
- 29 P. Xiao, H. Zhang, M. Dai and J. Nie, *Progress in Organic Coatings*, 2009, **64**, 510–514.
- 30 P. Esfandiari, S. C. Ligon, J. J. Lagref, R. Frantz, Z. Cherkaoui and R. Liska, *J. Polym. Sci. Part A: Polym. Chem.*, 2013, **51**, 4261–4266.
- 31 N. Moszner, W. Schöb and V. Rheinberger, *Polymer Bulletin*, 1996, **37**, 289–295.
- 32 E. Klemm, S. Sensfuß, U. Holfter and J. J. Flammersheim, *Angew. Makromolekulare Chemie*, 1993, 121–127.
- 33 C. Hoyle, R. Hensel and M. Grubb, *Polymer Photochemistry*, 1984, **4**, 69–80.
- 34 A. L. Andrady, ed., *Plastics and the environment*, Wiley, Hoboken, NJ, 2004.
- 35 Z. Belbakra, Z. M. Cherkaoui and X. Allonas, *Polymer Degradation and Stability*, 2014, **110**, 298–307.
- 36 M. Podgórski, E. Becka, S. Chatani, M. Claudino and C. N. Bowman, *Polymer chemistry*, 2015, **6**, 2234–2240.
- 37 M. Roth, A. Oesterreicher, F. H. Mostegel, A. Moser, G. Pinter, M. Edler, R. Piock and T. Griesser, *J. Polym. Sci. Part A: Polym. Chem.*, 2015, n/a-n/a.
- 38 S. Reinelt, M. Tabatabai, U. K. Fischer, N. Moszner, A. Utterodt and H. Ritter, *Beilstein journal of organic chemistry*, 2014, **10**, 1733–1740.
- 39 A. Oesterreicher, C. Gorsche, S. Ayalur-Karunakaran, A. Moser, M. Edler, G. Pinter, S. Schlogl, R. Liska and T. Griesser, *Macromolecular rapid communications*, 2016.
- 40 W. A. Green, *Industrial photoinitiators. A technical guide*, Taylor & Francis, Boca Raton, 2010.

- 41 J. P. Fouassier and J. Lalevée, *Photoinitiators for Polymer Synthesis. Scope, Reactivity and Efficiency*, Wiley, Weinheim, 2012.
- 42 G. Ullrich, P. Burtscher, U. Salz, N. Moszner and R. Liska, *Journal of Polymer Science Part A: Polymer Chemistry*, 2006, **44**, 115–125
- 43 W. A. Green, *Industrial photoinitiators. A technical guide*, CRC Press, Boca Raton, 2010.
- 44 *International journal of toxicology*, 2007, **26 Suppl 3**, 89–118.
- 45 *EFSA Journal*, 2015, **13**, 4086.
- 46 *EFSA Journal*, 2014, **12**, 3643.
- 47 *EFSA Journal*, 2015, **13**, 4149.
- 48 *EFSA Journal*, 2012, **10**, 2588.

## 6 Co-Authorship Publications, Patents and Conference Contributions

Radl, Simone; Kreimer, Manuel; Griesser, Thomas; Oesterreicher, Andreas; Moser, Andreas; Kern, Wolfgang; Griesser, Thomas; Schlögl, Sandra: New strategies towards reversible and mendable epoxy based materials employing [4 $\pi$ s+4 $\pi$ s] photocycloaddition and thermal cycloreversion of pendant anthracene groups *Polymer* **2015**, 80, 76–87.

Manhart, Jakob; Ayalur-Karunakaran, Santhosh; Radl, Simone; Oesterreicher, Andreas; Moser, Andreas; Ganser, Christian; Teichert, Christian; Pinter, Gerald; Kern, Wolfgang; Griesser, Thomas; Schlögl, Sandra: Design and application of photo-reversible elastomer networks by using the [4 $\pi$ s+4 $\pi$ s] cycloaddition reaction of pendant anthracene groups *Polymer* **2016**, 102, 10–20.

Mostegel, Florian H.; Roth, Meinhart; Gassner, Martina; Oesterreicher, Andreas; Piock, Richard; Edler, Matthias; Griesser, Thomas: Vinylcarbonates as low-toxic monomers for digital ink-jet inks: Promising alternatives to acrylate based systems *Progress in Organic Coatings* **2016**, 94, 116–123.

Roth, Meinhart; Oesterreicher, Andreas; Hennen, Daniel; Edler, Matthias; Kappaun, Stefan; Mostegel Florian H.; Griesser Thomas: Exploring Functionalized Benzophenones as Low-migration Photoinitiators for Thiol-Ene Formulations *European Polymer Journal* **2016**, *accepted and in press* DOI: 10.1016/j.eurpolymj.2016.11.004.

### Submitted:

Roth, Meinhart; Hennen, Daniel; Oesterreicher, Andreas; Mostegel, Florian H.; Samusjew, Aleksandra; Edler, Matthias; Maier, Eugen; Griesser Thomas: Highly Water-soluble alpha-Hydroxyalkylphenone Based Photoinitiator for Low-migration Applications; Submitted to: *Macromolecular Rapid Communications*, in Sept, **2016**

Edler, Matthias; Mostegel, Florian H.; Roth, Meinhart; Oesterreicher, Andreas; Kappaun, Stefan; Griesser, Thomas (2016): Enhancing the Stability of UV Curable Thiol/Vinyl Carbonate Resins. Submitted to: Journal of Applied Polymer Science, in July, **2016**.

## 6.1 Patents

AT514594B1, Photoinitiator (WO2015031927A1);

Roth, M.; Griesser, T.; Edler, M.; Billiani, J.; Kappaun, S.; Mostegel, F.; Oesterreicher, A.;

WO2015158718A1, Patent Application - Resin composition suitable for printing and printing method utilizing the same;

Griesser, T.; Oesterreicher, A.; Roth, M.; Edler, M.; Mostegel, F.H.; Gassner, M.; Billiani, J.;

DE102015015143A1, Patent Application - Hybridtinte auf Wasserbasis sowie Verfahren zur Herstellung eines mit dieser Tinte gedruckten Artikels;

Griesser, T.; Edler, M.; Samusjew, A.; Oesterreicher, A.; Mostegel, F. H.; Piock, R.; Lenz, S.; Roth, M.; Billiani, J.;

GB1518033.4, Patent Application - Printable Ester Based Resin Compositions and Printing Method utilizing the same;

Griesser, T.; Oesterreicher, A.; Roth, M.; Edler, M.; Mostegel, F.H.; Billiani, J.;

## 6.2 Conference Contributions

Oesterreicher A., Wolfberger A., Daschiel U., Schmidt V., Jerrar A., Teichert C., Griesser T. *Fabrication of 3D Microstructures by Two-Photon Induced Cross-linking of ROMP Derived Polymers*, Photopolymerization Fundamentals Jackson Hole, Wyoming, USA, 22 – 25 Sept 2013

Oesterreicher A., Wolfberger A., Daschiel U., Schmidt V., Jerrar A., Teichert C., Griesser T. *Manufacturing of 3D – Polymer Microstructures via Two-Photon Induced Thiol-Ene Reaction*, IUPAC Polymer World Congress - Macro 2014, Chiang Mai, Thailand, 6 – 11 Jul 2014



Oesterreicher A., Wiener J., Roth M., Moser A., Mostegel F., Edler M., Samusjew A., Pinter G., Grießer T. 27<sup>th</sup> *Synthesis and Characterization of Biocompatible Monomers for Thiol-yne Based Photopolymers*, International Conference on Photochemistry, Jeju Island, Korea, 28 Jun – 2 Jul 2015

Oesterreicher A., Wiener J., Roth M., Moser A., Mostegel F., Samusjew A., Edler M., Pinter G., Grießer T. *Promising Biocompatible Monomers for Thiol-yne Based Photopolymers*, Regional Conference Polymer Processing Society Graz 2015, Graz, Austria, 21 - 25 Sep 2015

Oesterreicher A., Wiener J., Roth M., Moser A., Mostegel F., Edler M., Pinter G., Griesser T. *Photopolymerisierbare Monomere für den 3D Druck von biokompatiblen Strukturen*, 25. Leobener Kunststoff-Kolloquium, Leoben, Austria, 14 – 15 Apr 2016

# 7 APPENDIX

## 7.1 List of Abbreviations and Acronyms

4BC	1,4-Butandiol dibut-3-yn-1-yl carbonate
4MPC	1,4-Butandiol dipent-4-yn-2-yl carbonate
4PC	1,4-Butanediol dipropargyl carbonate
4PE	1,4-Butanediol dipropargyl ether
AlCl <sub>3</sub>	Aluminum chloride
AMT	Additive manufacturing technology
BABC	2,2-Bis[4-(2-hydroxy)ethoxyphenyl]propane dibut-3-yn-1-yl carbonate
BHT	Butylated hydroxytoluene
BisAEPE	2,2-Bis[4-(2-(prop-2-yn-1-yloxy)ethoxyphenyl)]propane
BisAPE	2,2-Bis[4-(prop-2-yn-1-yloxy)phenyl]propane
BuAc	1,4-Butanediol diacrylate
BuBE	1,4-Butanediol dibut-3-yn-1-yl ether
BuMAc	1,4-Butanediol dimethacrylate
BuOH	3-Butyne-1-ol
BuVC	1,4-Butanediol divinyl carbonate
BuVE	1,4-Butanediol divinyl ether
CAD	Computer aided design
CDI	1,1'-Carbonyldiimidazole
CT	Computer tomographic
DBC	Di(but-1-yne-4-yl)carbonate
DF	Defect fraction
DIOPA	Diisooctylphosphinic acid
DiPETMP	Dipentaerythritolhexa(3-mercaptopropionate)
DLP	Direct light projection
DMA	Dynamic Mechanical Analysis

DMF	Dimethylformamide
DMSO	Dimethylsulfoxide
DQ	Double quantum (refers to solid state NMR spectroscopy)
$D_{res}$	Residual dipolar coupling
$E'$	Storage modulus (DMA)
EC50	Half maximal effective concentration
EDT	2,2'-(Ethylenedioxy)diethanethiol
ETAHC	Ethanolamine hydrochloride
FN	Shrinkage force
FT-IR	Fourier Transformed Infrared Spectroscopy
FWHM	Full width at half-maximum of tan delta
$G'$	Storage modulus (Photorheology)
$G''$	Loss modulus (Photorheology)
GC-MS	Gas chromatography mass spectroscopy
HCl	Hydrogen chloride
HEA	2-Hydroxyethyl acrylate
HEMA	2-Hydroxyethyl methacrylate
I2959	Irgacure 2959
ICP-MS	Inductively coupled plasma - mass spectrometry
LOD	Limit of detection
MC	Overall monomer conversion
$MC_g$	Conversion at the gel point
MEHQ	Hydroquinone monomethyl ether
MRI	Magnetic resonance imaging
MTE	2-(2-Methoxyethoxy)ethanethiol
NaH	Sodium hydride
NaOH	Sodium Hydroxide
NMR	Nuclear magnetic resonance
PETMP	Pentaerythritoltetra(3-mercaptopropionat)

Photo-DSC	Photo Differential Scanning Calorimetry
PI	Photoinitiator
PI - 9	Prop-2-yn-1-yl phenyl(2,4,6-trimethylbenzoyl)phosphinate
PI-4	2-Hydroxy-2-methyl-1-(4-(prop-2-yn-1-yloxy)phenyl)propan-1-one
PLA	Poly(lactic acid)
RT-FT-IR	Real-Time Fourier Transformed Infrared Spectroscopy
RT-NIR	Real-time near infrared
SLA	Stereolithography
SOCl <sub>2</sub>	Thionyl chloride
TATT	Triallyl-1,3,5-triazine,2,4,6(1H,3H,5H)trione
TCBC	Tricyclo[5.2.1.0 <sup>2,6</sup> ]decane-4,8-dimethanol dibut-3-yn-1-yl carbonate
T <sub>g</sub>	Glass transition temperature
t <sub>gel</sub>	Time to reach gelation
t <sub>max</sub>	Time to reach the maximum of delta H during photo-DSC measurements
TMPC	1,1,1-Tris(hydroxymethyl)propane tripropargyl carbonate
TMPP	Trimethylolpropanetrakis(3-mercaptopropionat)
TMPS	Silane tetraethyl tetraakis(propane-1-thiol)
TPO-L	Irgacure TPO-L
ΔH	Reaction enthalpy
η	Viscosity
ρ	Density
σ	Surface tension

## 7.2 List of Figures

Figure 1: Left: Water-soluble model compounds [HEA = 2-hydroxyethyl acrylate, HEMA = 2-hydroxymethyl acrylate, BuOH = 3-butyn-1-ol, ETAHC = ethanolamine hydrochloride, MTE = 2-(2-methoxyethoxy)ethanethiol]. Right: Double bond conversion of HEA/MTE (squares), HEMA/MTE (triangle) and HEA/ETAHC (circles) under simulated physiological conditions.....6	6
Figure 2: Test results of in-vitro cytotoxicity tests. .... 10	10
Figure 3: Photo-DSC plots of investigated monomers. Left: 4PC (solid), 4BC (chain dotted), 4MPC (dotted), BuAc (chain double dotted) and BuMAc (dashed). Right: BuAc (chain double dotted), BuMAc (solid, left only), DBC/TMPMP (dotted), DBC/PETMP (dashed), DBC/DiPETMP (chain dotted). Light starts at 0 s..... 12	12
Figure 4: Real-time FT-IR measurements: Conversion of alkyne and thiol moieties. Left: BuBE (open triangle) / TMPMP (diamond), BuPE (open square) / TMPMP (circle). Right: Conversion of (meth)acrylates. Right: BuAc (square) and BuMAc (triangle). .... 13	13
Figure 5: Triple bond (alkyne carbonates) and double bond ((meth)acrylates) conversion versus illumination time. .... 14	14
Figure 6: Conversion of the alkyne monomers BisAEPE (square) and BisAPE (triangle) in alkyne/TMPS formulations versus illumination time including thermal post-curing. .... 14	14
Figure 7: Storage modulus and tan delta versus temperature. Left: BuAc. (dashed) and the stoichiometrically balanced polymerization of BuBE/TMPS (dotted) and BuPE/TMPS (solid). Right: BisAEPE/TMPS (solid) and BisAPE/TMPS (dashed). .... 19	19
Figure 8: Storage modulus and tan delta from DMA measurements of investigated polymer samples. Left: 4MPC/PETMP (solid), 4BC/PETMP (dashed), BuAc (chain dotted). Right: TMPC/PETMP (solid), BABC/PETMP (dashed). .... 20	20
Figure 9: Storage modulus and tan delta from DMA measurements of investigated polymer samples. Left: 4PC/20TMPS (solid), 4PC/PETMP (dashed). Right: TCBC/DiPETMP (dashed) and TCBC/PETMP (solid). .... 21	21
Figure 10: Water absorption of DBC/PETMP, DBC/DiPETMP and DBC/TMPS. .... 22	22
Figure 11: Charpy impact strength and $T_g$ of DBC/PETMP, DBC/DiPETMP, BuAc and PLA.* ..... 23	23
Figure 12: Left: Determination of the gelpoint ( $G'/G'' = 1$ , -). Right: Measurement of the normal force $F_N$ . BuAc (chain double dotted), DBC/TMPMP (dotted), DBC/PETMP (dashed), DBC/DiPETMP (chain dotted). Light starts at 0 s..... 24	24
Figure 13: Left: DMA plots of DBC/TMPMP (chain dotted), DBC/PETMP (solid) and DBC/DiPETMP (dashed). Right: Measured Charpy impact strengths for DBC derived polymers and BuAc. .... 25	25
Figure 14: Weight losses during degradation for the formulations a) 4PC/PETMP, b) 4BC/PETMP, c) 4MPC/PETMP d) 4PC/5TMPS, e) 4PC/10TMPS, f) 4PC/20TMPS, g) 4PC/EDT, h) BC/EDT, i) MPC/EDT and PLA (left only) in 1 M NaOH (left) and 1 M HCl (right) at 45 °C. .... 26	26
Figure 15: 3D printed test patterns from a TCBC/DiPETMP formulation (scale on the left shown in cm). .... 27	27

Figure 16: Absorption spectra of the synthesized photoinitiators and the commercially available reference substances (1.0 mM in acetonitrile). Left: I2959 (solid line), PI – 4 (dotted line); right: TPO-L (solid line), PI – 9 (dashed line). ..... 31

Figure 17: Conversion of alkyne ether groups of PI - 4 (red circle) and PI - 9 (black square) during UV illumination (left) and results of photo-DSC measurements ( $t_{max}$  and peak height) of different concentrations (shown in wt%) of PI – 4 and I2959 in a DBC/PETMP resin formulation (right). 32

Figure 18: Results of migration studies of PI - 4 and P - 9 and their references in a thiol-ene (BuVC/TMPMP) resin (left) and PI – 4 and its reference at two different concentrations, respectively, in a thiol-yne resin (DBC/PETMP) (right). ..... 33

## 7.3 List of Tables

Table 1: EC50 values obtained from cytotoxicity tests. ....	9
Table 2: Density ( $\rho$ ), surface tension ( $\sigma$ ) and viscosity ( $\eta$ ) of TMPS and PETMP. ....	11
Table 3: Summary of photo-DSC ( $t_{\max}$ ) and RT-FT-IR measurements (conversion) of alkyne monomers in combination with thiols, including reference samples (BuAc and BuMAc). ....	12
Table 4: Viscosity increase after 20 h of investigated stabilizers including $t_{\max}$ , $\Delta H$ and $h$ from photo-DSC measurements. ....	16
Table 5: Analysis of the normalized DQ curves obtained for the different samples at 100 °C. ....	18
Table 6: Results of DMA measurements of alkyne ethers. ....	18
Table 7: Results of the DMA measurements of alkyne carbonate/PETMP photopolymers. ....	20
Table 8: Storage moduli and $T_g$ s of photocured TATT/TMPS, DBC/PETMP and DBC/DiPETMP resins before and after storage in water for 24h. ....	21
Table 9: Investigated parameters of DBC/thiol formulations and their corresponding photopolymers including reference sample BuAc. ....	24
Table 10: Photopolymerization parameters obtained by Photo-DSC. ....	31

## 7.4 List of Schemes

Scheme 1: Radical mediated thiol-yne reaction. ....	5
Scheme 2: Synthesis of but-1-yn-4-yl ethers. ....	7
Scheme 3: Synthesis of alkyne carbonates. ....	7
Scheme 4: Structures of the investigated alkyne monomers including reference substances. ....	8
Scheme 5: Chemical structures of investigated thiols. ....	10
Scheme 6: Investigated stabilizers. ....	15
Scheme 7: Synthesis of photoinitiator PI - 4. ....	29
Scheme 8: Synthesis of the photoinitiator PI - 9. ....	30
Scheme 9: Incorporation of PI - 4 into the thiol-ene network during photopolymerization. ....	32

## 8 References

- 1 M. Schwentenwein and J. Homa, *Int. J. Appl. Ceram. Technol.*, 2015, **12**, 1–7.
- 2 R. Liska, M. Schuster, R. Inführ, C. Turecek, C. Fritscher, B. Seidl, V. Schmidt, L. Kuna, A. Haase, F. Varga, H. Lichtenegger and J. Stampfl, *J. Coat. Technol. Res.*, 2007, **4**, 505–510.
- 3 J. Banks, *IEEE Pulse*, 2013, **4**, 22–26.
- 4 B. C. Gross, J. L. Erkal, S. Y. Lockwood, C. Chen and D. M. Spence, *Anal. Chem.*, 2014, **86**, 3240–3253.
- 5 A. Dawood, B. M. Marti, V. Sauret-Jackson and A. Darwood, *Br Dent J*, 2015, **219**, 521–529.
- 6 A. Bandyopadhyay, S. Bose and S. Das, *MRS Bull.*, 2015, **40**, 108–115.
- 7 L. E. Murr, E. Martinez, K. N. Amato, S. M. Gaytan, J. Hernandez, D. A. Ramirez, P. W. Shindo, F. Medina and R. B. Wicker, *J. Mater. Res. Techn.*, 2012, **1**, 42–54.
- 8 D. L. Bourell, H. L. Marcus, J. W. Barlow and J. J. Beaman, *Int. J. Powder Metall*, 1992, **28**, 369–381.
- 9 P. H. Warnke, H. Seitz, F. Warnke, S. T. Becker, S. Sivananthan, E. Sherry, Q. Liu, J. Wiltfang and T. Douglas, *J Biomed Mater Res B Appl Biomater*, 2010, **93**, 212–217.
- 10 A. Zocca, P. Colombo, C. M. Gomes, J. Günster and D. J. Green, *J. Am. Ceram. Soc.*, 2015, **98**, 1983–2001.
- 11 B. Wendel, D. Rietzel, F. Kühnlein, R. Feulner, G. Hülder and E. Schmachtenberg, *Macromol. Mater. Eng.*, 2008, **293**, 799–809.
- 12 R. D. Goodridge, C. J. Tuck and R. Hague, *Prog Mater Sci*, 2012, **57**, 229–267.
- 13 H. N. Chia and B. M. Wu, *J Biol Eng*, 2015, **9**, 4.
- 14 M. Schuster, C. Turecek, G. Weigel, R. Saf, J. Stampfl, F. Varga and R. Liska, *J. Polym. Sci. A Polym. Chem.*, 2009, **47**, 7078–7089.
- 15 D. W. Hutmacher, M. Sittinger and M. V. Risbud, *Trends Biotechnol*, 2004, **22**, 354–362.
- 16 J. R. Tumbleston, D. Shirvanyants, N. Ermoshkin, R. Januszewicz, A. R. Johnson, D. Kelly, K. Chen, R. Pinschmidt, J. P. Rolland, A. Ermoshkin, E. T. Samulski and J. M. DeSimone, *Science (New York, N.Y.)*, 2015, **347**, 1349–1352.
- 17 R. Felzmann, S. Gruber, G. Mitteramskogler, M. Pastrama, A. R. Boccaccini and J. Stampfl, in *Biomedical Engineering 2013*.
- 18 S. C. Ligon-Auer, M. Schwentenwein, C. Gorsche, J. Stampfl and R. Liska, *Polym. Chem.*, 2016, **7**, 257–286.
- 19 A. Oesterreicher, S. Ayalur-Karunakaran, A. Moser, F. H. Mostegel, M. Edler, P. Kaschnitz, G. Pinter, G. Trimmel, S. Schlögl and T. Griesser, *J. Polym. Sci. Part A: Polym. Chem.*, 2016, **54**, 3484–3494.
- 20 A. Oesterreicher, J. Wiener, M. Roth, A. Moser, R. Gmeiner, M. Edler, G. Pinter and T. Griesser, *Polym. Chem.*, 2016, **7**, 5169–5180.
- 21 A. Oesterreicher, C. Gorsche, S. Ayalur-Karunakaran, A. Moser, M. Edler, G. Pinter, S. Schlogl, R. Liska and T. Griesser, *Macromol. Rapid Commun*, 2016, **37**, 1701–1706.



- 22 M. Roth, A. Oesterreicher, F. H. Mostegel, A. Moser, G. Pinter, M. Edler, R. Piock and T. Griesser, *J. Polym. Sci. Part A: Polym. Chem.*, 2016, **54**, 418–424.
- 23 A. Oesterreicher, A. Moser, M. Edler, H. Griesser, S. Schlögl, M. Pichelmayer and Griesser Thomas, *Macrom Mater Eng*, submitted on October 14, 2016.
- 24 J. V. Crivello and E. Reichmanis, *Chem. Mater.*, 2014, **26**, 533–548.
- 25 J. P. Fouassier, *Photoinitiation, Photopolymerization, and Photocuring: Fundamentals and Applications*, Hanser Publisher, New York, 1995.
- 26 A. B. Scranton, C. N. Bowman, R. W. Peiffer, *Photopolymerization: Fundamentals and Applications*, American Chemical Soc, Washington, DC, 1997, vol. 673.
- 27 N. S. Allen, *Photopolymerization and Photoimaging Science and Technology*, Elsevier Applied Science, London, 1st edn., 1989.
- 28 C. Hull, *Apparatus for production of three-dimensional objects by stereolithography*. US 4575330 A, 1986.
- 29 F. P. W. Melchels, J. Feijen and D. W. Grijpma, *Biomaterials*, 2010, **31**, 6121–6130.
- 30 N. J. Mankovich, D. Samson, W. Pratt, D. Lew and J. Beumer, *Otolaryngol. Clin. North Am.*, 1994, **27**, 875–889.
- 31 F. Valente, G. Schioli and A. Sbrenna, *Int. J. Oral Maxillofac. Implants*, 2009, **24**, 234–242.
- 32 A. Curodeau, E. Sachs and S. Caldarise, *J. Biomed. Mater. Res.*, 2000, **53**, 525–535.
- 33 B. Husár, C. Heller, M. Schwentenwein, A. Mautner, F. Varga, T. Koch, J. Stampfl and R. Liska, *J. Polym. Sci. A Polym. Chem.*, 2011, **49**, 4927–4934.
- 34 A. Woesz, M. Rumpler, J. Stampfl, F. Varga, N. Fratzi-Zelman, P. Roschger, K. Klaushofer and P. Fratzi, *Mater. Sci. Eng. C*, 2005, **25**, 181–186.
- 35 T. Weigel, G. Schinkel and A. Lendlein, *Expert Rev. Med. Devices*, 2014, **3**, 835–851.
- 36 S. Bose, S. Vahabzadeh and A. Bandyopadhyay, *Mater. Today*, 2013, **16**, 496–504.
- 37 C. Gorsche, K. Seidler, P. Knaack, P. Dorfinger, T. Koch, J. Stampfl, N. Moszner and R. Liska, *Polym. Chem.*, 2016, **7**, 2009–2014.
- 38 P. Dorfinger, J. Stampfl and R. Liska, *MSF*, 2015, **825-826**, 53–59.
- 39 D. Karalekas and A. Aggelopoulos, *J. Mater. Process. Tech.*, 2003, **136**, 146–150.
- 40 L. S. Andrews and J. J. Clary, *J. Toxicol. Environ. Health*, 1986, **19**, 149–164.
- 41 M. Friedman, J. F. Cavins and J. S. Wall, *J. Am. Chem. Soc.*, 1965, **87**, 3672–3682.
- 42 A. Mautner, X. Qin, G. Kapeller, G. Russmüller, T. Koch, J. Stampfl and R. Liska, *Macromol. Rapid Commun*, 2012, **33**, 2046–2052.
- 43 I. Vroman and L. Tighzert, *Materials*, 2009, **2**, 307–344.
- 44 J. C. Middleton and A. J. Tipton, *Biomaterials*, 2000, **21**, 2335–2346.
- 45 T. Matsuda and M. Mizutani, *J. Biomed. Mater. Res.*, 2002, **62**, 395–403.
- 46 C. Heller, M. Schwentenwein, G. Russmüller, F. Varga, J. Stampfl and R. Liska, *J. Polym. Sci. A Polym. Chem*, 2009, **47**, 6941–6954.
- 47 C. Heller, M. Schwentenwein, G. Russmüller, T. Koch, D. Moser, C. Schopper, F. Varga, J. Stampfl and R. Liska, *J. Polym. Sci. A Polym. Chem*, 2011, **49**, 650–661.

- 48 B. Husar and R. Liska, *Chem. Soc. Rev.*, 2012, **41**, 2395.
- 49 A. Mautner, B. Steinbauer, S. Orman, G. Russmüller, K. Macfelda, T. Koch, J. Stampfl and R. Liska, *J. Polym. Sci. Part A: Polym. Chem.*, 2016, **54**, 1987–1997.
- 50 C. N. Bowman and C. J. Kloxin, *AIChE J.*, 2008, **54**, 2775–2795.
- 51 C. E. Hoyle, T. Y. Lee and T. Roper, *J. Polym. Sci. A Polym. Chem.*, 2004, **42**, 5301–5338.
- 52 J. A. Carioscia, H. Lu, J. W. Stanbury and C. N. Bowman, *Dent. Mater.*, 2005, **21**, 1137–1143.
- 53 T. M. Roper, T. Kwee, T. Y. Lee, C. A. Guymon and C. E. Hoyle, *Polymer*, 2004, **45**, 2921–2929.
- 54 J. P. Fouassier and J. F. Rabek, eds., *Radiation Curing in Polymer Science and Technology. Volume III Polymerisation Mechanisms*, Elsevier Science Publishers Ltd., 1993.
- 55 A. Lowe and C. Bowman, *Thiol-X Chemistries in Polymer and Materials Science*, RSC Publishing, Cambridge, 2013.
- 56 M. Podgórski, E. Becka, M. Claudino, A. Flores, P. K. Shah, J. W. Stansbury and C. N. Bowman, *Dent. Mater.*, 2015, **31**, 1255–1262.
- 57 S. Reinelt, M. Tabatabai, N. Moszner, U. K. Fischer, A. Utterodt and H. Ritter, *Macromol. Chem. Phys.*, 2014, **215**, 1415–1425.
- 58 A. B. Lowe, *Polym. Chem*, 2010, **1**, 17.
- 59 A. B. Lowe, *Polymer*, 2014, **55**, 5517–5549.
- 60 S. Parker, R. Reit, H. Abitz, G. Ellson, K. Yang, B. Lund and W. E. Voit, *Macromol. Rapid Commun*, 2016, **37**, 1027–1032.
- 61 M. Podgorski, S. Chatani and C. N. Bowman, *Macromol. Rapid Commun*, 2014, **35**, 1497–1502.
- 62 M. Podgórski, E. Becka, S. Chatani, M. Claudino and C. N. Bowman, *Polym. Chem.*, 2015, **6**, 2234–2240.
- 63 S. Reinelt, M. Tabatabai, U. K. Fischer, N. Moszner, A. Utterodt and H. Ritter, *Beilstein J. Org.*, 2014, **10**, 1733–1740.
- 64 J. A. Carioscia, L. Schneidewind, C. O'Brien, R. Ely, C. Feeser, N. Cramer and C. N. Bowman, *J. Polym. Sci. A Polym. Chem.*, 2007, **45**, 5686–5696.
- 65 B. D. Fairbanks, T. F. Scott, C. J. Kloxin, K. S. Anseth and C. N. Bowman, *Macromolecules*, 2009, **42**, 211–217.
- 66 C. E. Hoyle, A. B. Lowe and C. N. Bowman, *Chem. Soc. Rev.*, 2010, **39**, 1355.
- 67 J. W. Chan, J. Shin, C. E. Hoyle, C. N. Bowman and A. B. Lowe, *Macromolecules*, 2010, **43**, 4937–4942.
- 68 J. W. Chan, H. Zhou, C. E. Hoyle and A. B. Lowe, *Chem. Mater*, 2009, **21**, 1579–1585.
- 69 B. D. Fairbanks, E. A. Sims, K. S. Anseth and C. N. Bowman, *Macromolecules*, 2010, **43**, 4113–4119.
- 70 D. Pretzel, B. Sandmann, M. Hartlieb, J. Vitz, S. Hölzer, N. Fritz, N. Moszner and U. S. Schubert, *J. Polym. Sci., Part A: Polym. Chem.*, 2015, **53**, 1843–1847.
- 71 P. Theato and H.-A. Klok, eds., *Functional polymers by post-polymerization modification*, Wiley-VCH, Weinheim, 1st edn., 2013.

- 72 A. S. Quick, de los Santos Pereira, Andres, M. Bruns, T. Bückmann, C. Rodriguez-Emmenegger, M. Wegener and C. Barner-Kowollik, *Adv. Funct. Mater.*, 2015, **25**, 3735–3744.
- 73 D. P. Nair, M. Podgórski, S. Chatani, T. Gong, W. Xi, C. R. Fenoli and C. N. Bowman, *Chem. Mater*, 2014, **26**, 724–744.
- 74 E. D. Bergmann, D. Ginsburg and R. Pappo, *Org. react.*, 1959, **10**, 179–556.
- 75 H. Peng, C. Wang, W. Xi, B. A. Kowalski, T. Gong, X. Xie, W. Wang, D. P. Nair, R. R. McLeod and C. N. Bowman, *Chem. Mater.*, 2014, **26**, 6819–6826.
- 76 A. Williamson, *Philosophical Magazine Series 3*, 1850, **37**, 350–356.
- 77 I. N. Michaelides, B. Darses and D. J. Dixon, *Org. Lett*, 2011, **13**, 664–667.
- 78 S. P. Rannard and N. J. Davis, *Org. Lett.*, 1999, **1**, 933–936.
- 79 P. Esfandiari, S. C. Ligon, J. J. Lagref, R. Frantz, Z. Cherkaoui and R. Liska, *J. Polym. Sci. Part A: Polym. Chem*, 2013, **51**, 4261–4266.
- 80 *International journal of toxicology*, 2007, **26 Suppl 3**, 89–118.
- 81 *EFSA Journal*, 2015, **13**, 4086.
- 82 *EFSA Journal*, 2014, **12**, 3643.
- 83 *EFSA Journal*, 2015, **13**, 4149.
- 84 *EFSA Journal*, 2012, **10**, 2588.
- 85 M. Sangermano, *Pure Appl. Chem*, 2012, **84**, 2089–2101.
- 86 P. J. Flory and J. Rehner, *J. Chem. Phys.*, 1943, **11**, 521.
- 87 P. J. Flory, *Principles of polymer chemistry*, Cornell Univ. Press, Ithaca, NY, 1953.
- 88 P. J. Flory, *J. Chem. Phys.*, 1950, **18**, 108.
- 89 R. Graf, D. E. Demco, S. Hafner and H. W. Spiess, *Solid State Nucl Magn Reson*, 1998, **12**, 139–152.
- 90 M. Schneider, L. Gasper, D. E. Demco and B. Blümich, *J. Chem. Phys.*, 1999, **111**, 402.
- 91 K. Saalwächter, *Prog. Nucl. Magn. Reson. Spectrosc.*, 2007, **51**, 1–35.
- 92 K. Saalwächter, P. Ziegler, O. Spyckerelle, B. Haidar, A. Vidal and J.-U. Sommer, *J. Chem. Phys.*, 2003, **119**, 3468.
- 93 N. Moszner, W. Schöb and V. Rheinberger, *Polym. Bull.*, 1996, **37**, 289–295.
- 94 E. Hassan, Y. Wei, H. Jiao and M. Yu, *JFBI*, 2013, **6**, 85–94.
- 95 C. Gorsche, T. Koch, N. Moszner and R. Liska, *Polym. Chem.*, 2015, **6**, 2038–2047.
- 96 R. M. Ginde and R. K. Gupta, *J. Appl. Polym. Sci.*, 1987, **33**, 2411–2429.
- 97 A. Oesterreicher, M. Roth, D. Hennen, F. H. Mostegel, M. Edler, S. Kappaun and T. Griesser, *Eur. Polym. J*, 2016, DOI: 10.1016/j.eurpolymj.2016.10.040.
- 98 C. G. Williams, A. N. Malik, T. K. Kim, P. N. Manson and J. H. Elisseeff, *Biomaterials*, 2005, **26**, 1211–1218.
- 99 S. Benedikt, J. Wang, M. Markovic, N. Moszner, K. Dietliker, A. Ovsianikov, H. Grützmacher and R. Liska, *J. Polym. Sci. Part A: Polym. Chem.*, 2016, **54**, 473–479.
- 100 W.D. Davies, F.D. Jones, J. Garrett, I. Hutchinson and G. Walton, *Surf. Coat. Int., Part B: Coat. Trans.*, 2001, 169–242.

- 101 R. Klos, H. Gruber and G. Greber, *J Macromol Sci Part A*, 1991, **28**, 925–947.
- 102 J. Lalevée, X. Allonas, S. Jradi and J.-P. Fouassier, *Macromolecules*, 2006, **39**, 1872–1879.
- 103 Du Pont, *Organic Polymers*, GB925117, 1963.
- 104 P. Xiao, H. Zhang, M. Dai and J. Nie, *Prog. Org. Coat.*, 2009, **64**, 510–514.
- 105 J. Yang, R. Tang, S. Shi and J. Nie, *Photochem. Photobiol. Sci.*, 2013, **12**, 923–929.
- 106 M. Roth, D. Hennen, A. Oesterreicher, F. H. Mostegel, S. Kappaun, M. Edler and T. Griesser, *Eur. Polym. J*, 2016, DOI: 10.1016/j.eurpolymj.2016.11.004.
- 107 G. Ullrich, P. Burtscher, U. Salz, N. Moszner and R. Liska, *J. Polym. Sci. Part A: Polym. Chem.*, 2006, **44**, 115–125.
- 108 T. I. Briggs, G. G. S. Dutton and E. Merler, *Can. J. Chem.*, 1956, **34**, 851–855.
- 109 S. Jockusch, I. V. Koptug, P. F. McGarry, G. W. Sluggett, N. J. Turro and D. M. Watkins, *J. Am. Chem. Soc.*, 1997, **119**, 11495–11501.
- 110 U. Kolczak, G. Rist, K. Dietliker and J. Wirz, *J. Am. Chem. Soc.*, 1996, **118**, 6477–6489.
- 111 J. P. Fouassier and J. Lalevée, *Photoinitiators for Polymer Synthesis. Scope, Reactivity and Efficiency*, Wiley, Weinheim, 2012.

## 9 Curriculum Vitae

Name: Dipl.-Ing. Andreas Oesterreicher  
Date of birth: April 30, 1986 in Innsbruck  
Nationality: Austria  
E-mail: andi.oester@gmail.com

---

### Education and Qualifications

- 2013 – 2016** University of Leoben – Chair of Chemistry of Polymeric Materials  
PhD thesis under supervision of Assoc. Prof. DI Dr. Thomas Griesser  
Title: Thiol-yne Derived Resins for 3D Printing of Biocompatible Structures
- 2011 – 2012** Safer Future Youth Development Project, Freetown, Sierra Leone  
Civil Service
- 2005 – 2011** Graz University of Technology - Technical Chemistry  
Master thesis under supervision of Dipl.-Chem. Univ. Dr. Frank Wiesbrock  
Title: Preparation of polyurethane-based recyclates with special consideration of C3- and C4-(poly)-ethers
- 2008 – 2009** McMaster University, Hamilton, Canada - Joint Study Exchange Program  
Focus: Material Science
- 2004 – 2005** Graz University of Technology – Process Engineering
- 1996 – 2004** Bundesrealgymnasium Bludenz